MOLECULAR X-RAY SPECTRA OF PHOSPHORUS-BEARING COMPOUNDS

A THESIS SUBMITTED TO THE GRADUATE DIVISION OF THE
UNIVERSITY OF HAWAII IN PARTIAL FULFILLMENT
OF THE REQUIREMENTS FOR THE DEGREE OF

MASTER OF SCIENCE

IN CHEMISTRY

JUNE 1972

By

Kathleen M. Myers

Thesis Committee:

George Andermann, Chairman
Roger E. Cramer
Burton L. Henke

We certify that we have read this thesis and that in our opinion it is satisfactory in scope and quality as a thesis for the degree of Master of Science in Chemistry.

THESIS COMMITTEE

_____

Chairman

_____

_____

DEDICATION

Lovingly, to the majority of this department who thought I would never produce.

ACKNOWLEDGMENT

This research does not represent a singular effort. Several people contributed to my total graduate school experience and thus to this thesis. First of all, my parents for their support in my efforts and for making this all possible; a very special thanks to Mr. H. Collins Whitehead who sired our "bastardized spectrometer," his patient assistance considerably eased the way; Professor Quintus Fernando of the University of Arizona for donating his phosphorus compounds and thus the initial stimulus for this research project; "Rog" for his CNDO program, helpful discussions--academic and not-so-academic--and even, in retrospect, for his nagging; Mrs. Ethyl McAfee for proofreading this manuscript; and, of course, the Chemistry faculty--their doubts instilled incentive.

Lastly, but most importantly, a very deep debt of gratitude to "Uncle George" for having faith!

TABLE OF CONTENTS

LIST OF TABLES

LIST OF TABLES (Continued)

LIST OF FIGURES

LIST OF FIGURES (Continued)

LIST OF FIGURES (Continued)

CHAPTER I

Introduction

As indicated in a recent review article by Urch,[1] x-ray photon spectra arising from electron transitions provide a powerful tool for the elucidation of the electronic structure of materials. Accordingly, photon emission which originates in the outermost orbitals reflects changes that occur in the vicinity of an atom upon bond formation. Thus, shifts in peak positions, changes in band shapes, and splittings of bands provide valuable information concerning electronic structure.

As indicated by Andermann,[2] photon emission spectroscopy possesses an inherent advantage over other electronic methods. Due to the essentially atomic nature of the initially ionized state and the large emission energies, photon spectroscopy of solids, for example, is capable of high resolution of spectral transitions, unlike u.v. absorption spectroscopy of solids which necessarily involves broad bands under poor resolution. Furthermore, x-ray photon emission spectroscopy is representative of the bulk sample favoring it over x-ray induced photoelectron spectroscopy which is representative of surface material only.[3]

The effects of chemical bonding upon x-ray spectra were first noted over fifty years ago,[4] but lay uninterpreted primarily due to the lack of a rigorous bonding theory. More recently, the application of molecular orbital concepts has led to the resurgence of interest in x-ray photon emission spectroscopy.

Much of the work, at first, centered upon transition metal complexes due to their large transition energies and easier measurement in the hard x-ray region. In 1965 Best[5] provided a reasonable interpretation of the K x-ray emission spectra of a series of tetrahedral transition metal oxy-anions, while Seka and Hanson[6] interpreted the K absorption spectra of many transition metal complexes on a molecular orbital model. Fischer[7,8] similarly reported on the $L_{2,3}$ emission and absorption spectra for some titanium and vanadium compounds. In 1967 Andermann suggested the use of molecular spectroscopic concepts for interpretation of x-ray emission spectra.[9] Work was then extended to the compounds of the second periodic row elements, in particular to their oxy-anions. Dodd and Glenn[10] investigated the K emission spectra of fourfold and sixfold coordinated oxides of magnesium, aluminum, and silicon, while the sulfur and chlorine spectra were studied by several people including Best,[11] Andermann and Whitehead,[12] and Nefedov, et al.,[13,14,15] all interpretations agreeing fairly well on the main spectral features. The sulfur and chlorine work is further supplemented by the rigorous molecular orbital calculations of Manne,[16] Hillier,[17] and Bishop.[18,19]

In the considerable work done on the compounds of the elements of the second periodic row, however, information on the compounds of phosphorus is limited. Nefedov and Fomichev[14] have looked at the L spectra of one phosphorus compound, and Urch[20] has discussed the L spectra of a series of phosphorus compounds, but this is rather scanty information. More complete is the work of Hillier[17] on PO_4^{-3} in which rigorous molecular orbital <u>ab initio</u> SCF calculations for the molecule in relation to the Kβ and $L_{2,3}$ spectra and photoelectron spectra are

discussed. The only other rigorous calculation for phosphorus is by Boyd and Lipscomb[21] who have done ab initio SCF calculations on the hypothetical PO_2^- anion; but obviously no spectral data exists for comparison.

Curiously enough complete K and L spectra do exist for an entire series of phosphorus salts, the K spectra having been investigated by Fichter,[22] and the L spectra by Henke,[23] but neither author offers molecular interpretation.

Studies to date have dealt with relatively simple bonding situations in which the central atom is surrounded by one type of ligand and possesses over-all high symmetry. Any evaluation of molecular bonding needs to be extended to more general situations where more than one type of ligand may be bonded to the central atom and in which the molecular symmetry is reduced. In this aspect lies the rationalization of this thesis. It is intended to look at phosphorus bonded to a series of different types of ligands and in different combinations of these ligands. One series of compounds is of the type $Ni\,/\!\!-S_2P(R)_2-\!\!/_2$, where R may be an alkyl or alkoxy group, and the arrangement about the phosphorus atom is approximately tetrahedral. In order to interpret the bonding in these compounds, it appeared necessary first to understand completely the nature of phosphorus bonding; this was envisioned to be accomplished by the investigation of a series of simple phosphorus salts of the type PO_4^{-3}, HPO_3^{-2}, $H_2PO_2^-$, where phosphorus is bonded to one or two different ligand types in an approximately tetrahedral arrangement. The $H_2PO_2^-$ was thought to be of particular advantage in the study of the $Ni\,/\!\!-S_2P(R)_2-\!\!/_2$ compounds.

A complete study of bonding appeared to require the consideration of all electronic transitions since each spectral series contains unique information. Most authors have investigated only the K or L spectral series giving an incomplete picture of the bonding. Andermann and Whitehead[12] were the first to consider the K and L spectra together with the core photoelectron spectra for a series of chlorine and sulfur oxy-anions. Their results raised many interesting aspects that appeared to require further investigation but demonstrated clearly the need for simultaneous evaluation of $K\beta$ and $L_{2,3}$ spectra.

This work, thus, involves three specific areas:

(1) the evaluation of the bonding in phosphorus compounds, in general, by means of photon spectroscopy and application of molecular orbital concepts with specific concern to the effects of a second ligand type;

(2) the simultaneous evaluation of the $K\beta$ and $L_{2,3}$ spectra for these compounds, along with the determination of the corresponding molecular levels; and

(3) the use of the concepts developed above for a series of "simple" phosphorus compounds as applied to a series of more sophisticated compounds of the type $Ni\left[S_2P(R)_2\right]_2$.

CHAPTER II

Theory

As mentioned previously, it was the development of the application of molecular orbital methods that revived interest in x-ray spectroscopy as a tool for electronic studies. Appendix C gives a brief description of the molecular orbital approach to bonding with an appropriate example. This section discusses the relevance of molecular orbital concepts to x-ray photon emission spectroscopy as a guide to the interpretation of the experimental results given in Chapter IV. Below, a brief description is provided of the x-ray photon emission process as viewed from various models.

X-rays are emitted[24] when inner shell vacancies are filled by electron transitions from outer shell orbitals. This process is shown diagrammatically in Figure 1 for the K and L spectral series of an isolated atom. The energy, $h\nu$, of the emitted photon corresponds to the difference in the energy between the two states; i.e., $h\nu = E_1 - E_2$.

The opposite process, x-ray absorption, results[24] when an inner shell electron is excited to one of the empty valence orbitals, as indicated in Figure 2. X-ray emission and absorption spectroscopy together are capable of locating both filled and empty valence orbitals.

In molecules the valence orbitals are directly involved in bond formation, producing a new set of energy levels from which transitions are possible. Two theories have been offered to explain the resulting x-ray spectra.

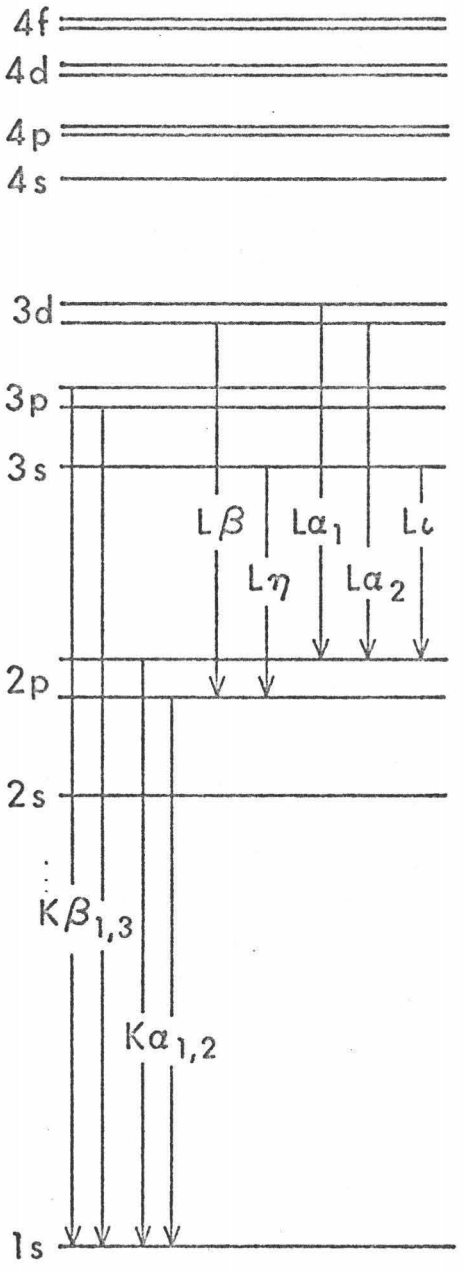

Figure 1

K and L Emission

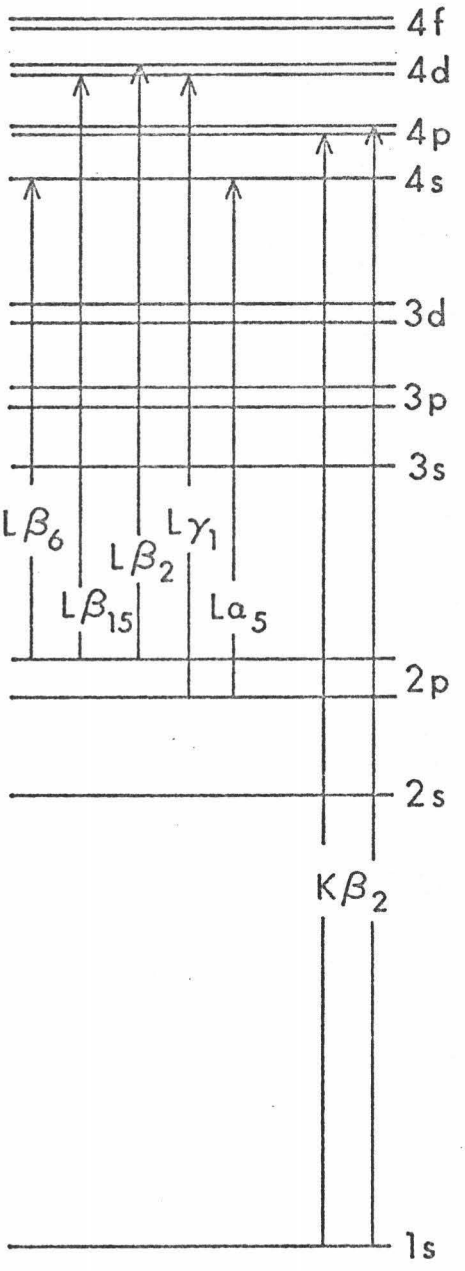

Figure 2

K and L Absorption

According to valence band theory,[25] the bonding orbitals comprise a delocalized valence band of varying electron charge density. Ignoring selection rules, the resulting transitions then represent a density of states for the valence band. The energy level diagram for this model is shown in Figure 3. This model may be appropriate for bonding situations in which each atom is bonded to many other atoms in a truly delocalized lattice, for example, in a semiconductor such as silicon.

Molecular orbital theory, on the other hand, proposes a set of discrete energy levels resulting from atomic interactions of "nearest neighbors" as representing the valence electron charge density.[26] This situation is shown for a molecule of T_d symmetry in Figure 4. Representative of this model are chemical compounds in which certain atoms are directly bonded together into a discrete entity which has little interaction with other such species. This network of strong and weak bonding results in an essentially isolated molecule giving sharp spectral lines as compared to the broad-band spectra for the valence band model.

In the aforementioned diagrams, transitions to inner levels are shown as arising from certain selected outer orbitals, indicating the transition probabilities governing x-ray transitions. For the isolated-atom model under the Russell-Saunders coupling scheme, electric dipole transitions are allowed[27] only when the changes in quantum numbers in changing states obey the following conditions:

$$\Delta L = \pm 1, \Delta J = 0 \text{ or } \pm 1$$

where L is the resultant orbital momentum for the atom produced by the coupling of electron's individual angular momentum, and J is the resultant total angular momentum produced by coupling of the resultant orbital (L) and spin (S) momenta.

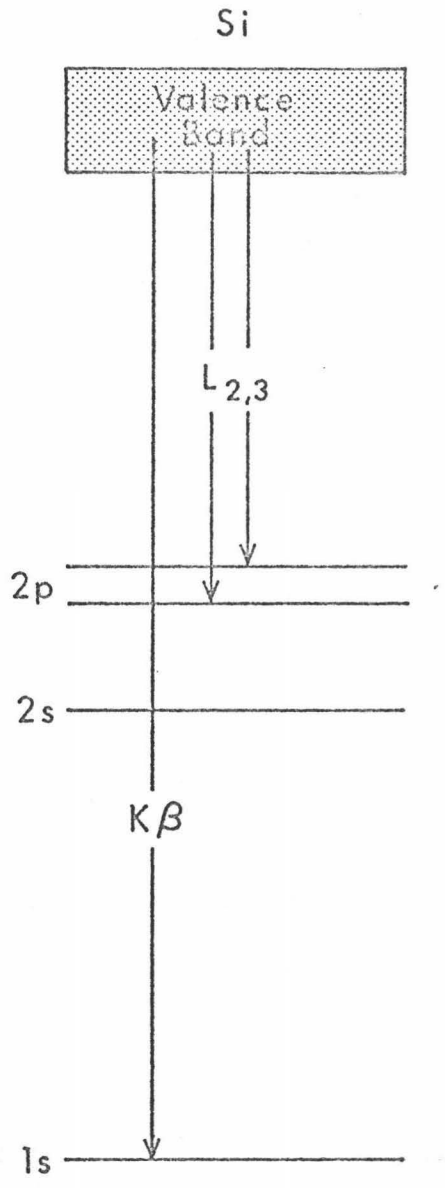

Figure 3

Valence Band Model

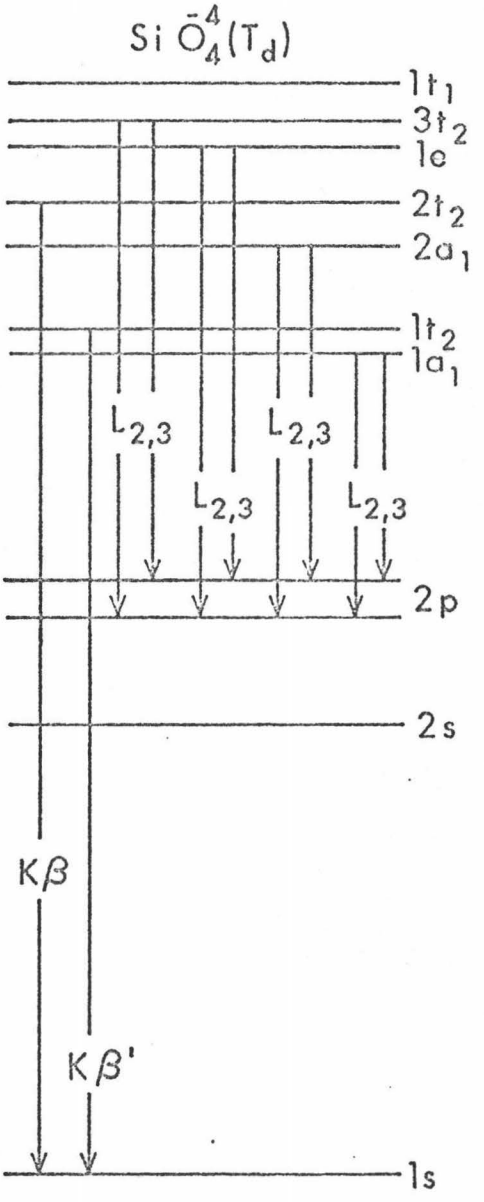

Figure 4

Molecular Orbital Model

Therefore K spectra arise from p ⟶ s transitions whereas L spectra represent s ⟶ p or d ⟶ p changes. The ability to so distinguish electrons of different symmetries due to their spatial selectivity gives x-ray spectroscopy particular advantage over photoelectron spectroscopy.[3]

Furthermore, the essentially atomic nature of the inner level offers x-ray spectroscopy as a viable and superior alternative to u.v. absorption spectroscopy. For solids the interpretation of u.v. absorption spectra is hindered by the numerous possible states to which the valence electron may be excited. Along with the inherently low resolution, mentioned previously, this makes the assignment of transitions difficult. Solution work offers no alternative, as solvent-solute interactions prohibit an accurate description of the excited, as well as, the ground state.[28] Also, possible charge transfer transitions from solute to solvent complicate the resulting spectra and interpretation.

Molecular orbital theory is concerned with the "local environment" of an entity as determined by the specific atoms bonded together in a discrete unit. Application of molecular orbital concepts to photon spectra may then be considered as describing the environment of the emitting atom probed by x-ray spectroscopy. This environment is describable in terms of molecular symmetry. Since the Hamiltonian operator commutes with the symmetry operator, the eigenfunctions for a molecule may form a basis for the irreducible representations of the symmetry group to which the molecule belongs, thereby incorporating group theoretical concepts into the molecular orbital arguments. It is here that the molecular situation, while derived from the linear combination

of atomic orbitals, deviates significantly from the atomic. For example, in an atom, 's' and 'p' orbitals are clearly of two different types; but in the molecule, a group of 's' orbitals arranged tetrahedrally about a central atom are no longer 's' in character. They now transform as an $a_1 + t_2$ group of orbitals and may interact with the 'p' orbitals of the central atom which transform as t_2. It is then possible for 's' orbitals in molecules to participate in transitions which are forbidden atomically. Most importantly, an atomic orbital may contribute to several molecular orbitals of different energies, thus splitting a single characteristic atomic emission line into two or more distinct lines. These molecular transitions are also governed by selection rules reflecting transition probabilities, and thus retain in the molecule the spatial selectivity inherent in the atom.

For photon spectroscopy these selection rules may be derived analogously to u.v. absorption transitions. In order for a transition to be "allowed," the transition matrix element R_{mn} must be of finite magnitude; i.e.:

$$R_{mn} = \langle \Psi_m | \hat{\mu} | \Psi_n \rangle \neq 0 \qquad (1)$$

where Ψ_m is the final state molecular orbital function, Ψ_n the initial state wave function and $\hat{\mu}$ is the electric dipole moment operator. This transition matrix element will only be non-zero if the triple product, represented above, transforms as or contains the totally symmetric representation.[29] But this says nothing of the intensity of an allowed transition which is determined by the squares of the atomic coefficients comprising the molecular orbitals. According to Manne,[30] the intensity for the molecular situation is derived analogously to the atomic; for a

dipole allowed transition the spontaneous emission probability, I, is related to the transition energy, E, and the transition moment, R_{mn}, through:

$$I \sim E^3/R_{mn}/^2 \qquad (2)$$

where $R_{mn} = \langle \Psi_m / \sum_i e\vec{r}_i / \Psi_n \rangle$, and $\hat{\mu} = \sum e\vec{r}_i$, where $\vec{r}_i$ is the electric dipole vector.

These wave functions are approximated by the molecular orbital wave functions for the ground state of the neutral molecule each with one electron missing. Under this condition, R_{mn} reduces to the one electron dipole matrix element between the two vacated molecular orbitals. For Kβ one of these is the central atom 1s orbital and the other is the delocalized molecular orbital Ψ_i, which is expressed in terms of the available valence atomic orbitals as:

$$\Psi_i = \sum_K \chi_K C_{Ki} \qquad (3)$$

to give:

$$R_{mn} = \sum_K \langle \chi_{1s} | e\vec{r}_i | \chi_K \rangle C_{Ki} \qquad (4)$$

In summation, all but the dominant one-center central atom terms $\langle \chi_{1s} | e\vec{r}_i | \chi_{2p} \rangle$ are neglected; then

$$I \sim \sum_{K=2p} C_{Ki}^2 \qquad (5)$$

i.e., the relative emission probability will depend only on the amount of 'p' character of the central atom in the molecular orbital describing the vacancy in the final state; all other atomic contributions will be negligible. Manne's assignment for Kβ transitions then is on an intensity model; most others have concurred. Andermann and Whitehead,[12] on the other hand, have argued for the possibility of significant contributions from all other atomic orbitals, as well as lattice perturbations,

to explain any unpredictable intensity contour. Their assignment, then, considers a combined scheme of an energy plus an intensity model.

While the intensity problem currently inhibits the full quantitative interpretation of $L_{2,3}$ photon emission lines, it is seen from a detailed evaluation of interpretation of the Kβ spectra, that Kβ transitions will result from molecular orbitals with large 'p' contribution. According to Manne's rules, the $L_{2,3}$ spectra will reflect significant 's' and 'd' character in molecular orbitals, provided that 3d orbital population is high for compounds containing second row elements.

For a molecule of high symmetry, following Manne's arguments, the Kβ and $L_{2,3}$ spectra will exhibit few common features. As the symmetry is lowered there is significant orbital mixing which may result in molecular orbitals capable of producing both K and L transitions and thus mutual spectral features. Andermann and Whitehead[12] have proposed such a model; if:

$$E_i = h\nu - \overline{V}_i \qquad (6)$$

where E_i is the energy of the ith molecular orbital in which a transition originates; $h\nu$ is the photon emission energy which is experimentally determined; and $\overline{V}$ is the binding energy of the inner orbital electron, as determined by photoelectron spectroscopy; then it should be possible to show that:

$$h\nu_k - \overline{V}_k = h\nu_L - \overline{V}_L$$

i.e., for certain transitions:

$$E_i\ (K) = E_i\ (L) \qquad (7)$$

However, any two such mutual transitions will not necessarily be of equal intensity in both spectra, either under Manne's or Andermann's

arguments. For example, band C for ClO_3^- in the $L_{2,3}$ spectrum, as shown in Figure 5, has been attributed by Andermann and Whitehead[12] to an a_1 molecular orbital. This same molecular orbital has been designated by Manne[16] as the origin of band ß in the Kβ spectrum shown in Figure 6. While the band is quite prominent in $L_{2,3}$, it is barely resolvable in Kβ. Determination of any such mutual spectral transitions then necessitates the simultaneous evaluation of Kβ and $L_{2,3}$ spectra.

Molecular orbital concepts are fairly well established for molecules involving atoms of the first periodic row; however, difficulties are encountered when it is assumed that models using simple collections of atomic orbital functions are also applicable to molecules of the second row elements. When this model attempts to incorporate 3d orbitals into the bonding schemes to describe the bonding of penta- and hexa-coordinated structures, the 3d orbitals are found to be so diffuse that overlap with ligand orbitals is negligible. This suggests that either 3d orbitals do not contribute significantly to the bonding or that they are modified drastically in a molecular environment to make bonding feasible. This aspect has been reinvestigated by several people recently[31,32,33,34,35,36,37] leading to the possible involvement of 3d orbitals in the bonding on two factors: the number of 'd' orbitals in the bonding configuration and the magnitude of formal charge induced on the central atom. This evidence is qualitative and argumentative. However, more recent work has presented quantitative evidence for inclusion of 3d orbitals in bonding. Hillier and Saunders[38] have found molecular properties consistent with experiment and over-all decreases in molecular energy as a result of ab initio SCF calculations on a series of second row molecules. Also Boyd and Lipscomb[21]

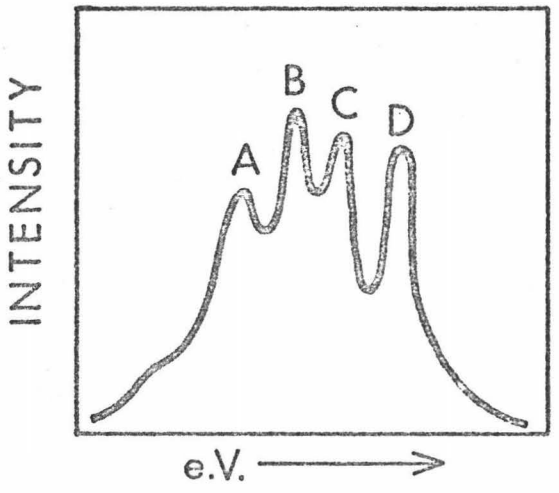

Figure 5

Cl $L_{2,3}$ Emission Spectrum for ClO_3^-

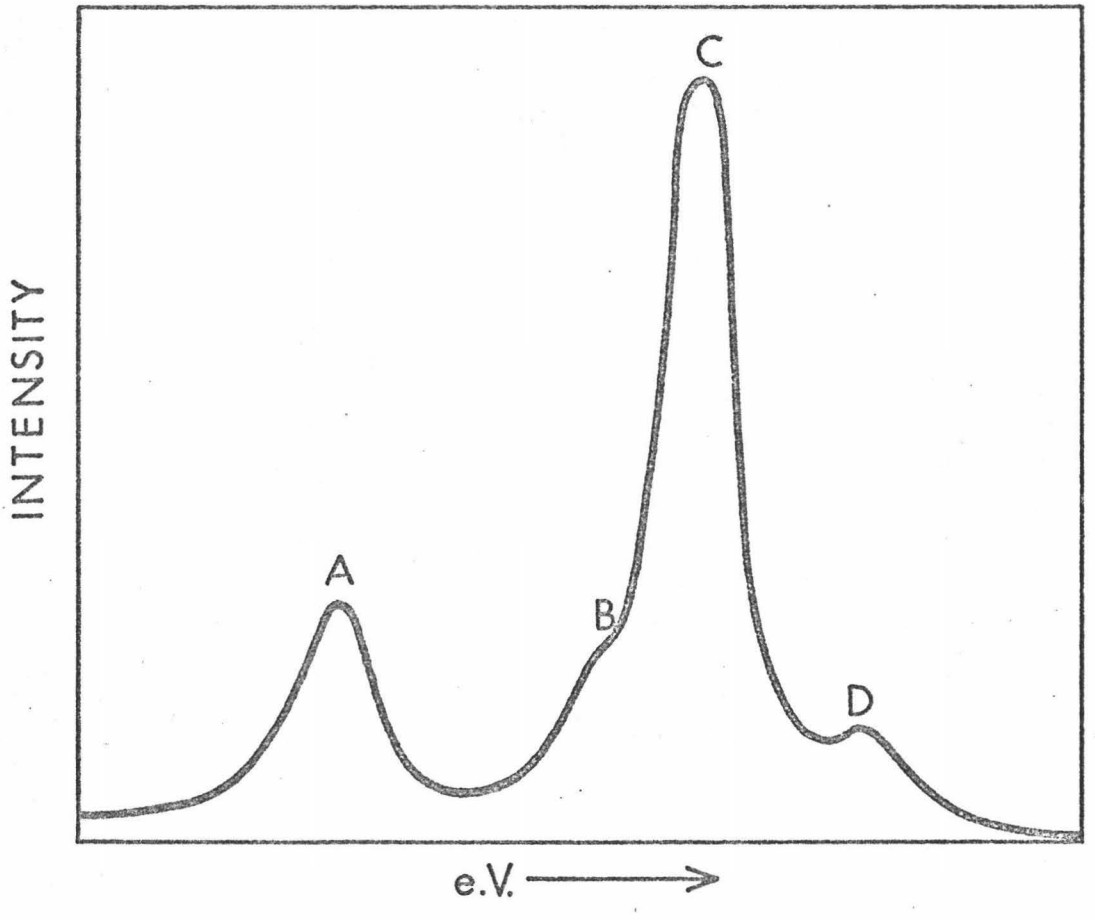

Figure 6

Cl Kβ Spectrum for ClO_3^-

have indicated large 3d orbital contribution to the hypothetical PO_2^- as a result of rigorous calculations. Thus the correlation of theoretical calculations with observation is better when 3d orbitals are included, it being necessary to include them in order to obtain results comparable with the few ab initio calculations available.[34,36,38]

In the above discussion it has been shown that, for the most part, computational and experimental considerations have been extended to simple bonding situations in which all ligand atoms are of the same type. The more general bonding scheme, however, may involve a combination of different ligand atoms. Each of these ligands may interact with the central atom in its own unique manner and may further interact with one another to produce a set of energy levels significantly different from that for the unsubstituted molecule. It is the main intent of this thesis to consider exactly these sorts of problems.

Manne[16] has investigated such a situation for SO_3F^- and predicts three additional energy levels to those for SO_3^{-2}; but since the experimental spectrum does not split out these levels, he attaches no significance to the location of the additional levels. He further finds a significant decrease in all the energy levels over that for SO_3^{-2} or SO_4^{-2}. This is the only example available correlating molecular orbital calculations with x-ray emission data for evaluation of different ligands on a central atom. More complex systems may exist, of course, depending upon the size of the ligand substituted and the difference between the bonding ligands. For example, if oxygen in PO_4^{-3} is replaced by sulfur to give $PS_2O_2^{-2}$, d orbitals may be available in both phosphorus and sulfur adding to the basis set that must be considered.

A more subtle change in bonding may occur with a less drastic change in ligand. For example, if PO_4^{-3} is converted to $PO_3(OH)^{-2}$, crystallographic data[39] suggests that there are two different phosphorus-oxygen bonds formed and, therefore, two different ligands are present.

The concepts discussed here have been used as basic tools to interpret trends in experimental results. A truly quantitative evaluation of bonding is beyond the scope of this thesis, but experimental work should provide material to evaluate existing concepts. In this respect, Hillier and Saunders,[38,17] while predicting significant 3d orbital contribution from rigorous calculations, have investigated photoelectron and x-ray emission spectra[17] for experimental evidences of their calculations. It is experimental interpretation that evaluates quantitative predictions. This is the purpose here, to look for experimental evidence for effects of changing ligand or for 3d orbital participation on the basis of previously developed molecular orbital concepts.

CHAPTER III

Experimental

In this section the instrumental features of the double-crystal x-ray spectrometer, as modified for phosphorus evaluation, will be discussed in detail before summarizing the instrumental operating conditions and sample preparation.

The spectrometer available to this lab was a Norelco vacuum single-crystal spectrometer which, with a PET (002) crystal, and 0.020 inch x 4 inch collimation of the beam incident upon the crystal, and 0.010 inch x 5/8 inch collimation of the reflected beam, gave a resolving power of 350, as shown in Figure 7 for second order Mn $K\alpha_{1,2}$. Figure 8 shows a representative single-crystal scan for one of the phosphorus salts, $Ca_3(PO_4)_2$, with a resolving power of 200. It was this kind of low resolution which had precipitated the design of a high resolving double-crystal unit by Whitehead, Layfield, and Andermann.[40] A brief diagrammatical representation and description of this continuously scanning instrument is given in Appendix A. Obtaining high resolution spectra for phosphorus on this instrument proved to be rather complex, as modification of the double-crystal unit into a novel "hybrid spectrometer" was necessary.

The double-crystal unit was designed so as to be attached onto the 2θ arm of the single-crystal mount thereby replacing the detector, as discussed in Appendix A. The instrument was provided with ability for simultaneous scanning of both crystals or for independent rotation of

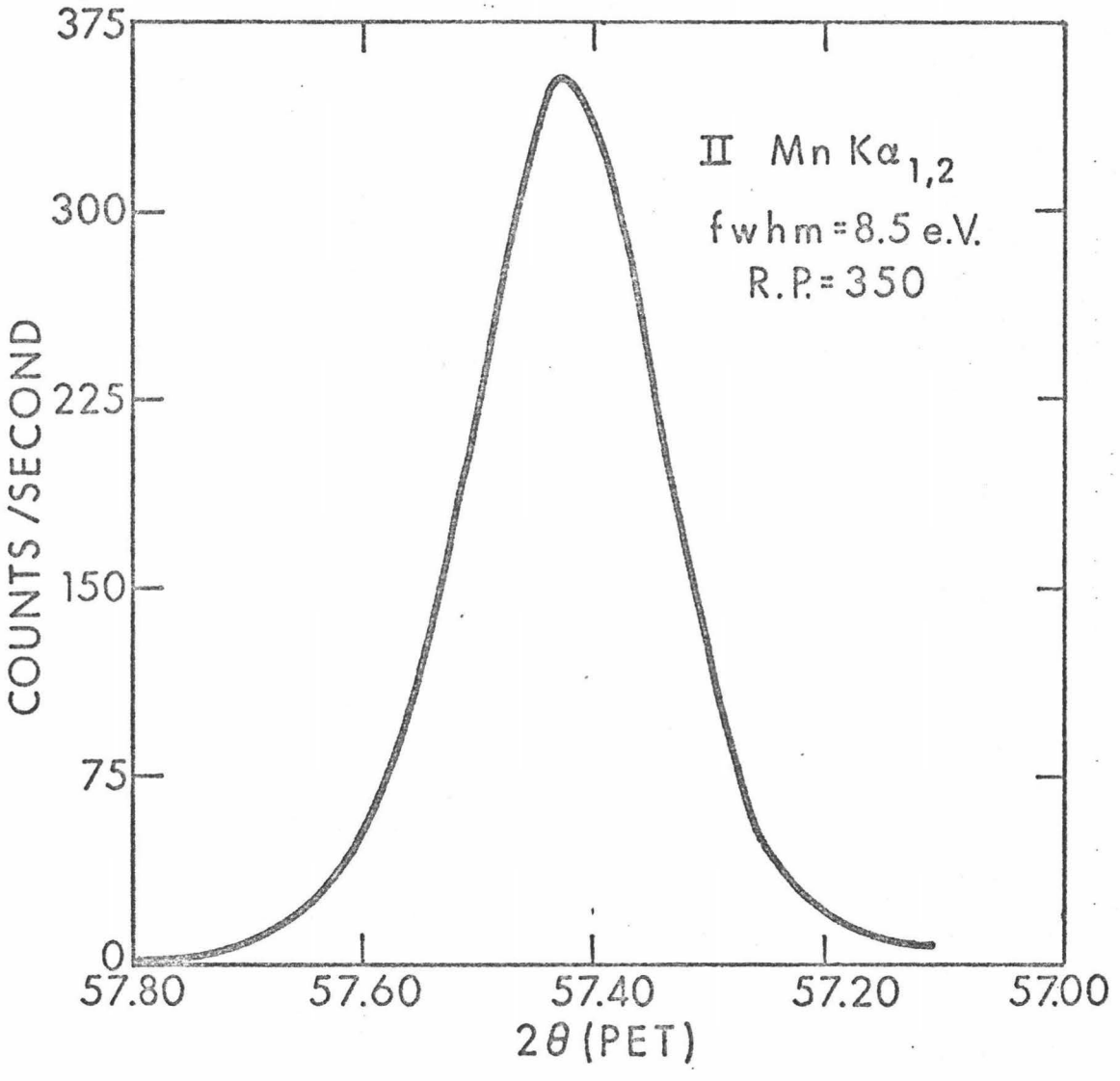

Figure 7

$K\alpha_{1,2}$ Emission Spectrum of Mn Obtained from Single Crystal Scan (PET)

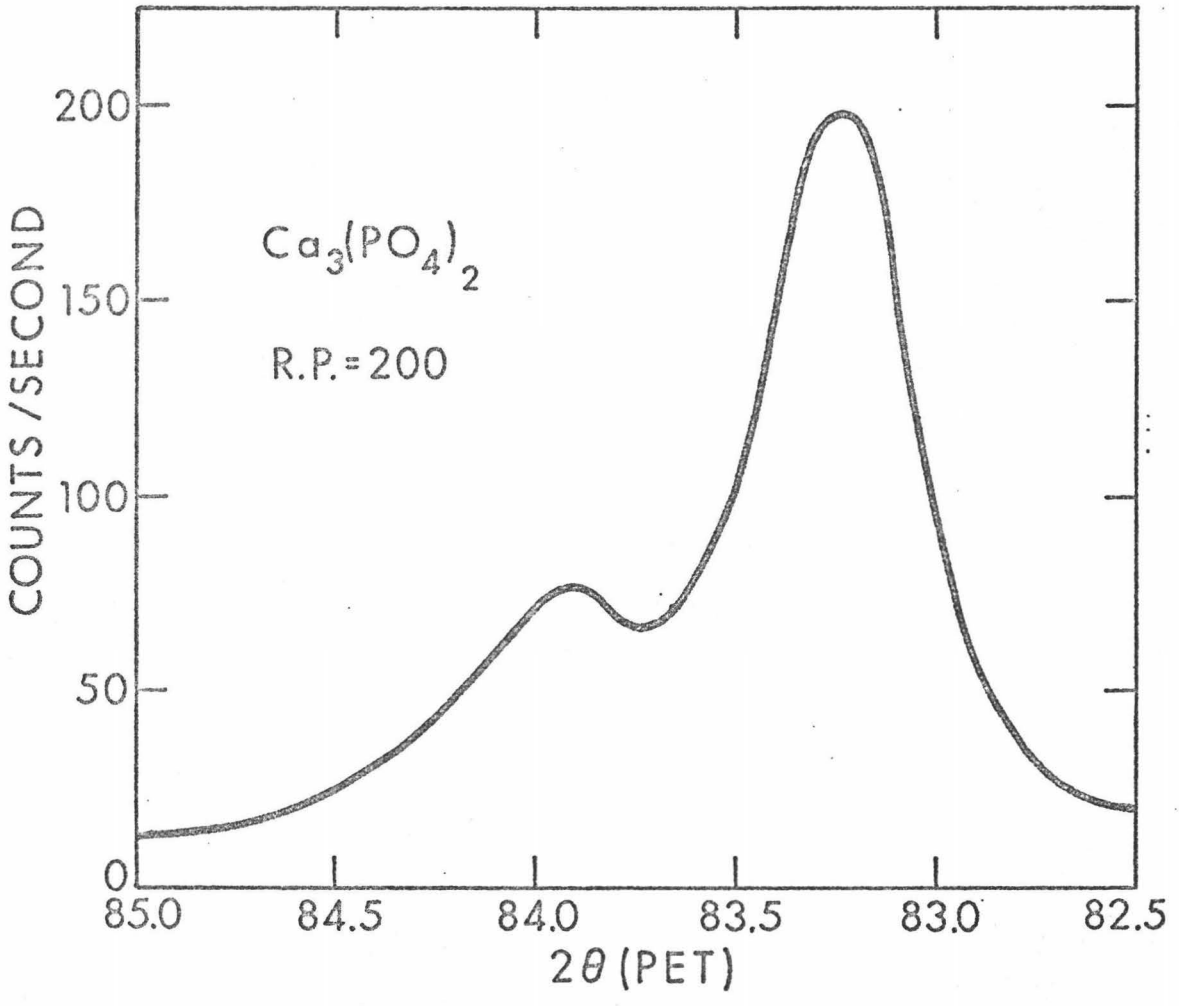

Figure 8

Single Crystal Scan of PKβ
Emission Spectrum for $Ca_3(PO_4)_2$

the second crystal. The first arrangement is more commonly used and is capable of covering a large spectral region while producing a faithful intensity contour. The second arrangement, however, while generally capable of high resolution, covers a very limited spectral region the width of which depends upon the angular spread of the beam incident upon the second crystal. Both methods were investigated here, the results will be discussed below, but first an explanation of the crystal system used is necessary.

Resolution capabilities with a double-crystal spectrometer are highly dependent upon the type of crystals and their physical condition. Whitehead, et al.[40] had previously determined that two calcite crystals were capable of 1 - 2 eV resolution for the soft x-ray region, and it was desired to employ a double calcite crystal system here. Furthermore, calcite's 2d spacing (6.0706 Å) would provide optimum dispersion for phosphorus radiation (5.80 Å). However, mechanical limitations of 116° 2θ on the goniometer prohibited this arrangement. In fact, the long wavelength of phosphorus radiation severely limited the choice of crystals.

Three factors must be considered in the choice of crystals:

1) resolving capabilities

2) reflectivity for maximum intensity

3) a large $\lambda/2d$ value for maximum dispersion.

No one crystal qualified in all three respects for phosphorus, and the two best qualified--quartz and calcite--were eliminated for mechanical reasons; the third choice of two PET crystals fulfilled the second and third requirements fairly well, but the resolution needed to be evaluated. Second order Mn $K\alpha_{1,2}$ and first order P$K\beta$ for NaH_2PO_4 were scanned by

simultaneous rotation of both crystals; the resultant spectra are shown in Figures 9 and 10. Resolving power of about 450 was obtained corresponding to only 5.4 eV resolution for phosphorus which was clearly inappropriate for the work to be done here. Apparently the presence of extensive mosaic structure in PET did not allow good resolution.

Fichter[22] had previously investigated the Kβ spectra for a series of phosphorus salts using a curved quartz-crystal spectrometer with a resolution of 1.5 eV. For comparison with Fichter's work, a resolution of 1.5 to 2.0 eV is needed here.

As already mentioned, independent rotation of the second crystal provides high resolution; this position was thus provided with a calcite crystal while maintaining PET in the first position. Such an arrangement is not so strictly limited by mechanical considerations due to the destruction of the 2:1 geometrical relationship between the two crystals, extending the upper limit of operation to $147^{o}2\theta$. The resulting crystal arrangement is shown diagrammatically in Figure 11b. The alignment of this hybrid spectrometer is similar to that for the normal two-crystal operation. Third order Fe $K\alpha_{1,2}$ radiation was employed for the alignment since its wavelength lies quite close to that for phosphorus Kβ. Since the double crystal unit is attached to the 2θ arm, the detector is placed in the second crystal position, as seen in Figure 11a, and the first crystal is then aligned so as to focus the beam reflected from PET onto the center of rotation of the calcite crystal. The detector is then placed at a position appropriate to the calcite crystal which is now placed on the 2θ arm, as seen in Figure 11b. Further alignment of the second crystal is made by adjustment of the crystal holder support on the 2θ arm and by

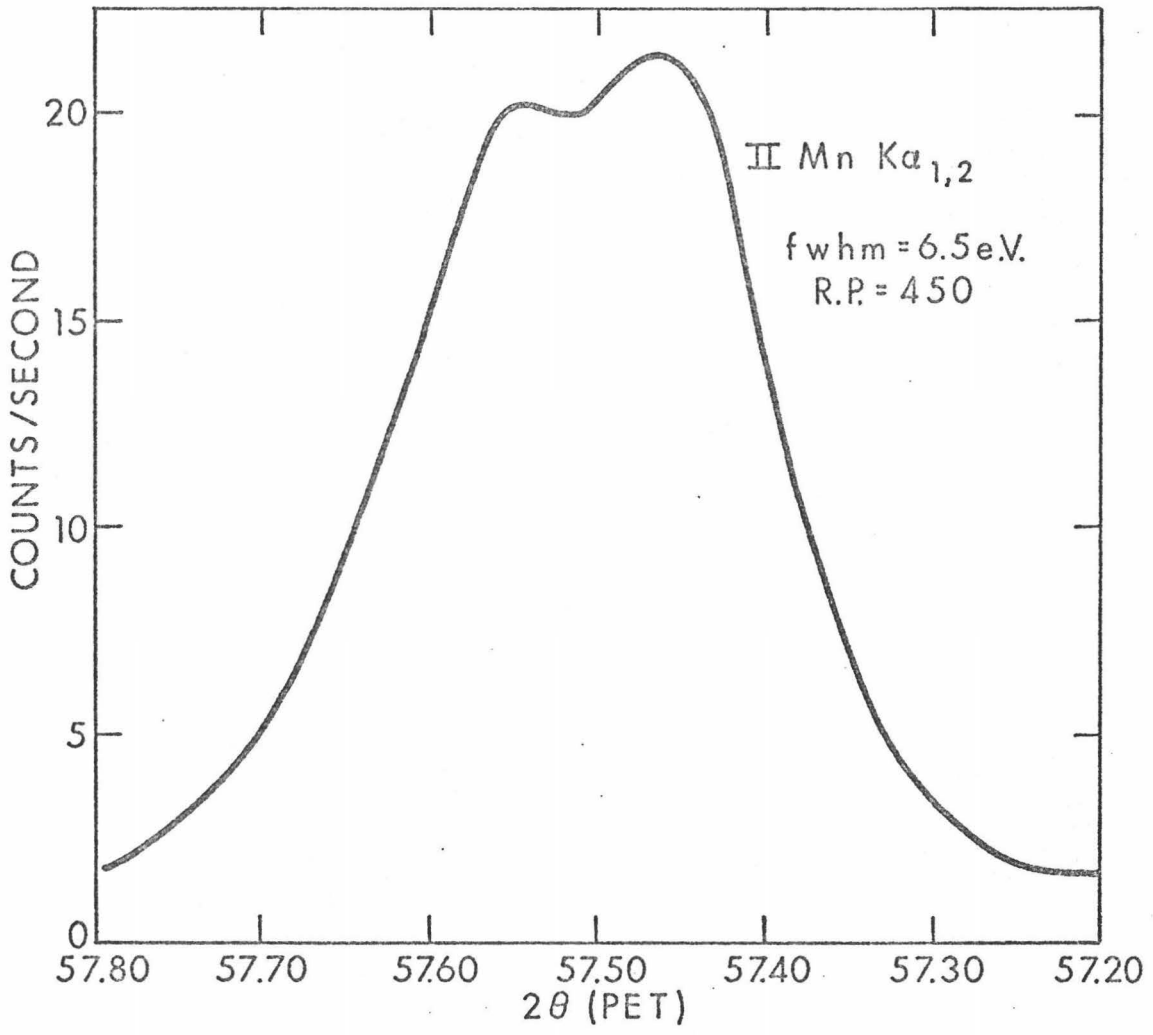

Figure 9

$K\alpha_{1,2}$ Emission Spectrum of Mn Obtained from Double Crystal (PET) Scan

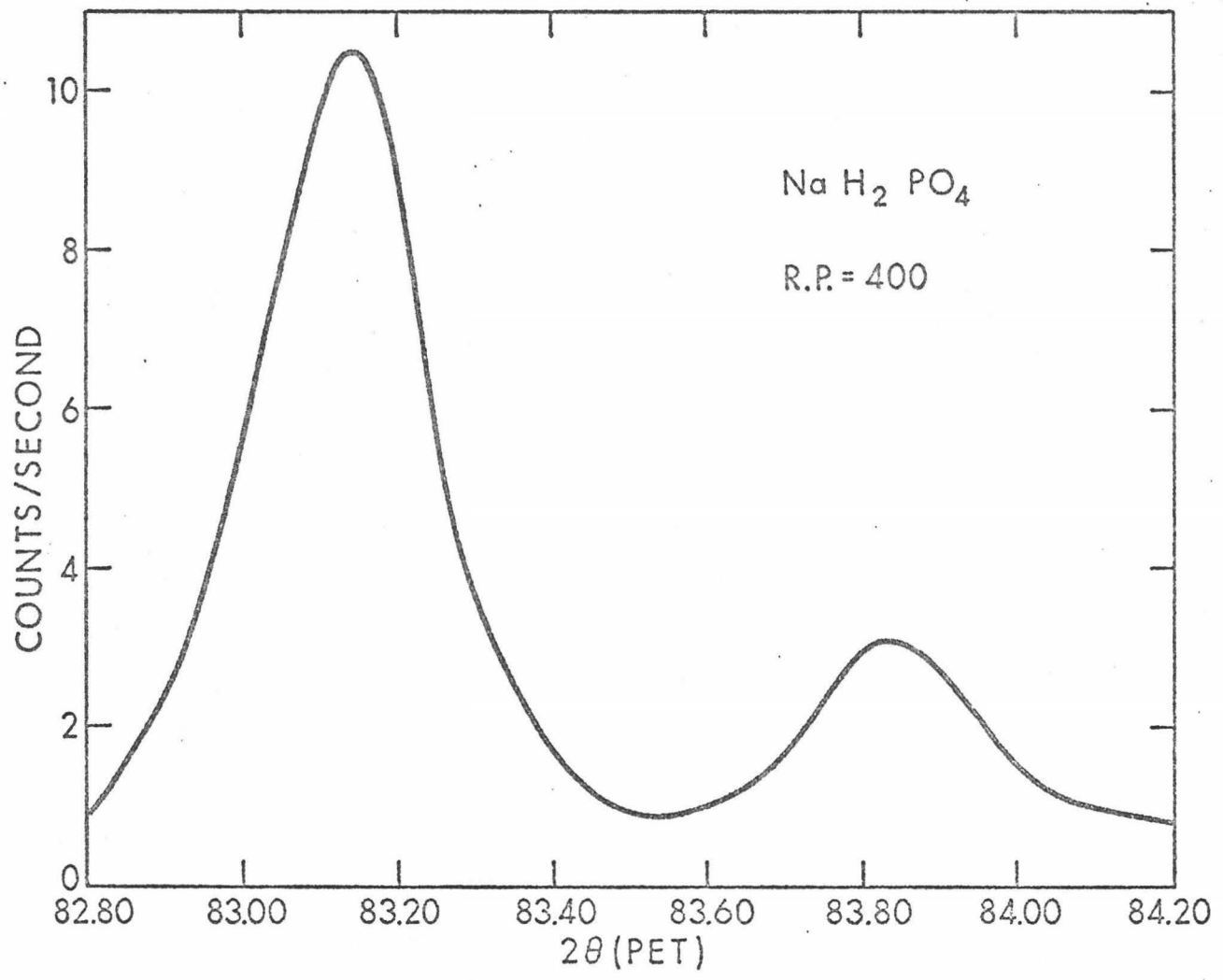

Figure 10

PKβ Emission Spectrum for NaH_2PO_4 Obtained from Double Crystal (PET) Scan

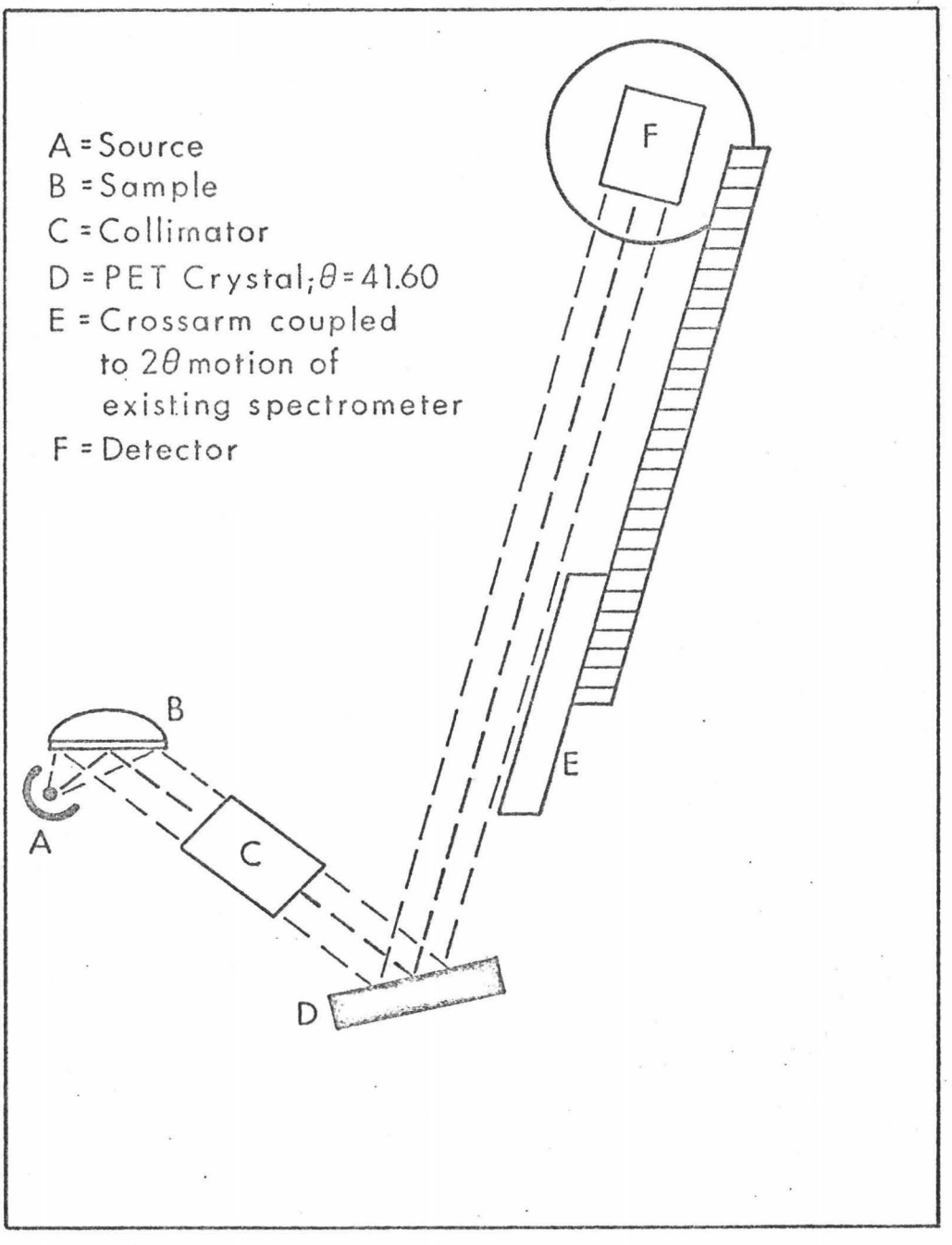

Figure 11a

Alignment of PET With Respect to Center of Rotation of Second Crystal Axis

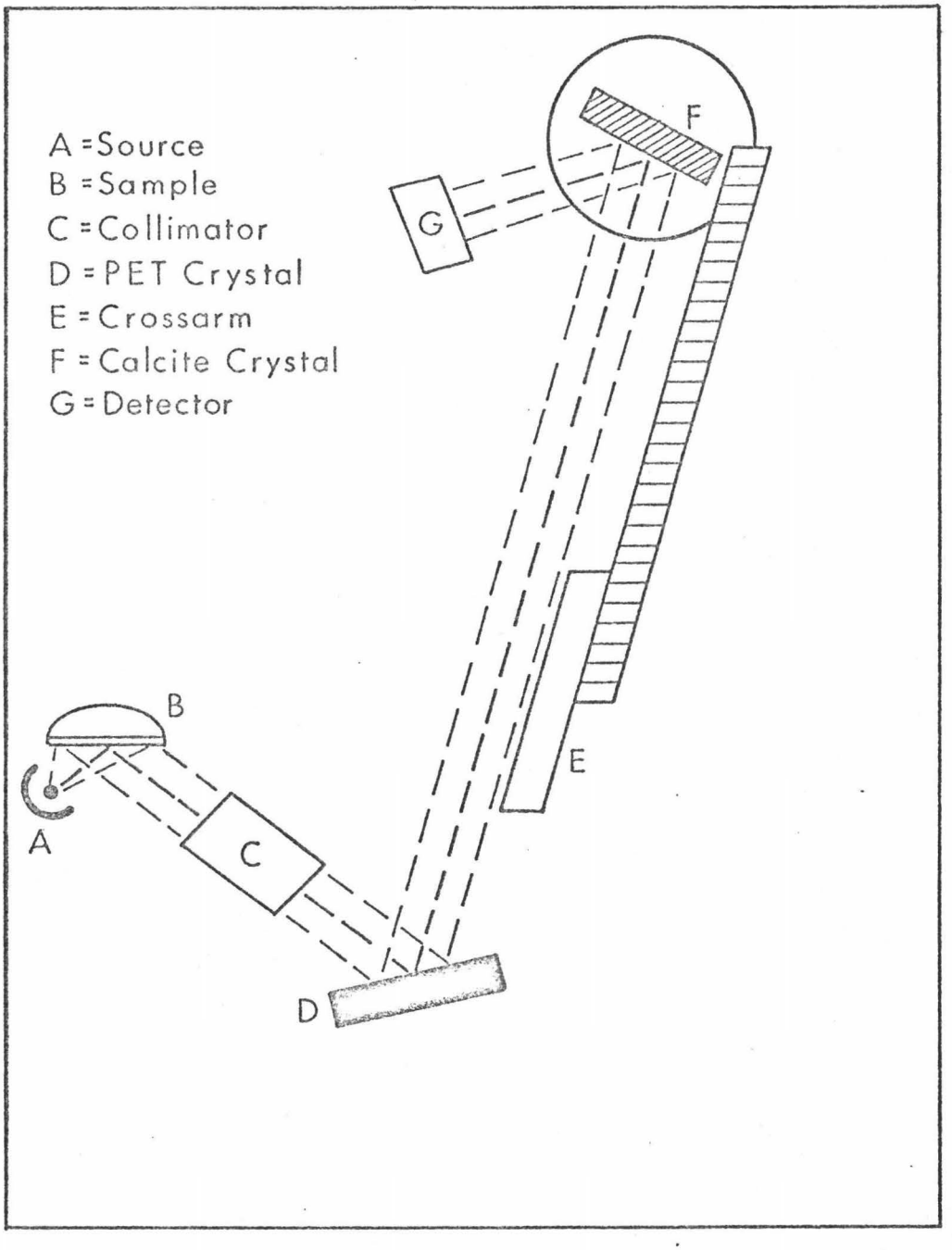

Figure 11b

Alignment of PET-Calcite
"Hybrid Spectrometer"

adjustment of the holder itself. Thus radiation reflected at 41.60°2θ by PET (002) is reflected at 72.83°2θ by calcite (100), a difference of 31.23°2θ over the double PET arrangement.

An evaluation of the double-crystal arrangement was accomplished using second order Mn $K\alpha_{1,2}$ reflected from PET and first order Mn $K\alpha_{1,2}$ reflected from calcite; third order Fe $K\alpha_{1,2}$ was also evaluated. Several scans were made to check the reproducibility, stability, and instrumental variables; the resulting Mn $K\alpha_{1,2}$ spectrum is given in Figure 12. The resolving power increased from 450, for second order Mn $K\alpha_{1,2}$ from the double PET arrangement, to 525 for first order Mn $K\alpha_{1,2}$ from the PET-calcite system. More significant is the resulting spectrum for third order Fe $K\alpha_{1,2}$ which, since its wavelength (5.80 Å) lies closer to that for phosphorus $K\beta$ than does II Mn $K\alpha_{1,2}$ (4.20 Å), should better describe the spectrometer's performance for phosphorus. The spectrum is shown in Figure 13. Figure 14 shows the single PET crystal scan for comparison. A resolving power of 1400 is obtained for the PET-calcite arrangement; peak positions for four successive runs were reproducible within 0.06 eV supplying the necessary resolution and instrumental stability. Also shown in Figure 15 is a spectrum of III Fe $K\alpha_{1,2}$ obtained by simultaneous rotation of both PET and calcite crystals. The resolving power has been decreased to 900 and the intensity contour has been significantly distorted. The independent calcite rotation at fixed settings of the PET crystal clearly offers the best spectral performance for this "hybrid spectrometer."

With sufficient resolution thus available, the spectrometer was applied to phosphorus $K\beta$ studies. Figure 16 is a scan of $Ca_3(PO_4)_2$;

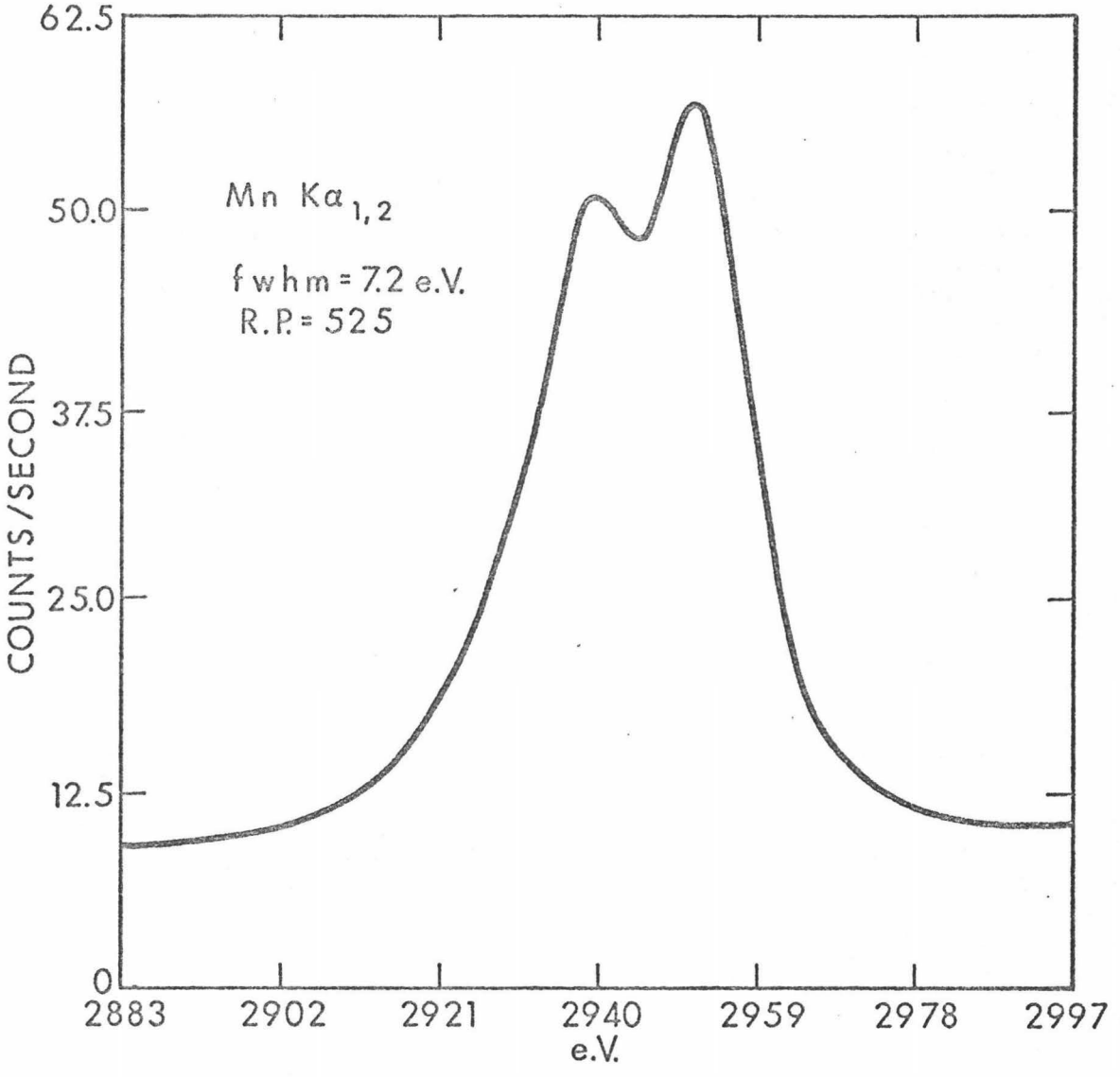

Figure 12

Mn $K\alpha_{1,2}$ Emission Spectrum Obtained from "Hybrid Spectrometer"

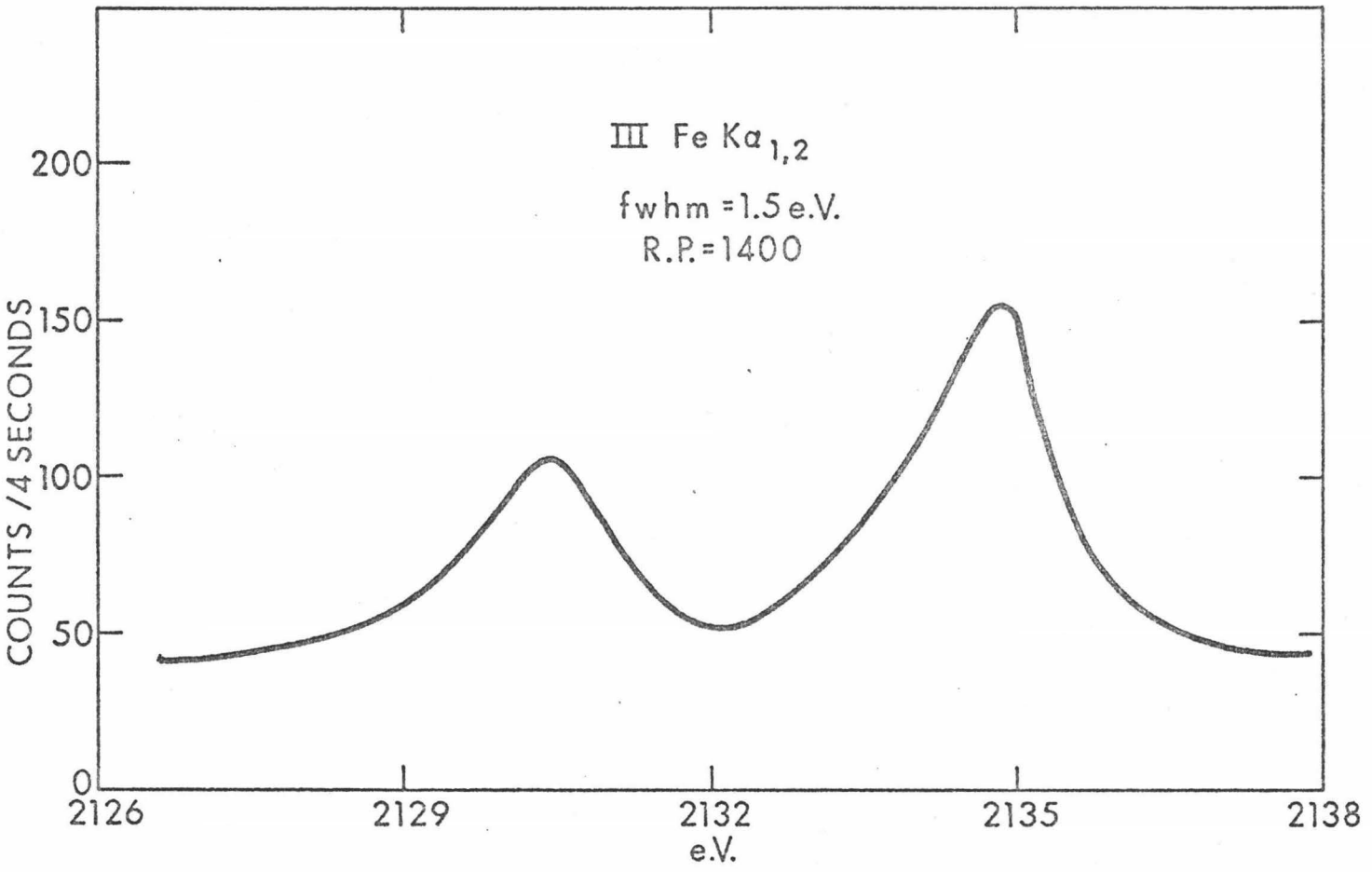

Figure 13

III Fe $K\alpha_{1,2}$ Emission Spectrum Obtained from Hybrid Spectrometer

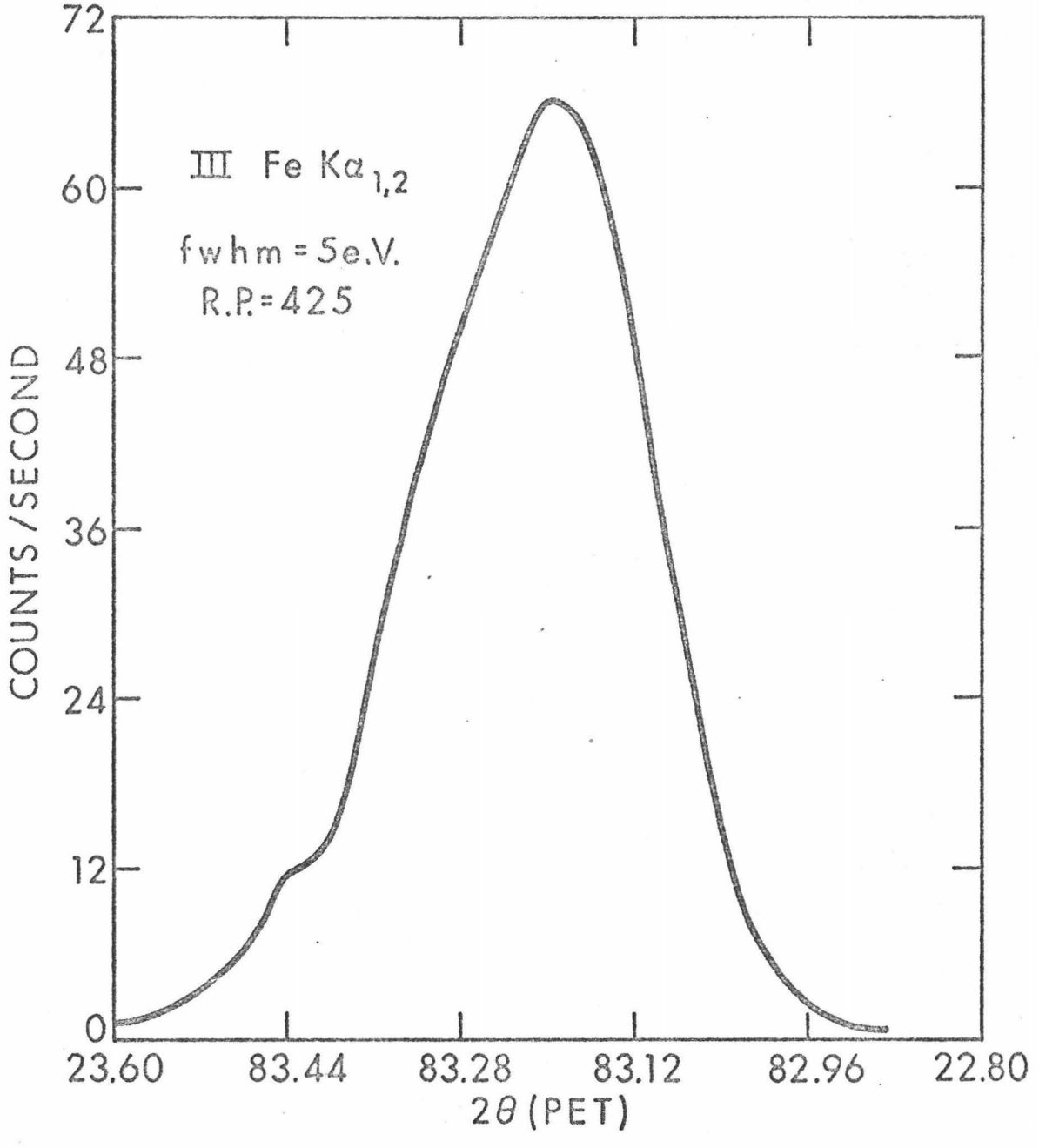

Figure 14

III Fe $K\alpha_{1,2}$ Emission Spectrum from Single Crystal (PET) Scan

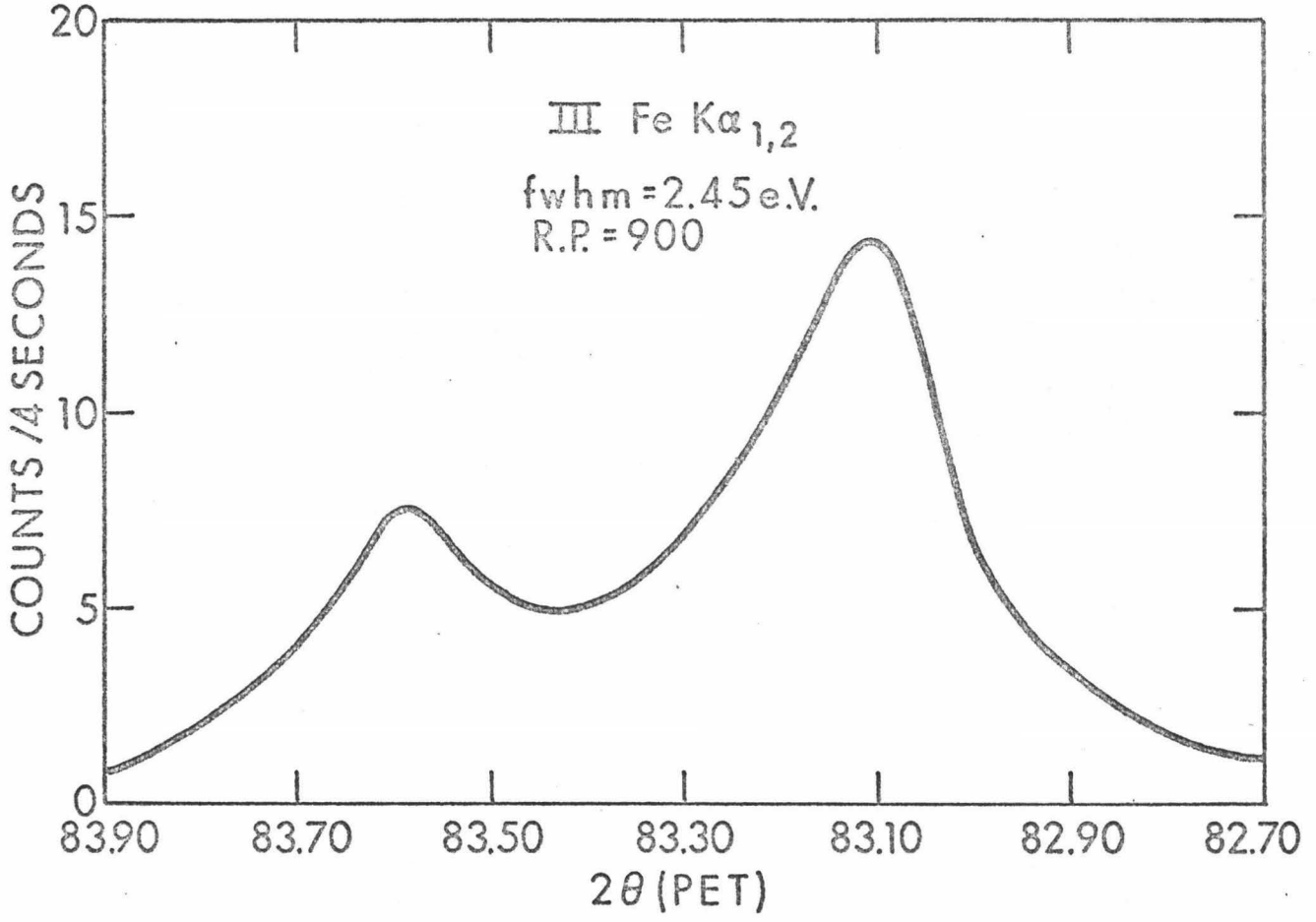

Figure 15

III Fe $K\alpha_{1,2}$ Emission Spectrum;
Simultaneous Rotation of Both Crystals

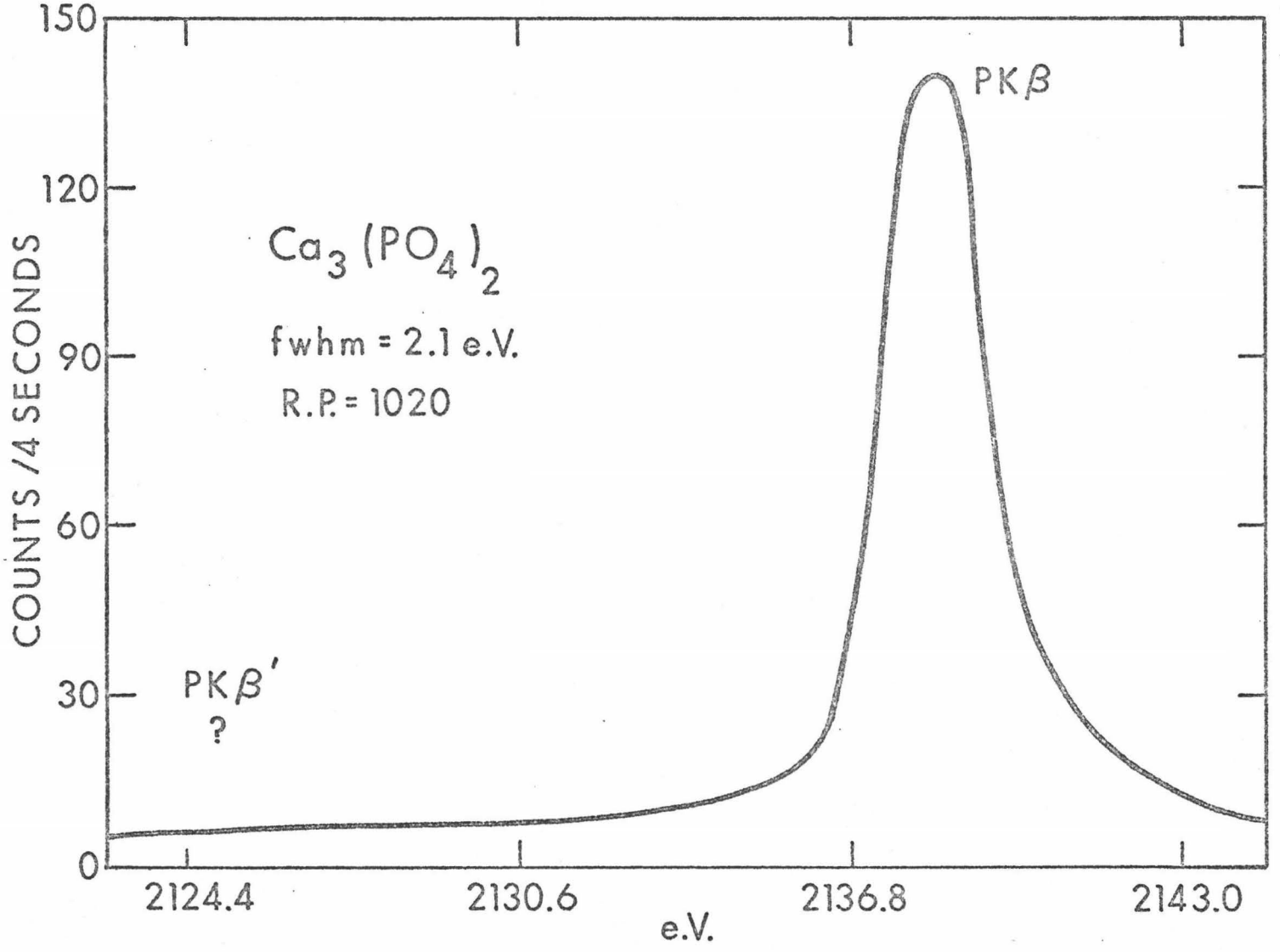

Figure 16

PKβ for $Ca_3(PO_4)_2$ Obtained from "Hybrid Spectrometer" with PET at 83.05°2θ

comparison with Figure 8, while exhibiting superior resolution, indicates that only half of the Kβ spectrum has been covered by the independent second crystal scan--clearly demonstrating the limitation of this method. In order to investigate the full Kβ spectrum it appeared necessary to obtain calcite scans at several settings of PET and then to piece together the resulting normalized sections.

This dependence of the spectral distribution upon the first crystal's setting necessitated an evaluation of the effect of this crystal's properties upon the resulting spectra. Three factors were considered:

1) 2θ setting of the PET crystal

2) mosaic structure of PET

3) collimation of the beam incident upon PET

These were investigated with respect to their effect upon the III Fe $K\alpha_1$ to III Fe $K\alpha_2$ ratio which ideally is 2; therefore, the angular range over which the proper intensity ratio can be obtained represents the extent of a faithful intensity contour for a second crystal scan. The results are shown graphically in Figures 17 to 19; the plateaus represent the angular range for proper intensity contour within about 15 percent deviation. For the first PET crystal studied a range of 0.12^{o} 2θ was obtained which, together with the III Fe $K\alpha_1$ - III Fe $K\alpha_2$ separation of 4.33 eV represents a useful range of 6.5 eV. Outside of this region distortion increases greatly. Therefore, in order to obtain a true representation of the full 20 eV Kα spectrum three settings of PET would be necessary.

In substituting a PET crystal of a more mosaic structure, Figure 18, an angular range of 0.275^{o}2θ corresponding to about 10.0 eV is obtained

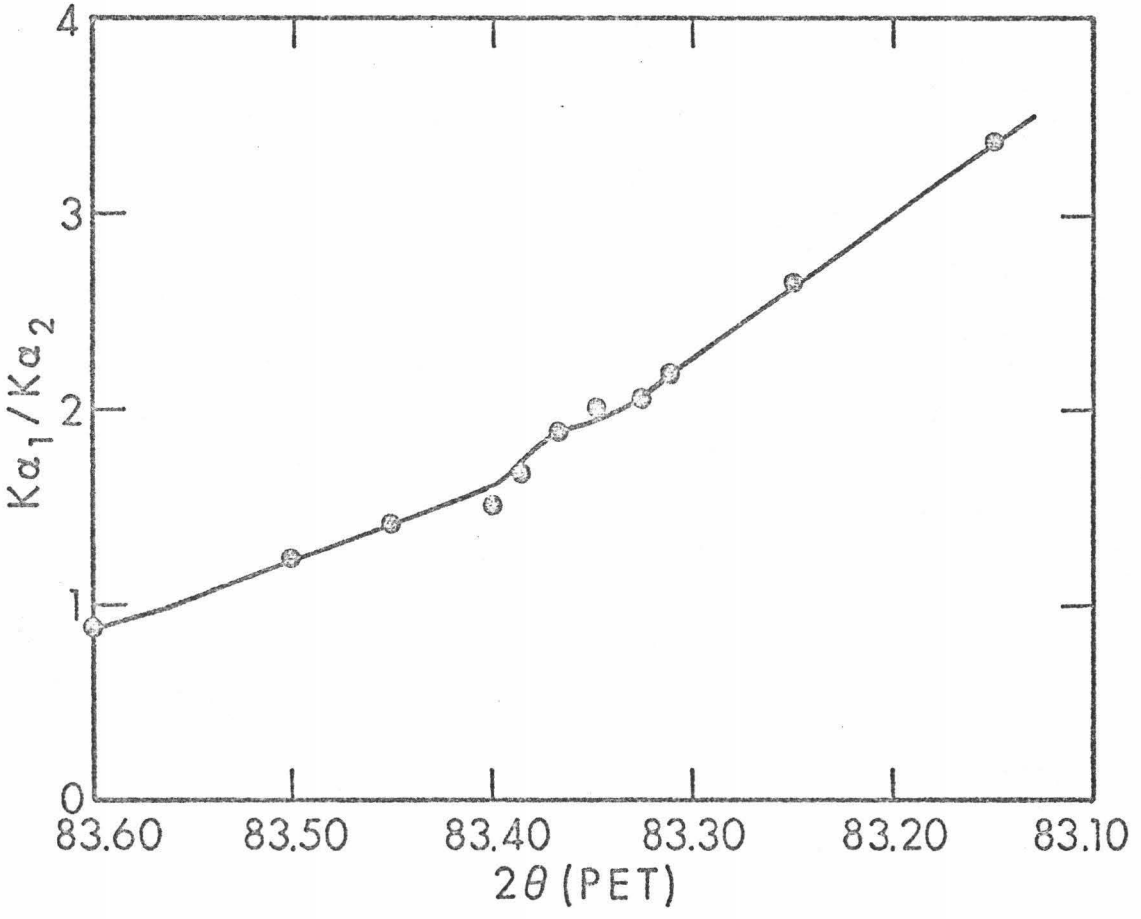

Figure 17

Effect of Coarse Collimation on
III Fe $K\alpha_1$/III Fe $K\alpha_2$; (PET #1)

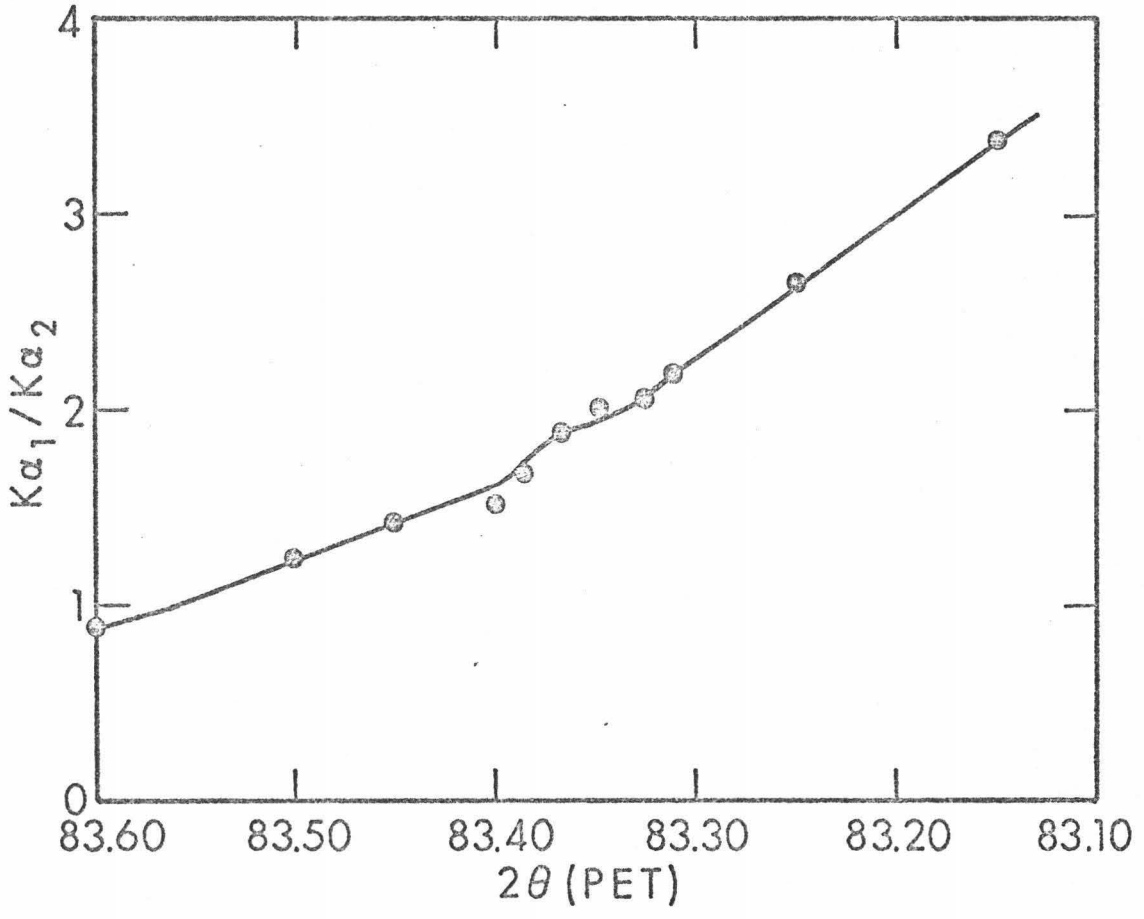

Figure 17

Effect of Coarse Collimation on
III Fe $K\alpha_1$/III Fe $K\alpha_2$; (PET #1)

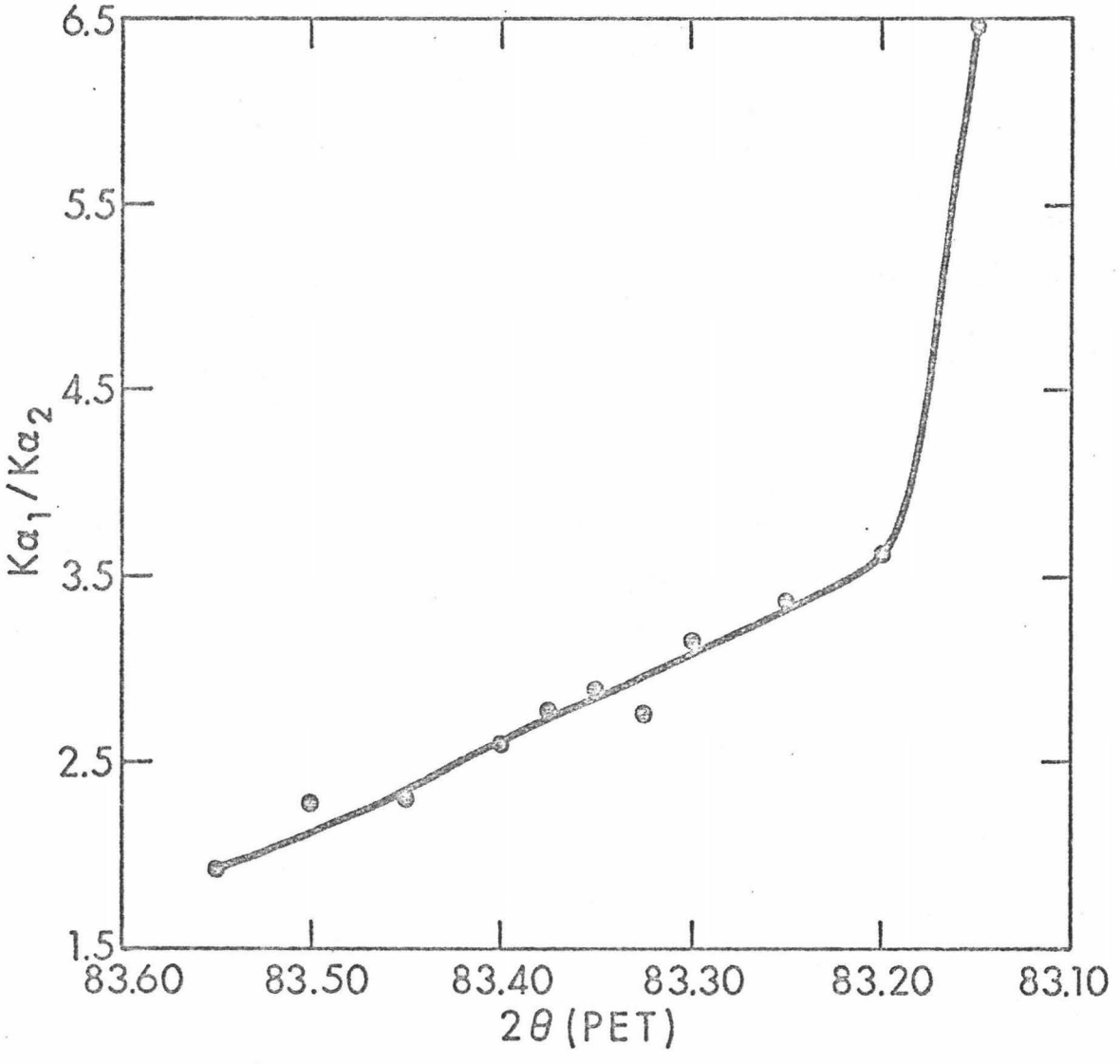

Figure 18

Effect of Mosaic Structure
of PET upon III Fe $K\alpha_1$/III Fe $K\alpha_2$

necessitating two PET settings for a true intensity representation. Therefore, the mosaic structure of the first crystal directly determines the intensity distribution produced by the second crystal and affects the applicability of this hybrid spectrometer.

Figure 19 represents the effects of collimation of the beam incident upon the first crystal; the more "perfect" crystal was used for this investigation. When the 0.020 inch primary collimation was replaced by a 0.005 inch x 4 inch collimator, a decrease from $0.12^{o}2\theta$ to $0.012^{o}2\theta$ in flexibility of setting of the first-crystal results; this corresponds to a 4.5 eV range which would require four settings of the PET crystal for full spectral evaluation. These effects are directly a result of the Bragg equation. The more coarsely collimated beam, being more divergent, contains many different rays which can form the proper Bragg angles with the mosaic structure of the crystal so that there is a range of angular settings over which the crystal may be positioned and still yield a reasonably faithful intensity distribution. As the beam becomes more parallel or the crystal more nearly "perfect," the angular range of the crystal becomes more limited. Fine collimation and a nearly perfect crystal would, therefore, represent the most restrictive situation for this type of hybrid spectrometer arrangement. Obviously, the simultaneous scanning of two identical crystals would not exhibit this distortion as the wavelength range reflected by crystal A forms the proper Bragg angles with the second crystal B without restriction. Increased mosaic structure may decrease the over-all resolution, but would not distort the intensity distribution.

Evaluation of the full phosphorus spectra, therefore, entailed three separate scans of calcite at different settings of PET #1. Although

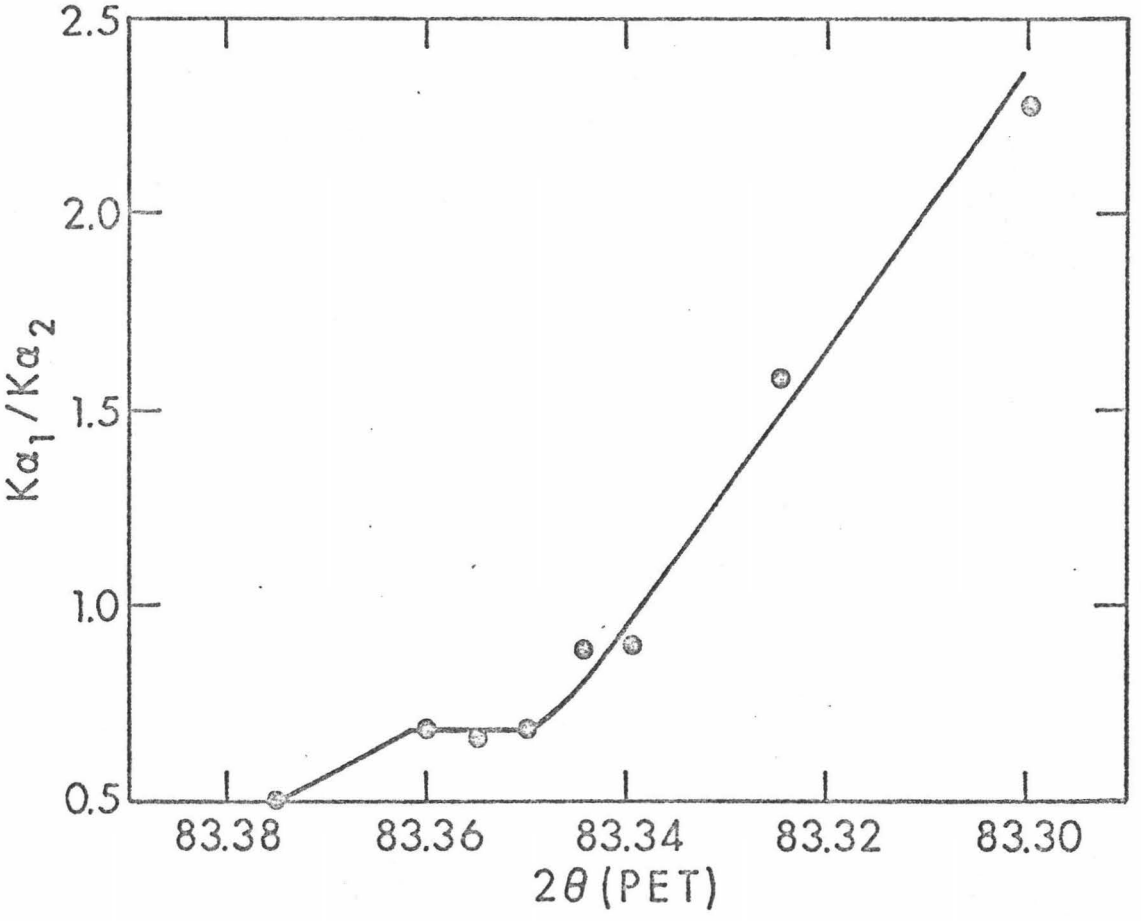

Figure 19

Effect of Fine Collimation on
III Fe $K\alpha_1$/III Fe $K\alpha_2$; (PET #1)

PET #2 gave a larger angular range, it produced considerably lower intensities which could not be afforded. The normalization and combining of the three spectral regions was possible by the scanning of a standard sample as a reference at each setting of the first crystal.

Sample spectra for $Ca(H_2PO_4)_2$ and III Fe $K\alpha_{1,2}$ at each setting of PET are given in Figures 20 to 25; the extent of distortion may be realized from the deviation of the III Fe $K\alpha_1$/III Fe $K\alpha_2$ ratio from the actual value of 2:1.

The normalization processes are discussed fully in Appendix B; a brief discussion is offered here.

The energy scale normalization is necessary due to the independent scan of the second crystal which is rotated by a dial calibrated in units of 12 seconds of arc which must be converted to 2θ values for each crystal used. This conversion was accomplished by standardizing and applying the dispersion relationship to the III Fe $K\alpha_{1,2}$ spectrum for which the Fe emission lines are known exactly.

The dispersion for the antiparallel arrangement is the sum of the dispersions for the two crystals.

$$D = \frac{d\theta}{d\lambda} = \frac{n}{2d_A \, Cos\theta_A} + \frac{n}{2d_B \, Cos\theta_B} \qquad (8)$$

and thus the dispersion increases nonlinearly for increasing angular setting of each crystal. Therefore, the dispersion will change both with setting of the PET crystal and during scanning of calcite. The experimentally determined dispersion is shown graphically in Figure 26 which represents the calcite position as a function of PET setting. It is seen that both III Fe $K\alpha_1$ and III Fe $K\alpha_2$ emission lines change at the same rate and that this change is approximately linear over the range

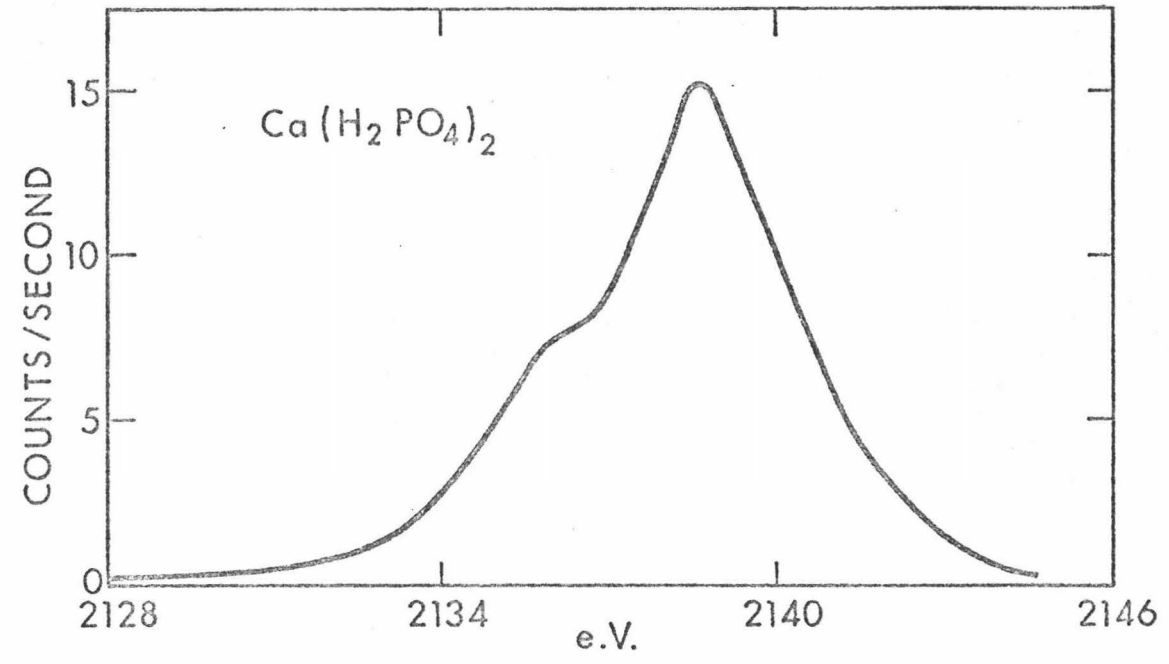

Figure 20

PKβ Spectrum with PET set at 83.05°2θ

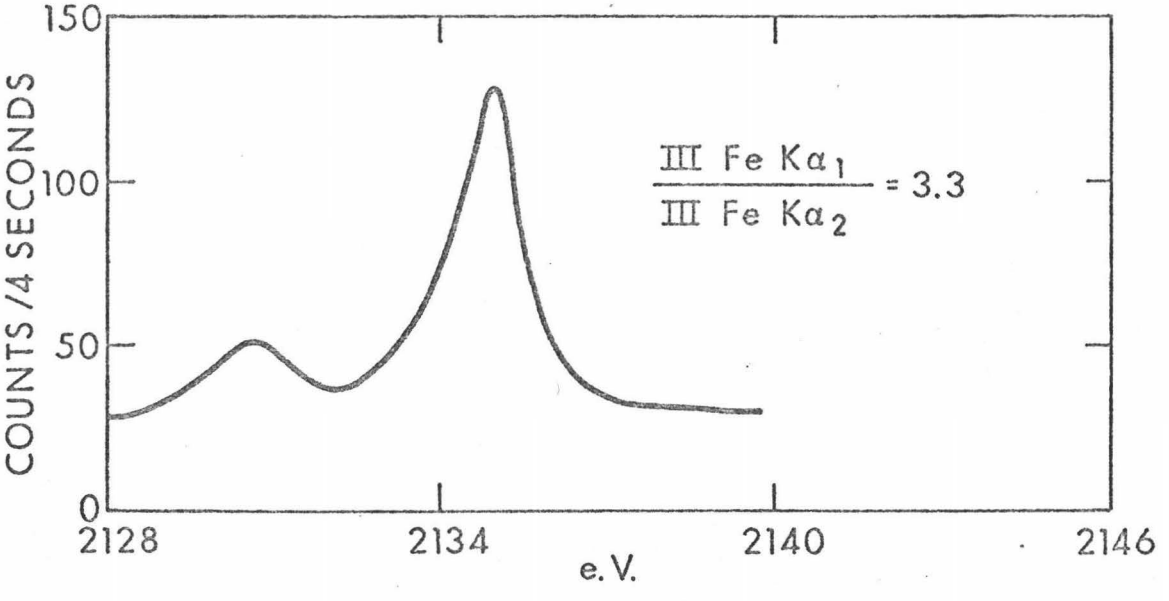

Figure 21

III Fe $K\alpha_{1,2}$ Spectrum with PET set at 83.05°2θ

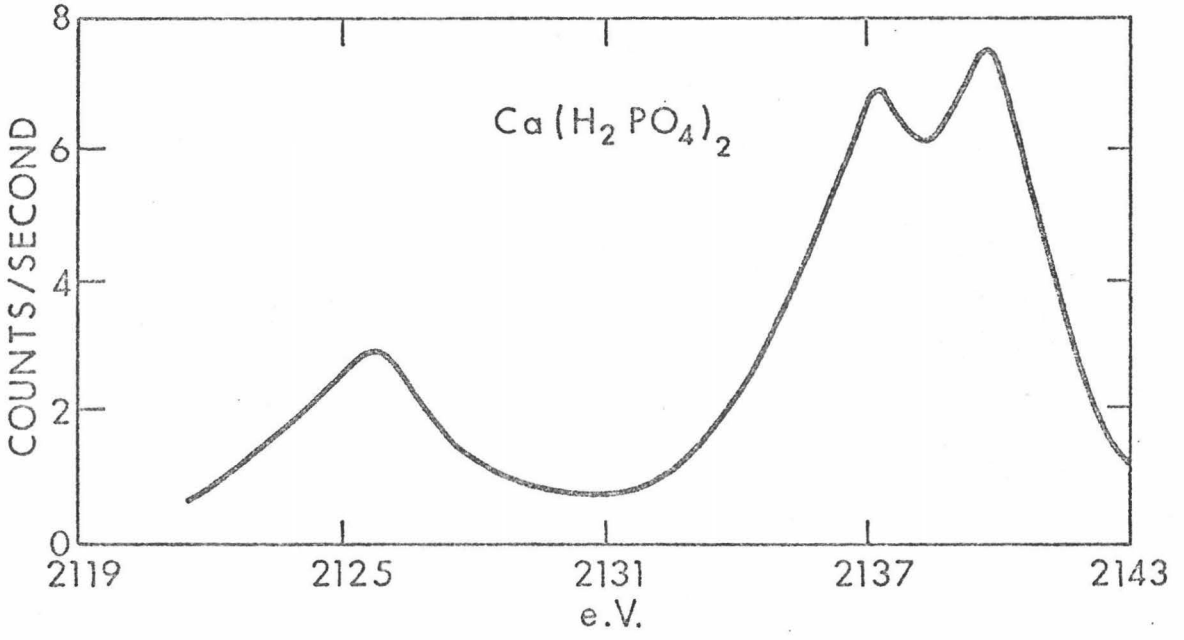

Figure 22

PKβ Spectrum with PET set at 83.40°2θ

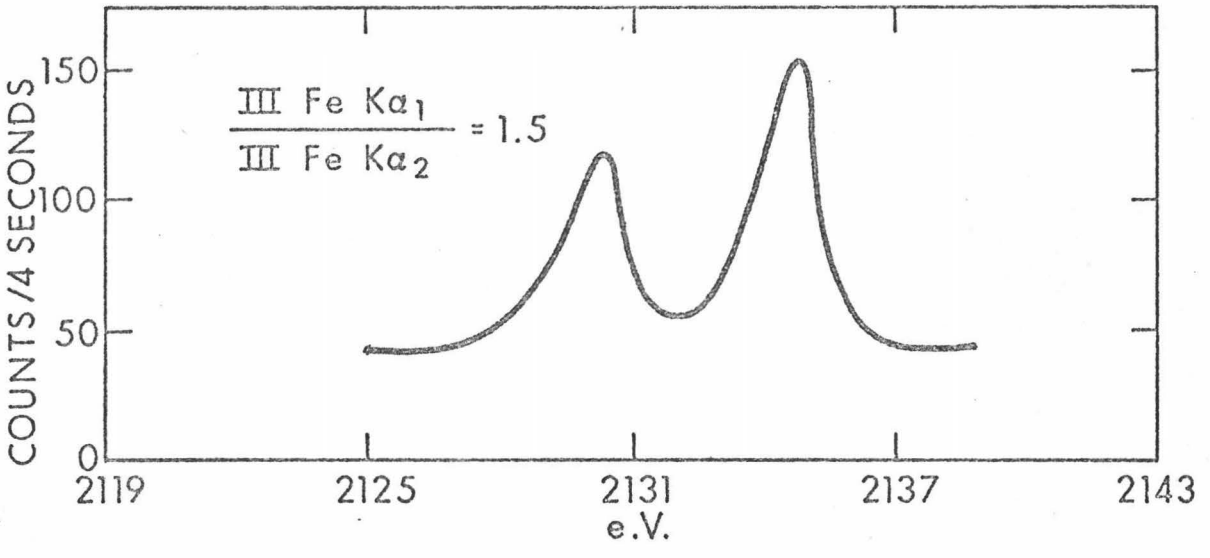

Figure 23

III Fe $K\alpha_{1,2}$ Spectrum with PET set at 83.40°2θ

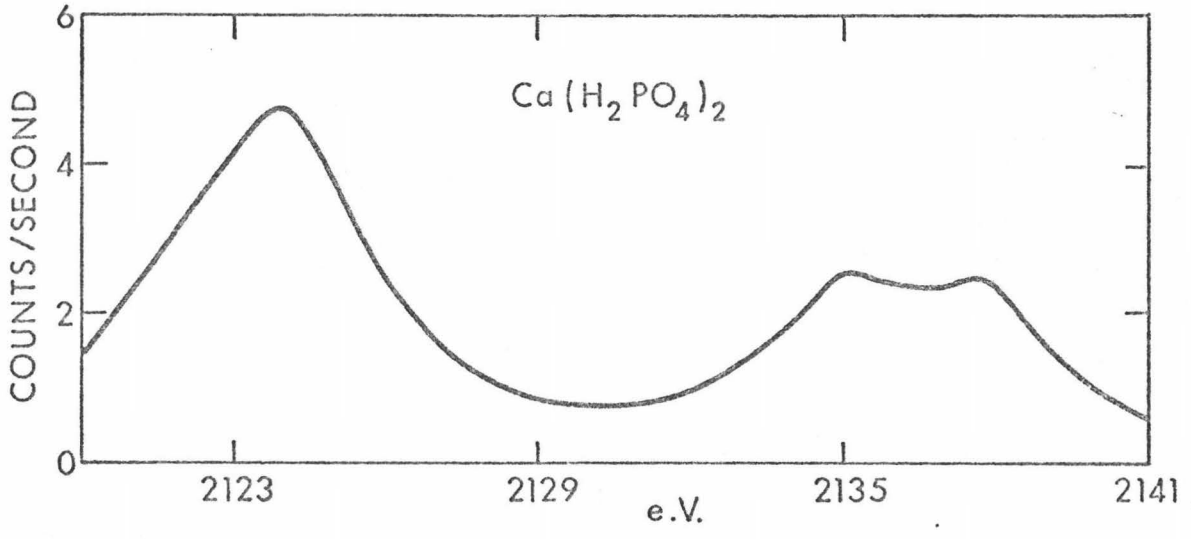

Figure 24

PKβ Spectrum with PET set at 83.60°2θ

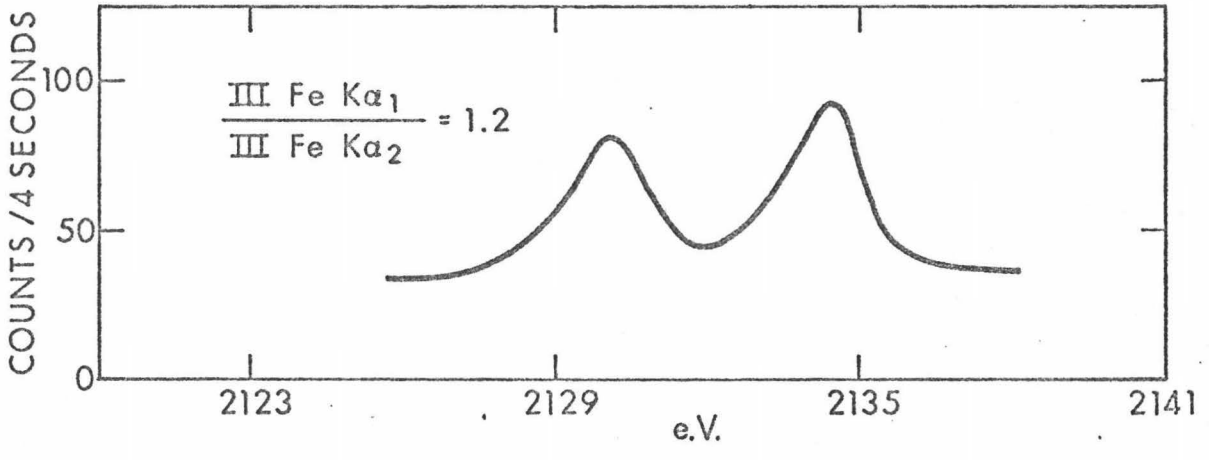

Figure 25

III Fe $K\alpha_{1,2}$ Spectrum with PET set at 83.60°2θ

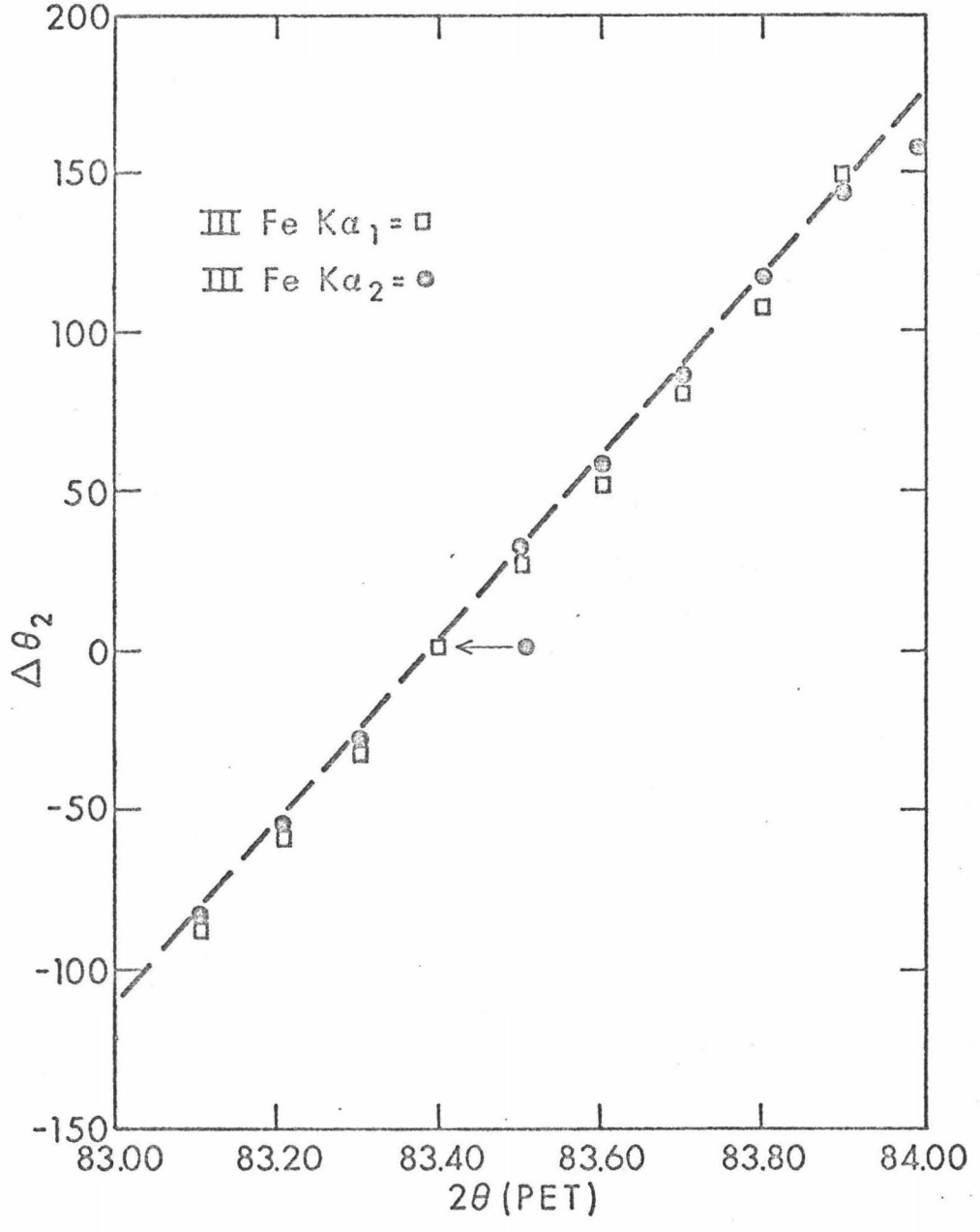

Figure 26

Shift in θcalcite as a Function of θPET

useful here. The III Fe $K\alpha_1$ - III Fe $K\alpha_2$ separation therefore served as an experimental dispersion from which an energy scale could be derived. A dispersion value was obtained for each setting of PET used, but due to the linear relationship observed above (Figure 26) the dispersion was assumed constant during any one scan.

Results appear to be quite good; two lines were needed for evaluation. On the high-energy side, $PK\beta$ for red phosphorus was determined to be 2139.89 eV; Fichter reports a value of 2139.85 eV. Unfortunately, no standard emission line was available on the low-energy side for comparison. The $K\beta$ - $K\beta'$ separation for $Ca_3(PO_4)_2$ was, therefore, compared to that for Na_3PO_4 as published by Fichter.[22] According to Fichter, $K\beta$ = 2137.70 eV and $K\beta'$ = 2124.50 eV, a difference of 13.20 eV; for $Ca_3(PO_4)_2$ calculated from the experimental dispersion, $K\beta$ = 2137.97 eV and $K\beta'$ = 2124.48 eV, a difference of 13.49 eV and an apparent discrepancy of 1.5 percent in the separation.

The intensity normalization is discussed in Appendix B. Figure 27 shows a spectrum for $CaHPO_3$ obtained at PET 83.40°2θ and a corrected spectrum obtained from the normalization and piecing together of the three spectra obtained at PET settings of 83.05°, 83.40°, and 83.60°2θ. As seen, the scan at 83.40°2θ fairly well approximates the true intensity contour; the remaining spectra in Section IV are, therefore, uncorrected spectra obtained at a PET setting of 83.40°2θ.

The successful calibration of the instrument and the reproducibility of spectral features to within 0.06 eV indicate that our "hybrid double-crystal spectrometer" is capable of quantitative, as well as qualitative, evaluation.

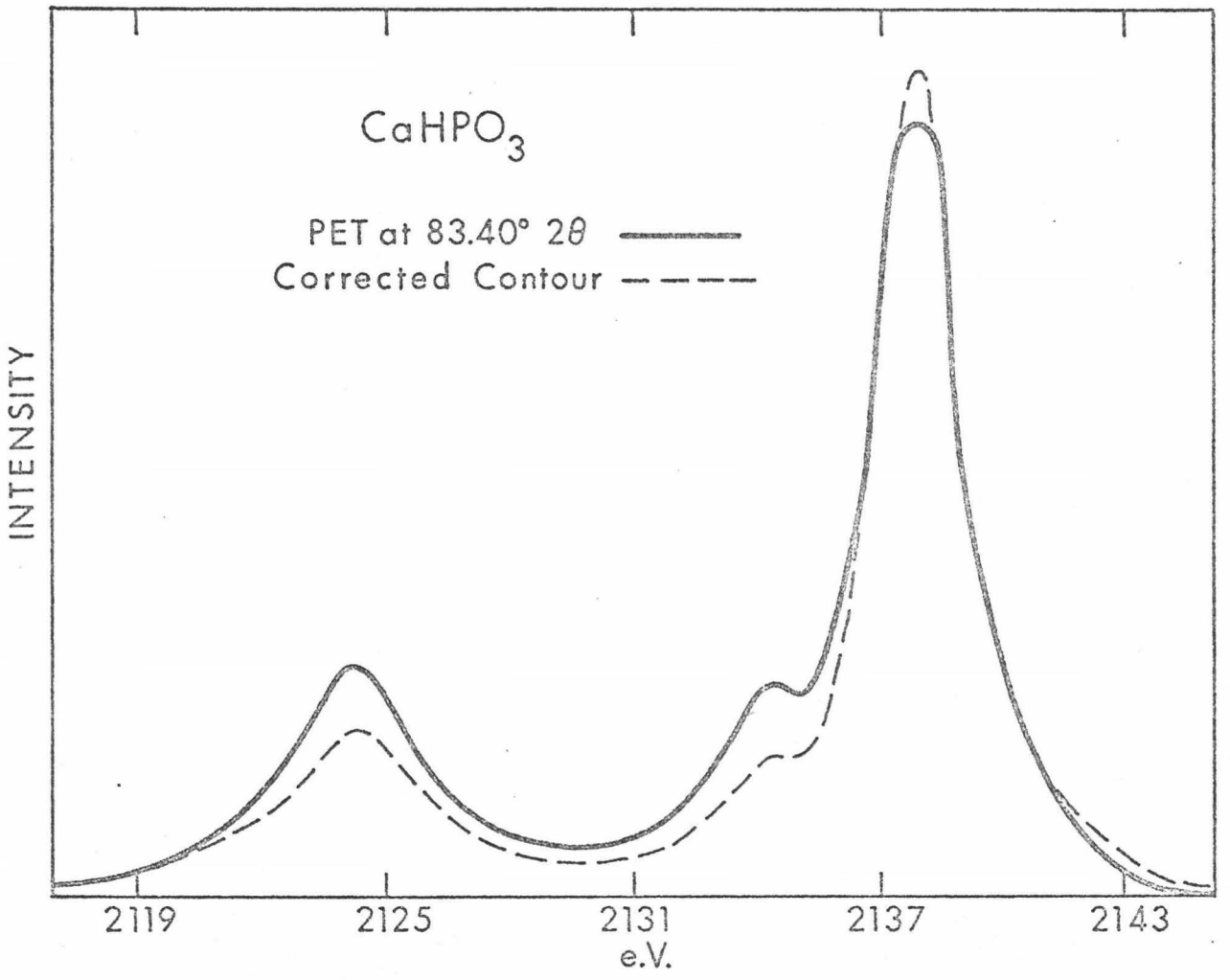

Figure 27

Correction of Intensity Contour for $CaHPO_3$

Operation

Before any double-crystal work was attempted, all of the compounds were investigated for effects of decomposition.

The sodium salts of the phosphorus oxy-anions were found to decompose rapidly in an inexplicable manner upon irradiation, as was previously noted by Wiech,[41] while the calcium salts proved quite stable in the x-ray beam. Figure 28 is an example of the stability of the calcium salts. Each compound was irradiated for a total of three hours, spectral data being recorded each hour; decomposition effects were small over-all and negligible for the first 90 minutes. The salts were all reagent grade chemicals and no further purification was made.

The Ni $\overline{/}\,S_2P(R)_2\,\overline{\backslash}_2$ compounds donated by Professor Quintus Fernando of the University of Arizona, Tucson, also exhibited negligible decomposition effects; a sample of radiation effects is shown in Figure 29. One of the compounds, the pyridine adduct of Bis (0 0' diethydithiophosphinato) Nickel (II), exhibited a tendency to lose pyridine unless kept in a pyridine atmosphere. Exposure to radiation may also have induced pyridine loss, as would be indicated by the change in color from green to purple characteristic of the parent compound. However, no significant spectral changes were observed on the phosphorus $K\beta$ spectra.

All samples were ground manually to a fine powder from which a briquette of "infinite" thickness was prepared. Spectra were run in a helium atmosphere at 45 kv and 60 ma with a 3 kw chromium tube and gas flow proportional counter with P - 10 gas set at 1600 v. Pulse-height analysis was used to discriminate against stray tube radiation and background radiation from calcium; the use of a 1.0 v baseline and 3.0 v window increased the peak to background ratio by a factor of 2.

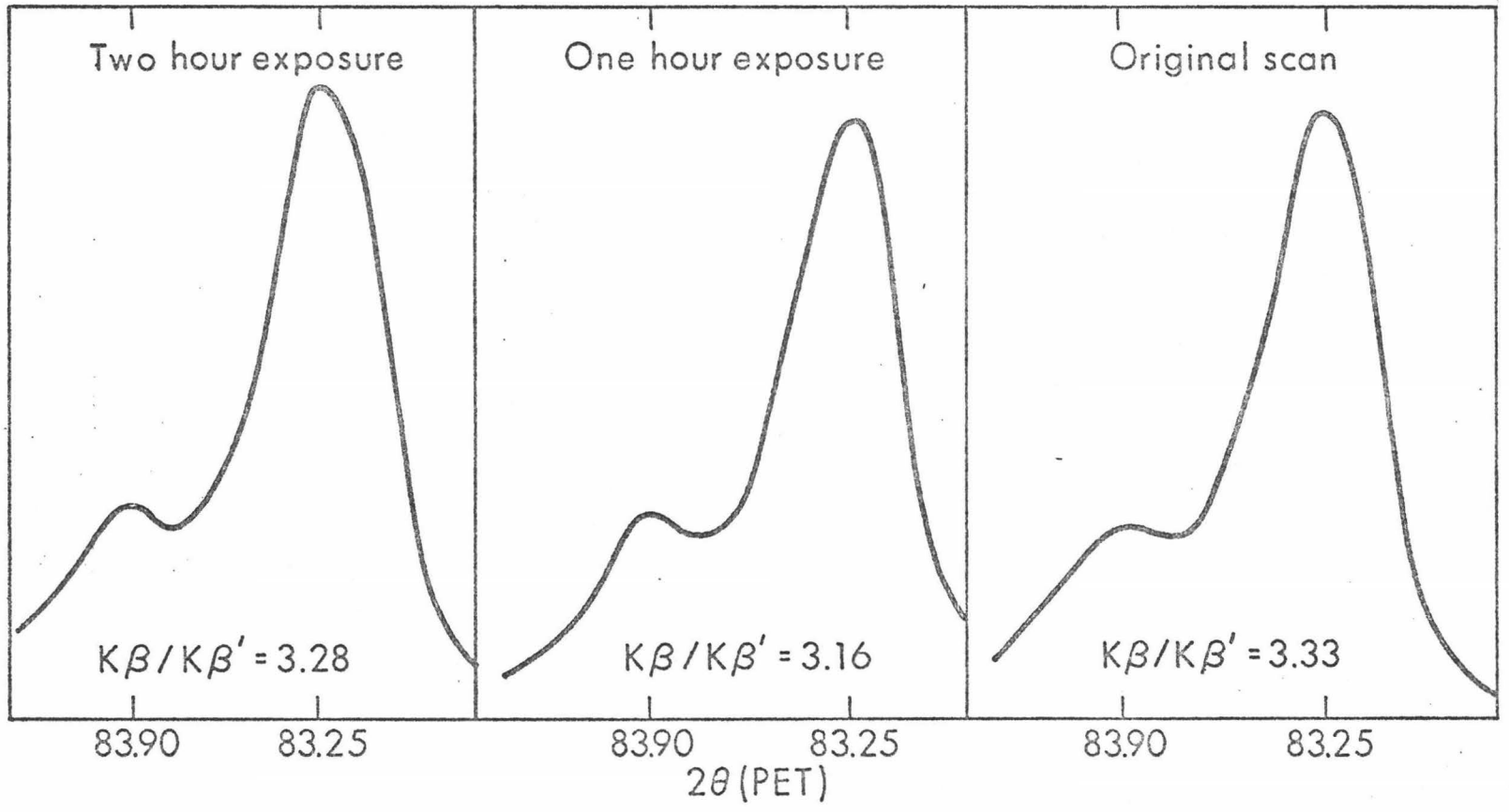

Figure 28

Decomposition Effects for $CaHPO_4$

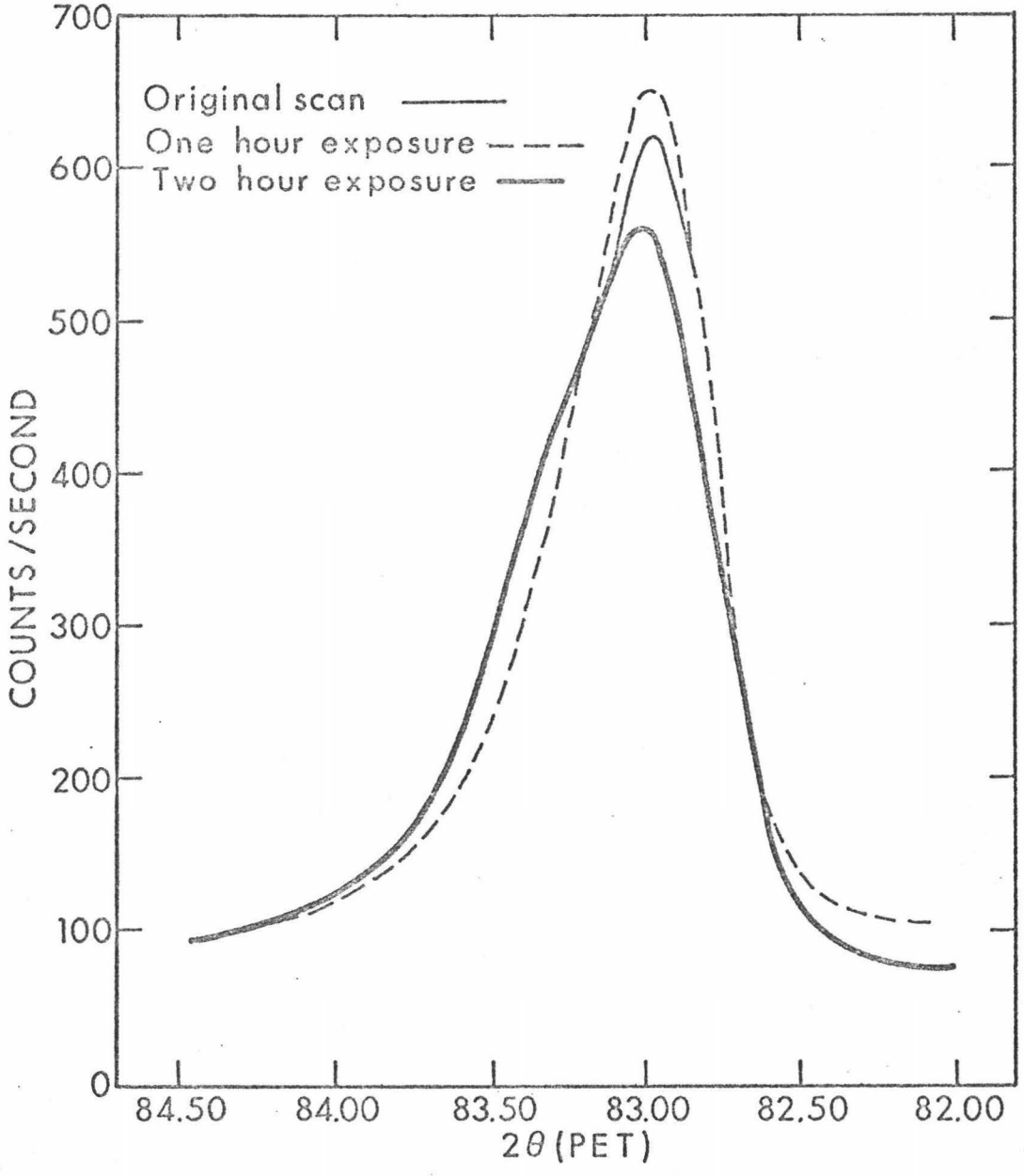

Figure 29

Decomposition Effects on Ni $\overline{/}\overline{S_2P(C_2H_5)_2}\overline{/}_2$

Three settings of PET were used, 83.05°2θ, 83.40°2θ, and 83.60°2θ; one-hundred-second counts were taken for each point and each spectrum required from 70 to 100 points. III Fe $K\alpha_{1,2}$ standard was run after each phosphorus point-by-point scan to provide a constant check on the wavelength stability of the system, and to provide a standard for wavelength and intensity calibration.

Where any spectral feature was suspect, a fresh sample was scanned over that particular region as a check. The running of each spectra averaged from 90 to 120 minutes.

CHAPTER IV

Results and Discussion

In this section the experimental results and their interpretation will be presented; the interpretation will be semi-quantitative as appropriate CNDO/2 calculations have been performed.

Two series of compounds were studied; the results of the phosphorus oxy-anions will be presented first, then the Ni $\overline{[}S_2P(R)_2\overline{]}_2$ compounds will be discussed on the basis of information gained from the phosphorus salts.

The following phosphorus oxy-anions were investigated:

$Ca_3(PO_4)_2$	$CaHPO_4$	$Ca(H_2PO_4)_2$	H_3PO_4	$CaHPO_3$	$Ca(H_2PO_2)_2$
Td	C_{3v}	C_{2v}	C_{3v}	C_{3v}	C_{2v}

$Ca_3(PO_4)_2$, $CaHPO_4$, and $Ca(H_2PO_4)_2$ are the tri-, di-, and monobasic salts of phosphoric acid, H_3PO_4. Data in Table 1 indicate one type of bond for PO_4^{-3} and two distinct bonds for $CaHPO_4$, $Ca(H_2PO_4)_2$, and H_3PO_4. It was on this basis that the symmetries were assigned.

The Kβ spectra for all compounds were obtained in this lab; the $L_{2,3}$ spectra for $H_2PO_4^-$, HPO_3^{-2}, and $H_2PO_2^-$ were furnished by Henke[23] while that for PO_4^{-3} was published by Wiech.[41] The $L_{2,3}$ spectra were not available for HPO_4^{-2} and H_3PO_4; however, this does not appear to have hindered the assignment made here.

Figures 30-36 show the Kβ spectra for phosphorus and its salts while the $L_{2,3}$ spectra are presented in Figures 37 to 41.

Table 1

Crystallographic Data for Phosphorus Oxy-Anions

Compound	Bond	Length[a]	Angle	Degrees[a]
PO_4^{-3}	P-O	1.56 Å	O-P-O	109.5
HPO_4^{-2}	P-O	1.519 Å	OH-P-O	108.4
	P-OH	1.576 Å	O-P-O	110.5
$H_2PO_4^-$	P-O	1.498 Å	O-P-O	114.2°
	P-OH	1.606 Å	OH-P-OH	112.2°
			O-P-OH	107.6°
H_3PO_4	P-O	1.503 Å	OH-P-O	112.7°
	P-OH	1.553 Å	OH-P-OH	106.1°
HPO_3^{-2}	P-H	1.17 Å	H-P-O	109°
	P-O	1.51 Å	O-P-O	110°
$H_2PO_2^-$	P-H	1.39 Å	H-P-O	109°
	P-O	1.505 Å	H-P-H	< 109.5°
			O-P-O	> 109.5°

[a]Bond lengths and bond angles given represent average values.[39,42,43,44,45,46]

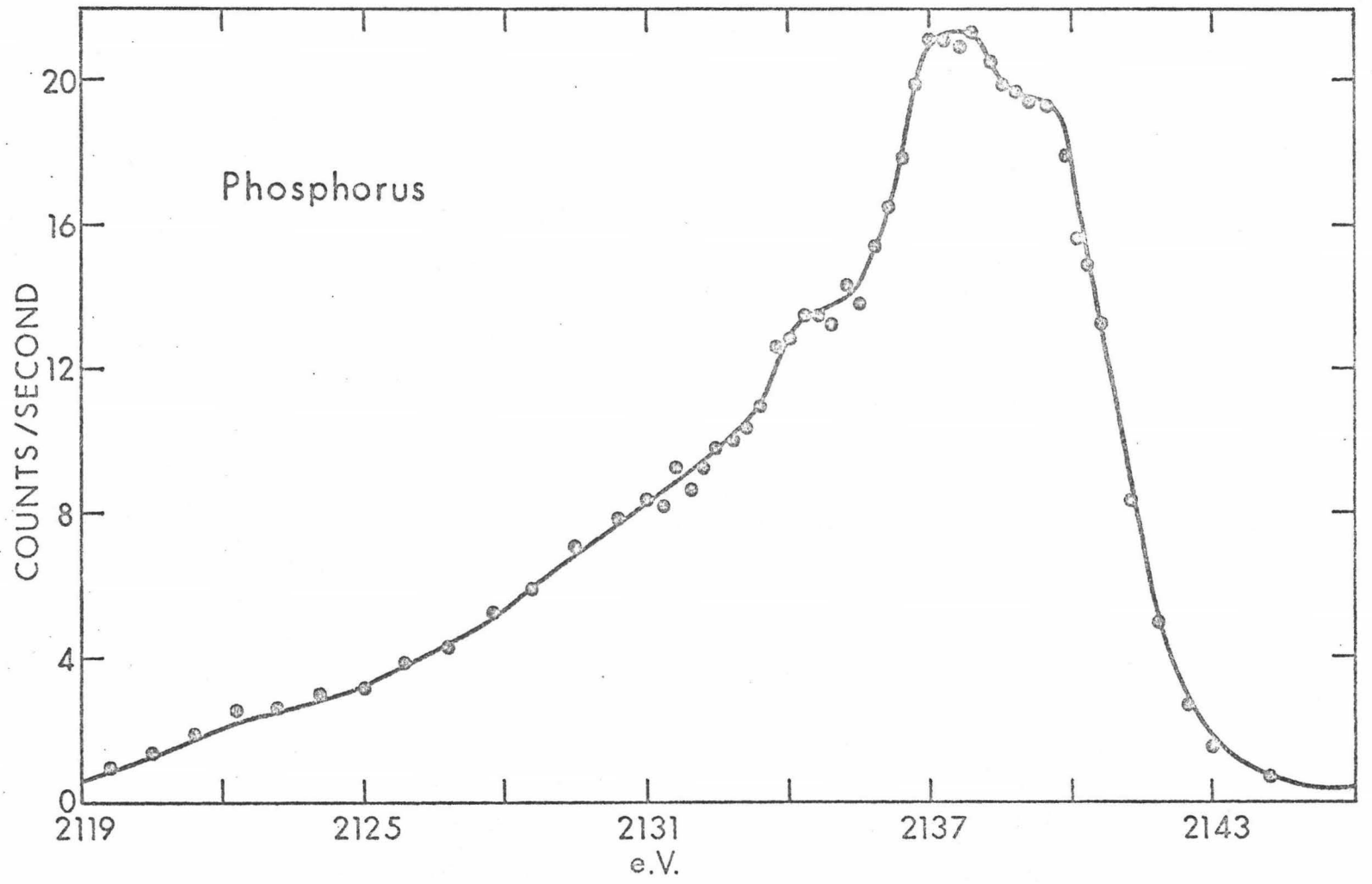

Figure 30

Kβ Emission Spectrum of $P_{(red)}$

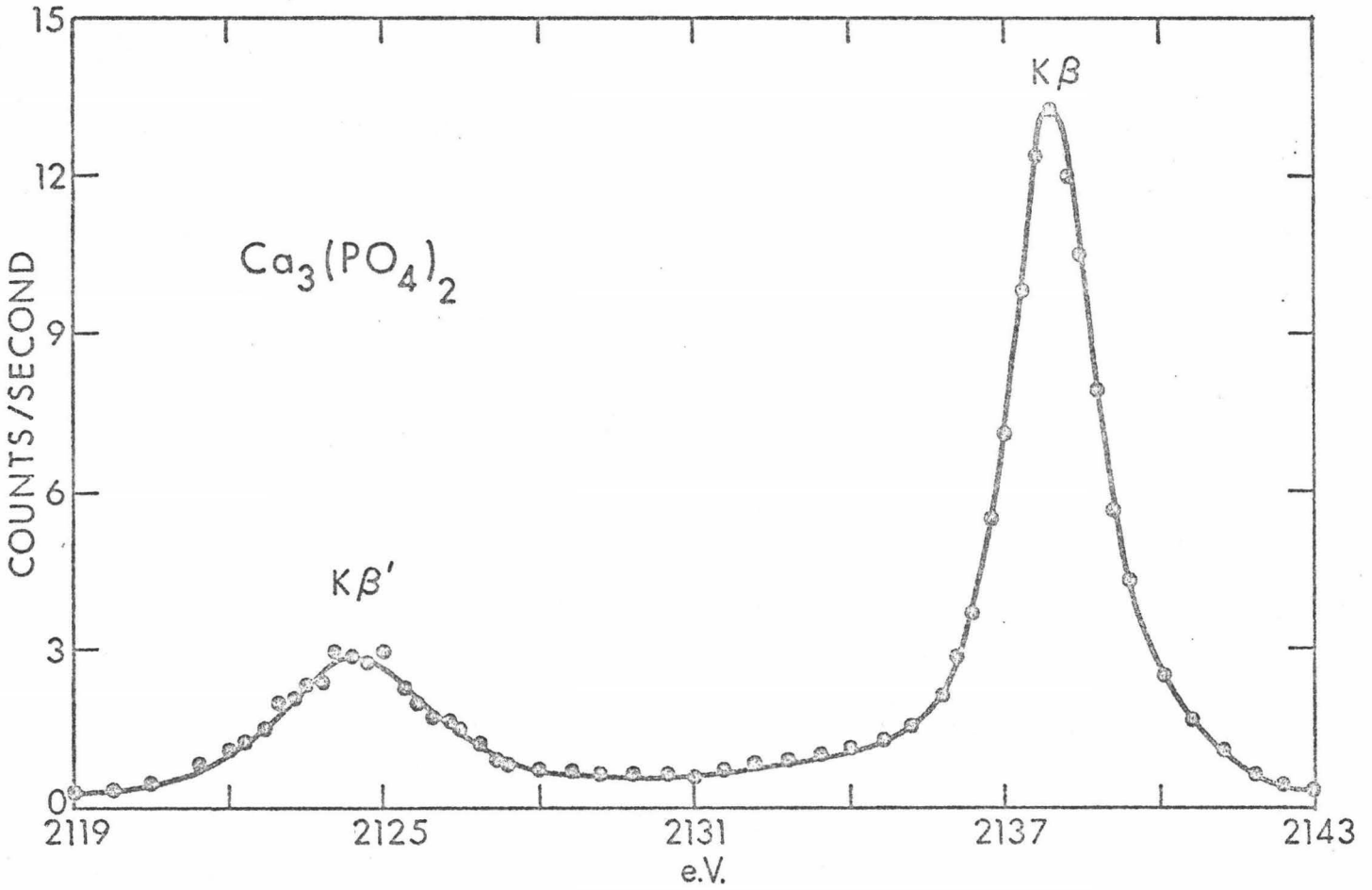

Figure 31

Kβ Emission Spectrum of $Ca_3(PO_4)_2$

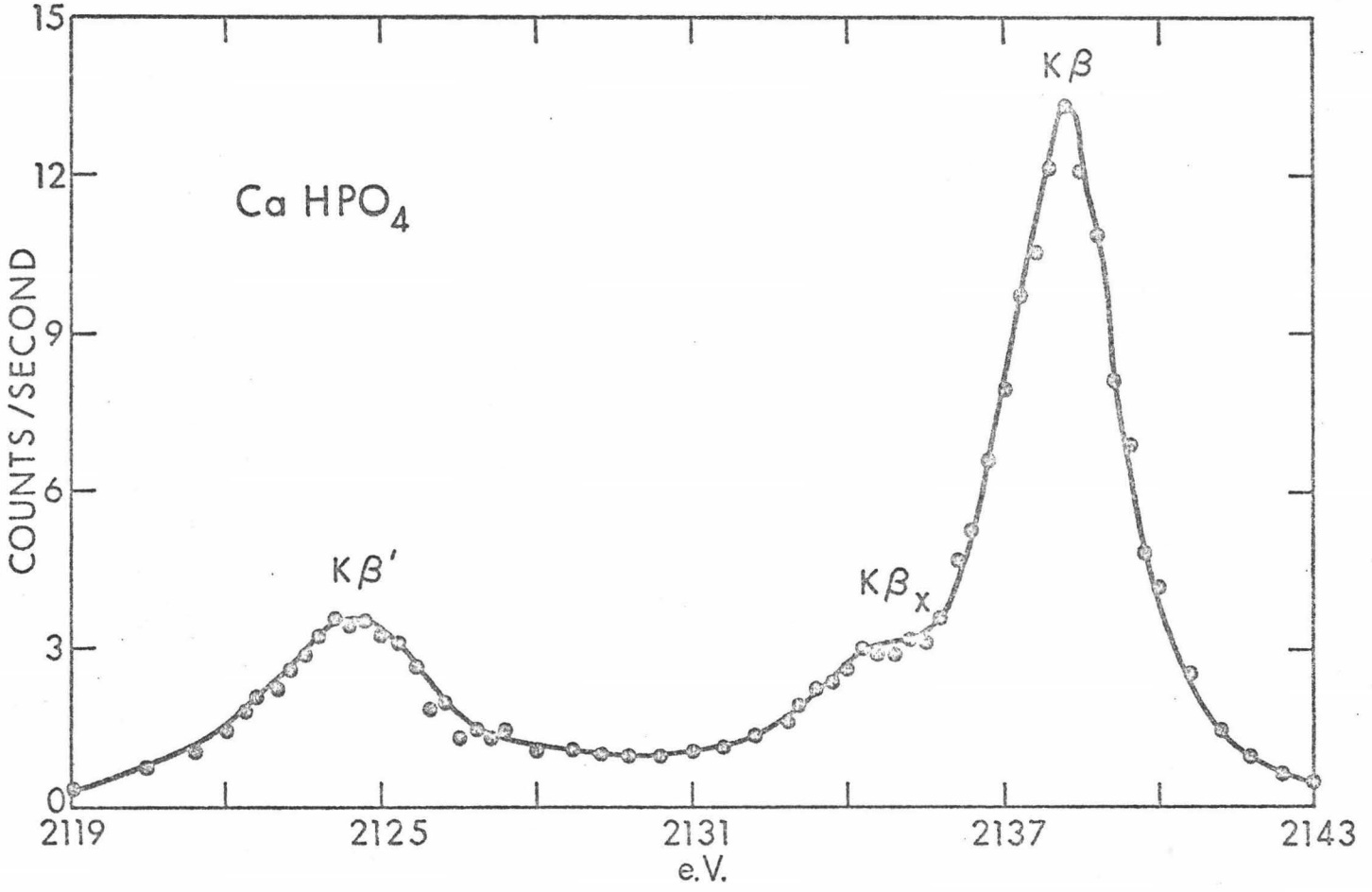

Figure 32

Kβ Emission Spectrum of $CaHPO_4$

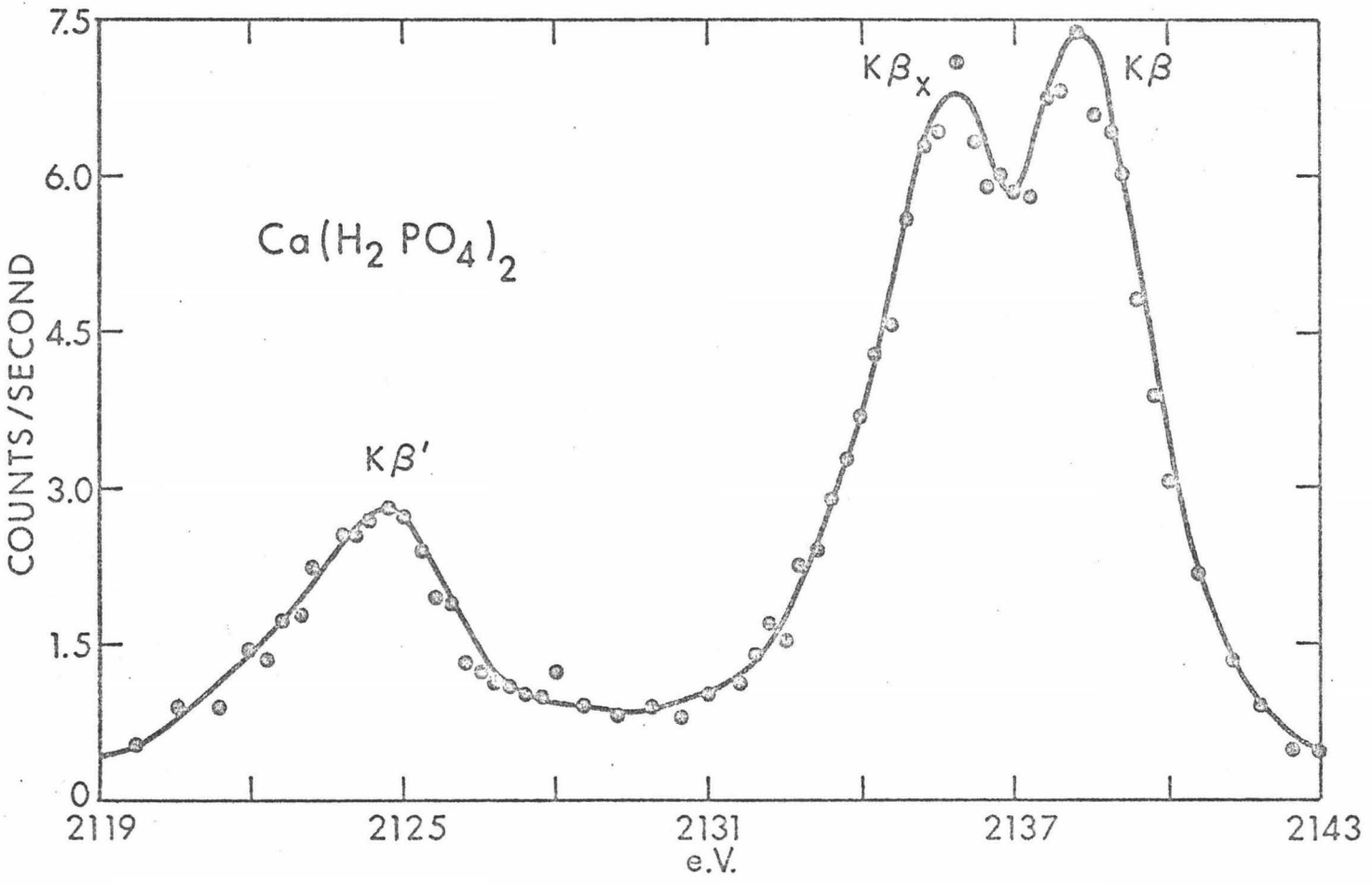

Figure 33

Kβ Emission Spectrum of $Ca(H_2PO_4)_2$

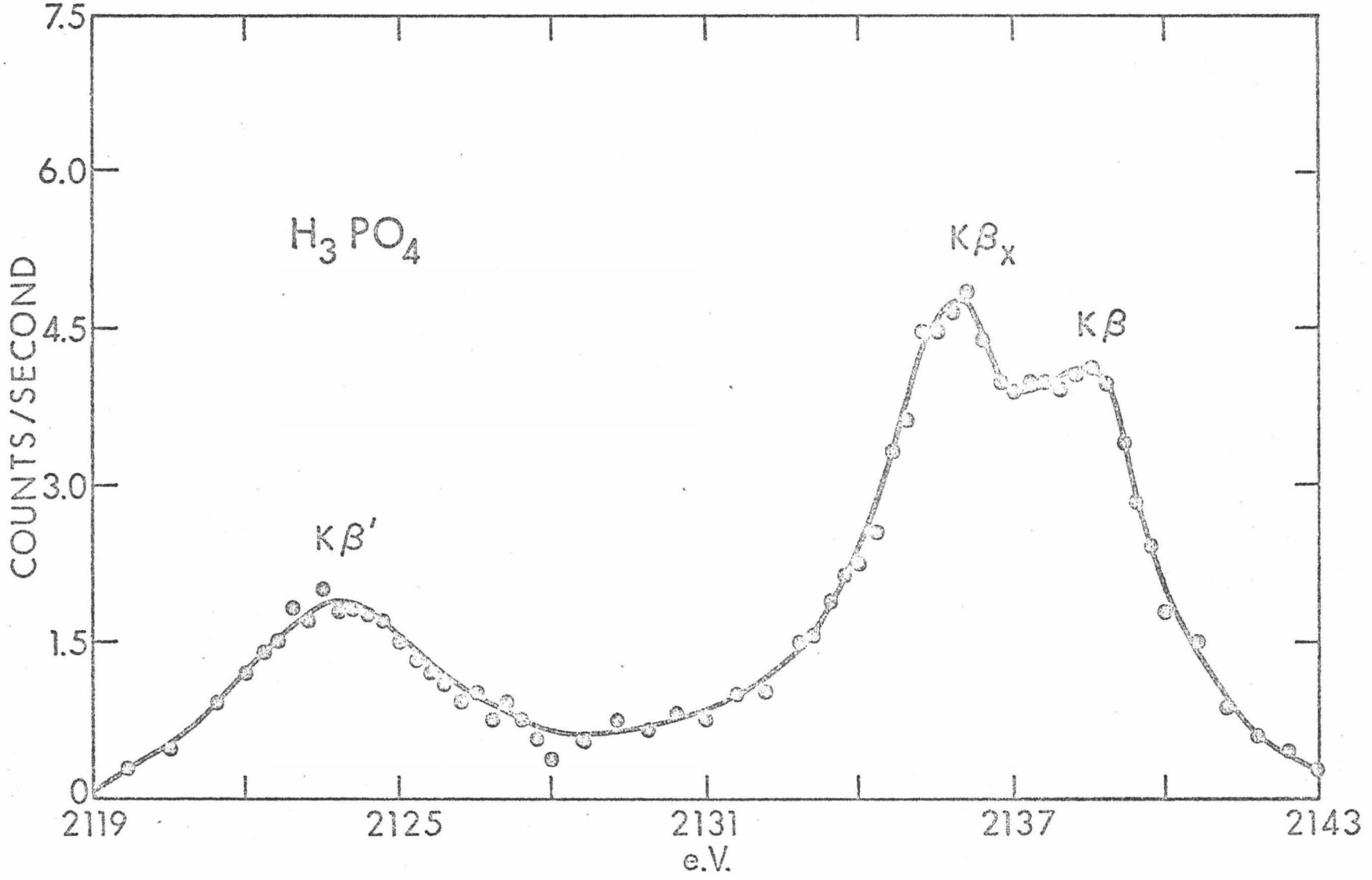

Figure 34

$K\beta$ Emission Spectrum of H_3PO_4

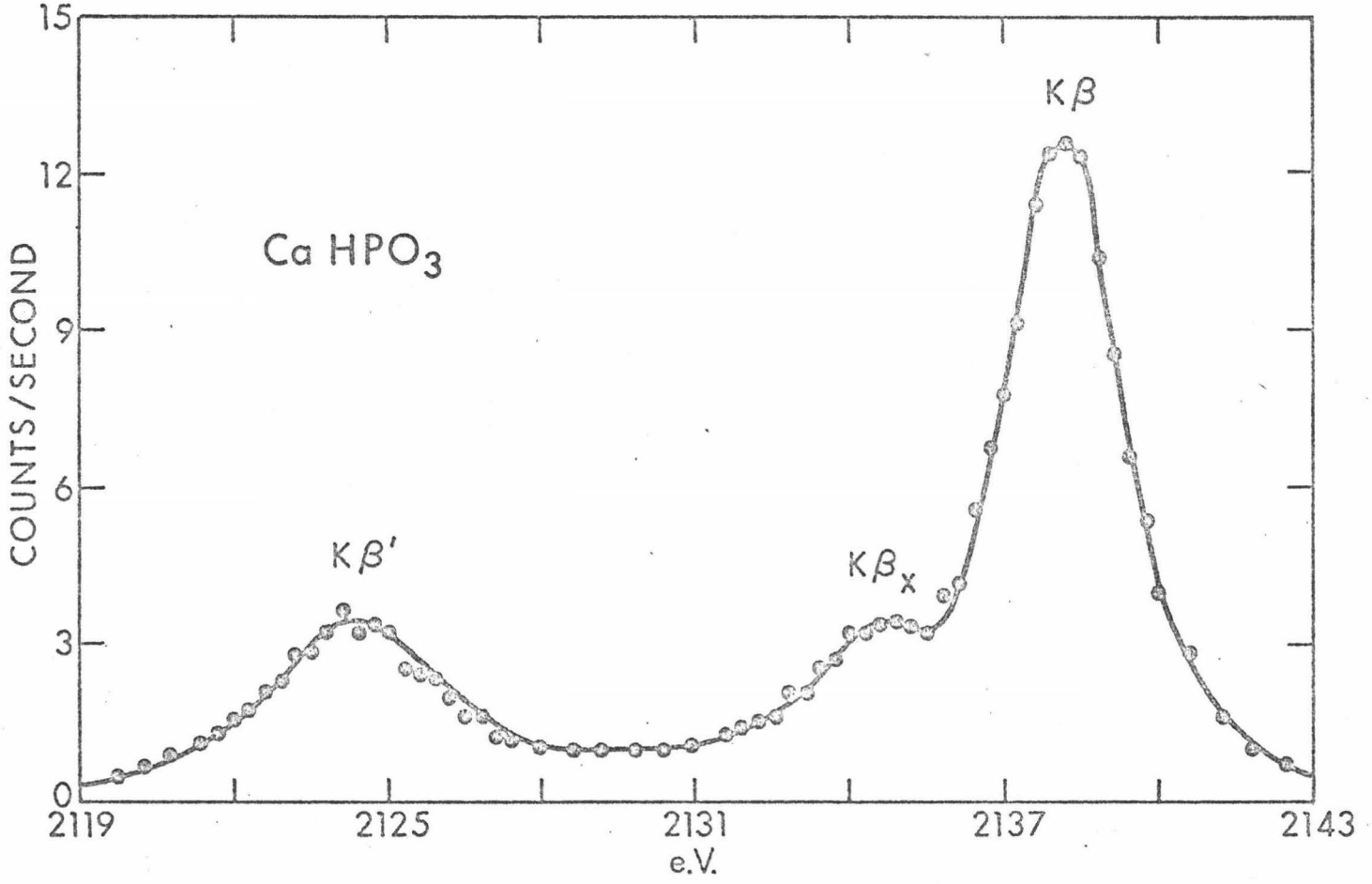

Figure 35

Kβ Emission Spectrum of $CaHPO_3$

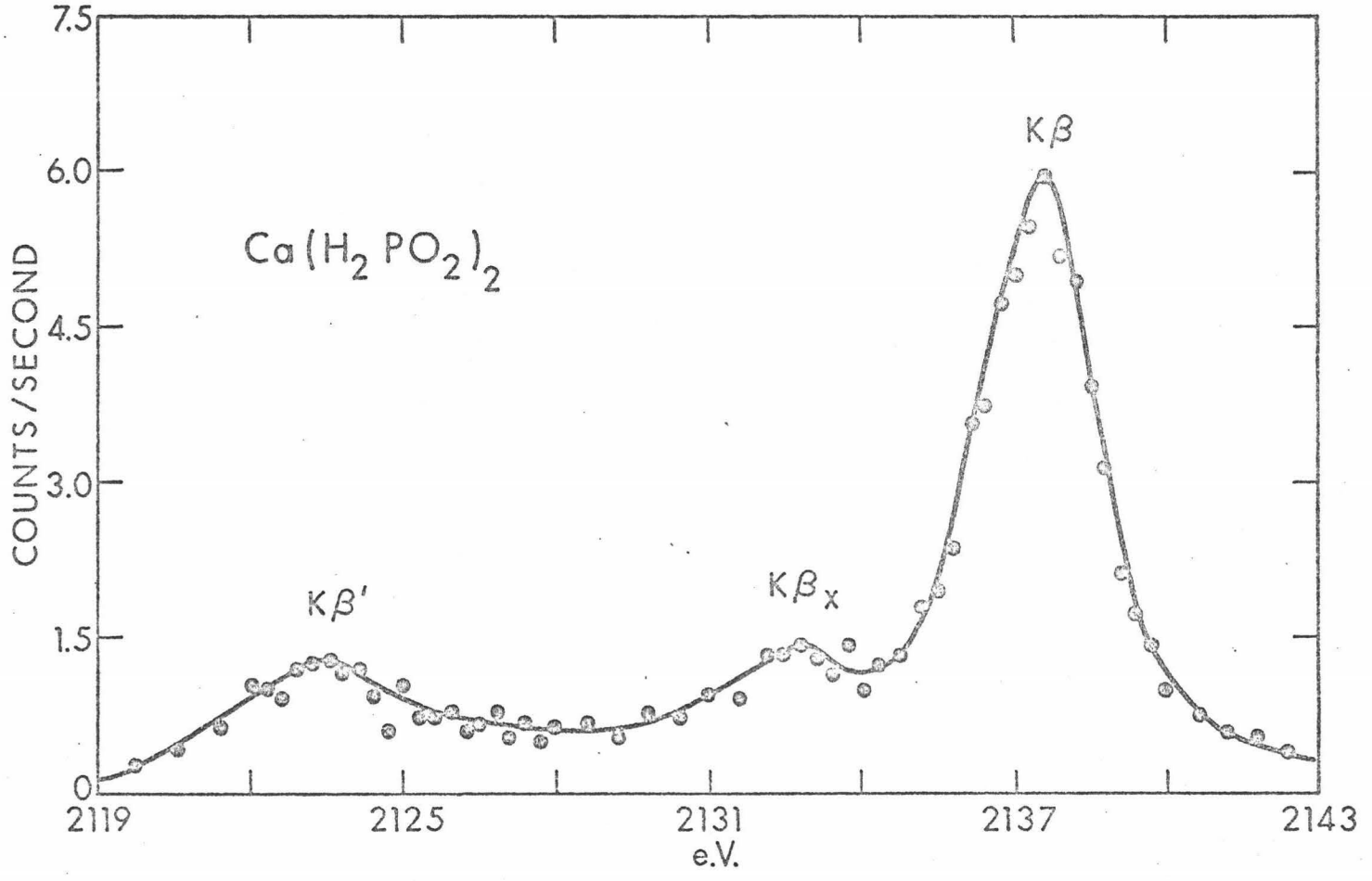

Figure 36

Kβ Emission Spectrum of $Ca(H_2PO_2)_2$

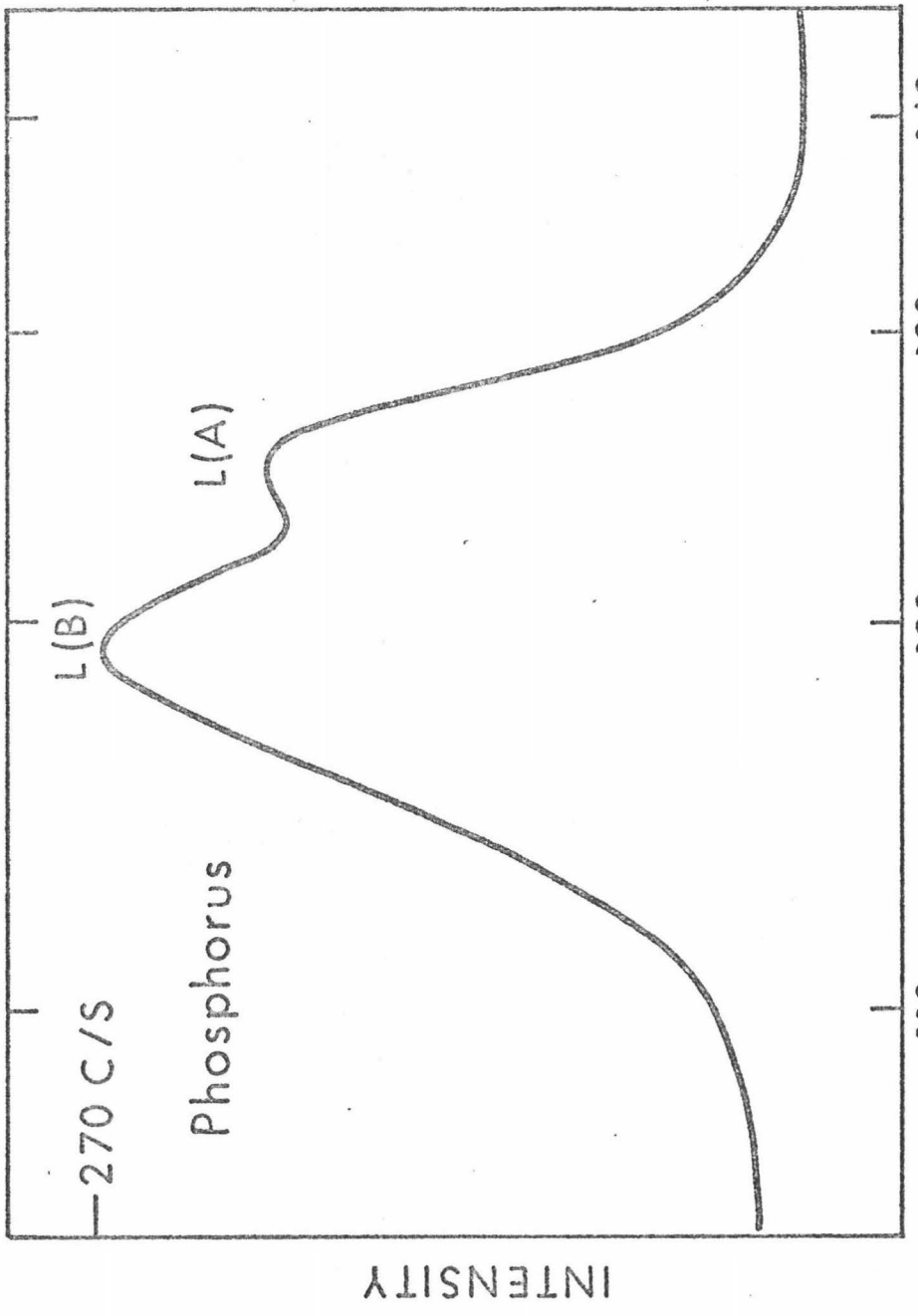

Figure 37

$L_{2,3}$ Emission Spectrum of $P_{(red)}$

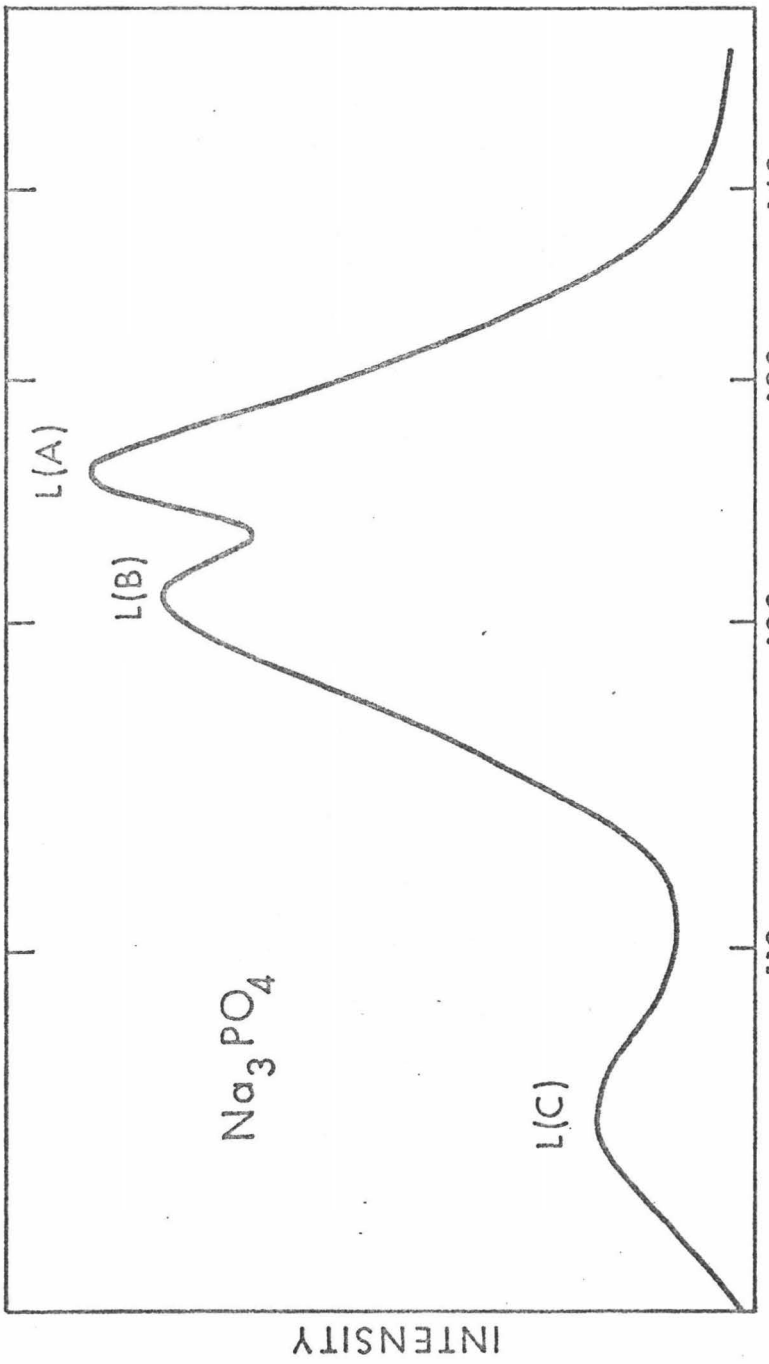

Figure 38

$L_{2,3}$ Emission Spectrum of Na_3PO_4

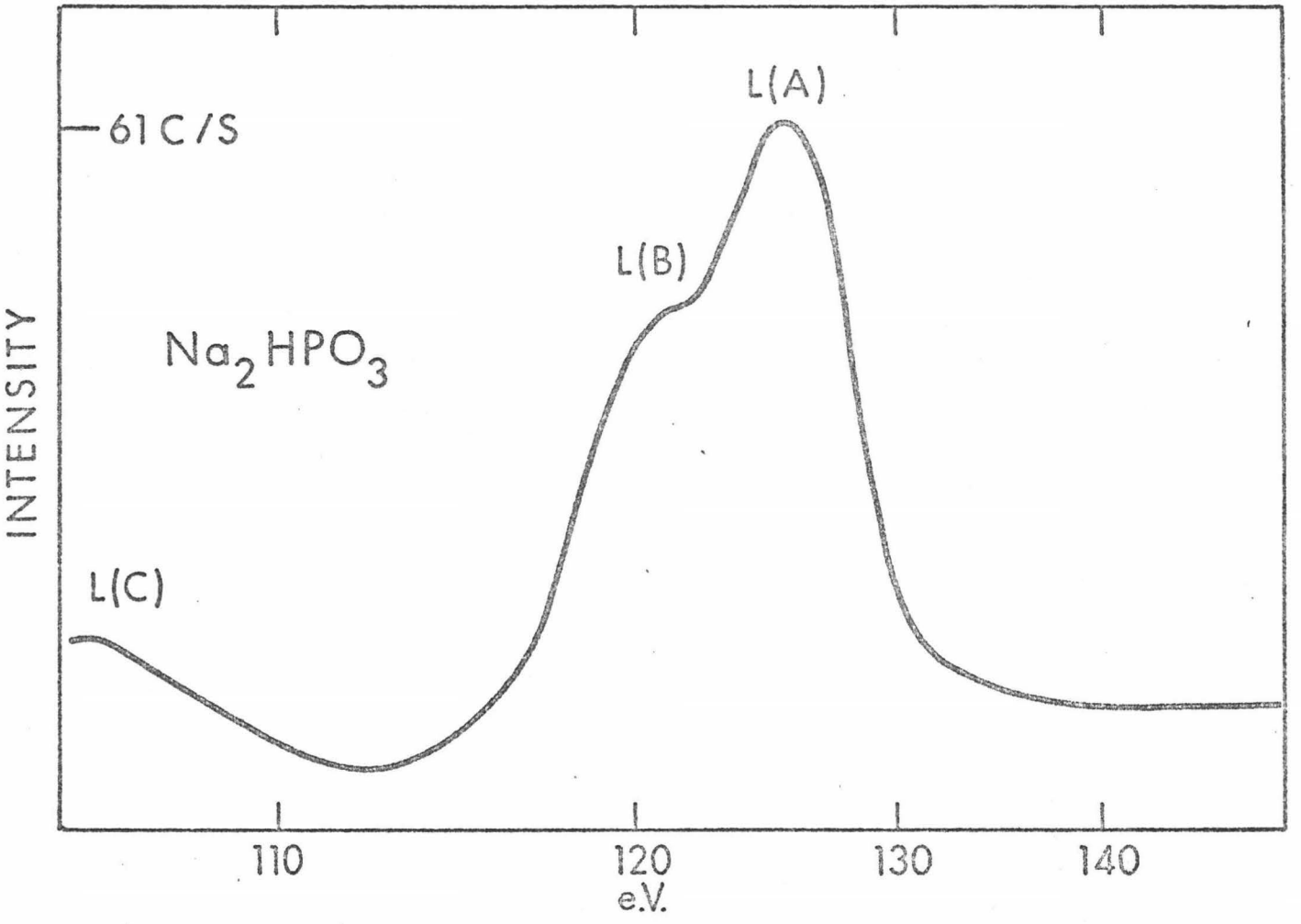

Figure 39

$L_{2,3}$ Emission Spectrum of Na_2HPO_3

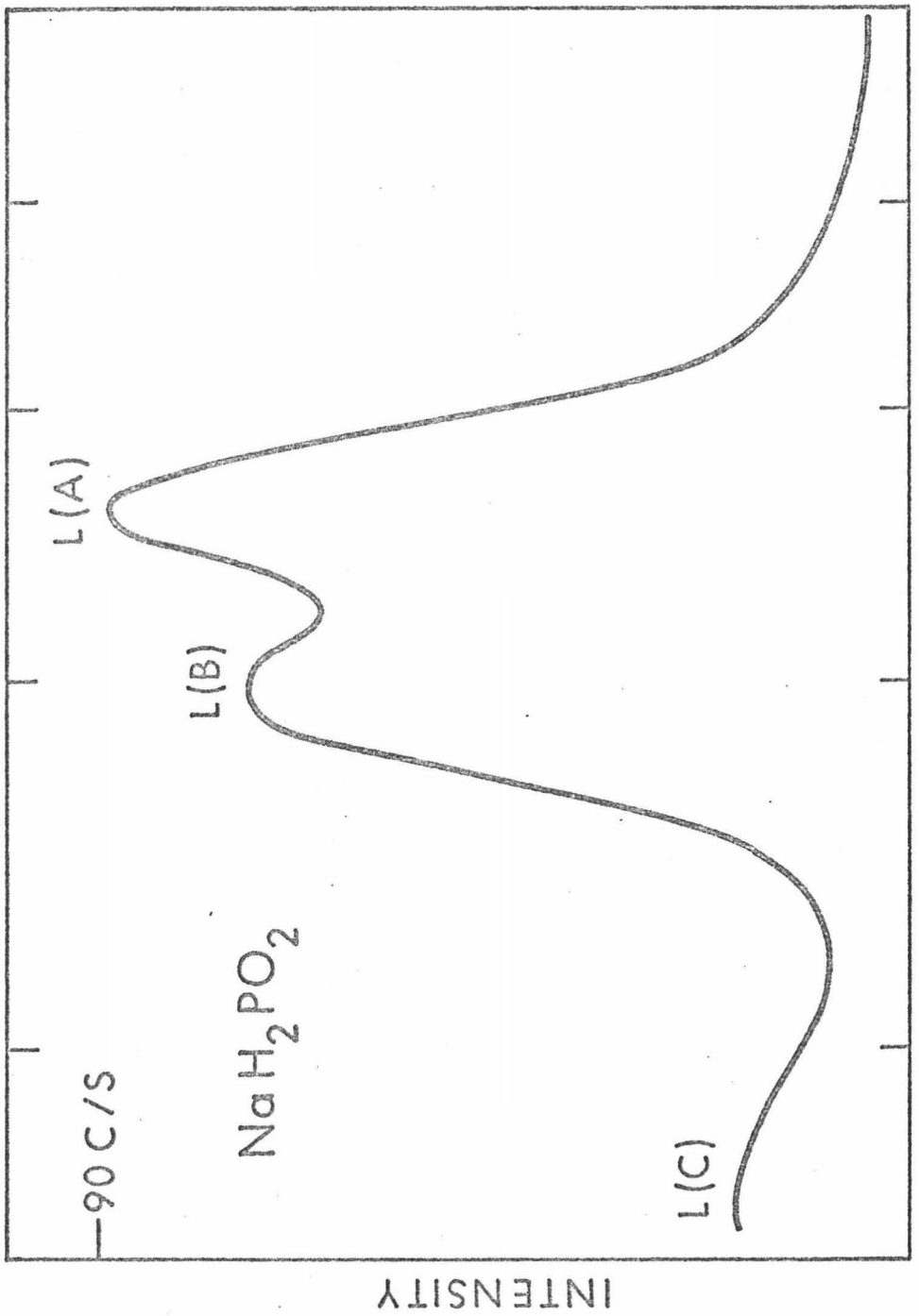

Figure 40

$L_{2,3}$ Emission Spectrum of NaH_2PO_2

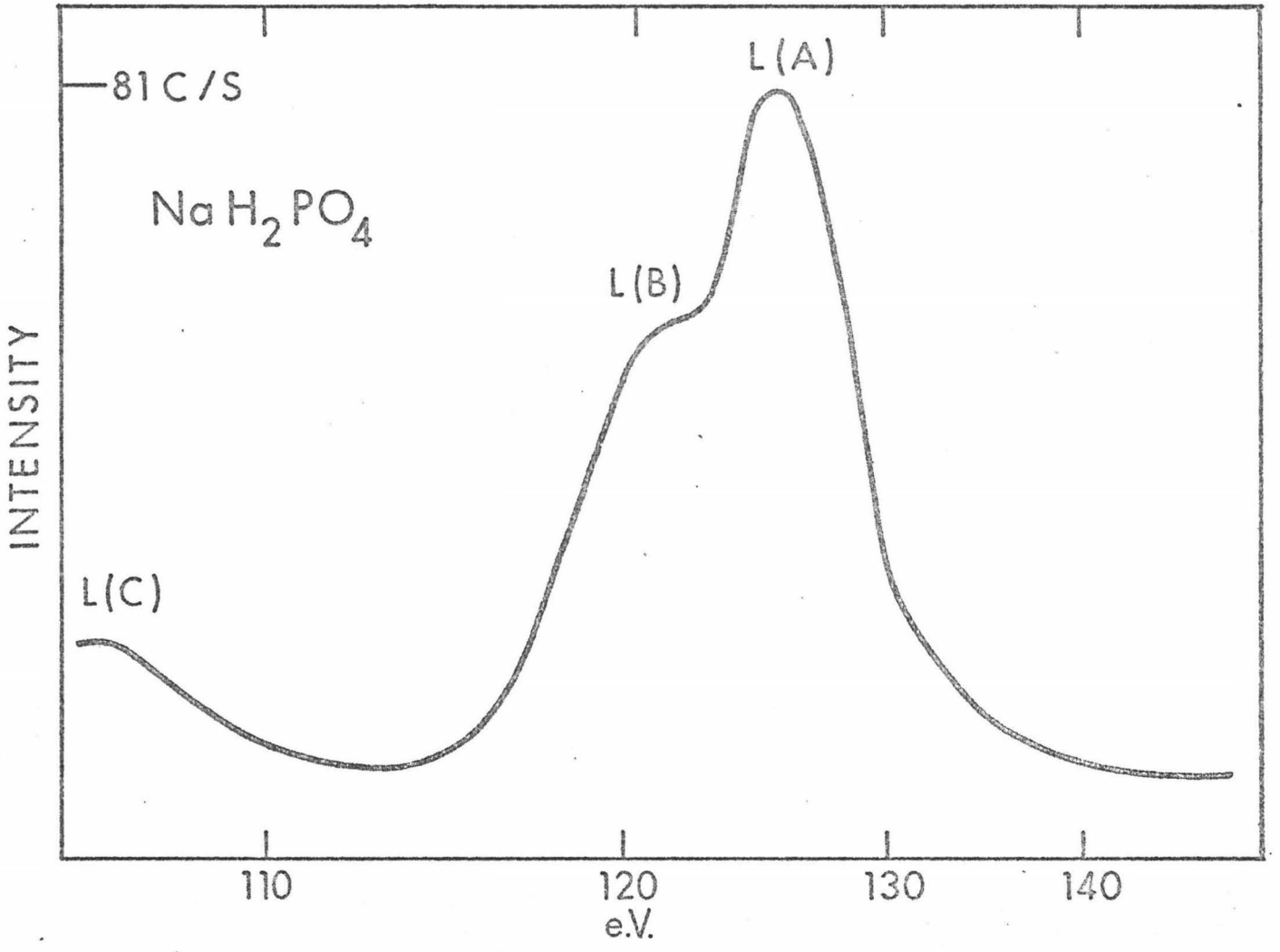

Figure 41

$L_{2,3}$ Emission Spectrum of NaH_2PO_4

The first step in the spectral assignment is the determination of the appropriate selection rules from equation (1) and using group theoretical arguments. Table 2 gives the allowed transitions for T_d, C_{3v}, and C_{2v} symmetries for both the Kβ and the $L_{2,3}$ spectra. It is seen that as the symmetry decreases from Td to C_{2v}, the resulting loss of degeneracy allows many more transitions to occur which may lead to complex spectra.

Next, simultaneous evaluation of Kβ and $L_{2,3}$ requires determination of the values for equation (6) ($E_i = h\nu - \overline{V}_i$). Table 3 lists the $\overline{V}_i$ values for the 2p level as determined by Jolly, et al.;[47] the 1s binding energies were not directly available but were derived from Jolly's data for 2p binding energies and Fichter's $K\alpha_1$ information.[22] Setting $K\alpha_1$ equal to the 2p binding energies of Jolly, $h\nu$ is the $K\alpha_1$ transition energy and then:

$$E_i\ (K) = h\nu_{K\alpha_1} - \overline{V}_K$$

$$B\ E_{(2p)} = K\alpha_1 - \overline{V}_K$$

These 1s binding energies are also given in Table 3.

In order to calculate $E_i(K)$ and $E_i(L)$, it is necessary to subtract the tabulated $\overline{V}_i$ values from the observed transition energies, $h\nu$. The results for $E_i(K)$ and $E_i(L)$ are given in Table 4.

Molecular orbital calculations are also necessary for the ordering of molecular orbital energy levels and atomic coefficients in these orbitals. Hillier[17] has performed rigorous ab initio SCF calculations on PO_4^{-3}, but no calculations at all have been done for the other compounds. Therefore, CNDO/2 calculations were performed for all of the compounds including PO_4^{-3} for comparison with Hillier's calculations.

Table 2

Selection Rules for T_d, C_{3v} and C_{2v} Symmetries

Symmetry	Spectral Transition	ϕ_m	$\hat{\mu}$	ϕ_n	Allowed Transitions
T_d :	Kβ	a_1 (1s)	t_2 (x,y,z)	t_2	$t_2 \longrightarrow a_1$
	$L_{2,3}$	t_2 (2p)	t_2 (x,y,z)	a_1,e,t_1,t_2	$a_1 \longrightarrow t_2$; $e \longrightarrow t_2$; $t_1 \longrightarrow t_2$; $t_2 \longrightarrow t_2$
C_{3v} :	Kβ	a_1 (1s)	$a_1(z)$ e(x,y)	a_1, e	$a_1 \longrightarrow a_1$; $e \longrightarrow a_1$
	$L_{2,3}$	a_1,e (2p)	$a_1(z)$ e(x,y)	a_1,a_2,e	$a_1 \longrightarrow a_1$; $e \longrightarrow a_1$; $a_1 \longrightarrow e$; $e \longrightarrow e$; $a_2 \longrightarrow e$
C_{2v} :	Kβ	a_1 (1s)	$a_1(z)$;$b_1(x)$; $b_2(y)$	a_1;b_1;b_2	$a_1 \longrightarrow a_1$; $b_1 \longrightarrow a_1$; $b_2 \longrightarrow a_1$
	$L_{2,3}$	$a_1(z)$;$b_1(x)$; $b_2(y)$	$a_1(z)$; $b_1(x)$;$b_2(y)$	a_1;a_2; b_1;b_2	a_1 $b_1 \longrightarrow a_1$ b_2 a_1 $a_2 \longrightarrow b_1$ b_1 a_1 $a_2 \longrightarrow b_2$ b_2

Table 3

Binding Energies for K and L Shells

Compound	$\bar{V}_K$ [a]	V_L [47]
P	2143.82 eV	130.1 eV
PO_4^{-3}	2146.57	132.1
HPO_4^{-2}	2147.15	132.7
$H_2PO_4^-$	2148.34	133.9
H_3PO_4	--	--
HPO_3^{-2}	2147.28	132.9
$H_2PO_2^-$	2146.62	132.4

---

[a] Derived from Fichter's values of $h\nu$ for $K\alpha$ and Jolly's values for 2p binding energy applied to: $E_i = h\nu - \bar{V}_K$.

Table 4

Transition Energies and Corresponding E_i Values

Line	$h\nu$	$-E_i$(K)	Compound	Line	$h\nu$	$-E_i$(L)
$K\beta$	2139.85 eV	4.00	P	L(A)	125.5 eV	4.6
$K\beta_x$	2137.25	6.60		L(B)	119.1	11.1
$K\beta$	2137.70	8.87	PO_4^{-3}	L(A)	126.4	5.7
$K\beta'$	2124.50	22.07		L(B)	119.6	12.5
				L(C)	107.8	24.3
$K\beta$	2138.23	8.92		L(A)	--	--
$K\beta_x$	2134.86	12.29	HPO_4^{-2}	L(B)	--	--
$K\beta'$	2124.21	22.94		L(C)	--	--
$K\beta$	2138.50	9.84		L(A)	125.5	8.4
$K\beta_x$	2135.78	12.56	$H_2PO_4^-$	L(B)	121.2	12.7
$K\beta'$	2124.60	23.70		L(C)	108.0	26.0
$K\beta$	2138.54	--		L(A)	--	--
$K\beta_x$	2135.93	--	H_3PO_4	L(B)	--	--
$K\beta'$	2123.30	--		L(C)	--	--
$K\beta$	2137.70	9.58		L(A)	125.0	7.9
$K\beta_x$	2133.30	13.98	HPO_3^{-2}	L(B)	121.0	11.9
$K\beta'$	2124.20	23.08		L(C)	108.0	25.0
$K\beta$	2137.75	8.87		L(A)	126.0	6.4
$K\beta_x$	2133.03	13.59	$H_2PO_2^-$	L(B)	119.4	13.0
$K\beta'$	2124.20	22.40		L(C)	108.0	24.0

Hillier had included 3d orbital participation in his calculations on the basis of valence photoelectron data, $L_{2,3}$ emission spectra, and the better correlation between his calculations and experimental results when 3d orbitals are included. On the basis of Hillier's findings, therefore, 3d orbital participation has been assumed for the other molecules and has been incorporated into the CNDO calculations. Their inclusion makes a significant effect upon the subsequent interpretation.

In performing the calculations for the oxy-anions the cations were neglected, as were the neighboring anions and matrix properties. In effect, then, the phosphorus oxy-anions were considered isolated anionic species.

The CNDO program and calculations are discussed more fully in Appendix C. The resulting molecular energy levels, and their eigenvalues and atomic parameters are given in Tables 6, 8, 10, 12, 14 and 15. Table 5 gives the results of Hillier's calculations on PO_4^{-3}.

The atomic parameters listed for the CNDO calculations are merely the sum of the eigenvectors for each atomic orbital; they are listed either as bonding or as antibonding with the central atom. For example, for $2t_2$ of PO_4^{-3} the atomic parameter of 1.48 for the phosphorus 3p orbital represents the sum of the eigenvectors for p_x, p_y, and p_z; an analogous situation exists for the five 3d orbitals; the phosphorus 3s coefficient is zero. The coefficients of the individual ligand orbitals are then similarly summed and referred to each phosphorus orbital as to whether it is bonding or antibonding. Oxygen then has a total 2s atomic parameter of zero with respect to phosphorus' 3p bonding parameter of 0.49. Similarly, the 2p bonding parameter is 5.05 while the antibonding

Table 5

Hillier's Calculated Electronic Structure of PO_4^{-3}

Valence Orbital	Energy	Atomic Components (%) Phosphorus Orbital			Oxygen Orbital	
		3s	3p	3d	2s	2p
$1t_1$	15.3 eV	--	--	--	--	100
$3t_2$	13.5	--	--	13	1	86
1e	11.8	--	--	21	--	79
$2t_2$	9.0	--	28	2	6	63
$2a_1$	6.1	28	--	--	21	51
$1t_2$	-8.9	--	12	3	84	1
$1a_1$	-11.6	26	--	--	71	3

is 1.87; this is then considered as strongly bonding with phosphorus. These values are not meant as a quantitative measurement of the contribution of atomic orbitals to the total bonding molecular orbital, but rather are a qualitative representation of the extent of bonding between two atomic orbitals based on a geometric model. Thus, for $2t_2$ in PO_4^{-3}, phosphorus 3p may be considered as antibonding with oxygen 2s but strongly bonding with oxygen 2p. In a case where the bonding and antibonding contributions are equal, the orbitals may be considered as nonbonding with the central atom orbital.

The actual CNDO eigenvalues and eigenvectors obtained from the program are given in Appendix C.

This presentation does not provide a quantitative rationalization of the observed intensity contour. To a first approximation, as shown by Manne,[30] the intensity of the transition may be taken as the sum of the squares of the central atom's atomic coefficients. For the $2t_2$, the intensity of the $K\beta$ band would then be proportional to 0.54 Although this neglects the contribution of ligand atoms, according to Manne's arguments it is a reasonable approximation and will be invoked here in the assignment of spectral bands.

Comparison of the CNDO calculated molecular energy levels ($\mathcal{E}_i$) with the experimental E_i values shows that the calculated values are consistently higher than the experimental; there is therefore no direct correlation between the two on an absolute value basis. However, the theoretical and experimental results may be correlated on a relative basis by comparing the differences between levels. For example, although $E_i(K) \neq \mathcal{E}_i$ and $E_j(L) \neq \mathcal{E}_j$, where $\mathcal{E}_i$ and $\mathcal{E}_j$ are the calculated ith and

jth molecular energy levels respectively, $E_i(K) - E_j(L)$ may be correlated with $\mathcal{E}_i - \mathcal{E}_j$. Similarly, comparing two bands in the same spectrum: $E_i(K) - E_m(K)$ may be correlated with $\mathcal{E}_i - \mathcal{E}_m$. Such a correlation is made here both as an evaluation of the CNDO program and as support for the assignments made.

Comparison of the CNDO results for PO_4^{-3} with those obtained by Hillier indicate the limitations and usefulness of this approximation approach. First of all, the CNDO calculation has reversed the ordering of the $2t_2$ and 1e levels; 1e is a π bonding level consisting of phosphorus 3d and oxygen 2p bonding, while the $2t_2$ level is predominantly a σ bonding level which gives rise to the main spectral band in Kβ. In view of the considerable separation between these two levels (2.8 eV) indicated by Hillier's calculations, this is the most serious discrepancy in the CNDO calculation. The second notable feature is the over-all lower energies obtained by the CNDO method, which may be attributable to the choice of atomic parameters used to describe the molecular system. This discrepancy does not hinder the assignment. A significant discrepancy does exist, however, in the atomic components listed for the $3t_2$ level. According to Hillier, this level consists of phosphorus 3d and oxygen 2s and 2p; the CNDO calculation, however, indicates a significant contribution from the phosphorus 3p. In effect, then, according to Manne's intensity agruments, two transitions would be observed in the Kβ according to Hillier's ab initio calculations ($1t_2$ and $2t_2$), while three transitions are possible according to the CNDO results ($1t_2$, $2t_2$, $3t_2$), although the transition due to $3t_2$ would be weaker than that from either $1t_2$ or $2t_2$. Note in Figure 31 that only two Kβ bands are observed in agreement with the more rigorous calculations. The CNDO calculations

do, however, give a fair qualitative representation of the bonding. While the relatively close-lying levels may be reversed, the over-all ordering is in fair agreement with more rigorous calculations and the qualitative atomic contribution to molecular orbitals may be deduced.

The CNDO calculations offered here are not meant as a quantitative description of the electronic structure of the molecules but rather as a qualitative guide to assignment of spectral features and understanding of the over-all, general bonding. In particular, it is desirable to have CNDO-calculated evidence for the origin of the $K\beta_x$ band noted experimentally in all of the molecules except PO_4^{-3}. The growth of this $K\beta_x$ band with increasing substitution of a hydroxy ligand for an oxygen ligand suggests that it may be due to the presence of two different types of ligands and not necessarily to just a lowering of symmetry. CNDO-calculated evidence for a set of energy levels due to the presence of a second ligand type would yield considerable support for such an assignment.

With all of the necessary information now available, each compound will be discussed individually.

$Ca_3(PO_4)_2$ (Td): Tribasic calcium phosphate

Since only $t_2 \longrightarrow a_1$ transitions are allowed in $K\beta$ the assignment follows immediately, in accordance with identical assignment for these transitions for ClO_4^- and SO_4^{-2}, as shown by Andermann and Whitehead.[12]

$$K\beta : 2t_2 \longrightarrow 1s$$

$$K\beta' : 1t_2 \longrightarrow 1s$$

According to the energy-level diagram (Tables 5 and 6), a transition from $3t_2$ is also allowed on the high-energy side of the $K\beta$, but this is not

Table 6

CNDO-Calculated Electronic Structure of PO_4^{-3}

Valence Orbital	Energy	Atomic Components				
		Phosphorus Orbital			Oxygen Orbital	
		3s	$\sum$3p	$\sum$3d	$\sum$2s	$\sum$2p
$1t_1$	11.71 eV	0	0	0	(0)(0)*	(7.15)(0)*
$3t_2$	10.49	0	0.76	--	(0)(0.52)*	(5.71)(0.80)*
		--	--	1.22	(0.09)(0.86)*	(9.91)(0.90)*
$2t_2$	6.93	0	1.48	--	(0)(0.49)*	(5.05)(1.87)*
		--	--	0.86	(0.77)(0.08)*	(4.60)(4.84)*
1e	6.90	0	0	1.24	(0)(0)*	(5.70)(2.44)*
$2a_1$	5.53	0.53	0	0	(0)(0.80)*	(2.04)(0)*
$1t_2$	-10.06	0	0.94	--	(4.43)(0)*	(0.20)(0.12)*
		--	--	0.87	(7.26)(0)*	(0.17)(0.27)*
$1a_1$	-12.19	0.49	0	0	(1.72)(0)*	(0.30)(0)*

*Indicates antibonding contribution.

observed here or for other similar compounds.[16,17] This is in agreement with Manne's arguments, since the 3p atomic contribution to this molecular orbital is small (CNDO) or zero (Hillier).

The assignment of the $L_{2,3}$ spectrum is less straightforward as a_1, t_2, e and t_1 are all allowed. As seen in Table 4, $E_i(K\beta)$ lies almost directly between $E_i(L(A))$ and $E_i(L(B))$ so that apparently these three molecular levels produce separate transitions, with L(A) and L(B) originating in molecular orbitals lying respectively above and below that for $K\beta$. L(A) is then associated with the $(3t_2 + 1e)$ levels and L(B) with the $2a_1$ level.

$E_i(L(C))$ is of about the same value as $E_i(K\beta')$, suggesting a transition from a molecular orbital with a large oxygen 2s coefficient. However, this value is about 2 eV below that for $E_i(K\beta')$, this being approximately the difference between $E_i(K\beta')$ and $E_i(L(C))$ for all subsequent compounds, suggesting that the lower-lying $1a_1$ is involved. Since $1a_1$ has a large 3s coefficient and $1t_2$ a large 3d coefficient, both orbitals may be active in $L_{2,3}$.

A reasonable $L_{2,3}$ spectral assignment is then as follows:

$$L(A): \quad 3t_2 + 1e \longrightarrow 2p$$

$$L(B): \quad 2a_1 \longrightarrow 2p$$

$$L(C): \quad 1a_1 + 1t_2 \longrightarrow 2p$$

The $1t_1$ orbital has not been included in the L(A) band since it is composed solely of oxygen 2p orbitals and is nonbonding.

Further evidence for the above assignment comes from comparison of the relative internal consistency of the experimental results with the calculations of Hillier and those of our CNDO program. These data are

given in Table 7. In the first column is given the experimental $E_i(K)-E_j(L)$, $E_i(K)-E_m(K)$, or $E_j(L)-E_n(L)$ values, while the corresponding calculated $\mathcal{E}_i-\mathcal{E}_j$, $\mathcal{E}_i-\mathcal{E}_m$ or $\mathcal{E}_j-\mathcal{E}_n$ values are given in columns 2 and 3. The values in parentheses under the CNDO column are the values obtained when only $3t_2$ instead of $3t_2$+1e is used for the L(A) band, since the CNDO calculation reverses the order for $2t_2$ and 1e, thus giving too low a value for 1e. When this value in parenthesis is used, the correlation with Hillier's calculations improves greatly. Agreement between Hillier's values and experimental values is very good and lends considerable support to the assignment made above. A correlation diagram aligning the $K\beta$ and $L_{2,3}$ spectra with one another by means of their $E_i(K)$ and $E_j(L)$ values is given in Figure 42. This diagram further directly correlates the experimentally determined E_i values with the theoretically determined E_i values; the s, p and d intensity parameters determined by the sum of the squares of the individual eigenvectors in each molecular orbital (see equation 3) are also indicated for each level. It is these intensity parameters that determine the intensity of a transition according to Manne's arguments. Thus all of the pertinent spectral and calculated data are correlated on a single scale by this diagram.

Note that the $E_i(K)$ and $E_i(L)$ values occur in the order:

$$E_i(L(C)) < E_i(K\beta') << E_i(L(B)) < E_i(K\beta) < E_i(L(A))$$

in agreement with the calculated molecular energy level sequence:

$$1a_1 < 1t_2 << 2a_1 < 2t_2 < (1e + 3t_2)$$

Hillier et al. have made the same assignment and further cite photoelectron data to support the assignment. Hillier's group observes three spectral regions upon ionization of the valence shell; first, a low-energy broad

Table 7

Comparison of Calculated Eigenvalues ($\mathcal{E}$) with Experimental Energy Levels (E)

$E_i - E_j$	$\mathcal{E}_i - \mathcal{E}_j$ (Hillier)	$\mathcal{E}_i - \mathcal{E}_j$ (CNDO)
PKβ - PL(B)	$2t_2 - 2a_1$	$2t_2 - 2a_1$
-8.87 - (-12.5)	9.0 - 6.1	6.93 - 5.53
3.6 eV	2.9 eV	1.40 eV
PL(A) - PL(B)	$(3t_2+1e) - 2a_1$	$(3t_2+1e) - 2a_1$
-5.7 - (-12.5)	12.7 - 6.1	8.70 - 5.53
6.8 eV	6.6 eV	3.17 eV (4.96)
PL(A) - PKβ	$(3t_2+1e) - 2t_2$	$(3t_2+1e) - 2t_2$
-5.7 - (- 8.87)	12.7 - 9.0	8.70 - 6.93
3.2 eV	3.7 eV	1.77 eV (3.56)
PL(A) - PL(C)	$(3t_2+1e) - 1a_1$	$(3t_2+1e) - 1a_1$
-5.7 - (-24.3)	12.7 - (-11.6)	8.70 - (-12.19)
18.6 eV	24.3 eV	20.89 eV (22.68)
PKβ - PKβ'	$2t_2 - 1t_2$	$2t_2 - 1t_2$
-8.87 - (-22.07)	9.0 - (-8.9)	6.93 - (-10.06)
13.20 eV	17.9 eV	16.99 eV

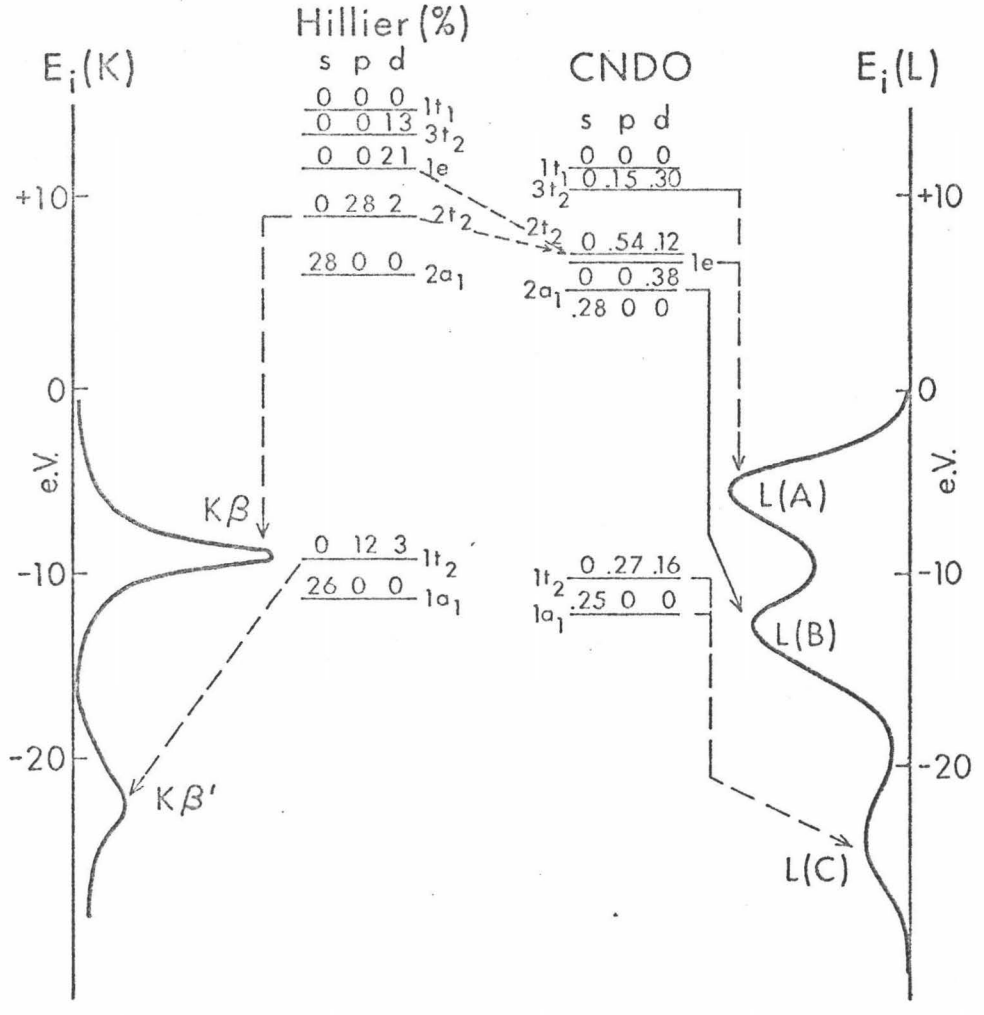

Figure 42

Correlation Diagram for PO_4^{-3}

band is assigned to the ($1t_1 + 3t_2 + 1e$) molecular orbitals and is taken to represent 3d orbital participation in the bonding of PO_4^{-3}; at higher energy, a doublet with 2.5 eV separation is attributed to the ($2t_2 + 2a_1$) orbitals; and at about 11.6 eV to higher energies, a not-well-resolved doublet is assigned as ionization from the $1a_1 + 1t_2$ levels.

This information then correlates with Hillier's $K\beta$ and $L_{2,3}$ assignments which are the same as made here. However, Hillier bases his $L_{2,3}$ assignment for PO_4^{-3} on spectra obtained by Nefedov et al.,[14] but KH_2PO_4 was used for their experimental work, and we have assigned a C_{2v} not a T_d symmetry to this compound. Our $L_{2,3}$ spectrum is from Wiech[41] who used Na_3PO_4 which is of T_d symmetry and reflects the true bonding situation. For his photoelectron work, however, Hillier does use a T_d phosphate, Li_3PO_4, and his work is not suspect.

The assignment of $K\beta$ and $L_{2,3}$ spectra made here stresses three factors. First, for PO_4^{-3} the $K\beta$ and $L_{2,3}$ spectra are mutually exclusive. Second, it is important to consider both energy and intensity factors in making spectral assignments; as witnessed, for example, in the inclusion of both $1a_1$ and $1t_2$ in the L(C) band and in the absence of a transition in $K\beta$ from the "allowed" $3t_2$ level. Third, evidently 3d orbital participation is significant in bonding for phosphorus, as seen in the assignment of the L(A) band and the significant 3d coefficients resulting from Hillier's ab initio calculations. The $K\beta$ spectrum then consists of transitions from molecular orbitals with large 3p coefficients, while the $L_{2,3}$ spectrum reflects significant 3s and 3d contributions to the molecular orbitals. To make a significant spectral contribution it is not sufficient for a transition to be merely "allowed," it must be of sufficient intensity

to be "observed." This consideration is particularly interesting in the contention made here for 3d orbital participation in the bonding. The absence of a transition in $K\beta$ for $3t_2$ suggests that either the $3t_2 + 1e + 1t_1$ orbitals are completely nonbonding and are localized on oxygen, or that the electron density has been significantly shifted to other orbitals on phosphorus. The former case would give transitions which, according to Manne's arguments, would not be observed in either $K\beta$ or $L_{2,3}$, but the latter case would give a transition active either in $K\beta$ or in $L_{2,3}$ depending upon whether the oxygen 2p orbitals have become bonding with phosphorus 3p or 3d orbitals. Assuming the participation of phosphorus 3d orbitals in bonding, this then would be the situation for the observance of band A in $L_{2,3}$ and the lack of a transition from $3t_2$ in $K\beta$. If phosphorus 3p orbitals participate at all in this bonding, then the transition would become active in $K\beta$, and it is possible to calculate where this band would be observed; it may, for example, be active but concealed in the main $K\beta$ band. If both phosphorus 3p and 3d orbitals participate in this bonding with oxygen 2p then the same molecular orbital will give rise to both $K\beta''$ and $L_{2,3}(A)$ bands, $E_i(K\beta'') = E_i(L(A)) = -5.7$ eV, and then:

$$E_i(K\beta'') = h\nu - \bar{v}_k = -5.7 \text{ eV}$$

$$h\nu - 2146.57 \text{ eV} = -5.7 \text{ eV}$$

$$h\nu(K\beta'') = 2140.8 \text{ eV}$$

Examination of the $K\beta$ spectrum at 2141 eV reveals a region removed from the main $K\beta$ band and of small intensity, suggesting that phosphorus 3p orbitals do not participate in the bond and that $3t_2$ is not active in $K\beta$--in agreement with Hillier's calculations and the $K\beta$ assignment made here.

It is interesting to note, however, that 2141 eV is the region for the occurrence of the main band $PK\beta$ for elemental phosphorus (Figure 30). Furthermore, Table 4 shows that $E_i(K\beta)$ and $E_i(L(A))$ are in good agreement, suggesting that the high-energy bands in both spectra originate in the same molecular orbital. This orbital may then reflect P_{3p}-P_{3d} bonding which, from intensity arguments alone, would give transitions active in both $K\beta$ and $L_{2,3}$. Upon formation of the oxy-anions, this high-energy band in $K\beta$ is suppressed, while that at 2137 eV participates in bond formation as observed, for example, in the spectrum for PO_4^{-3}. Although this band disappears in $K\beta$, it increases in intensity in $L_{2,3}$ as may be expected due to greater electron density available in oxygen which can be transferred to phosphorus 3d. Since oxygen 2p has, in effect, replaced phosphorus 3p in this bonding, this band would not be observable in $K\beta$ according to Manne's arguments.

Although these spectral features are offered as further experimental support for phosphorus 3d orbital participation in bonding, it is not meant as conclusive evidence. It does, however, form substantial basis for inclusion of these orbitals in the spectral assignments made here.

In assigning the $K\beta$ and $L_{2,3}$ spectra for the other oxy-anions, a few spectral features are worth noting beforehand. First, the $L_{2,3}$ spectra for all of the compounds strongly resemble that for PO_4^{-3}, suggesting analogous transitions for these lower symmetry molecules. Furthermore, all molecular $L_{2,3}$ spectra are very similar to that for elemental phosphorus. Second, the L(A)-L(B) separation of about 4.5 eV is approximately the same as that for $K\beta$ - $K\beta_x$, suggesting mutual transitions.

$CaHPO_3$ (C_{3v}): Calcium phosphite

For C_{3v}, two transitions are allowed in Kβ: e $\longrightarrow$ a_1 and a_1 $\longrightarrow$ a_1 (Table 2).

This leads to the assignment of the main band in Kβ (Figure 35) to the close-lying $3a_1$+2e levels which must be the orbitals split from $2t_2$ in decreasing symmetry from T_d to C_{3v}. These orbitals have significant 3p coefficients and are bonding with oxygen 2p orbitals as seen in Table 8. The 3e level lies about 3 eV above 2e and its inclusion in Kβ is questionable; however, it has a very large phosphorus 3p contribution and a strong bonding coefficient with oxygen 2p. In view of the good correlation between the spectral assignment made for PO_4^{-3} and Manne's arguments, this orbital is included in the Kβ assignment. Furthermore, for HPO_3^{-2}, inclusion of this orbital accounts for the 50 percent increase in half-width for HPO_3^{-2} PKβ (3 eV) over PO_4^{-3} (2 eV), and also considerably improves the correlation between experimental and theoretical peak separations.

PKβ' lying about 14 eV below PKβ must be due to the 1e level which, as seen in Table 8, reflects very large oxygen 2s coefficient which is strongly bonding with phosphorus 3p.

$E_i(K\beta_x)$ lies 4.40 eV below $E_i(K\beta)$. According to the energy level sequence in Table 8 only one molecular level lies between Kβ and Kβ', this is the $2a_1$ level which, according to the CNDO calculations, lies 4.9 eV below the average energy value for the ($3a_1$+2e+3e) levels in good agreement with experiment. While the Kβ band corresponds to a transition from orbitals predominantly oxygen 2p and phosphorus 3p in nature, this $2a_1$ level is predominantly phosphorus 3s and 3p and hydrogen 1s in

Table 8

CNDO-Calculated Electronic Structure of HPO_3^{-2}

Valence Orbital	Energy	Atomic Components: Phosphorus Orbital			Hydrogen Orbital	Oxygen Orbital	
		3s	$\sum$3p	$\sum$3d	1s	$\sum$2s	$\sum$2p
$1a_2$	4.18 eV	0	0	0	(0)(0)*	(0)(0)*	(2.16)(0)*
4e	2.89	0	0.24	--	(0)(0)*	(0)(0.45)*	(5.42)(2.93)*
		--	--	1.34	(0)(0)*	(0.27)(0.71)*	(10.24)(4.24)*
$4a_1$	2.28 eV	0.10	--	--	(0)(0.46)*	(0)(0.15)*	(1.80)(0)*
		--	0.11	--	(0.46)(0)*	(0)(0.15)*	(1.80)(0)*
		--	--	0.43	(0.46)(0)*	(0)(0.15)*	(1.39)(0.41)*
3e	1.52	0	1.00	--	(0)(0)*	(0.05)(0.52)*	(5.84)(0.53)*
		--	--	1.08	(0)(0)*	(0.67)(0.67)*	(6.44)(6.36)*
2e	-1.39	0	0.68	--	(0)(0)*	(0)(0.29)*	(2.57)(1.37)*
		--	--	0.98	(0)(0)*	(0.29)(0.29)*	(5.06)(2.50)*
$3a_1$	-1.53	0.23	--	--	(0)(0.18)*	(0)(0.39)*	(1.50)(0.75)*
		--	0.43	--	(0.18)(0)*	(0)(0.54)*	(1.50)(0.75)*
		--	--	0.13	(0)(0.18)*	(0.39)(0)*	(2.11)(0)*
$2a_1$	-5.36	0.46	--	--	(0.60)(0)*	(0)(0.60)*	(1.14)(0)*
		--	0.35	--	(0.60)(0)*	(0.60)(0)*	(0)(1.14)*
		--	--	0.12	(0.60)(0)*	--	(0.44)(0.70)*
1e	-18.25	0	0.82	--	(0)(0)*	(4.20)(0.60)*	(0.21)(0.11)*
		--	--	0.91	(0)(0)*	(4.54)(0)*	(0.14)(0.17)*
$1a_1$	-20.62	0.47	0.11	0.09	(0.14)(0)*	(1.47)(0)*	(0.25)(0)*

*Denotes antibonding contribution.

character, and thus represents a strong bonding between hydrogen and phosphorus. $K\beta$ and $K\beta_x$ must then be considered as reflecting molecular orbitals formed by two different ligands with the central phosphorus atom.

The $K\beta$ spectrum is then assigned as:

$$K\beta : 3a_1 + 2e + 3e \longrightarrow 1s$$

$$K\beta_x : 2a_1 \longrightarrow 1s$$

$$K\beta' : 1e \longrightarrow 1s$$

where $K\beta$ and $K\beta'$ may be considered as representing the phosphorus-oxygen bonding and $K\beta_x$ the phosphorus-hydrogen bonding.

Again the $L_{2,3}$ spectral assignment is more difficult as a_1, a_2 and e are all active. The most obvious feature is the low-energy band C in Figure 39, corresponding to an $E_i(L(C))$ equal to -25 eV. This is analogous to the PO_4^{-3} spectrum and again $E_i(L(C))$ lies about 2 eV below $E_i(K\beta')$, as seen in Table 4, and is attributable to the $1a_1$ and 1e levels reflecting a large oxygen 2s contribution to the phosphorus-oxygen bond.

The L(A)-L(B) separation is 4.0 eV, compared to 4.4 eV for $PK\beta$ and $PK\beta_x$, a good correlation if these bands are attributable to the same molecular levels. However, both $E_i(L(A))$ and $E_i(L(B))$ lie on the high-energy side of $E_i(K(\beta))$ and $E_i(K\beta_x)$ by about 2 eV. Also, the strong resemblance between this spectrum and that for PO_4^{-3} suggests an analogous assignment. Lying above the orbitals active in $PK\beta$ are $4a_1$, 4e and $1a_2$; $1a_2$ is nonbonding and will not be observable; on the other hand, $4a_1$ and 4e have large 3d coefficients with oxygen 2p; they are assigned as the source of the L(A) band.

The L(B) band's origin is not immediately obvious. The band lies almost directly between $E_i(K\beta)$ and $E_i(K\beta_x)$, as seen in Table 4, and

cannot be associated with either of these levels. There is no molecular energy level lying between $2a_1$ ($K\beta_x$) and $3a_1 + 2e + 3e$ ($K\beta$) to which this band may be assigned.

$E_i(L(B))$ has a value of -11.9 eV, corresponding very nicely to the average value of $E_i(K\beta)$ and $E_i(K\beta_x)$ (-11.8 eV), and it thus appears that L(B) contains contributions from $2a_1$ and 2e + 3e levels. This assignment is, furthermore, consistent with an intensity assignment, as $2a_1$ has a significant 3s coefficient while 2e and 3e have very large 3d coefficients, and thus all three levels must be active in both $K\beta$ and $L_{2,3}$. Higher resolution of the $L_{2,3}$ spectrum is needed to resolve these two contributions to the L(B) band, but note that the $L_{2,3}$ spectrum bands are quite broad and may well conceal two or more transitions. While the $K\beta$ spectrum is nicely correlated with the P - O and P-H bonding for $K\beta$ and $K\beta_x$, respectively, the bands in $L_{2,3}$ are not so clearly defined. The $L_{2,3}$ assignment is then as follows:

$$PL(A) : \quad 4a_1 + 4e \longrightarrow 2p$$

$$PL(B) : \quad 2a_1 + 2e + 3e \longrightarrow 2p$$

$$PL(C) : \quad 1a_1 + 1e \longrightarrow 2p$$

Further support for the assignment comes from fairly good correlation between experimental values and the CNDO calculations, as seen in Table 9. The correlation diagram is shown in Figure 43.

$Ca(H_2PO_2)_2$ (C_{2v}): Calcium hypophosphite

For C_{2v}, a_1, b_1, and b_2 are all active. The $K\beta$ spectrum (Figure 36) for $H_2PO_2^-$ is similar to that for HPO_3^{-2}, suggesting the spectral distinction between the P - O and P - H bonds for $H_2PO_2^-$.

Table 9

Comparison of Calculated Eigenvalues ($\mathcal{E}$) with Experimental Levels (E)

HPO_3^{-2}

$E_i - E_j$	$\mathcal{E}_i - \mathcal{E}_j$ (CNDO)
$PK\beta - PK\beta_X$ -9.58 - 13.98 4.40 eV	$(3a_1+2e+3e) - 2a_1$ -0.47 - (-5.36) 4.89 eV
$PK\beta$ - PL(B) -9.58 - (11.9) 2.30 eV	$(3a_1+2e+3e) - \overline{/(2e+3e)+2a_1\_/}$ -0.47 - (-2.72) 2.25 eV
PL(A) - PL(B) -7.9 - (-11.9) 4.0 eV	$(4a_1+4e) - \overline{/(2e+3e)+2a_1\_/}$ 2.59 - (-2.72) 5.31 eV
PL(A) - $PK\beta$ -7.9 - (-9.58) 1.7 eV	$(4a_1+4e) - (3a_1+2e+3e)$ 2.59 - (-0.47) 3.06 eV
$PK\beta - PK\beta'$ -9.58 - (-23.08) 13.50 eV	$(3a_1+2e+3e) - 1e$ 0.47 - (-18.25) 17.78 eV

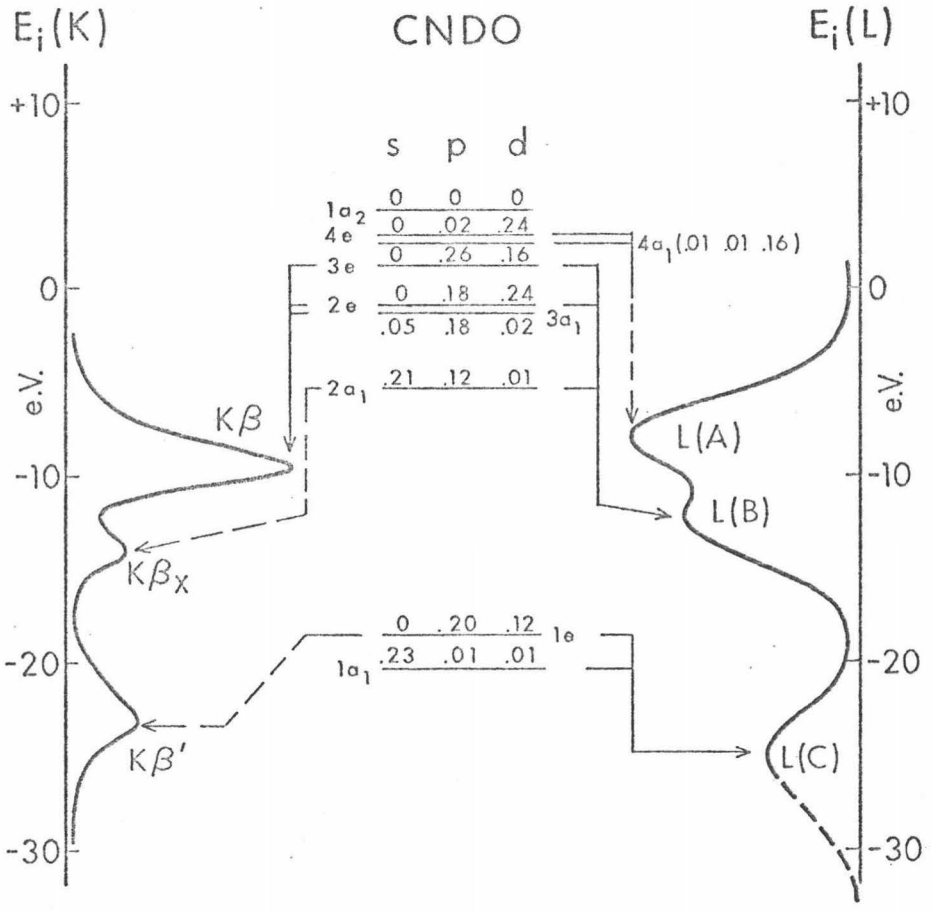

Figure 43

Correlation Diagram for HPO_3^{-2}

Investigation of the CNDO calculated electronic structure for $H_2PO_2^-$, Table 10, reveals three close-lying levels $2b_2$, $3b_2$, $3a_1$ with significant phosphorus 3p coefficients and which are strongly bonding with oxygen but nonbonding with hydrogen. These levels then define the P - O bonding and may be denoted as the $K\beta$ band.

About 4 eV below these levels lies another set of molecular energy levels with large phosphorus 3p coefficients which may give rise to the $K\beta_x$ band. The $1b_1$ level is only slightly bonding with both hydrogen and oxygen, while the $2a_1$ level has large bonding coefficients with both hydrogen 1s and oxygen 2s. The $2b_1$ level, however, has the largest 3p coefficient and is strongly bonding with hydrogen 1s only.

The two lowest-lying molecular levels, $1a_1$ and $1b_2$, again represent orbitals with very large oxygen 2s bonding coefficients and constitute the $K\beta'$ band. Note that for HPO_3^{-2} the lower-lying $1a_1$ level wasn't active in $K\beta$ although it has as large an oxygen 2s coefficient as does $1b_2$ for $H_2PO_2^-$; this is a typical example of the greater orbital mixing resulting from a lowering of symmetry.

The assignment for $H_2PO_2^-$ is then analogous to that for HPO_3^{-2};

$$K\beta : 2b_2 + 3b_2 + 3a_1 \longrightarrow 1s$$

$$K\beta_x : 2a_1 + 2b_1 + 1b_1 \longrightarrow 1s$$

$$K\beta' : 1a_1 + 1b_2 \longrightarrow 1s$$

It is interesting to note that the $K\beta$ band for $H_2PO_2^-$ has a half-width equal to that for HPO_3^{-2} (3 eV), which is consistent with the number of active molecular orbitals assigned to each band.

The $L_{2,3}$ spectrum (Figure 40) resembles that for PO_4^{-3} and HPO_3^{-2} and an analogous assignment is anticipated. $E_i(L(C))$ again lies about

Table 10

CNDO-Calculated Electronic Structure of $H_2PO_2^-$

Valence Orbital	Energy	Atomic Components: Phosphorus Orbital			Hydrogen Orbital	Oxygen Orbital	
		3s	$\sum$3p	$\sum$3d	$\sum$1s	$\sum$2s	$\sum$2p
$1a_2$	-5.92	0	0.02	0.43	(0)(0)*	(0)(0.08)*	(2.40)(1.68)*
$4a_1$	-6.80	0	0.10	--	(1.19)(0)*(0.02)(0.02)*		(1.34)(1.34)*
		--	--	0.74	(1.57)(0)*(0.04)(0.02)*		(1.82)(2.18)*
$3a_1$	-7.12	0.07	--	--	(0)(0.59)*	(0)(0.20)*	(1.78)(0)*
		--	0.41	--	(0.59)(0.33)*	(0)(0.40)*	(3.56)(0)*
		--	--	0.48	(0.59)(0.33)*	(0)(0.36)*	(2.72)(0.84)*
$3b_2$	-7.68	0	0.25	--	(0)(0)*	(0)(0.14)*	(1.36)(0.58)*
		--	--	0.50	(0)(0)*	(0.14)(0.14)*	(1.94)(1.94)*
$2b_2$	-7.71	0	0.41	--	(0)(0)*	(0)(0.22)*	(1.98)(0)*
		--	--	0.31	(0)(0)*	(0.22)(0.22)*	(1.94)(1.94)*
$2b_1$	-10.53	0.01	0.81	0.02	(1.23)(0)*	(0)(0)*	(1.16)(1.16)*
$1b_1$	-10.64	0.08	--	--	(0)(0.17)*	(0)(0.18)*	(1.14)(0.84)*
		--	0.51	--	(0.17)(0.10)*	(0)(0.36)*	(2.08)(1.68)*
		--	--	0.51	(0.20)(0.17)*	(0.36)(0.18)*	(4.80)(0.84)*
$2a_1$	-14.58	0.60	--	--	(0.80)(0)*	(0)(0.44)*	(0.88)(0)*
		--	0.34	--	(0.82)(0)*	(0.88)(0)*	(0)(0.76)*
		--	--	0.33	(1.20)(0.40)*	(1.32)(0)*	(0.34)(0.54)*
$1b_2$	-27.62	0	0.32	--	(0)(0)*	(1.30)(0)*	(0.03)(0.03)*
		--	--	0.33	(0)(0)*	(2.60)(0)*	(0.08)(0.04)*
$1a_1$	-29.26	0.41	--	--	(0.16)(0)*	(1.22)(0)*	(0.14)(0)*
		--	0.27	--	(0)(0.16)*	(2.44)(0)*	(0.28)(0)*
		--	--	0.26	(0)(0.32)*	(3.66)(0)*	(0.18)(0.10)*

*Indicates antibonding contribution.

2 eV below $E_i(K\beta')$ and is attributable to the $1a_1 + 1b_2$ levels with large oxygen 2s coefficients. Note that whereas for HPO_3^{-2} the lower energy of $E_i(L(C))$ compared to $E_i(K\beta')$ was due to the inclusion in L(C) of the lower energy $1a_1$ level, for $H_2PO_2^-$ both the $1a_1$ and $1b_2$ levels are active in both $K\beta$ and $L_{2,3}$, and the same energy may be expected for $E_i(K\beta')$ and $E_i(L(C))$. The occurrence of $E_i(L(C))$ at lower energy than $E_i(K\beta')$ may then be attributed to the much higher intensity of the $1a_1$ molecular level which will tend to "shift" the intensity maximum to a lower value.

$E_i(L(A))$ lies about 2 eV above $E_i(K\beta)$ and may be attributed to the bonding between phosphorus 3d orbitals and its ligands. The $4a_1$ and $1a_2$ molecular orbitals with their negligible 3p and large 3d coefficients are immediately assignable to the L(A) band. However, the $3a_1$ and $3b_2$ levels, assigned to $K\beta$, also have significant 3d coefficients--and they lie quite close in energy to the two higher energy orbitals. For $H_2PO_2^-$ as for HPO_3^{-2} there is, then, overlapping transitions in $K\beta$ and $L_{2,3}$--a result of the low symmetry of these molecules. It may be noted that the $4a_1$ level is strongly bonding with hydrogen but nonbonding with oxygen. Hydrogen then participates in bonding with both phosphorus 3p and 3d orbitals.

As for HPO_3^{-2}, the interesting spectral feature in $L_{2,3}$ for $H_2PO_2^-$ is the L(B) band. $E_i(L(B))$ lies only 0.60 eV above $E_i(K\beta_x)$, suggesting that the same molecular orbitals are active in both spectra. Investigation of the table shows that the $2a_1$ and $1b_1$ levels do have significant 3s and/or 3d coefficients and will be active in $L_{2,3}$. The $2b_1$ level, however, will not contribute due to insignificant 3s and 3d coefficients;

this is the orbital that has the largest hydrogen-bonding coefficient and it therefore follows that, as for HPO_3^{-2}, there is no clear distinction between P - O and P - H bonding in $L_{2,3}$ as appears to be the case with $K\beta$.

The $L_{2,3}$ spectrum then is assigned as:

$$L(A) : \quad 3b_2 + 3a_1 + 4a_1 + 1a_2 \longrightarrow 2p$$

$$L(B) : \quad 2a_1 + 1b_1 \longrightarrow 2p$$

$$L(C) : \quad 1a_1 + 1b_2 \longrightarrow 2p$$

The correlation diagram for $K\beta$ and $L_{2,3}$ for $H_2PO_2^-$ is given in Figure 44.

$Ca(H_2PO_4)_2$ (C_{2v}): Monobasic calcium phosphate

The $K\beta$ spectrum for $H_2PO_4^-$ (Figure 33) shows two high-energy bands which, in analogy with HPO_3^{-2} and $H_2PO_2^-$, may be due to the presence of two ligand types, although oxygen and hydroxy are not as distinctly differentiated as are oxygen and hydrogen, and the intensity of the $K\beta_x$ band is quite intense here. Investigation of the CNDO calculated structure, Table 12 reveals two molecular levels, $3a_1+2b_2$, with significant 3p coefficients, which are strongly bonding with the hydroxy ligand but exhibit very small coefficients with oxygen 2p. These levels are about 4 eV below the next set of levels, $4a_1$, $4b_2$, $5b_2$, and $4b_1$, which have significant bonding coefficients with oxygen but not with hydroxy. It therefore appears that there are two sets of energy levels again generated by two different types of ligands. However, there are two molecular orbitals, $2b_1+3b_1$, lying between those assigned to P - OH and P - O bonding which are antibonding and nonbonding, respectively, with hydroxy and only slightly bonding with oxygen. In energy they lie closer to the orbitals defining P - O bonding. The bonding in $H_2PO_4^-$ does not, then,

Table 11

Comparison of Calculated Eigenvalues ($\mathcal{E}$) with Experimental Energy Levels (E)

$H_2PO_2^-$

$E_i - E_j$	$\mathcal{E}_i - \mathcal{E}_j$
$PK\beta - PK\beta_X$	$(2b_2+3b_2+3a_1) - (2a_1+1b_1+2b_1)$
-8.87 - (-13.59)	-7.50 - (-11.92)
4.72 eV	4.42 eV
$PK\beta - PL(B)$	$(2b_2+3b_2+3a_1) - (2a_1+1b_1)$
-8.87 - (-13.0)	-7.50 - (-12.61)
4.13 eV	5.11 eV
PL(A) - PL(B)	$(3b_2+3a_1+4a_1+1a_2) - (2a_1+1b_1)$
-6.4 - (-13.0)	-6.88 - (-12.61)
6.6 eV	5.73 eV
PL(A) - $PK\beta$	$(3b_2+3a_1+4a_1+1a_2) - (2b_2+3b_2+3a_1)$
-6.4 - (-8.87)	-6.88 - (-7.50)
2.47 eV	0.62 eV
$PK\beta - PK\beta'$	$(2b_2+3b_2+3a_1) - (1a_1+1b_2)$
-8.87 - (-22.40)	-7.50 - (-28.44)
13.53 eV	20.94 eV

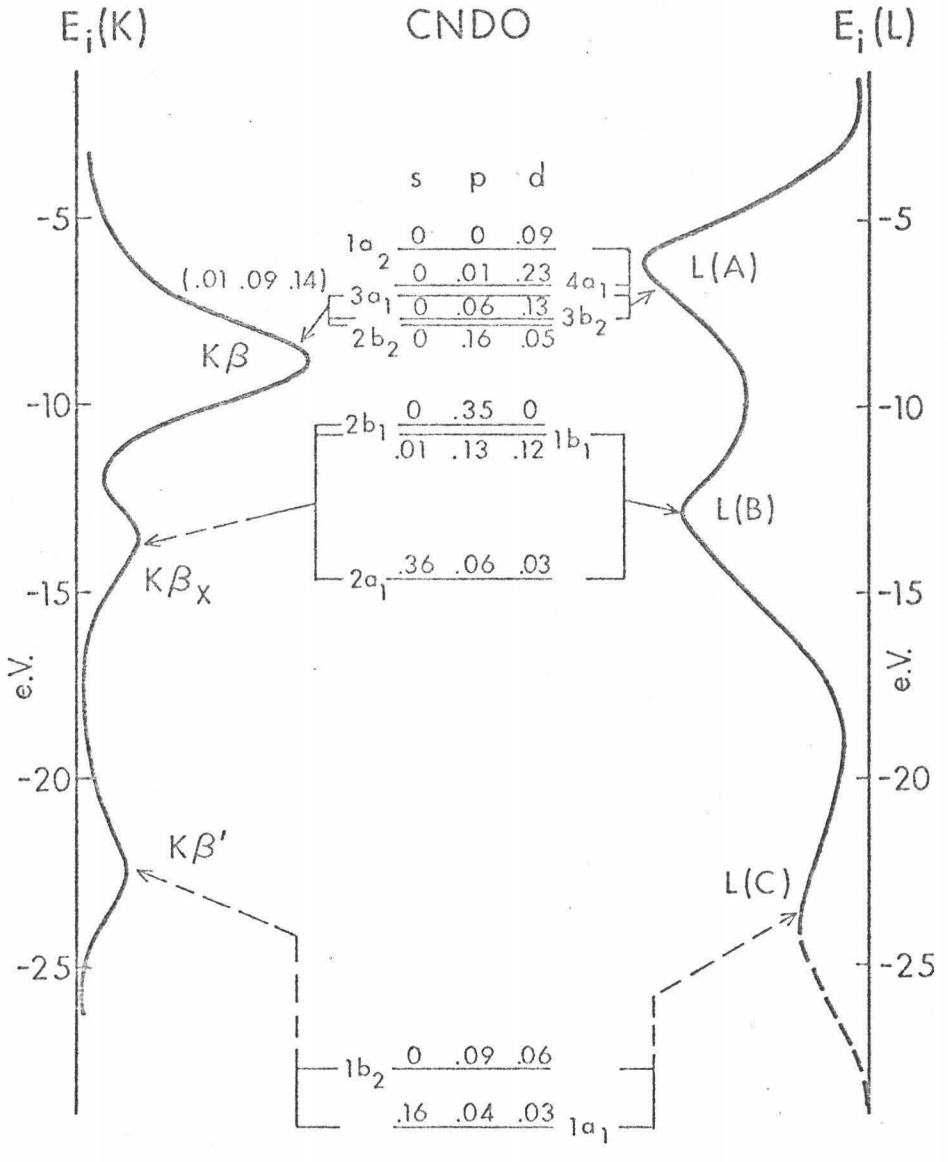

Figure 44

Correlation Diagram for $H_2PO_2^-$

Table 12

CNDO-Calculated Electronic Structure of $H_2PO_4^-$

Valence Orbital	Energy	Atomic Components: Phosphorus Orbital			Oxygen Orbital		"Hydroxy"** Orbital	
		3s	Σ3p	Σ3d	Σ2s	Σ2p	Σ2s	Σ2p
$6a_1$	-5.90	0	0.10	--	(0.03)(0)*	(1.01)(1.33)*	(0)(0)*	(0.68)(0.68)*
		--	--	0.29	(0)(0.04)*	(2.78)(0.36)*	(0)(0)*	(1.10)(0.94)*
$6b_2$	-6.60	0	0	0.28	(0)(0)*	(1.73)(0)*	(0)(0)*	(1.04)(1.04)*
$4b_1$	-6.66	0	0.49	--	(0)(0.36)*	(2.16)(0)*	(0)(0)*	(0.56)(0.56)*
		--	--	0.39	(0)(0.48)*	(2.36)(0.57)*	(0)(0)*	(0.78)(0.68)*
$5b_2$	-7.30	0	0.17	--	(0)(0)*	(1.02)(0)*	(0)(0.08)*	(0.42)(1.10)*
		--	--	0.24	(0)(0)*	(1.02)(0.52)*	(0.16)(0)*	(2.62)(0.42)*
$5a_1$	-8.44	0.33	--	--	(0)(0.32)*	(0.99)(0.08)*	(0)(0.24)*	(0)(0.70)*
		--	0.11	--	(0.16)(0.32)*	(1.08)(0.81)*	(0.48)(0)*	(1.40)(0)*
		--	--	0.52	(0.16)(0.48)*	(2.44)(0.16)*	(0.72)(0)*	(1.74)(0.36)*
$4b_2$	-10.60	0	0.19	--	(0)(0)*	(0.68)(0)*	(0)(0.14)*	(0.98)(0.84)*
		--	--	0.44	(0)(0)*	(0.68)(0.34)*	(0.28)(0)*	(1.68)(1.96)*
$4a_1$	-10.81	0.18	--	--	(0)(0.22)*	(0.86)(0)*	(0)(0.06)*	(0)(0.22)*
		--	0.45	--	(0.11)(0.22)*	(1.40)(0.61)*	(0.12)(0)*	(0.44)(0)*
		--	--	0.49	(0.22)(0.22)*	(1.75)(0.87)*	(0.06)(0.12)*	(0.22)(0.44)*

Table 12 (Continued)

CNDO-Calculated Electronic Structure of $H_2PO_4^-$

Valence Orbital	Energy	Atomic Components: Phosphorus Orbital 3s	Phosphorus Orbital Σ3p	Phosphorus Orbital Σ3d	Oxygen Orbital Σ2s	Oxygen Orbital Σ2p	"Hydroxy"** Orbital Σ2s	"Hydroxy"** Orbital Σ2p
$3b_1$	-12.09	0	0.43	--	(0)(0.21)*	(0.75)(0.24)*	(0)(0)*	(1.68)(1.68)*
		--	--	0.38	(0.29)(0)*	(0.82)(0.54)*	(0)(0)*	(2.32)(2.42)*
$3b_2$	-12.17	0	0	0.54	(0)(0)*	(0.93)(0)*	(0)(0)*	(1.58)(1.58)*
$2b_1$	-12.20	0.05	--	--	(0)(0.11)*	(0.21)(0)*	(0)(0)*	(1.46)(0.72)*
		--	0.29	--	(0)(0.11)*	(0.21)(0.13)*	(0)(0)*	(1.44)(2.90)*
		--	--	0.47	(0.11)(0.12)*	(0.14)(0.32)*	(0)(0)*	(5.08)(1.46)*
$2b_2$	-14.66	0	0.36	--	(0)(0)*	(0.28)(0)*	(0.20)(0)*	(1.74)(0)*
		--	--	0.15	(0)(0)*	(0.14)(0.28)*	(0.40)(0)*	(3.48)(0)*
$3a_1$	-16.15	0.38	--	--	(0)(0.28)*	(0.30)(0)*	(0.06)(0)*	(1.52)(0)*
		--	0.26	--	(0.28)(0.14)*	(0.20)(0.30)*	(0.12)(0)*	(3.04)(0)*
		--	--	0.17	(0.42)(0.14)*	(0.02)(0.64)*	(0.18)(0)*	(2.88)(1.68)*
$1b_1$	-27.92	0	0.42	--	(1.93)(0)*	(0.01)(0.02)*	(0)(0)*	(0.10)(0.08)*
		--	--	0.37	(2.57)(0)*	(0)(0.03)*	(0)(0)*	(0.16)(0.14)*
$2a_1$	-28.89	0.31	--	--	(1.21)(0)*	(0)(0.08)*	(0)(0.30)*	(0.18)(0)*
		--	0.33	--	(1.21)(0.61)*	(0.09)(0.05)*	(0.60)(0)*	(0)(0.36)*
		--	--	0.34	(1.82)(0.61)*	(0.15)(0.04)*	(1.80)(0)*	(0.12)(0.42)*

Table 12 (Continued)

CNDO-Calculated Electronic Structure of $H_2PO_4^-$

Valence Orbital	Energy	Atomic Components						
		Phosphorus Orbital			Oxygen Orbital		"Hydroxy"** Orbital	
		3s	Σ3p	Σ3d	Σ2s	Σ2p	Σ2s	Σ2p
$1b_2$	-32.42	0	0.24	--	(0)(0)*	(0.04)(0)*	(1.22)(0)*	(0)(0.08)*
		--	--	0.26	(0)(0)*	(0.02)(0.04)*	(2.44)(0)*	(0)(0.16)*
$1a_1$	-33.27	0.35	--	--	(0.27)(0)*	(0.09)(0)*	(1.18)(0)*	(0)(0)*
		--	0.16	--	(0.13)(0.27)*	(0.06)(0.09)*	(2.39)(0)*	(0)(0)*
		--	--	0.17	(0.26)(0.27)*	(0.01)(0.08)*	(3.54)(0)*	(0)(0)*

*Denotes antibonding contribution..

**"Hydroxy" orbitals denote the orbitals of the oxygen atoms bonded to hydrogen so as to form the "hydroxy" ligand as compared to the non-hydrogenated oxygen ligands; the hydrogen orbitals have not been included in the orbitals denoted as "hydroxy."

The term "hydroxy" is meant merely to distinguish between the hydrogenated and non-hydrogenated oxygen ligands.

directly parallel the case for $H_2PO_2^-$, which is of the same symmetry, but rather appears to offer a continuing series of molecular orbitals which change from predominantly $P_{3p} - O_{2p}H$ in nature to predominantly $P_{3p} - O_{2p}$, in proceeding to higher energies. This is more clearly seen from the bonding coefficients for the two ligands; there is a change from a strongly bonding hydroxy ligand to nonbonding to antibonding, and smaller over-all coefficients in proceeding from $3a_1$ through $4b_1$. In the same series the oxygen ligand's coefficients change from weakly bonding to very strongly bonding. Therefore, while there is some justification for assigning the $K\beta$ and $K\beta_x$ bands to molecular orbitals composed of phosphorus with oxygen and hydroxy ligands, respectively, it is more pertinent to denote the $K\beta$ spectrum as a superposition of two $K\beta$ emission spectra, one describing the P - O, and the other the P - OH bonding. This difference between $H_2PO_4^-$ and $H_2PO_2^-$ is a result of the similarities of the oxygen and hydroxy ligands as compared with the oxygen and hydrogen ligands, and also because of the larger number of orbitals for $H_2PO_4^-$ which may interact.

The $K\beta'$ band must again be due to a transition from a molecular orbital which corresponds to phosphorus 3p--oxygen 2s bonding. Three orbitals are active in $K\beta'$ for H_2PO_4: $1b_2 + 2a_1 + 1b_1$, all with significant phosphorus 3p coefficients, although the $1b_1$ orbital will probably contribute the most to the band's intensity. Note that the CNDO calculation indicates a 4 eV separation between $1a_1 + 1b_2$ and $2a_1 + 1b_1$ and, furthermore, indicates that the $1a_1 + 1b_2$ orbitals are due to phosphorus 3p-hydroxy 2s bonding, while the $2a_1 + 1b_1$ orbitals similarly describe phosphorus 3p-oxygen 2s bonding. Only one transition is noted here, however, and it must contain contributions from both $P - O_{2s}H$ and $P - O_{2s}$.

The $K\beta$ spectrum is then assigned as:

$$K\beta : 4a_1 + 4b_2 + 5b_2 + 4b_1 \longrightarrow 1s$$

$$K\beta_x : 3a_1 + 2b_2 + 2b_1 + 3b_1 \longrightarrow 1s$$

$$K\beta' : 1b_2 + 2a_1 + 1b_1 \longrightarrow 1s$$

Again the $L_{2,3}$ spectrum is more difficult to assign, especially here, due to the large mixing of orbitals. The $L_{2,3}$ spectrum is shown in Figure 41. The following E_i arrangement holds for $H_2PO_4^-$, which is the same as for $H_2PO_2^-$, and may be of use in assigning the $L_{2,3}$ spectrum for $H_2PO_4^-$:

$$E_i(L(C)) < E_i(K\beta') \ll E_i(L(B)) \leq E_i(K\beta_x) < E_i(K\beta) < E_i(L(A))$$

It appears that the molecular orbitals active in $K\beta_x$ are also active in L(B), while L(A) again reflects phosphorus 3d-oxygen 2p bonding. As with all previous molecules, the L(C) band lies about 2 eV below that for $E_i(K\beta')$; the lower energy of $E_i(L(C))$ must be due to the contributing intensity of the $1a_1$ orbital which will "shift" the peak maximum to a lower average value.

The $L_{2,3}$ spectrum is then assigned as:

$$L(A) : 4a_1 + 4b_2 + 5a_1 + 5b_2 + 4b_1 + 6b_2 + 6a_1 \longrightarrow 2p$$

$$L(B) : 3a_1 + 2b_1 + 3b_2 + 3b_1 \longrightarrow 2p$$

$$L(C) : 1a_1 + 1b_2 + 2a_1 + 1b_1 \longrightarrow 2p$$

This assignment shows that the $L_{2,3}$ and the $K\beta$ spectra share most of the same transitions with only $3b_2$, $6b_2$, and $6a_1$ being added to the $L_{2,3}$ assignment. The experimental and calculated values for the assignments made here are compared in Table 13. Note that the agreement is not as good as for PO_4^{-3}, HPO_3^{-2}, and $H_2PO_2^-$, a factor directly reflecting the greater mixing of orbitals for the very similar oxygen and hydroxy

Table 13

Comparison of Calculated Eigenvalues ($\mathcal{E}$) with Experimental Energy Levels (E)

$H_2PO_4^-$

$E_i - E_j$	$\mathcal{E}_i - \mathcal{E}_j$
$PK\beta - PK\beta_x$ -9.84 - (-12.56) 2.72 eV	$(4a_1+4b_2+5b_2+4b_1) - (3a_1+2b_2+2b_1+3b_1)$ -8.84 - (-13.78) 4.94 eV
$PK\beta - PL(B)$ -9.84 - (-12.7) 2.86 eV	$(4a_1+4b_2+5b_2+4b_1) - (3a_1+2b_1+3b_2+3b_1)$ -8.84 - (-13.15) 4.31 eV
$PL(A) - PK\beta$ -8.4 - (-9.84) 1.44 eV	$(4a_1+4b_2+5a_1+5b_2+4b_1+6b_2+6a_1) - (4a_1+4b_2+5b_2+4b_1)$ -8.04 - (-8.84) 0.80 eV
$PL(A) - PL(B)$ -8.4 - (-12.17) 4.3 eV	$(4a_1+4b_2+5a_1+5b_2+4b_1+6b_2+6a_1) - (3a_1+2b_1+3b_2+3b_1)$ -8.04 - (-13.15) 5.11 eV
$PK\beta - PK\beta'$ -9.84 - (-23.7) 13.86 eV	$(4a_1+4b_2+5b_2+4b_1) - (1b_2+2a_1+1b_1)$ -8.84 - (-29.74) 20.90 eV

ligands; also note that the calculated values are generally greater than the experimental.

The correlation diagram for the two spectral series is given in Figure 45.

$CaHPO_4$ (C_{3v}): Dibasic calcium phosphate

No $L_{2,3}$ spectral data are available for HPO_4^{-2} and H_3PO_4, but on the basis of assignments made already, the $K\beta$ spectrum for the two molecules are interpretable.

For HPO_4^{-2}, the $K\beta$ spectrum of Figure 32 exhibits two high-energy bands as for other C_{3v} molecules. The $K\beta$-$K\beta_x$ separation is 3.37 eV. The CNDO calculation indicates two sets of energy levels corresponding to molecular orbitals with large phosphorus 3p-hydroxy 2p bonding coefficients ($3a_1 + 2e$) and phosphorus 3p-oxygen 2p bonding coefficients ($4a_1 + 3e + 5a_1 + 4e$). Notice that there is considerably more mixing of orbital coefficients for HPO_4^{-2} than for HPO_3^{-2}, which is also of C_{3v} symmetry but with two distinctly different ligands; however, the mixing is not as extensive as for the lower symmetry $H_2PO_4^-$ molecule.

The $K\beta'$ band contains transitions from the $1a_1$, $2a_1$, and 1e molecular orbitals, although the 1e level contributes the most intensity to the band and the peak maximum should, therefore, be centered near this transition.

The $K\beta$ spectrum may therefore be assigned as:

$$K\beta : 4a_1 + 3e + 5a_1 + 4e \longrightarrow 1s$$

$$K\beta_x : 3a_1 + 2e \longrightarrow 1s$$

$$K\beta' : 1a_1 + 2a_1 + 1e \longrightarrow 1s$$

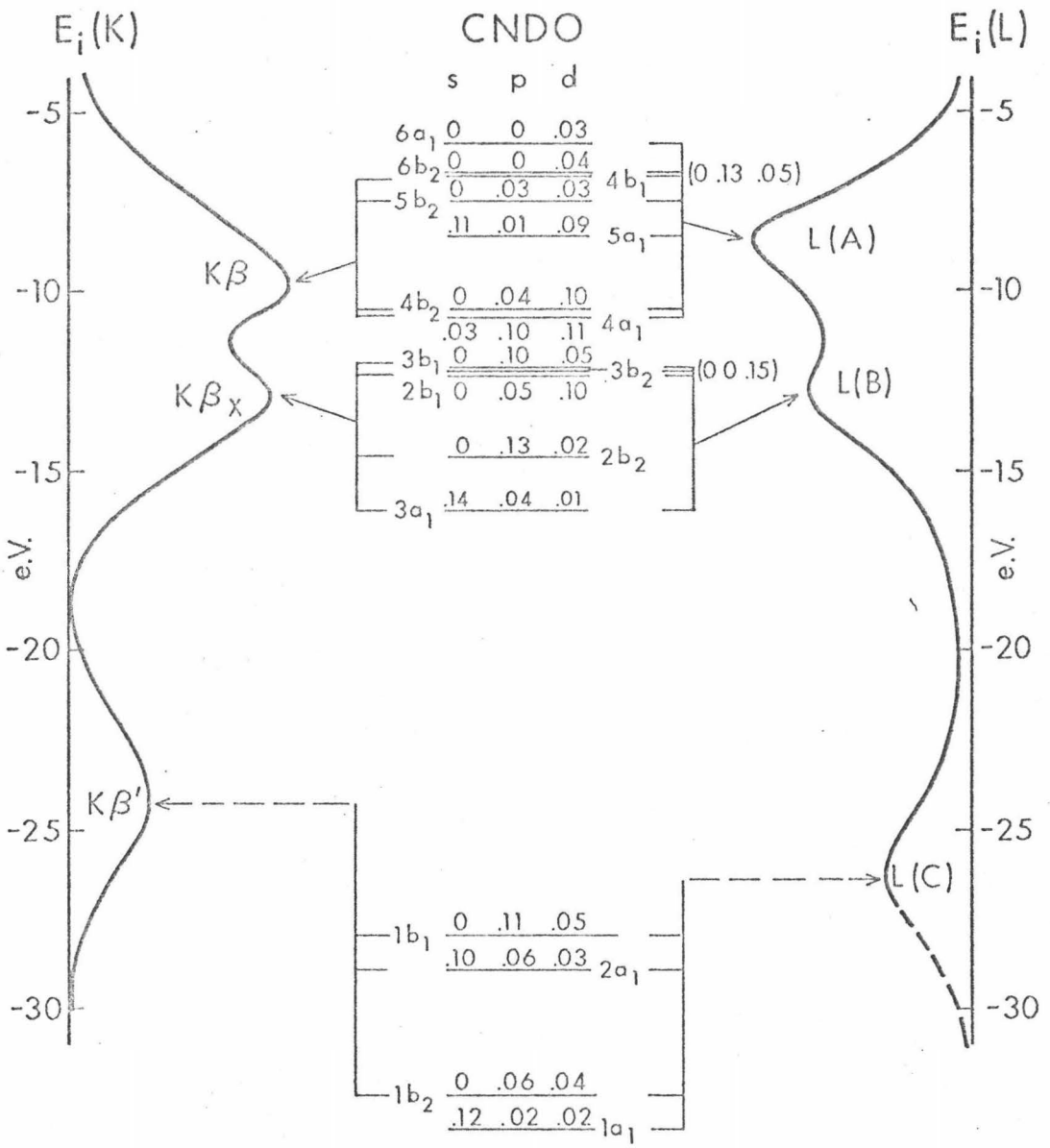

Figure 45

Correlation Diagram for $H_2PO_4^-$

Table 14

CNDO-Calculated Electronic Structure of HPO_4^{-2}

Valence Orbital	Energy	Atomic Components: Phosphorus Orbital			Oxygen Orbital		"Hydroxy"** Orbital	
		3s	Σ3p	Σ3d	Σ2s	Σ2p	Σ2s	Σ2p
$1a_2$	3.49	0	0	0	(0)(0)*	(2.18)(0)*	(0)(0)*	(0)(0)*
5e	2.58	0	0.10	--	(0.03)(0.30)*	(4.47)(3.31)*	(0)(0)*	(0.69)(0)*
		--	--	1.01	(0.07)(0.59)*	(9.09)(7.67)*	(0)(0)*	(0)(0.70)*
4e	1.88	0.02	0.80	--	(0.09)(0.68)*	(6.28)(1.04)*	(0)(0)*	(0)(0.11)*
		--	--	0.62	(0.09)(0.68)*	(6.38)(0.84)*	(0)(0)*	(0)(0)*
$5a_1$	-0.36	0.26	--	--	(0)(0.27)*	(1.72)(0)*	(0)(0.15)*	(0)(0.17)*
		--	0.22	--	(0.27)(0)*	(0)(0.72)*	(0)(0.15)*	(0)(0.17)*
		--	--	0.36	(0)(0.27)*	(1.65)(0.07)*	(0.15)(0)*	(0.17)(0)*
3e	-1.93	0.10	--	--	(0.07)(0.19)*	(1.63)(1.77)*	(0)(0.02)*	(0)(0.03)*
		--	0.82	--	(0.06)(0.41)*	(2.16)(1.82)*	(0)(0)*	(0.02)(0.03)*
		--	--	1.14	(0.41)(0.30)*	(5.55)(5.01)*	(0)(0)*	(0.02)(0.01)*
$4a_1$	-2.38	0.38	--	--	(0)(0.53)*	(1.63)(0.41)*	(0)(0.07)*	(0)(0.10)*
		--	0.38	--	(0)(0.53)*	(1.63)(0.41)*	(0.07)(0)*	(0.10)(0)*
		--	--	0.20	(1.26)(0.16)*	(3.56)(2.03)*	(0)(0.07)*	(0)(0.10)*
2e	-4.59	0.01	0.39	--	(0.03)(0.33)*	(1.58)(0.24)*	(0)(0)*	(2.40)(0)*
		--	--	0.79	(0.33)(0.03)*	(0.34)(1.56)*	(0)(0)*	(2.40)(0)*

Table 14 (Continued)

CNDO-Calculated Electronic Structure of HPO_4^{-2}

Valence Orbital	Energy	Atomic Components: Phosphorus Orbital			Oxygen Orbital		"Hydroxy"** Orbital	
		3s	Σ3p	Σ3d	Σ2s	Σ2p	Σ2s	Σ2p
$3a_1$	-8.34	0.25	--	--	(0)(0.30)*	(0.48)(0)*	(0.13)(0)*	(0.70)(0)*
		--	0.24	--	(0,30)(0)*	(0)(0.48)*	(0.13)(0)*	(0.70)(0)*
		--	--	0.11	(0.30)(0)*	(0.17)(0.31)*	(0.13)(0)*	(0.70)(0)*
1e	-18.87	0.04	--	--	(1.53)(1.46)*	(0.07)(0.06)*	(0)(0.02)*	(0.02)(0)*
		--	0.78	--	(4.19)(0.44)*	(0.18)(0.10)*	(0)(0)*	(0.09)(0)*
		--	--	0.81	(5.48)(0)*	(0.16)(0.15)*	(0)(0)*	(0)(0.07)*
$2a_1$	-20.61	0.42	--	--	(1.48)(0)*	(0.19)(0)*	(0)(0.14)*	(0.07)(0)*
		--	0.20	--	(1.48)(0)*	(0.19)(0)*	(0.14)(0)*	(0)(0.07)*
		--	--	0.19	(1.48)(0)*	(0.06)(0.13)*	(0.14)(0)*	(0)(0.07)*
$1a_1$	-25.91	0.25	--	--	(0.22)(0)*	(0.14)(0)*	(0.85)(0)*	(0)(0.01)*
		--	0.18	--	(0)(0.22)*	(0)(0.14)*	(0.85)(0)*	(0)(0.01)*
		--	--	0.14	(0)(0.22)*	(0.06)(0.08)*	(0.85)(0)*	(0)(0.01)*

*Denotes antibonding contribution.

**"Hydroxy" denotes distinction between hydrogenated and non-hydrogenated oxygen ligands.

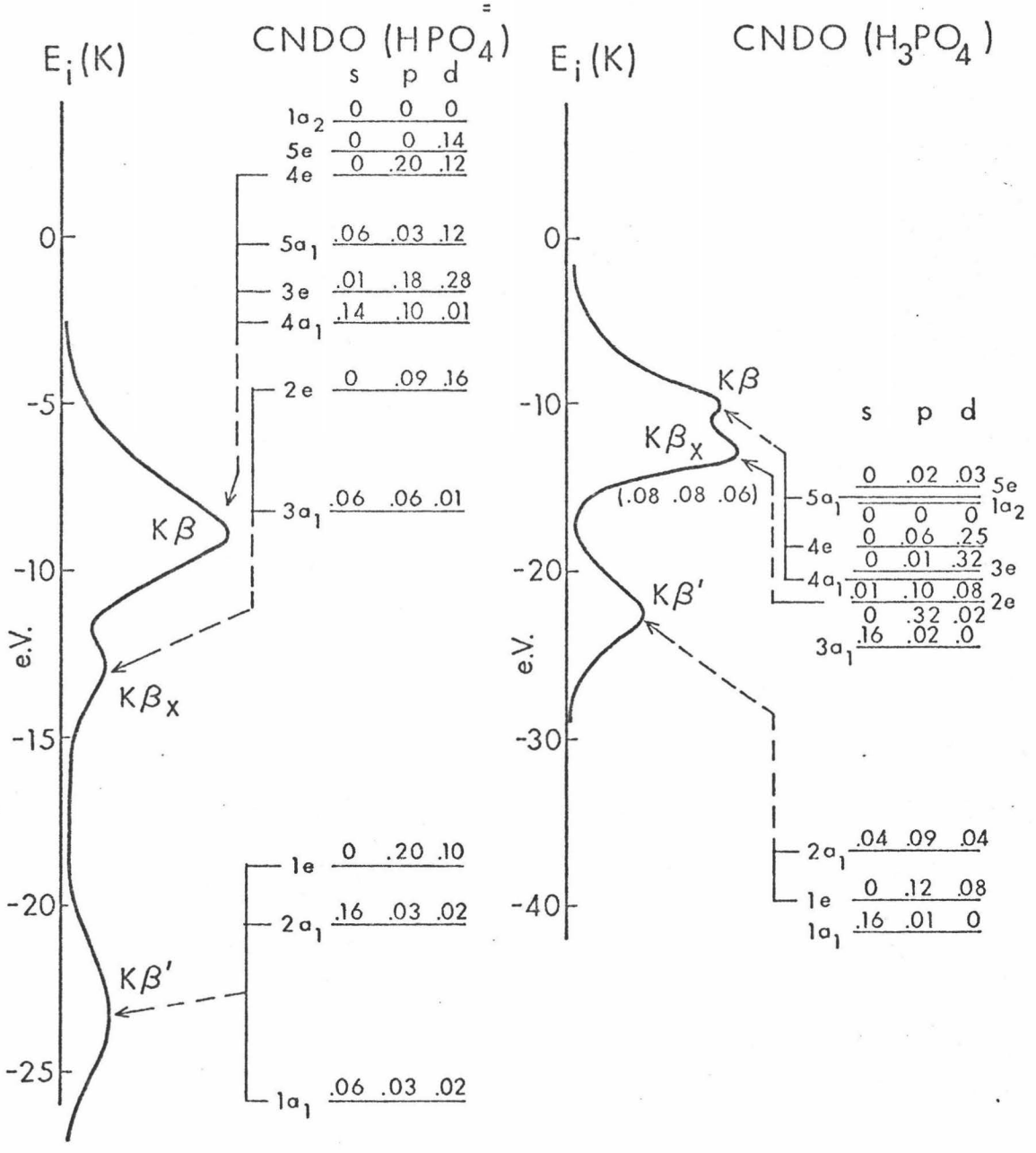

Figure 46

Correlation Diagrams for HPO_4^{-2} and H_3PO_4

The calculated $\mathcal{E}_i - \mathcal{E}_j$ value for $E_i(K\beta) - E_i(K\beta'_x)$ is 5.8 eV as compared with the experimental value of 3.4 eV. This assignment is shown diagrammatically in Figure 46.

H_3PO_4 C_{3v}: Phosphoric acid

Again, the two high-energy bands are obvious in the $K\beta$ spectrum for H_3PO_4 (see Figure 34); the lower energy band is anticipated to reflect the P - OH bonding and the higher energy band the P - O bonding. CNDO calculation, Table 15, shows two levels, $3a_1 + 2e$, which are strongly bonding between phosphorus 3p and hydroxy 2p, but only slightly bonding with oxygen 2p. These two levels may reasonably be attributed to $P_{3p} - O_{2p}H$ bonding. The higher-lying levels with significant phosphorus 3p coefficients have mixed bonding and antibonding coefficients with both oxygen and hydroxy ligands, although the over-all bonding with oxygen is greater than with the hydroxy ligand. The situation here, then, is similar to that for $H_2PO_4^-$, and the $K\beta$ spectrum may be described as a superimposed P - OH bonding contribution on a wide $K\beta$ band.

The $K\beta'$ band, in analogy with the other phosphorus oxy-anions, is attributable to the phosphorus 3p - oxygen 2s bonding molecular orbitals.

The $K\beta$ spectrum may then be assigned as:

$$K\beta : 4a_1 + 5a_1 + 4e \longrightarrow 1s$$

$$K\beta_x : 2e \longrightarrow 1s$$

$$K\beta' : 2a_1 + 1e \longrightarrow 1s$$

The experimental $K\beta - K\beta_x$ separation is 2.61 eV; the calculated $\mathcal{E}_i - \mathcal{E}_j$ value is 5.28 eV, a value considerably too large, as was the case for $\Delta\mathcal{E}_i$ values for $H_2PO_4^-$ and HPO_4^{-2}. The correlation between the experimental spectrum and the calculated electronic structure is shown diagrammatically in Figure 46.

Table 15

CNDO-Calculated Electronic Structure of H_3PO_4

Valence Orbital	Energy	Atomic Components: Phosphorus Orbital			Oxygen Orbital		"Hydroxy"** Orbital	
		3s	Σ3p	Σ3d	Σ2s	Σ2p	Σ2s	Σ2p
5e	-14.89	0	0.26	--	(0)(0)*	(1.91)(0)*	(0)(0)*	(2.07)(3.43)*
		--	--	0.42	(0)(0)*	(1.91)(0)*	(0)(0)*	(5.33)(3.08)*
$5a_1$	-15.57	0.29	--	--	(0)(0.22)*	(0.75)(0)*	(0)(0.24)*	(0)(0.82)*
		--	0.30	--	(0)(0.22)*	(0.75)(0)*	(0.24)(0)*	(0.82)(0)*
		--	--	0.26	(0)(0.22)*	(0.75)(0)*	(0.24)(0)*	(0.65)(0.17)*
$1a_2$	-15.86	0	0	0	(0)(0)*	(0.02)(0)*	(0)(0)*	(2.18)(0)*
4e	-18.56	0	0.47	--	(0)(0)*	(1.35)(0)*	(0.05)(0.52)*	(3.23)(3.97)*
		--	--	1.38	(0)(0)*	(1.35)(0)*	(1.04)(0.10)*	(8.82)(5.88)*
3e	-20.21	0.05	0.20	--	(0)(0.04)*	(0.46)(0)*	(0.17)(0.07)*	(3.68)(3.55)*
		--	--	1.66	(0)(0)*	(0.73)(0)*	(0.22)(0.22)*	(7.18)(6.39)*
$4a_1$	-20.46	0.11	--	--	(0)(0.10)*	(0.19)(0)*	(0.02)(0.01)*	(1.34)(0.74)*
		--	0.34	--	(0)(0.10)*	(0.19)(0)*	(0.01)(0.02)*	(0.74)(1.34)*
		--	--	0.48	(0.10)(0)*	(0.08)(0.19)*	(0.05)(0.04)*	(3.63)(2.61)*
2e	-21.97	0.02	0.87	--	(0)(0)*	(0.29)(0)*	(0.27)(0)*	(3.70)(0.14)*
		--	--	0.25	(0)(0)*	(0)(0.30)*	(0.54)(0)*	(7.19)(0.57)*

Table 15 (Continued)

CNDO-Calculated Electronic Structure of H_3PO_4

Valence Orbital	Energy	Atomic Components: Phosphorus Orbital			Oxygen Orbital		"Hydroxy"** Orbital	
		3s	Σ3p	Σ3d	Σ2s	Σ2p	Σ2s	Σ2p
$3a_1$	-24.46	0.42	--	--	(0)(0.14)*	(0.14)(0)*	(0)(0.08)*	(1.82)(0)*
		--	0.15	--	(0.14)(0)*	(0)(0.14)*	(0)(0.08)*	(1.82)(0)*
		--	--	0.04	(0.14)(0)*	(0)(0.14)*	(0)(0.08)*	(0.74)(1.08)*
$2a_1$	-36.79	0.20	--	--	(0.89)(0)*	(0)(0.02)*	(0)(0.28)*	(0.17)(0)*
		--	0.29	--	(0.89)(0)*	(0.02)(0)*	(0.28)(0)*	(0)(0.17)*
		--	--	0.21	(0.89)(0)*	(0.02)(0)*	(0.28)(0)*	(0.04)(0.08)*
1e	-39.79	0.04	--	--	(0.03)(0)*	(0)(0)*	(0.74)(1.97)*	(0.09)(0.12)*
		--	0.60	--	(0)(0)*	(0.04)(0)*	(4.13)(2.46)*	(0.11)(0.27)*
		--	--	0.67	(0)(0)*	(0.02)(0.02)*	(5.22)(0)*	(0.05)(0.41)*
$1a_1$	-41.67	0.40	--	--	(0.14)(0)*	(0.04)(0)*	(1.44)(0)*	(0.08)(0)*
		--	0.13	--	(0)(0.14)*	(0)(0.04)*	(1.44)(0)*	(0.08)(0)*
		--	--	0.08	(0)(0.14)*	(0)(0.04)*	(1.44)(0)*	(0.02)(0.07)*

*Denotes antibonding contribution.

**"Hydroxy" denotes distinction between hydrogenated and non-hydrogenated oxygen ligands.

Although the assignment of spectra from the CNDO calculations is difficult for $H_2PO_4^-$, HPO_4^{-2}, and H_3PO_4 due to the large number of orbitals and the extensive mixing of these orbitals, the spectra themselves are quite illustrative of the changes occurring with the change in bonding. As the hydroxy group in H_3PO_4 is replaced by an oxygen ligand, the $K\beta_x$ band decreases in intensity until it is not observed at all for the tetrahedral PO_4^{-3}, indicating the presence of but one ligand type. While these effects are clearly exhibited experimentally, it is gratifying that there is also theoretical semi-quantitative justification for the interpretation.

Photon emission spectroscopy is, therefore, capable of distinguishing two different phosphorus-ligand bonds, a distinction verified by semi-quantitative calculations. Further information about the bonding should be obtainable from other spectral features as peak shifts and half-widths of the spectral bands.

Table 16 lists the $K\beta$ transition energies and peak shifts relative to PO_4^{-3} for all the phosphorus oxy-anions. As seen, there is a consistent shift to higher energies for $K\beta$ and $K\beta_x$ in proceeding from PO_4^{-3} to H_3PO_4. Although valence-level shifts are not yet interpretable in terms of any bonding model, it is interesting to note that the shift to higher energies for these bands is in the opposite direction from the core-level shifts as given in Table 3; furthermore, for the phosphates the shift to higher energies occurs with substitution of the less electro-negative hydroxy ligand for oxygen. These factors suggest that the observed shifts may be due to changes in the valence-shell orbitals rather than in the core levels. Also of interest here is the considerably

Table 16

Spectral Shifts of Phosphorus Oxy-Anions

Compound	Line	$h\nu$ (eV)	eV
P	$K\beta$	2139.85	+2.15
	$K\beta_x$	2137.62	+2.76
PO_4^{-3}	$K\beta$	2137.70	--
	$K\beta'$	2124.50	--
HPO_4^{-2}	$K\beta$ *	2138.23	+0.53
	$K\beta_x$	2134.86	--
	$K\beta'$	2134.21	-0.29
$H_2PO_4^-$	$K\beta$	2138.50	+0.80
	$K\beta_x$	2135.78	+0.92
	$K\beta'$	2124.60	+0.10
H_3PO_4	$K\beta$	2138.54	+0.84
	$K\beta_x$	2135.93	+1.07
	$K\beta'$	2123.30	-1.20
HPO_3^{-2}	$K\beta$	2137.70	0.0
	$K\beta_x$	2133.30	-1.50
	$K\beta'$	2124.20	-0.30
$H_2PO_2^-$	$K\beta$	2137.75	+0.05
	$K\beta_x$	2133.03	-1.83
	$K\beta'$	2124.20	-0.30

---

*$K\beta_x$ values given with respect to HPO_4^{-2} $K\beta_x$; all other values are relative to PO_4^{-3}.

shorter P - O bond-length as compared to the P - OH bond-length in proceeding from PO_4^{-3} to H_3PO_4. This factor may be related to electro-negativity characteristics, as the more electro-negative oxygen ligand is better able to "back-bond" with the phosphorus 3d orbitals and to thus form π bonds. It seems that electronegativities and bond lengths may be somehow related to spectral shifts.

Comparison of PO_4^{-3} with HPO_3^{-2} and $H_2PO_2^{-}$ reveals similar effects. The main $K\beta$ band's position is about the same for all three molecules in spite of a considerable difference in the binding energies of the 1s shell for PO_4^{-3} and HPO_3^{-2}. Furthermore, the $K\beta_x$ band shifts to lower energies compared to the phosphates' shifts to higher values. It may be more significant, however, to discuss the shifts of the $K\beta_x$ band for HPO_3^{-2} and $H_2PO_2^{-}$ relative to the $K\beta'$ band of PO_4^{-3}, rather than with respect to the main $K\beta$ or $K\beta_x$ bands, since the $P_{3p} - H_{1s}$ bonding of HPO_3^{-2} and $H_2PO_2^{-}$ more nearly parallels that for $P_{3p} - O_{2s}$ than it does for $P_{3p} - O_{2p}$.

Investigation of the bonding in phosphorus oxy-anions has provided a wealth of information regarding ligand effects and several conclusions may be drawn: first, and most important, photon emission spectroscopy is capable of distinguishing between two different ligands bonded to the same central atom. Furthermore, the presence of the second ligand type significantly alters the over-all bonding for a molecule with respect to energy-level values, ordering of levels, and generation of new molecular orbitals characteristic of the new ligand.

Second, as the symmetry decreases, certain transitions become active in both $K\beta$ and $L_{2,3}$, as determined by means of the $E_i(K) = E_i(L)$ relationship proposed by Andermann and Whitehead.

Third, the assignment applicable on an energy basis is in agreement with Manne's intensity arguments.

Fourth, very good correlation between experimental results and theoretical calculations is possible for rigorously computed systems. Furthermore, semi-quantitative calculations give a good qualitative spectral interpretation which confirms observed spectral trends.

Fifth, invocation of 3d orbital participation was found useful to explain certain spectral features. While this in no way is meant as a conclusive evaluation of 3d orbital participation in bonding, it does suggest a need for further evaluation along the experimental line of investigation for similar evidence in other compounds.

Finally, from the observed shifting of bands upon change of ligand it appears possible to anticipate the spectral position of a transition due to specific central atom-ligand bonding.

Ni $\overline{/}\,S_2P(R)_2\,\overline{/}_2$ Compounds

For this series of compounds no $L_{2,3}$ nor binding energies were available and therefore no $E_i(K)$ and $E_i(L)$ values can be determined. However, certain conclusions can be drawn just on the basis of the $K\beta$ spectra presented here.

The compounds studied were:

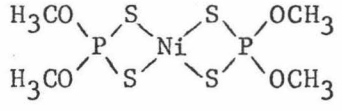

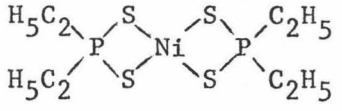

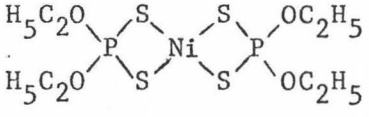

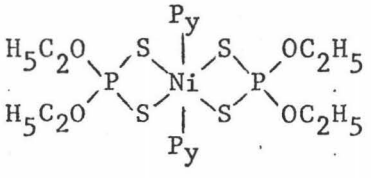

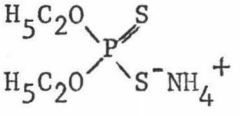

The resulting spectra are shown in Figures 47 to 51; the transition energies for each observed band are given in Table 18; and the CNDO results are given in Tables 19, 20, and 21. The CNDO calculations were not performed on the whole molecule but rather on just the $S_2PR_2^-$ segments. This was done in this manner both for practical reasons, i.e., ease of calculations and cost and limited computer capabilities, and for theoretical reasons, i.e., the entire molecule has D_{2h} symmetry, but it is the local symmetry about phosphorus that is of interest here, and that symmetry is C_{2v}. This approach is partially justified by the ionic nature of the nickel sulfur bond.[49,50]

The spectra of $Ni[S_2P(OC_2H_5)_2]_2$, $Ni[S_2P(OC_2H_5)_2]_2 \cdot 2py$, and $(C_2H_5O)_2P(=S)S^-NH_4^+$ all resemble one another, and the assignment is similar on all three. CNDO calculations were performed only on $Ni[S_2P(OC_2H_5)_2]_2$ as adduct formation with pyridine apparently does not directly affect the bonding in the original compound, and crystallographic data was not available for $(C_2H_5O)_2P(=S)S^-NH_4^+$.

The interpretation of the CNDO results is the same as for the oxy-anions except that there is a second atom, carbon, bonded to the ligand directly bonded to phosphorus. This second atom is considered as bonding or antibonding with respect to either oxygen or carbon and not to phosphorus, and is so designated in the table. Complete results are given only for the methoxy compound; the CNDO calculated eigenvectors and eigenvalues are given in Appendix C.

Table 17

Crystallographic Data for $Ni[S_2P(R)_2]_2$ Compounds

Bond Lengths and Angles*	$Ni[S_2P(OC_2H_5)_2]_2$	$Ni[S_2P(OC_2H_5)_2]_2 \cdot 2_{py}$	$Ni[S_2P(C_2H_5)_2]_2$
Ni - S	2.21 Å	2.49 Å	2.22 Å
S - P	1.97 Å	1.98 Å	2.01 Å
P - O	1.63 Å	1.58 Å	--
P - C	--	--	1.84 Å
O - C	1.51 Å	1.48 Å	--
C - C	1.60 Å	1.46 Å	1.54 Å
S - Ni - S	88.0°	81.7°	87.6°
Ni - S - P	84.5°	84.0°	86.1°
S - P - S	103.0°	110.4°	100.2°
S - P - O	not available	113.0°	--
S - P - C	--	--	113.9°
O - P - O	>101.7°	94.0°	--
C - P - C	--	--	101.7°
P - O - C	not available	121.2°	--
O - C - C	not available	107.6°	--
P - C - C	--	--	110.8°

*All values given are average values.[48,49,50]

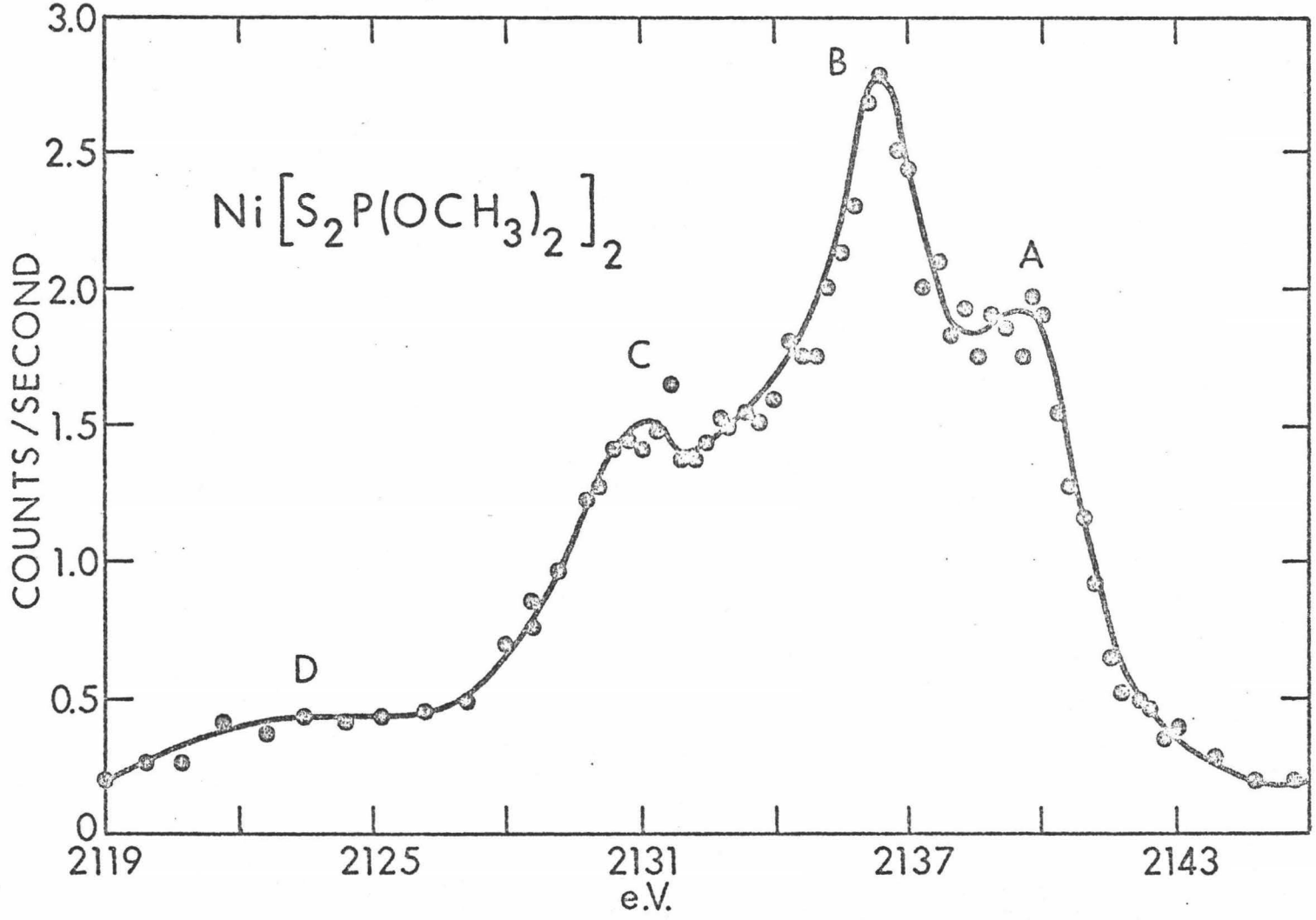

Figure 47

Kβ Emission Spectrum of Ni[S$_2$P(OCH$_3$)$_2$]$_2$

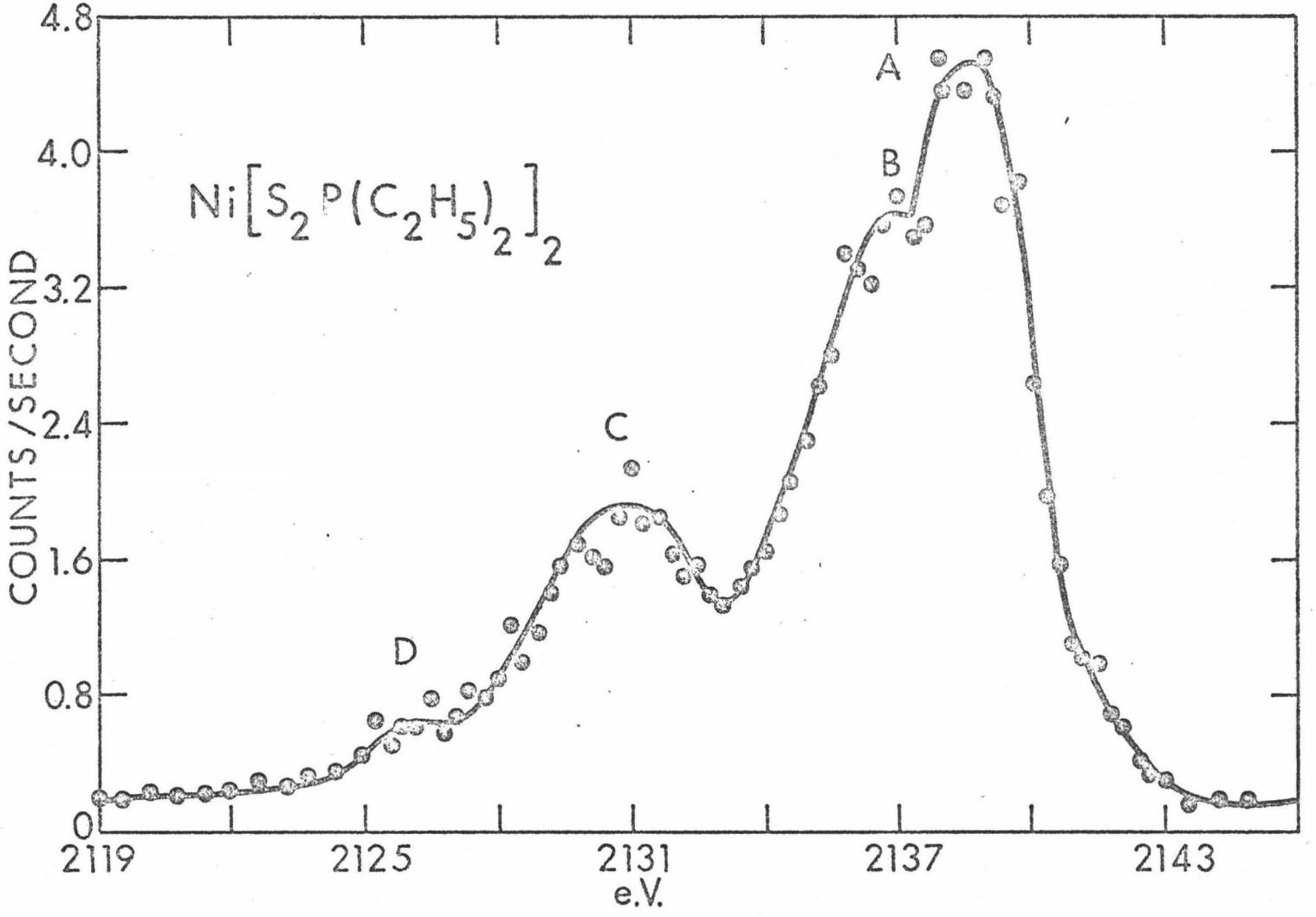

Figure 48

Kβ Emission Spectrum of Ni[S$_2$P(C$_2$H$_5$)$_2$]$_2$

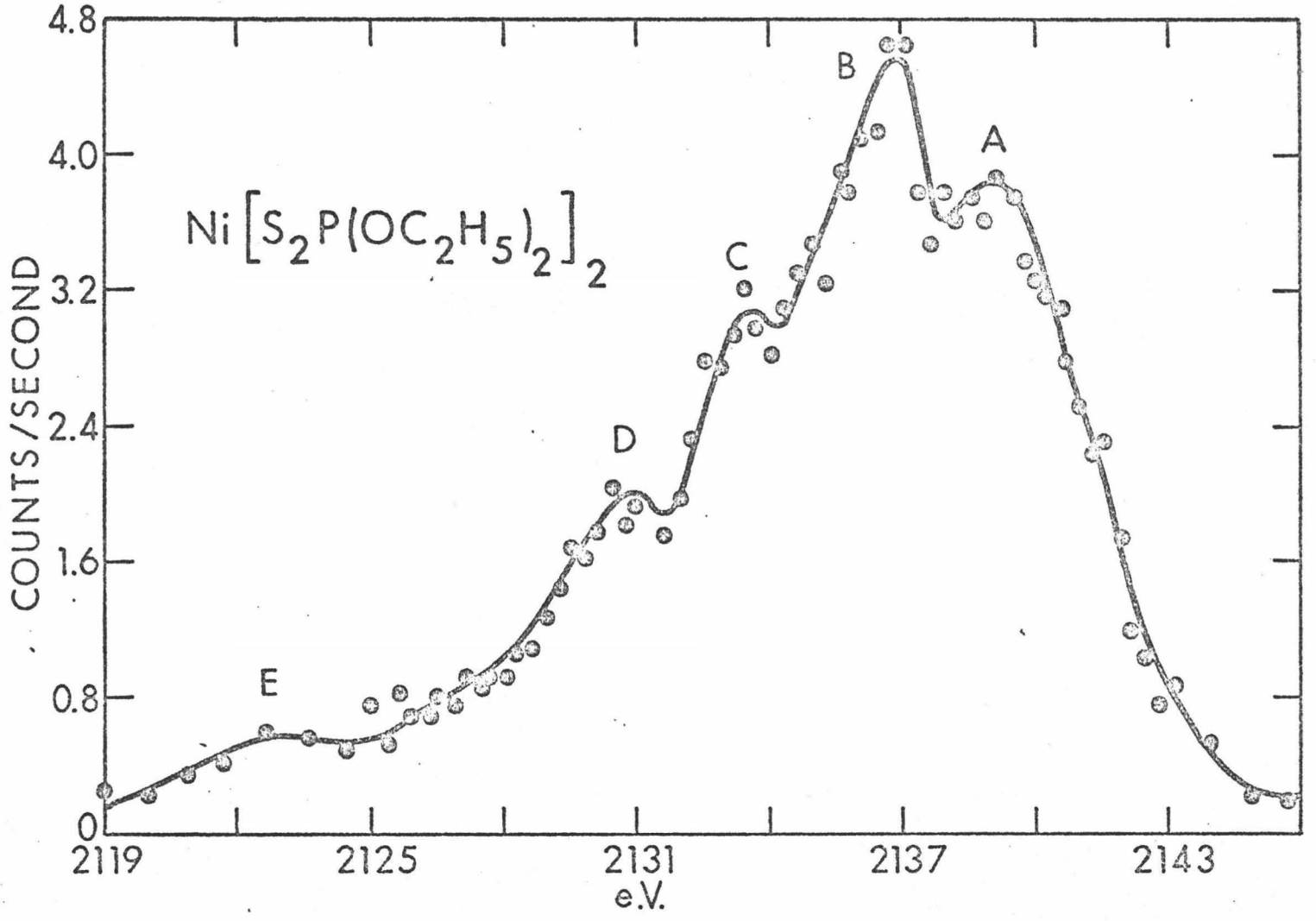

Figure 49

Kβ Emission Spectrum of Ni[S$_2$P(OC$_2$H$_5$)$_2$]$_2$

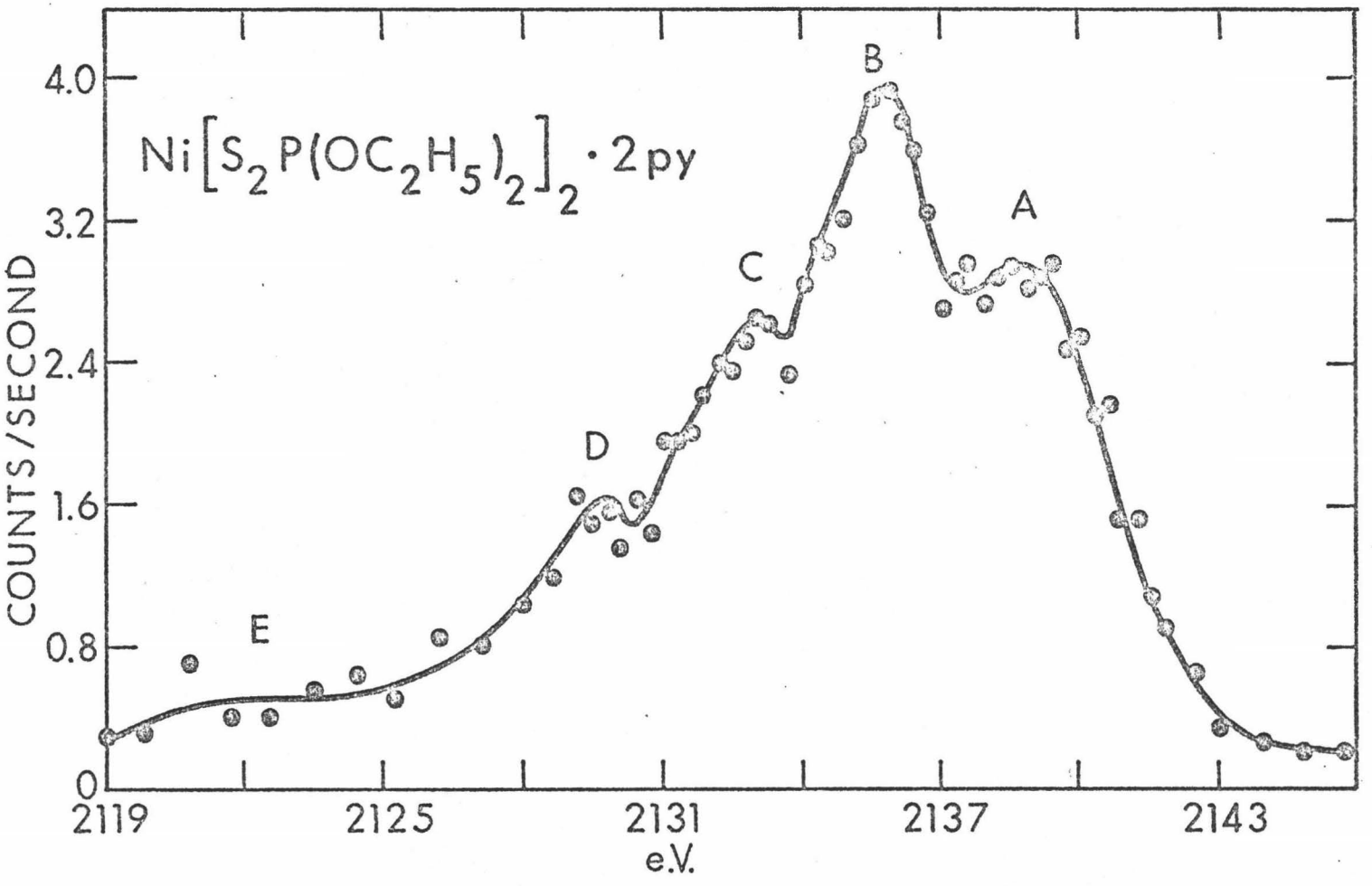

Figure 50

Kβ Emission Spectrum of Ni[S$_2$P(OC$_2$H$_5$)$_2$]$_2$ · 2py

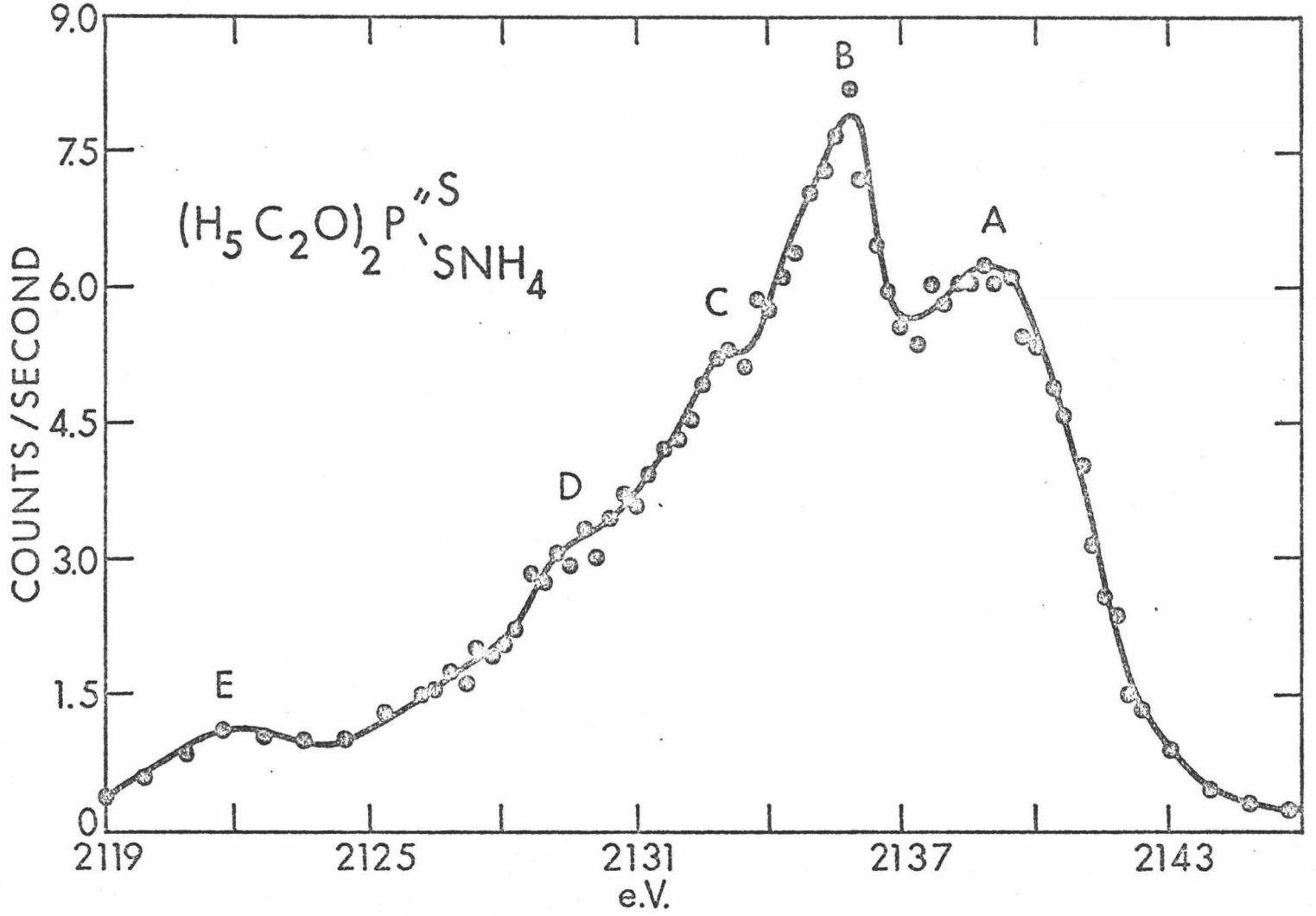

Figure 51

Kβ Emission Spectrum of $(H_5C_2O)_2P(=S)S^-NH_4^+$

Table 18

Transition Energies for $Ni[S_2P(R)_2]_2$ Compounds

Compound	$K\beta$ Line	Energy (eV)
$Ni[S_2P(OCH_3)_2]_2$	A	2139.76
	B	2136.39
	C	2131.35
	D	2122.4
$Ni[S_2P(C_2H_5)_2]_2$	A	2138.54
	B	2137.00
	C	2130.89
	D	2121.8
$Ni[S_2P(OC_2H_5)_2]_2$	A	2138.84
	B	2136.85
	C	2133.48
	D	2130.89
	E	2121.5
$Ni[S_2P(OC_2H_5)_2]_2 \cdot 2py$	A	2138.84
	B	2135.78
	C	2132.88
	D	2129.83
	E	2122.1
$(C_2H_5O)_2P(=S)S^-NH_4^+$	A	2138.89
	B	2135.78
	C	2132.88
	D	2129.67
	E	2121.79

$Ni[S_2P(OCH_3)_2]_2$: Bis (OO' dimethyl dithio phosphinato) Nickel (II)

Comparison of this spectrum, Figure 47, with that for $H_2PO_4^-$ (Figure 33) suggests that the high energy band A may be due to phosphorus-sulfur bonding, whereas the B band may arise from the phosphorus-oxygen bonding.

Table 19 gives the CNDO calculated electronic structure for $Ni[S_2P(OCH_3)_2]_2$ analogously to that for the phosphorus oxy-anions, and Table 20 lists the phosphorus 3p intensity parameters as determined from the sum of the squares of the eigenvectors comprising a molecular orbital. Thus Table 20 represents an approximate intensity evaluation, i.e., from this table it may be determined whether an "allowed" transition will be of sufficient intensity to be observed.

Analysis of the data in Table 19 shows that there is no sharp distinction between any set of levels, but rather a continuous series of energy levels in which the atomic coefficients reflect progressively lower oxygen and carbon contributions and higher sulfur contributions in proceeding to higher energies. This makes the assignment difficult on an energy basis alone, and there are no $E_i(K)$ values to aid in the assignment. Therefore, the assignment made for these compounds will be primarily on an intensity model; this should be a reasonable approach, as it was found for the oxy-anions that the assignments applicable on an energy model agreed with that for an intensity model. An investigation of Table 19, then, reveals four sets of energy levels with distinctly different ligand atomic coefficients; these four sections may be correlated with the four spectral bands noted for $Ni[S_2P(OCH_3)_2]_2$.

Table 19

$Ni[S_2P(OCH_3)_2]_2$

Valence Orbital	Energy	Phosphorus			Sulfur		
		3s	$\sum$3p	$\sum$3d	$\sum$3s	$\sum$3p	$\sum$3d
$10a_1$	-3.91	0.01	0.01	0.30	(0)(0)*	(2.94)(0.03)*	(0)(0)*
$7b_2$	-5.16	0	0.01	0.36	(0)(0)*	(1.90)(0)*	(0)(0)*
$9a_1$	-6.96	0.01	0.60	--	(0)(0.54)*	(1.70)(0.08)*	(0.40)(0.11)*
		--	--	--	(0)(0.72)*	(1.59)(0.78)*	(0.30)(0.40)*
$6b_2$	-7.05	0	0.22	--	(0)(0)*	(1.09)(0)*	(0.35)(0)*
		--	--	0.42	(0)(0)*	(1.09)(0.53)*	(0.39)(0.20)*
$8a_1$	-7.86	0.21	--	--	(0)(0.24)*	(0.58)(0.35)*	(0.65)(0.48)*
		--	0.06	--	(0.10)(0.24)*	(0.63)(0.30)*	(0.07)(0.13)*
		--	--	0.64	(0.10)(0.34)*	(1.68)(0.98)*	(0.28)(0.33)*
$2a_2$	-9.26	0	0.10	--	(0)(0)*	(0.34)(0)*	(0.13)(0)*
		--	--	0.26	(0)(0)*	(0.52)(0.08)*	(0.24)(0.02)*
$4b_1$	-10.15	0.13	--	--	(0)(0.55)*	(0.97)(0)*	(0.26)(0)*
		--	0.48	--	(0.29)(0.55)*	(1.35)(0.68)*	(0.42)(0.18)*
		--	--	0.27	(0.58)(0.55)*	(1.62)(1.09)*	(0.58)(0.22)*
$3b_1$	-10.27	0.05	--	--	(0.06)(0.06)*	(0.15)(0.28)*	(0.05)(0.13)*
		--	0.26	--	(0)(0.18)*	(0.37)(0.54)*	(0.11)(0.27)*
		--	--	0.43	(0.18)(0.06)*	(0.84)(0.43)*	(0.35)(0.25)*
$5b_2$	-10.76	0	0.31	--	(0)(0)*	(0.22)(0)*	(0.14)(0)*
		--	--	0.13	(0)(0)*	(0.13)(0.18)*	(0.08)(0.12)*
$7a_1$	-11.99	0.32	--	--	(0)(0.46)*	(0.43)(0)*	(0.11)(0.03)*
		--	0.20	--	(0.38)(0.27)*	(0.30)(0.38)*	(0.15)(0.15)*
		--	--	0.19	(0.27)(0.38)*	(0.30)(0.38)*	(0.10)(0.20)*
$4b_2$	-13.41	0	0.16	--	(0)(0)*	(0.09)(0.06)*	(0.05)(0.04)*
		--	--	0.25	(0)(0)*	(0.15)(0)*	(0.08)(0.01)*

Oxygen		Carbon		
Σ 2s	Σ 2p	Σ 2s	Σ2p	
(0.04)(0.08)*	(0.44)(0.40)*	(0)(0.04)*	(0)(0.06)*	2s
		(0.04)(0.04)*	(0.06)(0.06)*	2p
(0.04)(0.04)*	(0.64)(0.64)*	(0)(0.06)*	(0.04)(0.08)*	2s
		(0.06)(0.06)*	(0.14)(0.10)*	2p
(0.06)(0.06)*	(0.66)(0.66)*	(0)(0.04)*	(0)(0.12)*	2s
(0.12)(0.06)*	(1.00)(0.98)*	(0.04)(0.04)*	(0.12)(0.14)*	2p
(0.02)(0)*	(0.08)(0.82)*	(0)(0.10)*	(0.02)(0.16)*	2s
(0)(0.64)*	(1.64)(0.16)*	(2.0)(0)*	(0.32)(0.12)*	2p
(0)(0.08)	(0)(1.14)*	(0)(0)*	(0.02)(0.02)*	2s
(0.08)(0)*	(1.14)(0)*	(0)(0)*	(0.04)(0.16)*	2p
(0.16)(0.08)*	(2.94)(0.48)*			
(0)(0.04)*	(0.73)(0.86)*	(0)(0.04)*	(0.04)(0.04)*	2s
(0.04)(0.04)*	(1.60)(1.60)*	(0.04)(0.04)*	(0.38)(0.94)*	2p
(0.04)(0)*	(0)(0.64)*	(0.02)(0)*	(0.10)(0.14)*	2s
(0)(0.08)*	(1.28)(0)*	(0.02)(0.02)*	(0.34)(0.24)*	2p
(0.04)(0.08)*	(0.76)(1.16)*			
(0.02)(0)*	(0.82)(0.50)*	(0.02)(0)*	(0.20)(0.06)*	2s
(0.02)(0.02)*	(1.32)(1.32)*	(0.02)(0.02)*	(0.51)(0.99)*	2p
(0.02)(0.04)*	(1.82)(2.14)*			
(0)(0.16)*	(1.64)(0)*	(0.02)(0)*	(0.10)(0.36)*	2s
(0.16)(0)*	(1.64)(1.64)*	(0.02)(0.02)*	(0.70)(0.40)*	2p
(0)(0.24)*	(1.06)(0)*	(0)(0.02)*	(0.10)(0.36)*	2s
(0.24)(0.24)*	(1.06)(1.06)*	(0.02)(0.02)*	(0.46)(0.71)*	2p
(0.24)(0.24)*	(0.90)(1.22)*			
(0.10)(0.10)*	(1.30)(0.50)*	(0)(0.14)*	(0)(1.00)*	2s
(0.20)(0)*	(1.30)(0.50)*	(0.28)(0)*	(2.12)(0)*	2p

Table 19 (Continued)

$Ni[S_2P(OCH_3)_2]_2$

Valence Orbital	Energy	Phosphorus			Sulphur		
		3s	Σ3p	Σ3d	Σ3s	Σ3p	Σ3d
$6a_1$	-14.65	0.20	--	--	(0.03)(0.31)*	(0.12)(0.05)*	(0.05)(0.03)*
		--	0.26	--	(0.31)(0.34)*	(0.17)(0.17)*	(0.13)(0.08)*
		--	--	0.26	(0.96)(0)*	(0.27)(0.24)*	(0.21)(0.11)*
$5a_1$	-16.91	0.07	0.24	--	(0.64)(0)*	(0.12)(0.08)*	(0.11)(0.05)*
				0.20	(0.77)(0.13)*	(0.12)(0.15)*	(0.04)(0.12)*
$1a_2$	-17.58	0	0.04	--	(0)(0)*	(0.10)(0.02)*	(0.06)(0)*
		--	--	0.21	(0)(0)*	(0.22)(0)*	(0.14)(0)*
$4a_1$	-17.91	0.08	--	--	(0.31)(0.12)*	(0.02)(0)*	(0)(0.02)*
		--	0.11	--	(0.43)(0)*	(0.02)(0)*	(0.02)(0)*
		--	--	0.25	(0.31)(0.31)*	(0.04)(0.02)*	(0.02)(0.04)*
$3b_2$	-17.93	0	0.20	--	(0)(0)*	(0.18)(0)*	(0.11)(0)*
		--	--	0.13	(0)(0)*	(0.14)(0.08)*	(0.11)(0.05)*
$1b_1$	-19.24	0.02	0.50	--	(1.55)(0)*	(0.26)(0.06)*	(0.14)(0.07)*
		--	--	0.16	(2.11)(0)*	(0.18)(0.24)*	(0.07)(0.32)*
$3a_1$	-22.87	0.45	--	--	(1.00)(0)*	(0.29)(0)*	(0.19)(0)*
		--	0.37	--	(1.00)(0.48)*	(0.44)(0.23)*	(0.22)(0.12)*
		--	--	0.18	(1.48)(0.48)*	(0.76)(0.14)*	(0.31)(0.15)*
$2b_2$	-25.85	0	0.11	--	(0)(0)*	(0)(0.03)*	(0.01)(0.02)*
		--	--	0.22	(0)(0)*	(0.03)(0)*	(0.03)(0.02)*
$2a_1$	-26.46	0.21	--	--	(0.07)(0)*	(0.06)(0)*	(0.04)(0)*
		--	0.19	--	(0.06)(0.07)*	(0.04)(0.06)*	(0.03)(0.04)*
		--	--	0.08	(0.06)(0.06)*	(0.04)(0.04)*	(0.03)(0.02)*
$1b_2$	-37.33	0	0.23	--	(0)(0)*	(0.07)(0)*	(0)(0.06)*
		--	--	0.20	(0)(0)*	(0.03)(0.07)*	(0.03)(0.03)*
$1a_1$	-37.99	0.28	--	--	(0.12)(0)*	(0.10)(0)*	(0.04)(0.02)*
		--	0.16	--	(0.05)(0.12)*	(0.06)(0.10)*	(0.06)(0.04)*
		--	--	0.21	(0.05)(0.12)*	(0.05)(0.10)*	(0.05)(0.06)*

Oxygen		Carbon		
Σ 2s	Σ 2p	Σ 2s	Σ 2p	
(0)(0)*	(1.20)(0.44)*	(0)(0)*	(0)(0)*	2s
(0)(0)*	(2.40)(0.88)*	(0.20)(0)*	(1.06)(0)*	2p
(0)(0)*	(2.84)(2.08)*			
(0)(0.08)*	(1.80)(0)*	(0)(0.04)*	(0.70)(0.18)*	2s
(0.08)(0)*	(1.90)(0.80)*	(0.04)(0.04)*	(0.98)(0.88)*	2p
(0)(0.22)*	(0.64)(0.46)*	(0.08)(0)*	(0)(0.42)*	2s
(0.22)(0.22)*	(1.10)(1.10)*	(0.08)(0.08)*	(1.14)(0.42)*	2p
(0.18)(0)*	(0.36)(0.76)*	(0.08)(0)*	(0)(0.50)*	2s
(0.18)(0)*	(0.36)(0.76)*	(0)(0.12)*	(1.64)(0)*	2p
(0.18)(0.18)*	(1.12)(1.12)*			
(0)(0.16)*	(1.02)(0)*	(0.04)(0)*	(0.68)(0.44)*	2s
(0.16)(0.16)*	(1.02)(1.02)*	(0.04)(0.04)*	(1.46)(1.12)*	2p
(0.06)(0.06)*	(0.80)(0.80)*	(0.02)(0)*	(0.12)(0.40)*	2s
(0.12)(0.06)*	(1.28)(1.12)*	(0.02)(0.02)*	(0.78)(0.52)*	2p
(0)(0.32)*	(0.50)(0)*	(0.04)(0)*	(0.24)(0)*	2s
(0.64)(0)*	(0)(1.00)*	(0.04)(0.04)*	(0.34)(0.24)*	2p
(0.96)(0)*	(0.32)(1.19)*			
(0.70)(0)*	(0.20)(0.16)*	(0)(0.74)*	(0.60)(0)*	2s
(1.40)(0)*	(0.40)(0.24)*	(1.48)(0)*	(0.02)(1.20)*	2p
(0.62)(0)*	(0.32)(0.14)*	(0)(0.76)*	(0.48)(0)*	2s
(1.24)(0)*	(0.64)(0.28)*	(1.52)(0)*	(0.02)(0.96)*	2p
(0.62)(0.62)*	(0.78)(0.14)*			
(1.0)(0)*	(0.14)(0.14)*	(0.68)(0)*	(0.38)(0)*	2s
(2.0)(0)*	(0.28)(0.28)*	(1.36)(0)*	(0.84)(0)	2p
(1.0)(0)*	(0.14)(0.08)*	(0.64)(0)*	(0.36)(0)*	2s
(2.0)(0)*	(0.58)(0.16)*	(1.28)(0)*	(0.80)(0)*	2p
(2.0)(0)*	(0.52)(0)*			

Table 20

CNDO-Calculated Electronic Structure of
Bis (00' dimethyl dithio phosphinato) Nickel (II)

Valence Orbital	Energy	Phosphorus $\Sigma 3p^2$ Coefficients	Valence Orbital	Energy	Phosphorus $\Sigma 3p^2$ Coefficients
$10a_1$	-3.91	0	$6a_1$	-14.65	0.04
$7b_2$	-5.16	0	$5a_1$	-16.91	0.04
$9a_1$	-6.96	0.19	$1a_2$	-17.58	0
$6b_2$	-7.05	0.05	$4a_1$	-17.91	0.01
$8a_1$	-7.86	0	$3b_2$	-17.93	0.04
$2a_2$	-9.26	0.01	$1b_1$	-19.24	0.13
$4b_1$	-10.15	0.13	$3a_1$	-22.87	0.07
$3b_1$	-10.27	0.03	$2b_2$	-25.85	0.01
$5b_2$	-10.76	0.10	$2a_1$	-26.46	0.02
$7a_1$	-11.99	0.02	$1b_2$	-37.33	0.05
$4b_2$	-13.41	0.03	$1a_1$	-37.99	0.01

The four lowest-lying levels, $1a_1$, $1b_2$, $2a_1$ and $2b_2$, have very large oxygen 2s coefficients which are strongly bonding with phosphorus 3p. These orbitals also have large carbon 2s bonding coefficients and a significant amount of carbon 2p is also mixed in. The sulfur coefficients are negligible in all four of these orbitals. These four low-energy orbitals may then be correlated with the low-energy band at 2122.4 eV and band D is designated as due to P_{3p}-$O_{2s}C_{2s}$ bonding which would directly correspond to the P_{3p}-O_{2s} bonding in the oxy-anions ($PK\beta'$). Note the small phosphorus 3p coefficients and the low intensity of this $K\beta'$ band--in agreement with Manne's arguments.

In the next two levels, $3a_1$ and $1b_1$, the carbon coefficients are quite small and only slightly bonding while the oxygen contribution has been significantly reduced and is nonbonding. The sulfur 3s coefficients, on the other hand, are quite large and strongly bonding; sulfur 3p and 3d contribution to these molecular orbitals is small. These orbitals may then be assigned as the origin of band C in the $K\beta$ spectrum and are attributable to P_{3p}-S_{3s} bonding in analogy with the P_{3p}-O_{2s} bonding in the oxy-anions; this analogy between the sulfur 3s bonding and oxygen 2s bonding is not surprising as sulfur and oxygen are often attributed similar chemical properties and behavior. Note that experimentally this band is considerably more intense than the analogous transition for oxygen in band D; the CNDO phosphorus 3p coefficients predict just such a situation, as the sum of the squares of the 3p coefficients for the $1a_1$, $1b_2$, $2a_1$, $2b_2$ orbitals is 0.09 while that for the two orbitals attributed to band C, $3a_1 + 1b_1$, is 0.20. Thus the C band should be about twice as intense as band D.

The next distinct set of levels extends from $3b_2$ (-17.93 eV) to $3b_1$ (-10.27 eV), a considerable range. The orbitals have large oxygen and carbon 2p bonding coefficients and small sulfur coefficients; the contribution from oxygen and carbon 2s is apparently negligible. Although the sulfur contribution to these orbitals is small, it increases toward the higher-lying levels; this same trend was observed for the oxy-anions with hydroxy ligands. Band B may then be correlated with these molecular orbitals and be designated as due to P_{3p}-$O_{2p}C_{2p}$ bonding. The large carbon coefficients necessitate its inclusion in this designation rather than a P_{3p}-O_{2p} notation as was applicable for the oxy-anions. This appears to be a rational designation, as electron density may extend over a three-atom system; this may be particularly rationalized if the center atom is highly electronegative, as is oxygen.

The next set of levels $4b_1$ (-10.15 eV) to $9a_1$ (-6.96 eV) are mixed with large oxygen 2p and sulfur 3p components; the carbon coefficients are negligible here. However, the sulfur coefficients are more prominent and in the higher-lying levels are dominant, the oxygen coefficients being negligible. These orbitals are then the origin of the high-energy band A in the spectrum, and in analogy with the other assignments is designated as due to P_{3p}-S_{3p} bonding.

Although there is mixing of oxygen, carbon, and sulfur in most of these levels above those for sulfur 3s, these coefficients are observed to become more sulfur- or oxygen-like in character in proceeding to higher or lower energies respectively, and, thus, the designation of these bands as due to phosphorus-sulfur or phosphorus-oxygen-carbon bonding in the molecule.

The highest-lying levels $7b_2$ and $10a_1$ have not been included in the assignment of band A because, although they have very large sulfur 3p coefficients, their phosphorus 3p coefficients are negligible and they would not contribute significantly to the intensity of the observed band.

The Kβ spectrum of $Ni[S_2P(OCH_3)_2]_2$ may then be assigned as:

$K\beta(A)$: $4b_1 + 6b_2 + 9a_1 \longrightarrow 1s$

$K\beta(B)$: $3b_2 + 5a_1 + 6a_1 + 4b_2 + 5b_2 + 3b_1 \longrightarrow 1s$

$K\beta(C)$: $3a_1 + 1b_1 \longrightarrow 1s$

$K\beta(D)$: $1a_1 + 1b_2 + 2a_1 + 2b_2 \longrightarrow 1s$

$Ni[S_2P(C_2H_5)_2]_2$: Bis (diethyl dithiophosphinato) Nickel (II)

The spectrum for this molecule is given in Figure 48. This molecule and the calculated results differ from the methoxy molecule only by the substitution of a methylene group (CH_2) for oxygen. The spectral interpretation is analogous to that for the methoxy compound with certain modifications for the absence of oxygen.

The CNDO calculations incidate a low-energy region consisting of the $2a_1$, $1b_1$, and $2b_2$ orbitals which have large carbon 2s coefficients and negligible carbon 2p and sulfur coefficients. This would be analogous to the phosphorus 3p - oxygen 2s low-energy levels observed for the oxy-anions and the $Ni[S_2P(OCH_3)_2]_2$ molecule. However, the oxygen 2s electrons in each case are not involved in σ bonding to another atom and may contribute considerable electron density to the phosphorus-oxygen bonding. The carbon 2s electrons, on the other hand, are directly involved in σ bond formation and are not as available as oxygen 2s to donate "extra" electron density to the phosphorus-carbon bonding. The

large carbon 2s coefficients in these low-lying molecular orbitals in analogy with the oxygen case is, therefore, surprising. However, the Kβ spectrum for this molecule does exhibit such a low-energy transition although a weak one. Band D may then be associated with P_{3p}-C_{2s}-C_{2s} bonding.

The next set of energy levels which may be correlated with the spectral results are the $3a_1$ and $2b_1$ molecular levels. The $3a_1$ and $2b_1$ levels contain very large sulfur 3s coefficients with a small mixing of carbon 2p; furthermore, these sulfur 3s orbitals are strongly bonding with phosphorus 3p, whereas the oxygen 2p orbitals are only slightly bonding. These two levels may then be assigned to P_{3p}-S_{3s} bonding as in the case for the methoxy compound. The $3b_2$ molecular orbital falls between $3a_1$ and $2b_1$ and has large carbon 2s coefficients with zero sulfur 3s contribution. However, the phosphorus 3p coefficient is only 0.01, compared to over 0.10 for each of the other two orbitals, and will contribute negligible intensity to the band and, therefore, is not included in the assignment.

The higher-energy levels are similar to those for the methoxy compound in that the levels consist of both sulfur and carbon coefficients in significant magnitude but become more prominently sulfur in the higher-lying levels. The separation between the series of orbitals defining a particular bonding is more prominent here than for the methoxy compound, aiding in the assignment. Thus the molecular levels $4a_1$ (-16.6 eV) and $4b_2$ (-15.2 eV) may be ascribed to bonding between phosphorus and carbon. Furthermore, both types of carbon--the carbon bonded directly to phosphorus and the carbon bonded to carbon--contribute strongly to this bonding, suggesting a delocalized P_{3p}-C_{2p}-C_{2p} system.

Table 21

CNDO-Calculated Electronic Structure of
Bis (diethyldithio phosphinato) Nickel (II)

Valence Orbital	Energy	$\sum 3p^2$ Phosphorus Coefficients	Valence Orbital	Energy	$\sum 3p^2$ Phosphorus Coefficients
$8a_1$	-4.40	0	$5a_1$	-14.39	0.01
$9b_2$	-5.16	0.06	$4b_2$	-15.17	0.12
$8b_2$	-5.39	0	$4a_1$	-16.61	0.06
$5b_1$	-6.13	0.05	$2b_1$	-18.58	0.10
$7a_1$	-7.39	0.18	$3b_2$	-21.37	0.01
$7b_2$	-7.87	0.06	$3a_1$	-22.01	0.11
$6b_2$	-8.58	0.02	$2b_2$	-23.61	0.03
$4b_1$	-8.72	0	$1b_1$	-23.92	0.02
$3b_1$	-9.00	0.13	$2a_1$	-26.54	0.03
$6a_1$	-11.16	0.08	$1b_2$	-43.14	0.03
$5b_2$	-13.52	0	$1a_1$	-44.49	0.01

The remaining levels from $6a_1$ to $9b_2$ have very large bonding coefficients for sulfur 3s and 3p to phosphorus 3p; some levels also have significant carbon 2p coefficients but these are neither as large as nor as strongly bonding as the sulfur contribution. These levels then are correlated with band A in the spectrum and are designated as due to P_{3p}-S_{3p} bonding.

The Kβ spectrum is then assigned as:

$K\beta(A)$: $(6a_1 + 3b_1 + 7b_2 + 7a_1 + 5b_1 + 9b_2) \longrightarrow 1s$

$K\beta(B)$: $(4a_1 + 4b_2) \longrightarrow 1s$

$K\beta(C)$: $(3a_1 + 2b_1) \longrightarrow 1s$

$K\beta(D)$: $(2a_1 + 1b_1 + 2b_2) \longrightarrow 1s$

Although the $4b_1$, $8b_2$, and $8a_1$ orbitals have quite large sulfur coefficients, their phosphorus 3p coefficients are negligible and they have, therefore, not been included in this assignment.

$Ni[S_2P(OC_2H_5)_2]_2$: Bis (O O' diethyldithiophosphinato) Nickel (II)

As mentioned previously, the assignment made here also applies to the pyridine adduct and the parent compound.

The assignment of bands A and B as arising from phosphorus-sulfur bonding and phosphorus-oxygen bonding, respectively, follows from arguments presented for the methoxy compound and is confirmed by the CNDO calculation. The orbitals $3b_1$ (-10.1 eV) to $11a_1$ (-6.9 eV) contain very large sulfur-bonding coefficients with respect to phosphorus 3p. Except for the $10b_2$ level, the oxygen and carbon contribution to these levels is small compared to that for sulfur.

The molecular orbitals from $8b_2$ (-11.7 eV) to $9b_2$ (-10.5 eV) are predominantly oxygen 2p in character, with a significant contribution

Table 22

CNDO-Calculated Electronic Structure of
Bis (00' diethyldithio phosphinato) Nickel (II)

Valence Orbital	Energy	Phosphorus $\sum 3p^2$ Coefficients	Valence Orbital	Energy	Phosphorus $\sum 3p^2$ Coefficients
$12a_1$	-3.87	0	$6b_2$	-15.15	0.04
$12b_2$	-5.09	0	$7a_1$	-15.22	0
$11a_1$	-6.89	0.18	$5b_2$	-17.90	0.02
$11b_2$	-7.05	0.06	$6a_1$	-18.07	0.07
$4b_1$	-7.75	0	$1b_1$	-18.67	0.11
$10b_2$	-10.09	0.04	$5a_1$	-21.21	0.01
$3b_1$	-10.10	0.11	$4b_2$	-21.48	0.01
$9b_2$	-10.49	0.03	$4a_1$	-22.98	0.04
$10a_1$	-10.93	0.05	$3b_2$	-23.76	0
$2b_1$	-11.25	0.01	$3a_1$	-24.08	0.04
$8b_2$	-11.70	0.02	$2b_2$	-32.30	0.03
$9a_1$	-13.40	0.03	$2a_1$	-32.84	0.01
$7b_2$	-14.96	0	$1b_2$	-38.70	0.03
$8a_1$	-14.97	0.01	$1a_1$	-39.05	0.01

from the carbons bonded directly to oxygen, as in the case for the methoxy compound, and these levels are again correlated with band B and designated as P_{3p}-O_{2p}-C_{2p} bonding.

The phosphorus-sulfur 3s bonding is also clearly described by the $1b_1$ (-18.7 eV) and $6a_1$ (-18.1 eV) levels; again the oxygen and carbon contribution to these levels is small.

The $1a_1$, $1b_2$, $2a_1$, and $2b_2$ orbitals are assigned to the low-energy band E and describe the P_{3p}-O_{2s}-C_{2s} bonding as was observed for the methoxy compound.

The calculations indicate another set of energy levels from $3a_1$ (-24.1 eV) to $5a_1$ (-21.2 eV) which are predominantly oxygen and carbon 2s and 2p in nature and which become smaller in oxygen magnitude and greater in carbon in proceeding to higher energies. Such a situation was also indicated for the methoxy compound and would predict a transition between bands D and E spectrally. However, no such transitions are observed; but the phosphorus 3p coefficients are small, and these transitions may be concealed in the "background" radiation.

One prominent spectral feature distinguishing this spectrum from that for the methoxy or alkyl compounds is band C at 2133.48 eV. This band is observed for all three ethoxy compounds but not for the methoxy, suggesting additional energy levels due to the second methylene group, or a splitting of the levels contained in band B for the methoxy compound. The CNDO calculations indicate a series of molecular orbitals from $5b_2$ (-17.9 eV) to $9a_1$ (-13.41 eV), just below the levels associated with P_{3p}-O_{2p}-C_{2p} bonding which also contain large oxygen and carbon coefficients. However, this lower-lying series of levels contains significant contributions from the carbons not directly bonded to phosphorus. Furthermore,

the magnitude of the oxygen coefficients increases while that for carbon decreases in proceeding to the higher-lying levels until finally, as the series converges with that assigned to the $K\beta$(B) band, the coefficients on the carbon once removed from phosphorus become negligible. It therefore appears that there are two bands attributable to phosphorus-oxygen-carbon bonding, differing in the character of carbon donated to the bonding.

This is not unlike the situation for the methoxy and ethyl compounds, however, since the levels attributed to band B become smaller in the contribution from the atom once removed from phosphorus and larger in the contribution from that directly bonded to phosphorus in proceeding to higher-lying levels in the series. Possibly under higher resolution a similar "extra" band may be observed for these compounds also. On the other hand, while it is possible to envision electron density spread over a three-atom system so as to yield one series of bonding levels, such delocalization over a four-atom system as P_{3p}-O_{2p}-C_{2p}-C_{2p} may not be so extensive, resulting in the generation of two series of molecular energy levels.

The $K\beta$ assignment then is as follows:

$K\beta$(A): $(3b_1 + 10b_2 + 11b_2 + 11a_1) \longrightarrow 1s$

$K\beta$(B): $(8b_2 + 2b_1 + 10a_1 + 9b_2) \longrightarrow 1s$

$K\beta$(C): $(5b_2 + 6b_2 + 8a_1 + 9a_1) \longrightarrow 1s$

$K\beta$(D): $(1b_1 + 6a_1) \longrightarrow 1s$

$K\beta$(E): $(1a_1 + 1b_2 + 2a_1 + 2b_2) \longrightarrow 1s$

Shift Studies

As for the phosphorus oxy-anions, the shifts with a change of ligand and band widths may give some useful information about bonding.

The band shifts with changing ligand appear to correlate with changes in bond lengths. Appropriate crystallographic data for $Ni[S_2P(OC_2H_5)_2]_2$, $Ni[S_2P(OC_2H_5)_2]_2 \cdot 2py$, and $Ni[S_2P(C_2H_5)_2]_2$ are given in Table 17.

Fernando[49] interprets the angle changes upon adduct formation on the basis of a simple electrostatic model. Complexing with pyridine reduces the net positive charge on the nickel atom and increases the net negative charge on the sulfur atoms. This latter effect results in an increase in the S-P-S angle, while the former effect lengthens the Ni-S bond length, and decreases the S-Ni-S angle. It is the S-P-S angle that may be of interest here. The increase in this angle results in a more nearly tetrahedral arrangement and thus a more stable state. One may naively expect an accompanying shift of the phosphorus-sulfur bonding band (A) to lower energies, however, no such shift is observed upon adduct formation.

The large decrease in the O-P-O angle has been attributed to repulsion between the pyridine molecules and methylene groups resulting in a more strained ring and a higher energy state. The phosphorus-oxygen band shifts to lower energy in this case.

A more interesting trend may be noted in comparing peak shifts with bond lengths. The pyridine adduct of the ethoxy compound is of special interest since adduct formation does not directly affect the bonding to phosphorus, and it would not be expected to significantly

alter the molecular orbitals formed for the ethoxy compound. As noted previously, the phosphorus-sulfur band (A) does not shift upon adduct formation, in spite of a large change in geometry; however, the P-S bond length increases only slightly (0.01 Å), suggesting some correlation between bond length and peak positions. Similarly, the phosphorus-oxygen bond length decreases considerably (0.05 Å) upon adduct formation and spectrally there is a shift of 1.07 eV to lower energies of band B. There is a decrease of 0.03 Å in the oxygen-carbon bond length as well, which is interesting in view of the assignment of band B to phosphorus-oxygen-carbon bonding.

The P_{3p}-S_{3p} band (A) does not shift for the parent compound, $(C_2H_5O)_2P\overset{S}{\diagdown}_{SNH_4}$, in comparison with the ethoxy compound, while band B shifts considerably to lower energies. While this spectral information is quite suggestive, especially in view of the ionic nature of the sulfur-nickel bond for the ethoxy compound and the double bond character of the phosphorus-sulfur bond, no crystallographic data is available for $(C_2H_5O)_2P\overset{S}{\diagdown}_{SNH_4}$ for correlation.

In addition to the possible correlation of bond lengths with peak shifts, there are also some interesting trends to be noted upon change of ligand. In changing from the ethoxy to the less electro-negative ethyl ligand there is not only a shift of band B, which has been attributed to phosphorus-carbon bonding, to higher energies (0.15 eV), but also a shift of band A, attributed to phosphorus-sulfur bonding to lower energies (0.29 eV). While no conclusions may be drawn here, it is interesting to note the change of electronegativity of the ligand and the direction of the shifts.

Perhaps the most significant shifts of all occur upon changing from an ethoxy to a methoxy ligand. These two ligands would be expected to behave similarly, yet it has already been noted that the ethoxy spectrum displays one more band than does the methoxy spectrum. One possible significant difference between the methoxy and ethoxy ligands is the greater electronegativity of the methoxy ligand. While the exact relationship between electronegativity and spectral shifts cannot at this time be postulated, it is curious to note that for the methoxy compound the band attributed to P-O bonding shifts to lower energies while that for P-S bonding shifts to higher energies in comparison with the ethoxy compound. These spectral shifts are just the opposite of those noted for the ethyl compound.

The shifts noted here for the $Ni[S_2P(R)_2]_2$ compounds are quite similar to those noted for the oxy-anions in that the observed shifts seem to be a function of ligand effects and, furthermore, there seems to be some correlation between both bond lengths, electronegativity concepts, and spectral shifts. However, the evidence here is inconclusive and is, by no means, meant as definitive.

Another spectral feature of interest are the very wide band widths for all of the compounds but in particular for $(OC_2H_5)_2P(=S)S^-NH_4^+$. As seen, the P-S band of this compound is not only broad but appears to "bulge" on the high-energy side. The most immediate explanation that would distinguish this molecule from the other ethoxy compounds is the presence of two distinct types of sulfur ligands bonded to phosphorus. The bonding for $(EtO)_2P(=S)S^-NH_4^+$ is intermediate between $Ca_3(PO_4)_2$ for which one spectral transition is observed due to equivalent P-O bonds

and H_3PO_4 with one P-O bond and three P-OH bonds (where the hydroxy unit is of considerable ionic character), and for which two transitions are observed. The $S^-NH_4^+$ bond is undoubtedly not as ionic as O^--Ca^+ but is more ionic than -OH, giving two similar, but still different, P-S bonds, and, therefore, two P-S transitions must be postulated. This broad band may then conceal two P-S transition lines. The width of this band may be realized from Figure 52 which superimposes spectra for $Ni[S_2P(C_2H_5)_2]_2$, $Ni[S_2P(OCH_3)_2]_2$, and $(OC_2H_5)_2P(=S)SNH_4$.

It may also be postulated, in analogy with the phosphorus oxy-anions, that the phosphorus 3d orbitals may be "back bonding" with the sulfur 3p orbitals, giving a series of high-energy orbitals which may be weakly active in $K\beta$. This would be more probable for the phosphorus-sulfur system than the phosphorus-oxygen since the ionic nickel-sulfur bond concentrates considerable residual electron density on the sulfur as compared with the oxygen. Fernando[48] states that the P-S bond has considerable double-bond character and this should result from the transfer of electron density from sulfur 3p and 3d to phosphorus 3d orbitals. The need for $L_{2,3}$ spectral evaluation is obvious!

However, speculation about 3d orbital participation is not necessary to explain these band widths. These molecules are composed of many molecular orbitals which, for C_{2v} symmetry, are all non-degenerate. Therefore, each band represents several transitions of varying energies resulting in broad band widths.

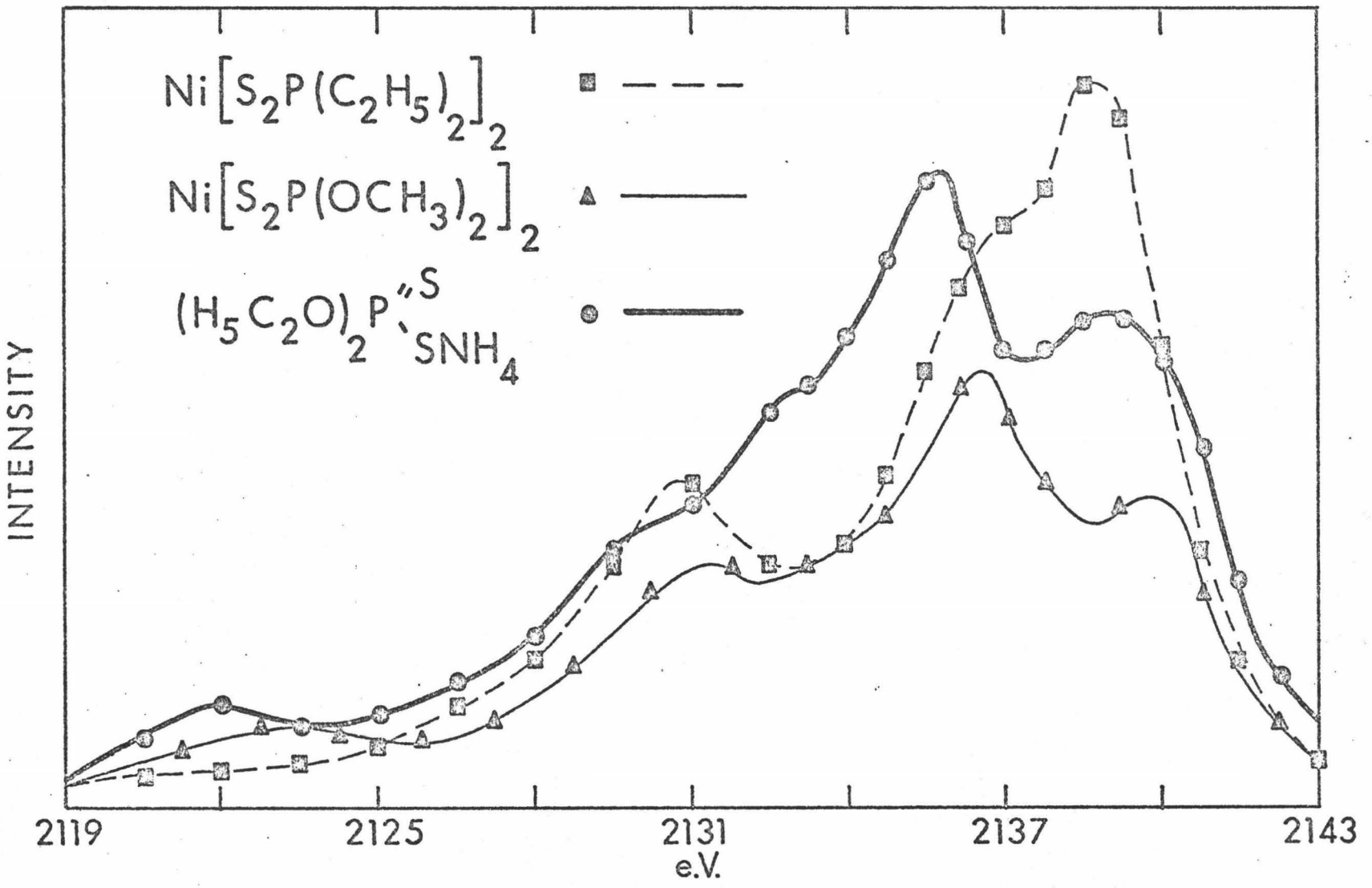

Figure 52
Band Width Comparison of Methoxy, Ethyl and "Parent" Compounds

CHAPTER V

Summary and Conclusions

The experimental and calculated results discussed above invite the following conclusions:

1) It has been shown, for the first time, that under favorable circumstances x-ray photon emission spectroscopy provides a probe for a localized bond, enabling the evaluation of the electronic structure of compounds, and further providing valuable insight into the bonding processes on both a practical and theoretical basis.

2) There is direct spectroscopic evidence that the extent of localization of a bond depends upon the specific ligands involved in the bonding; the greater the difference between these ligands, the more distinct will be the orbitals defining this bond. Furthermore, the larger the ligand, the more complicated is the bonding scheme and the greater the possibility of orbital mixing, as seen experimentally in proceeding from hydrogen to hydroxy to sulfur as ligands bonded to phosphorus.

3) The spectral results are easily interpretable on the basis of molecular orbital theory, and, furthermore, good correlation of spectra with calculations is possible even for "approximate molecular orbital methods." This aspect is particularly gratifying for the more complicated bonding situations.

4) $K\beta$ and $L_{2,3}$ spectra together with core photoelectron shift studies provide a complete description of the molecular bonding for our compounds, as all orbitals formed are active in either $K\beta$ or $L_{2,3}$ for the symmetries studied here.

5) From the observed spectral positions of the bands describing the bonding for a particular ligand, it appears possible to use x-ray emission spectroscopy for practical and specific ligand characterization and identification.

Suggestions for Further Work

The conclusions stated above call for further experimental and theoretical work to both confirm and extend the work presented here. The necessary work should include the following investigations:

1) The $L_{2,3}$ spectra for the Ni $\overline{/}S_2P(R)_2\overline{\backslash}_2$ compounds is necessary to fully understand the bonding to phosphorus in these compounds and to confirm the $K\beta$ assignment made here. The $L_{2,3}$ spectra may also provide further evidence for the participation of 3d orbitals in bonding of phosphorus.

2) Both $K\beta$ and $L_{2,3}$ spectra of sulfur in these compounds would provide a more complete bonding evaluation. In this respect it is desirable to obtain the emission spectra for all the ligands bonded to phosphorus. Since the ligands must possess the same bonding molecular orbitals as the central atom, their interpretation would give further insight to the total bonding scheme. For a true bonding representation, then, it is desirable to investigate all of the transitions for all of the bonded atoms.

3) It is desirable to perform further molecular orbital calculations on the compounds studied here. More rigorous calculations would be valuable, but even a comparison of "approximate methods" could prove useful. In this same respect it is also desired to perform these molecular orbital calculations on the molecule with a "hole" in the K shell as this better describes the true x-ray process.

4) Deconvolution of the spectra would be valuable for determination of the number of transitions represented by a particular band and thus provide better correlation with theory. This is particularly evident in the $K\beta$ spectra of the Ni $\underline{/}^{-}S_2P(R)_2\underline{-}^{-}/_2$ compounds with their very broad bands and large number of theoretically determined transitions.

5) The need to extend these concepts and investigations to compounds of other second row elements is obvious; of particular interest may be silicon and sulfur which bond in compounds similar to those of phosphorus.

APPENDIX A

Double Crystal Spectrometer

The double crystal unit designed by Whitehead, et al.,[40] is shown diagrammatically in Figure 53. The crystal arrangement is the anti-parallel mode for normal operation with two of the same crystals in positions D and H. In such an arrangement $\theta_1 = \theta_2 = \theta_3 = \theta_4$. The instrument is provided with continuous scanning ability and both crystals may be turned simultaneously, as the single crystal unit, or the second crystal may be rotated independently by a separate dial (N).

Each of the spectrometer parts labeled in the diagram is discussed below.

A: source

B: sample

C: primary collimator

D: first crystal

E: cross arm coupled to 2θ motion of existing spectrometer

F: internal flow proportional counter

G: shaft connected to E to translate 2θ motion to outside double crystal attachment

H: second crystal

I: crystal gear

J: crystal rack

K: external flow proportional counter

L: detector gear

M: detector rack

N: adjustor gear systems for fine adjustment of angular positions to second crystal (H) and external detector (K).

O: vacuum tight enclosure for soft x-ray region (3-20 Å)

The double crystal attachment takes advantage of the goniometer system of the one crystal unit to rotate the first crystal through an angle θ and a shaft (G) coupled to a cross arm (E) through an angle 2θ. The internal flow proportional counter (F) has been advanced so that it is out of the way of the double crystal operation; but it is still inside of the inner vacuum drum and may be used in alignment of the first crystal for use with the double crystal attachment. The 2θ motion is translated to the external parts of the attachment by the shaft (G) which is connected to the cross arm (E). The 2θ motion of the shaft maintains the center of rotation of the second crystal (H) in the center of the x-ray beam reflected from the first crystal (D). The second crystal is maintained at 3θ to the beam incident upon the first crystal by a 2:1 gear (I) and rack (J) system so as to maintain it at 4θ to the incident beam. The two separate adjustor gears (N) located at the bottom of the crystal rack and detector rack allow minor adjustments to be made independently on the second crystal and external detector.

The entire attachment is enclosed in a vacuum-tight enclosure (O) for operation in the soft x-ray region.

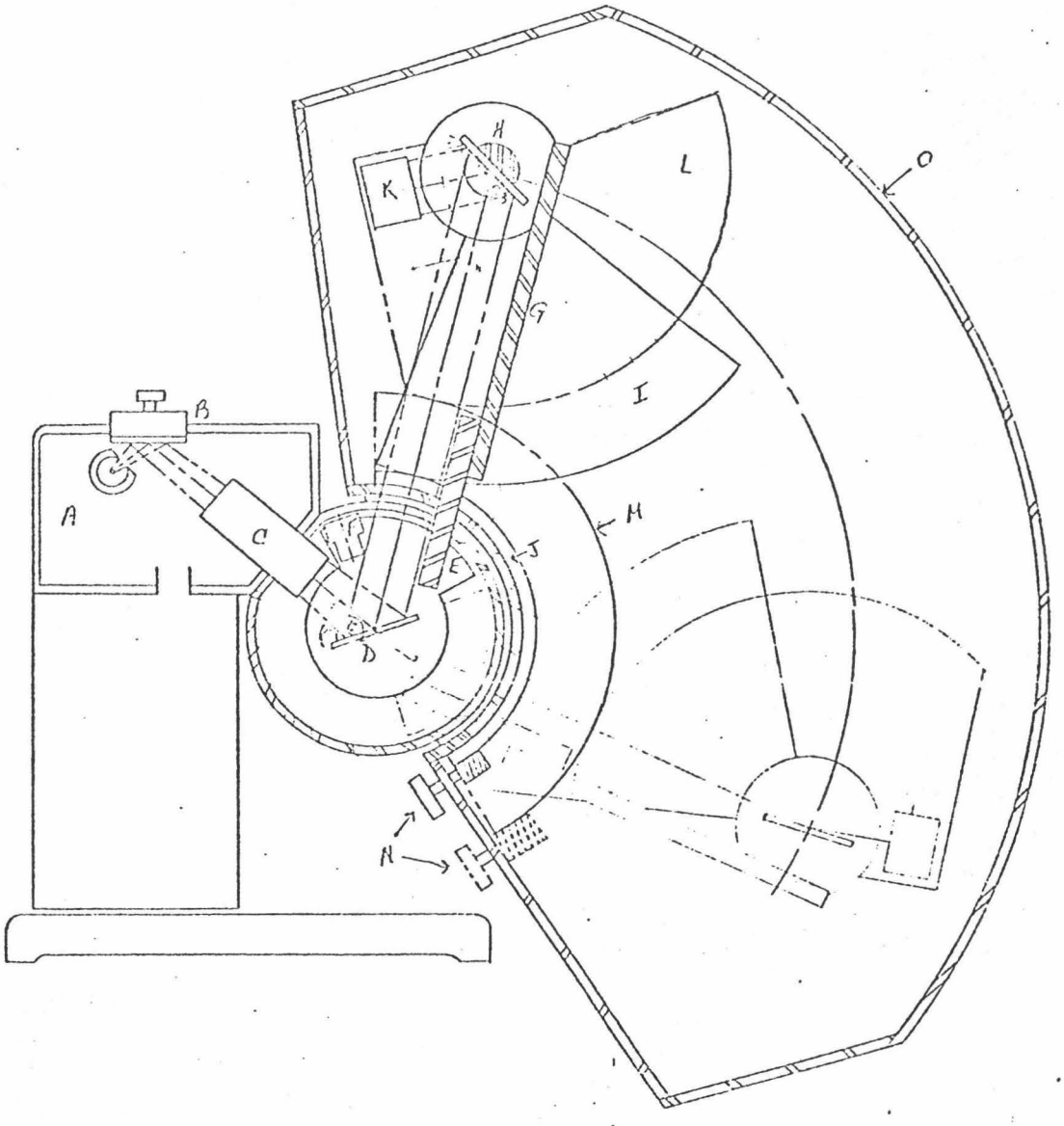

Figure 53

Double Crystal Spectrometer

APPENDIX B

Energy and Intensity Normalization

The normalization process involved two steps: establishment of an energy scale and correction of the intensity contour. It was necessary to first set up an appropriate energy scale as the intensity normalization entailed the joining of the energy scales of the three separate spectral segments before applying an intensity correction factor.

As mentioned in Chapter III, the dial rotating the second crystal is calibrated in units of 12 seconds of arc which is easily converted to degrees; the conversion from degrees to Angstroms then makes use of the dispersion relationship. The dispersion may be calculated from the derivative of Bragg's Law:

$$n\lambda = 2d \sin \theta$$

$$d\theta/d\lambda = n/2d \cos \theta$$

Alternately, the dispersion may be determined experimentally from the measured distance between two standard reference lines, as for example, between III Fe $K\alpha_1$ and III Fe $K\alpha_2$. In this manner the measured angular separation is correlated with the known Angstrom separation to give the dispersion value $d\theta/d\lambda$. The experimentally determined dispersion should then agree with the theoretically calculated values. However, the theoretical values calculated for each setting of PET and calcite consistently gave values higher than those determined experimentally. For example, for a PET setting of 83.40° 2θ the experimental dispersion was 40.04° θ/A while that determined from the Bragg equation derivative

was 41.25° θ/A. For this reason the experimental dispersion was used to establish the energy scale.

As mentioned in Chapter III, two factors must be considered in applying the dispersion relationship; first, the increasing dispersion upon higher angular setting of the PET crystal and second, the increasing dispersion during a scan of calcite to higher angles. Since the position of calcite was found to be a linear function of the PET setting (Figure 26), the dispersion was considered constant during any one scan at a specific PET setting. However, an individual dispersion was calculated for each setting of PET. The results of this calibration are discussed in Chapter III; the resultant energy scales are given in Tables 23, 24 and 25.

The intensity contour was corrected by piecing together three independently obtained sections; this method entailed the inherent problem of joining the energy scales properly. The choice of 83.05 and 83.60 2θ for scanning the main band ($K\beta$) and satellite ($K\beta'$) respectively was made because these were the positions providing maximum intensity for each of these bands as determined by single crystal PET scans. Therefore, for each of these scans the PET crystal has been set at the peak position. Since the crystal used for these studies gave a useful range of 6.5 eV, the intensity contour at 83.05 and 83.60 2θ should be correct to within about 3.2 eV on either side of the peak. Therefore, these 6.5 eV sections can be used without correction in piecing the spectra. The scan made with PET at 83.40 2θ is different. This position was chosen so as to give a 6.5 eV range which would just coincide with the ends of the useful ranges provided by the other two scans and so to

Table 23

Energy Scale for PET at 83.05°2θ

Scale Divisions	Ångstroms	Electron Volts	Scale Divisions	Ångstroms	Electron Volts
300	5.82754	2127.48	650	5.79799	2138.33
310	5.82669	2127.79	660	5.79714	2138.64
320	5.82585	2128.10	670	5.79630	2138.95
330	5.82501	2128.41	680	5.79546	2139.26
340	5.82416	2128.72	690	5.79461	2139.57
350	5.82332	2129.03	700	5.79377	2139.89
360	5.82247	2129.34	710	5.79292	2140.20
370	5.82163	2129.64	720	5.79208	2140.51
380	5.82078	2129.95	730	5.79123	2140.82
390	5.81994	2130.26	740	5.79039	2141.13
400	5.81910	2130.57	750	5.78955	2141.45
410	5.81825	2130.88	760	5.78870	2141.76
420	5.81741	2131.19	770	5.78786	2142.07
430	5.81656	2131.50	780	5.78701	2142.38
440	5.81572	2131.81	790	5.78617	2142.70
450	5.81487	2132.12	800	5.78532	2143.01
460	5.81403	2132.43	810	5.78448	2143.32
470	5.81319	2132.74	820	5.78364	2143.63
480	5.81234	2133.05	830	5.78279	2143.95
490	5.81150	2133.36	840	5.78195	2144.26
500	5.81065	2133.67	850	5.78110	2144.57
510	5.80981	2133.98	860	5.78026	2144.89
520	5.80896	2134.29	870	5.77941	2145.20
530	5.80812	2134.60	880	5.77857	2145.51
540	5.80728	2134.91	890	5.77773	2145.83
550	5.80643	2135.22	900	5.77688	2146.14
560	5.80559	2135.53	910	5.77604	2146.45
570	5.80474	2135.84	920	5.77519	2146.77
580	5.80390	2136.15	930	5.77435	2147.08
590	5.80305	2136.46	940	5.77350	2147.40
600	5.80221	2136.77	950	5.77266	2147.71
610	5.80137	2137.08	960	5.77182	2148.02
620	5.80052	2137.39	970	5.77097	2148.34
630	5.79968	2137.71	980	5.77013	2148.65
640	5.79883	2138.02	990	5.76928	2148.97
			1000	5.76844	2149.28

Table 24

Energy Scale for PET at 83.40°2θ

Scale Divisions	Å Angstroms	Electron Volts	Scale Divisions	Å Angstroms	Electron Volts
0	5.85987	2115.76	550	5.81411	2132.42
20	5.85821	2116.36	560	5.81328	2132.72
40	5.85654	2116.97	570	5.81245	2133.03
60	5.85488	2117.57	580	5.81161	2133.33
80	5.85321	2118.17	590	5.81078	2133.64
100	5.85155	2118.77	600	5.80995	2133.94
120	5.84989	2119.37	610	5.80912	2134.25
140	5.84822	2119.98	620	5.80829	2134.55
160	5.84656	2120.58	630	5.80745	2134.86
180	5.84489	2121.18	640	5.80662	2135.17
200	5.84323	2121.79	650	5.80579	2135.47
210	5.84240	2122.09	660	5.80500	2135.78
220	5.84157	2122.39	670	5.80413	2136.08
230	5.84073	2122.70	680	5.80329	2136.39
240	5.83990	2123.00	690	5.80246	2136.70
250	5.83907	2123.30	700	5.80163	2137.00
260	5.83824	2123.60	710	5.80080	2137.31
270	5.83741	2123.91	720	5.80000	2137.62
280	5.83657	2124.21	730	5.79913	2137.92
290	5.83574	2124.51	740	5.79830	2138.23
300	5.83491	2124.81	750	5.79747	2138.54
310	5.83408	2125.12	760	5.79664	2138.84
320	5.83325	2125.42	770	5.79581	2139.15
330	5.83241	2125.72	780	5.79500	2139.46
340	5.83158	2126.03	790	5.79414	2139.76
350	5.83075	2126.33	800	5.79331	2140.07
360	5.82992	2126.63	810	5.79248	2140.38
370	5.82909	2126.94	820	5.79165	2140.69
380	5.82825	2127.24	830	5.79081	2140.99
390	5.82742	2127.54	840	5.78998	2141.30
400	5.82659	2127.85	850	5.78915	2141.61
410	5.82576	2128.15	860	5.78832	2141.92
420	5.82493	2128.46	870	5.78749	2142.23
430	5.82409	2128.76	880	5.78665	2142.53
440	5.82326	2129.06	890	5.78582	2142.84
450	5.82243	2129.37	900	5.78499	2143.15
460	5.82160	2129.67	910	5.78416	2143.46
470	5.82077	2129.98	920	5.78333	2143.77
480	5.81993	2130.28	930	5.78249	2144.07
490	5.81910	2130.59	940	5.78166	2144.38
500	5.81827	2130.89	950	5.78083	2144.69
510	5.81744	2131.20	960	5.78000	2145.00
520	5.81661	2131.50	970	5.77917	2145.31
530	5.81577	2131.81	980	5.77833	2145.62
540	5.81494	2132.11	990	5.77750	2145.93
			1000	5.77667	2146.24

Table 25

Energy Scale for PET at 83.60°2θ

Scale Divisions	Å	Electron Volts	Scale Divisions	Å	Electron Volts
0	5.86369	2114.37	360	5.83414	2125.08
10	5.86287	2114.66	370	5.83332	2125.38
20	5.86204	2114.96	380	5.83249	2125.68
30	5.86122	2115.26	390	5.83167	2125.98
40	5.86040	2115.55	400	5.83085	2126.28
50	5.85958	2115.85	410	5.83003	2126.57
60	5.85876	2116.15	420	5.82921	2126.87
70	5.85794	2116.44	430	5.82839	2127.17
80	5.85712	2116.74	440	5.82757	2127.47
90	5.85630	2117.04	450	5.82675	2127.77
100	5.85548	2117.33	460	5.82593	2128.07
110	5.84973	2117.61	470	5.82511	2128.37
120	5.85384	2117.93	480	5.82429	2128.67
130	5.85302	2118.22	490	5.82347	2128.97
140	5.85219	2118.52	500	5.82264	2129.27
150	5.85137	2118.82	510	5.82182	2129.57
160	5.85055	2119.12	520	5.82100	2129.87
170	5.84973	2119.41	530	5.82018	2130.17
180	5.84891	2119.71	540	5.81936	2130.47
190	5.84809	2120.01	550	5.81854	2130.77
200	5.84727	2120.31	560	5.81772	2131.08
210	5.84645	2120.60	570	5.81690	2131.38
220	5.84563	2120.90	580	5.81608	2131.68
230	5.84481	2121.20	590	5.81526	2131.98
240	5.84399	2121.50	600	5.81444	2132.28
250	5.84317	2121.79	610	5.81362	2132.58
260	5.84234	2122.09	620	5.81279	2132.88
270	5.84152	2122.39	630	5.81197	2133.18
280	5.84070	2122.69	640	5.81115	2133.48
290	5.83988	2122.99	650	5.81033	2133.78
300	5.83906	2123.29	660	5.80951	2134.09
310	5.83824	2123.58	670	5.80869	2134.39
320	5.83742	2123.88	680	5.80787	2134.69
330	5.83660	2124.18	690	5.80705	2134.99
340	5.83578	2124.48	700	5.80623	2135.29
350	5.83496	2124.78	710	5.80541	2135.60

Table 25 (Continued)

Energy Scale for PET at 83.60°2θ

Scale Divisions	Ångstroms	Electron Volts	Scale Divisions	Ångstroms	Electron Volts
720	5.80459	2135.90	860	5.79310	2140.13
730	5.80377	2136.20	870	5.79227	2140.44
740	5.80295	2136.50	880	5.79145	2140.74
750	5.80212	2136.80	890	5.79063	2141.04
760	5.80130	2137.11	900	5.78981	2141.35
770	5.80048	2137.41	910	5.78899	2141.65
780	5.79966	2137.71	920	5.78817	2141.96
790	5.79884	2138.01	930	5.78735	2142.26
800	5.79802	2138.32	940	5.78653	2142.56
810	5.79720	2138.62	950	5.78571	2142.87
820	5.79638	2138.92	960	5.78489	2143.17
830	5.79556	2139.22	970	5.78407	2143.47
840	5.79474	2139.53	980	5.78325	2143.78
850	5.79392	2139.83	990	5.78242	2144.08
			1000	5.78160	2144.39

obtain the full 18 eV scan at one PET setting with a reasonable intensity contour (see Figure 27). However, this setting does not afford a true intensity representation for this section, the 83.40 2θ angle being too high. This may be seen in the distorted III Fe $K\alpha_{1,2}$ spectrum in Figure 54, since these lines occur in the same region as the $PK\beta$ segment of interest. Furthermore, the coincidence of III Fe $K\alpha_{1,2}$ lines with the distorted $PK\beta$ section makes them useful for correcting the intensity distribution; this was the approach used for intensity normalization of this middle segment. The actual III Fe $K\alpha_1$ and III Fe $K\alpha_2$ peak intensities from Figure 54 have been plotted in Figure 55 versus their corresponding energy values and a straight line relationship assumed for correction purposes. Since 83.40 2θ is the proper PET position for reflecting III Fe $K\alpha_2$ radiation, the intensity of this line may be considered absolute and the III Fe $K\alpha_1$ intensity then needs to be increased so as to give a 2:1 ratio with III Fe $K\alpha_2$; this is the source of the broken line in Figure 55. Thus, while these two straight lines do not represent a rigorous intensity contour calibration system, they may be used to approximate the percentage difference of the intensity contour at 83.40 2θ from the true contour. The percentage difference at each energy increment obtained from these plots may then be used to correct each point of another spectrum, e.g., each of the phosphorus spectra. When this middle segment has been so corrected, each of the three spectral segments is then joined together at the points of coincidence of the energy scales. The results for such a correction have been shown in Figure 27 for $CaHPO_3$; the main effect has been to significantly lower the intensity of this middle segment so that $K\beta_x$ is now lower in intensity

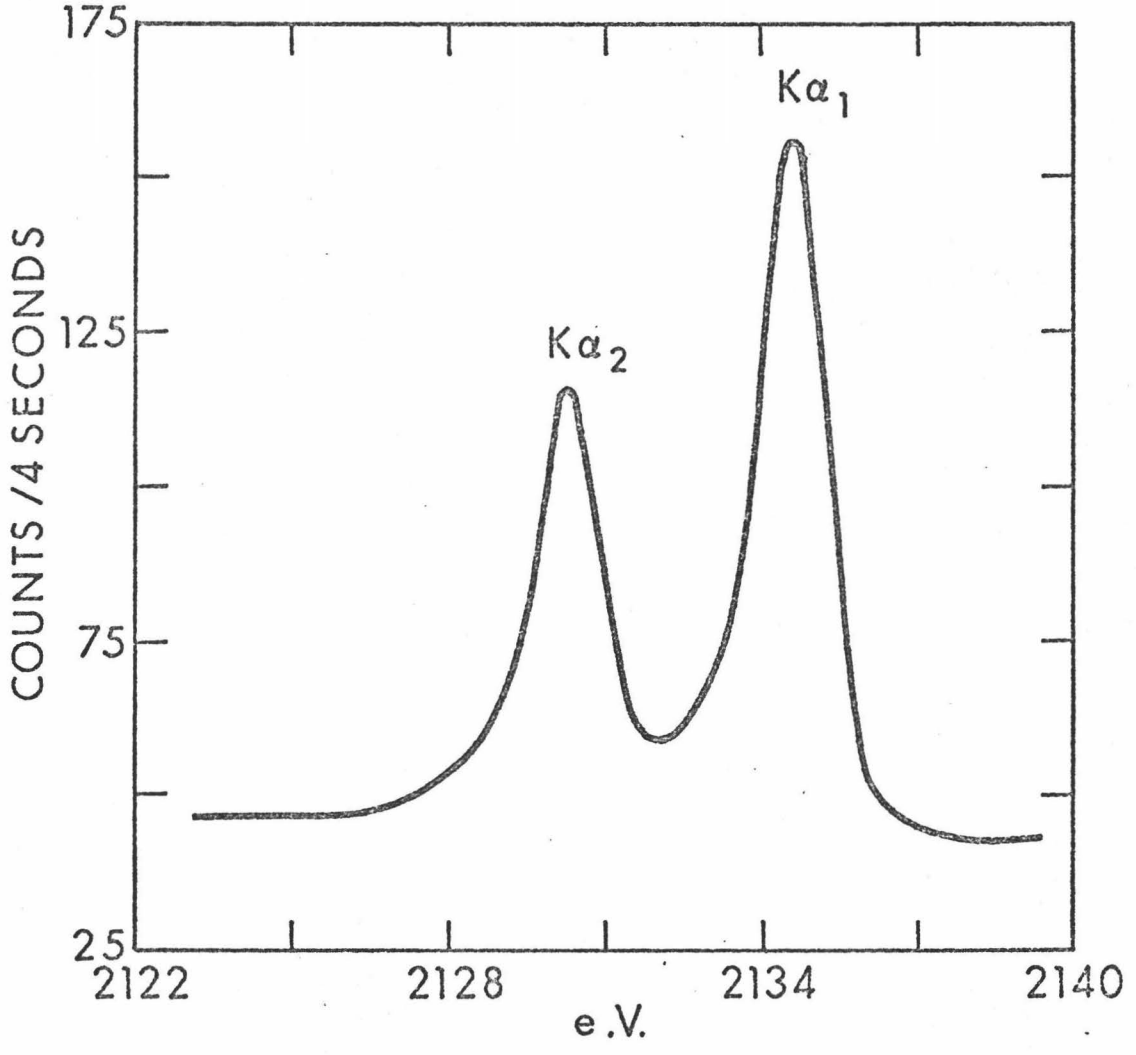

Figure 54

III Fe $K\alpha_{1,2}$ for PET Setting of 83.40°2θ

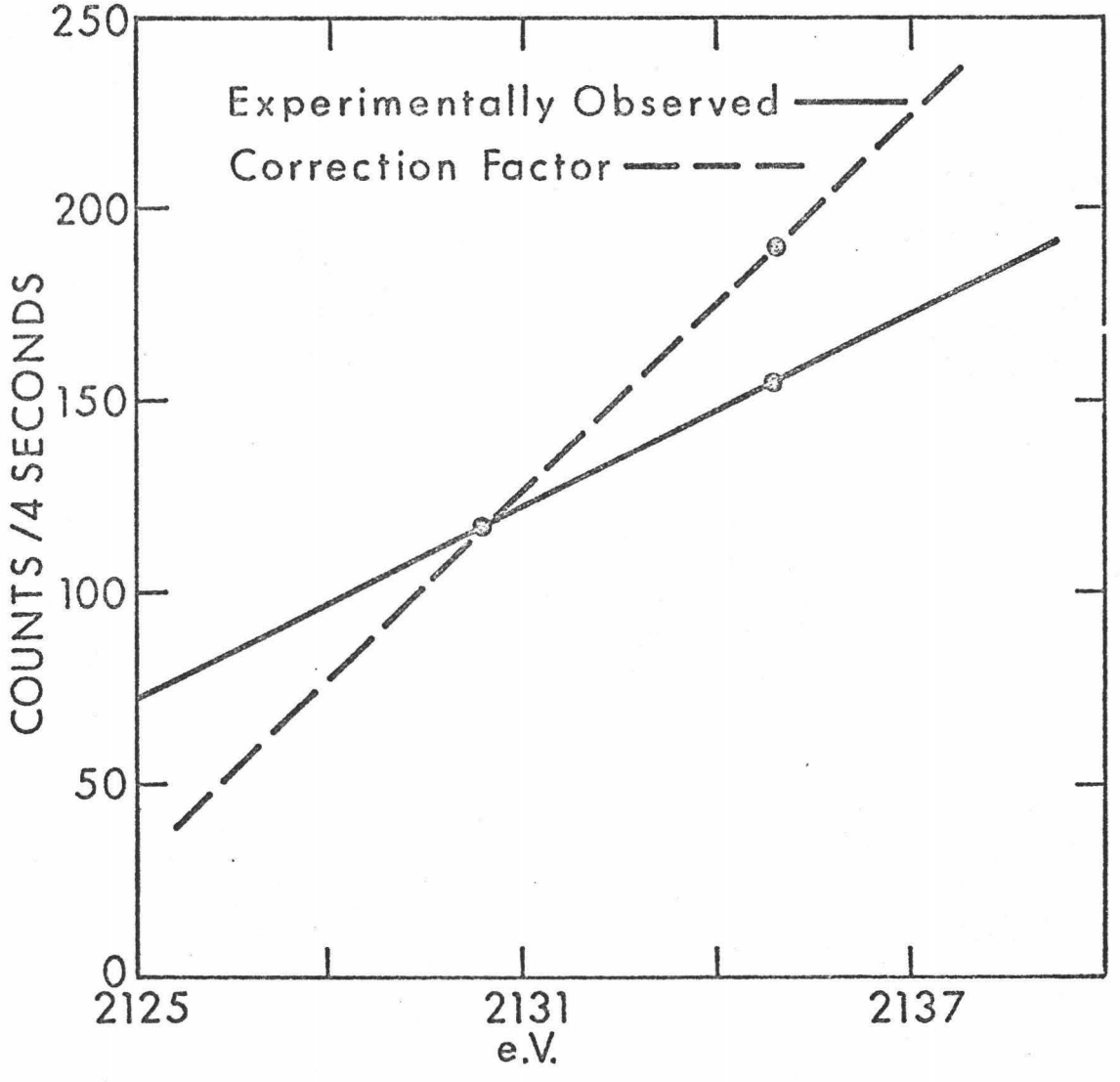

Figure 55

Intensity Correction Factor for III Fe $K\alpha_{1,2}$

than $K\beta'$, in better agreement with the $PK\beta$ distribution reported by Fichter.[22] Unfortunately, no other standard was available for correction and comparison with a previously published spectrum and a complete evaluation of this correction method is not possible.

APPENDIX C

Molecular Orbital Theory and CNDO Calculations

Molecular Orbital Theory

A complete treatment of molecular orbital theory is given in various texts and review articles;[26,51,52] a brief explanation of the molecular orbital approach, with a typical example, is offered here as a guide to understanding the work presented in Chapter IV.

The usual formulation of a molecular orbital assumes that it can be written as a linear combination of atomic orbitals:

$$\psi_i = \sum c_{ki} \chi_k$$

where c_{ki} is a coefficient describing the contribution of any atomic orbital (χ_k) to the molecular orbital (ψ_i). The complexity of the molecular orbital is dependent upon the basis set of atomic orbitals used to define the molecular orbital.

The ith eigenstate value of a given molecular orbital ψ_i may be found from the equation:

$$E_i = \int \psi_i^* \hat{H} \psi_i \, d\tau \Big/ \psi_i^* \psi_i \, d\tau$$

where $\hat{H}$ is the Hamiltonian operator. The actual energies of the molecular orbitals are found using the Variation Method in which the total energy is varied with respect to the coefficients (c_{ki}) so as to obtain a minimal value. This gives a set of secular equations:

$$\sum c_i (H_{ks} - E_{ks}) = 0$$

$H_{ks} = \int \chi_k \hat{H} \chi_s d\tau = \beta$: resonance integral, i.e., energy of interaction between χ_k and χ_s

$H_{kk} = \int \chi_k H \chi_k d\tau = \alpha$: coulomb integral

$S_{kk} = \int \chi_k \chi_k d\tau$ = +1 for normalized atomic orbital

$S_{ks} = \int \chi_k \chi_s d\tau$: $0 < S_{ks} < +1$: overlap integral (describes physical overlap in space of χ_k and χ_s

If the interaction of a set of n orbitals is being considered, there will be n equations corresponding to n possible values of s and each equation will have n terms as k takes the values 1-----n. The n possible values of E are then found by solving the determinant:

$$\left| H_{ks} - ES_{ks} \right| = 0$$

The calculations are simplified if S_{ks} ($k \neq s$) is set equal to zero--this is the neglect of overlap approximation--and if the interactions between nonadjacent orbitals are ignored--$H_{ks} = 0$--unless χ_k and χ_s are adjacent (Hückel Approximation).

Because the Hamiltonian Operator commutes with the symmetry operators, further computational simplification may be obtained by the application of symmetry. Thus, H_{ks} will only be nonzero if the wave functions χ_k and χ_s belong to the same irreducible representation, or are a linear combination of atomic orbitals chosen so as to correspond to the irreducible representation of the molecule.

As an example, consider a molecule of T_d symmetry (ML_4). First, it is necessary to classify the atomic orbitals according to their symmetry properties; this is done by determining how the orbitals transform under T_d symmetry.

M Valence Shell Orbitals		L Valence Shell Orbitals	
s (one orbital)	: a_1	s (four orbitals)	: $a_1 + t_2$
p (three orbitals):	t_2	p_z (four orbitals)	: $a_1 + t_2$
d (five orbitals)	: $t_2 + e$	$p_x p_y$ (eight orbitals):	$e + t_2 + t_1$

σ and π separability of the ligand 2p orbitals has been assumed here for simplicity, although this is not necessary in the actual calculations. By thus classifying the 25 valence orbitals under different irreducible representations the computations are considerably simplified. It is now necessary to consider the interactions of the four groups of orbitals, a_1, t_2, e and t_1.

a) σ bonding

a_1 representation:

1) M s orbital

2) orbital from the four ligands: $1/2(L_{as} + L_{bs} + L_{cs} + L_{ds})$

3) orbital from the four ligands: $1/2(L_{ap} + L_{bp} + L_{cp} + L_{dp})$

the determinant then is:

$$\begin{vmatrix} \alpha(M_s) - E & \beta_1 & \beta_2 \\ \beta_1 & \alpha(L_s) - E & 0 \\ \beta_2 & 0 & \alpha(L_p) - E \end{vmatrix}$$

t_2 representation:

M_p three orbitals: p_x, p_y, p_z

L_s three orthogonal orbitals of the type: $1/2(L_{as} + L_{bs} - L_{cs} - L_{ds})$

L_p three orthogonal orbitals of the type: $1/2(L_{ap} + L_{bp} - L_{cp} - L_{dp})$

the resultant 9 by 9 determinant is of the form of three identical 3 by 3 determinants since there are three identical and orthogonal systems present.

b) π bonding

t_2 representation:

M_d three orthogonal orbitals: d_{xy}, d_{xz}, d_{yz}

L_p three orthogonal orbitals: p_x, p_y, p_z

the resultant 6 by 6 determinant is of the form of three identical 2 by 2 determinants.

A similar method is used for e and t_1. From these determinants the appropriate molecular energy values are obtained upon substitution of appropriate values for α and β. The resultant series of molecular energy levels in order of increasing energy for a tetrahedral oxy-anion[17] are:

$$1a_1 < 1t_2 < 2a_1 < 2t_2 < 1e < 3t_2 < 1t_1$$

CNDO Calculations

The CNDO calculations were performed so as to obtain an ordering of the molecular energy levels and an idea of the atomic orbital contribution to each molecular orbital. The eigenvalues and corresponding eigenvectors for all of the compounds discussed in the text are given in the accompanying computer output; specific results for HPO_3^{-2} are discussed here.

The symmetries of the resultant molecular orbitals may be determined from consideration of the atomic coefficients of the central atom, phosphorus, and the symmetries of each of its orbitals. For example, the 3s atomic orbital on phosphorus transforms as a_1; if this orbital and the others transforming as a_1 have large coefficients while those transforming as e or a_2 have small coefficients, then the molecular orbital is assigned an a_1 symmetry. For T_d and C_{3v} symmetries this is straightforward and easily determined, but for C_{2v} symmetry the distinction is not always

EIGENVALUES AND EIGENVECTORS $HPO_3^=$

					1a$_1$	1e		2a$_1$	3a$_1$	2e		3e		4a$_1$	4e	
EIGENVALUES---					-0.7560	-0.6707	-0.6707	-0.1969	-0.0564	-0.0510	-0.0510	0.0560	0.0560	0.0840	0.1062	
					1	2	3	4	5	6	7	8	9	10	11	
1	1	P	S		0.4748	-0.0000	0.0000	-0.4556	-0.2294	-0.0000	0.0000	0.0000	-0.0000	-0.1004	-0.0000	
2	1	P	PX		-0.0000	-0.2967	-0.1112	-0.0000	0.0000	-0.2999	0.0356	-0.2498	-0.2585	0.0000	-0.0543	
3	1	P	PY		0.0000	0.1112	-0.2967	-0.0000	-0.0000	-0.0356	-0.2999	0.2585	-0.2408	0.0000	0.0667	
4	1	P	PZ		-0.1135	0.0000	-0.0000	-0.3546	0.4307	0.0000	-0.0000	-0.0000	0.0000	0.1132	-0.0000	
5	1	P	DZ2		-0.0932	0.0000	-0.0000	-0.1197	-0.1306	-0.0000	0.0000	-0.0000	-0.0000	0.4333	-0.0000	
6	1	P	DXZ		0.0000	0.1276	0.0478	0.0000	-0.0000	0.1787	-0.0212	-0.1417	-0.1521	-0.0000	0.1639	
7	1	P	DYZ		-0.0000	-0.0478	0.1276	0.0000	0.0000	0.0212	0.1787	0.1521	-0.1417	-0.0000	-0.2015	
8	1	P	DX-Y		-0.0000	-0.1788	-0.0670	0.0000	-0.0000	0.3146	-0.0373	-0.1205	-0.1293	0.0000	-0.1360	
9	1	P	DXY		-0.0000	-0.0670	0.1788	-0.0000	-0.0000	-0.0373	-0.3146	-0.1293	0.1205	-0.0000	-0.1671	
10	2	H	S		0.1419	-0.0000	0.0000	-0.6023	0.1766	0.0000	-0.0000	-0.0000	-0.0000	0.4610	-0.0000	
11	3	O	S		0.4903	0.1231	0.7396	0.1955	0.1259	-0.0464	-0.0622	0.0321	-0.1048	0.0539	0.0275	
12	3	O	PX		0.0309	-0.0251	0.0038	-0.0818	-0.2006	-0.3826	0.4426	-0.0311	0.1266	-0.0769	0.1328	
13	3	O	PY		0.0534	0.0143	-0.0031	-0.1416	-0.3474	0.3944	-0.0233	-0.0694	0.2127	-0.1331	-0.3402	
14	3	O	PZ		0.0127	0.0011	0.0064	-0.1776	0.2472	-0.0682	-0.0913	-0.1976	0.6450	-0.4071	0.0383	
15	4	O	S		0.4903	-0.7021	-0.2632	0.1955	0.1259	0.0771	-0.0091	0.0747	0.0822	0.0539	0.0488	
16	4	O	PX		-0.0617	-0.0008	-0.0003	0.1636	0.4011	0.2494	-0.0296	0.1761	0.1893	0.1537	0.4044	
17	4	O	PY		0.0000	0.0103	-0.0274	-0.0000	-0.0000	-0.0777	-0.6552	-0.0360	0.3056	-0.0000	-0.2367	
18	4	O	PZ		0.0127	-0.0060	-0.0023	-0.1776	0.2472	0.1131	-0.0134	-0.4598	-0.4936	-0.4071	0.1742	
19	5	O	S		0.4903	0.5789	-0.4764	0.1955	0.1259	-0.0306	0.0713	-0.1068	0.0246	0.0539	-0.0763	
20	5	O	PX		0.0309	-0.0164	-0.0193	-0.0818	-0.2006	-0.4755	-0.3408	0.1274	-0.0221	-0.0769	0.3583	
21	5	O	PY		-0.0534	-0.0087	-0.0117	0.1416	0.3474	-0.3889	0.0697	-0.2171	0.0542	0.1331	-0.5237	
22	5	O	PZ		0.0127	0.0050	-0.0041	-0.1776	0.2472	-0.0449	0.1047	0.6574	-0.1614	-0.4071	-0.2724	

					1a$_2$	5a$_1$	5e		6a$_1$	6e		7a$_1$	7e		
EIGENVALUES---					0.1062	0.1936	0.7205	0.8272	0.8272	0.8576	0.9656	0.9656	1.0032	1.0669	1.0669
					12	13	14	15	16	17	18	19	20	21	22
1	1	P	S		0.0000	-0.0000	-0.7004	0.0000	0.0000	-0.0679	0.0000	0.0000	0.0956	0.0000	-0.0000
2	1	P	PX		0.0667	-0.0000	-0.0000	0.0883	-0.6870	-0.0000	-0.0092	-0.1890	-0.0000	-0.3976	0.0495
3	1	P	PY		0.0343	0.0000	-0.0000	-0.6870	-0.0883	-0.0000	-0.1890	0.0092	-0.0000	-0.0495	-0.3976
4	1	P	PZ		-0.0000	-0.0000	-0.1131	-0.0000	-0.0000	0.7627	-0.0000	-0.0000	-0.2622	-0.0000	0.0000
5	1	P	DZ2		-0.0000	0.0000	-0.0805	0.0000	0.0000	-0.3480	0.0000	0.0000	-0.8329	-0.0000	0.0000
6	1	P	DXZ		-0.2015	0.0000	-0.0000	0.0594	-0.4621	-0.0000	0.0343	0.7017	-0.0000	0.3548	-0.0442
7	1	P	DYZ		-0.1639	0.0000	0.0000	-0.4621	-0.0594	-0.0000	0.7017	-0.0343	0.0000	0.0442	0.3548
8	1	P	DX-Y		0.1671	-0.0000	0.0000	-0.0386	0.3005	0.0000	0.0252	0.5160	0.0000	-0.6483	0.0807
9	1	P	DXY		-0.1360	-0.0000	-0.0000	-0.3005	-0.0386	-0.0000	-0.5160	0.0252	-0.0000	0.0807	0.6483
10	2	H	S		-0.0000	0.0000	0.4358	0.0000	0.0000	-0.2408	-0.0000	0.0000	0.3541	0.0000	-0.0000
11	3	O	S		0.0722	-0.0000	0.1339	-0.0603	-0.0460	0.0636	-0.0375	-0.0193	-0.1184	-0.1630	-0.2155
12	3	O	PX		-0.3935	0.5000	0.1345	-0.1661	0.1329	0.0926	-0.1659	0.1764	-0.0539	-0.1573	-0.0771
13	3	O	PY		-0.4642	-0.2887	0.2329	0.0013	-0.1489	0.1604	-0.0417	-0.1725	-0.0933	-0.1270	-0.2435
14	3	O	PZ		0.2578	-0.0000	0.0992	-0.2070	-0.1579	-0.1996	0.1864	0.0958	-0.1583	-0.0625	-0.0827
15	4	O	S		-0.0600	0.0000	0.1339	-0.0097	0.0752	0.0636	0.0021	0.0421	-0.1184	0.2681	-0.0334
16	4	O	PX		-0.4970	0.0000	-0.2590	0.0131	-0.1022	-0.1852	-0.0065	-0.1336	0.1077	-0.3103	0.0386
17	4	O	PY		-0.1926	0.5774	-0.0000	0.2364	0.0304	0.0000	0.2684	-0.0131	0.0000	-0.0113	-0.0905
18	4	O	PZ		-0.2140	-0.0000	0.0992	-0.0332	0.2582	-0.1996	-0.0102	-0.2094	-0.1583	0.1028	-0.0128
19	5	O	S		-0.0123	-0.0000	0.1339	0.0700	-0.0292	0.0636	0.0355	-0.0229	-0.1184	-0.1051	0.2489
20	5	O	PX		-0.2100	-0.5000	0.1345	0.1271	0.1706	0.0926	0.1823	0.1594	-0.0539	-0.1336	0.1133
21	5	O	PY		-0.2387	-0.2887	-0.2329	-0.0364	0.1444	-0.1604	-0.0246	0.1757	0.0933	0.0634	-0.2672
22	5	O	PZ		-0.0438	-0.0000	0.0992	0.2402	-0.1004	-0.1996	-0.1762	0.1136	-0.1583	-0.0403	0.0955

clear due to the greater orbital mixing and nondegenerate orbitals. In such a case it is necessary to consider the magnitude of the coefficients on the ligand orbitals and/or the effect of a symmetry operation upon the orbitals.

For HPO_3^{-2} the following symmetries were assigned to the atomic orbitals:

Phosphorus	Hydrogen	Oxygen
3s: a_1	1s: a_1	2s: $a_1 + e$
$3p_z$: a_1		2p: $a_1 + e + a_2$
$3p_x, 3p_y$: e		
$3d_{z2}$: a_1		
$3d_{x2-y2}, 3d_{xy}$: e		
$3d_{xz}, 3d_{yz}$: e		

The resultant assigned molecular orbital symmetries are indicated above each column of eigenvectors; the correlation between the atomic coefficients, atomic symmetries and the resultant assigned molecular symmetries is obvious.

It is next desired to determine which orbitals contribute to the bonding for each molecular orbital. Whether a particular ligand orbital is bonding or antibonding with the central phosphorus atom is determined from the geometrical arrangement of the orbitals and the signs associated with them. All orbitals are arranged in a cartesian coordinate system according to the right hand screw rule; thus the p_y and p_z orbitals may be pictured as:

p_y

p_z

Now, for any ligand orbital to be bonding with the phosphorus orbitals it must have the same sign in the region of maximum interaction. For example, if the phosphorus p_z orbital is to be bonding with hydrogen 1s in the following arrangement:

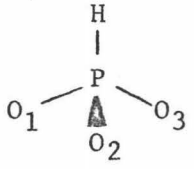

the hydrogen 1s orbital must have a positive sign if the phosphorus 3p is positive. However, if the phosphorus 3p orbital is to be bonding with oxygen (#3) $2p_y$, then the oxygen $2p_y$ orbital must carry a negative sign if the phosphorus $3p_y$ is positive. If oxygen $2p_y$ has a positive sign it is considered antibonding with phosphorus $3p_y$.

Although it is the square of the phosphorus coefficients that mainly determines the intensity of a band, the ligand orbitals do contribute to this intensity if they are bonding. But if the ligand orbitals are antibonding, they do not contribute any additional electron density; in this lies the rationale behind assigning a spectral band as describing the bonding to a particular ligand or ligand orbital.

A complete understanding of the CNDO methods and approximations may be gained from the publications of J. A. Pople, et al.,[53,54,55,56,57] who developed this approximate molecular orbital technique.

EIGENVALUES AND EIGENVECTORS PO_4^{-3}

					$1a_1$	$1t_2$			$2a_1$	$1e$		$2t_2$			
EIGENVALUES---					-0.4481	-0.3699	-0.3699	-0.3699	0.2531	0.2535	0.2535	0.2546	0.2546	0.2546	0.3855
					1	2	3	4	5	6	7	8	9	10	11
1	1	P	S		-0.4938	0.0000	0.0000	0.0000	0.5834	0.0000	-0.0000	0.0000	0.0000	-0.0000	-0.0000
2	1	P	PX		-0.0001	-0.3039	-0.0001	-0.0190	0.0000	0.0000	-0.0000	0.0617	-0.0482	0.4159	0.2100
3	1	P	PY		-0.0000	0.0003	-0.3045	-0.0024	-0.0000	-0.0000	-0.0002	0.0002	0.4195	0.0487	-0.0305
4	1	P	PZ		0.0000	-0.3190	-0.0024	0.3039	-0.0000	-0.0001	-0.0001	0.4178	0.0079	-0.0613	-0.0641
5	1	P	DZ2		0.0000	-0.0142	-0.0018	0.2271	0.0030	0.0000	0.0000	-0.1494	-0.0033	0.0293	-0.0964
6	1	P	DXZ		0.0000	0.1311	0.0001	0.0082	0.0000	-0.3554	0.0127	0.0169	-0.0133	0.1144	-0.1425
7	1	P	DYZ		0.0000	-0.0001	0.1313	0.0010	-0.0000	0.0127	0.3554	0.0001	0.1157	0.0134	0.0005
8	1	P	DX-Y		-0.0000	-0.1654	-0.0001	-0.0116	-0.0000	-0.2513	0.0090	-0.0241	0.0148	-0.1617	0.2582
9	1	P	DXY		0.0000	-0.0002	0.1353	0.0014	-0.0000	-0.0090	-0.2514	0.0000	0.1634	0.0190	0.0006
10	2	O	S		-0.4314	-0.0499	-0.0363	0.7987	-0.1997	0.0000	0.0000	-0.1079	-0.0018	0.0158	0.0349
11	2	O	PX		-0.0000	-0.0269	-0.0000	-0.0016	0.0000	-0.4497	0.0161	0.0721	-0.0964	0.4957	-0.2315
12	2	O	PY		-0.0000	0.0000	-0.0250	-0.0002	-0.0000	0.0161	0.4496	0.0003	0.4911	0.0570	0.0006
13	2	O	PZ		0.0544	0.0001	0.0000	-0.0016	-0.3728	0.0001	0.0001	-0.2889	-0.0048	0.0424	0.2264
14	3	O	S		-0.4314	-0.7354	0.0018	-0.3133	-0.1997	-0.0000	-0.0000	0.0229	0.0123	-0.1063	-0.1195
15	3	O	PX		0.0613	-0.0017	-0.0001	0.0083	-0.3515	-0.1550	0.0053	0.2145	0.0274	-0.2370	-0.0639
16	3	O	PY		-0.0000	0.0000	-0.0250	-0.0002	-0.0000	-0.0161	-0.4496	0.0001	0.4908	0.0570	0.0006
17	3	O	PZ		-0.0181	-0.0038	-0.0002	0.0214	0.1243	-0.4241	0.0151	0.4385	-0.0215	0.1838	0.2256
18	4	O	S		-0.4314	0.3926	0.6356	-0.2376	-0.1997	-0.0000	-0.0000	0.0435	0.0832	0.0555	0.0421
19	4	O	PX		-0.0257	-0.0138	0.0003	-0.0053	0.1757	0.3092	0.2491	-0.0756	-0.4390	0.2970	-0.3987
20	4	O	PY		-0.0444	0.0127	-0.0071	-0.0067	0.3044	-0.2597	0.0094	-0.2560	0.0714	-0.2697	-0.1331
21	4	O	PZ		-0.0181	0.0026	0.0071	0.0223	0.1243	0.1988	-0.3748	0.3843	-0.1319	-0.2092	0.0161
22	5	O	S		-0.4314	0.3937	-0.6511	-0.2478	-0.1997	0.0000	0.0000	0.0434	-0.0937	0.0350	0.0425
23	5	O	PX		-0.0257	-0.0187	-0.0103	-0.0055	0.1757	0.2906	-0.2705	-0.0754	0.2620	0.3668	-0.3395
24	5	O	PY		0.0444	-0.0107	0.0072	0.0064	-0.3044	0.2597	-0.0093	0.2560	-0.0638	0.2628	0.1357
25	5	O	PZ		-0.0181	0.0028	-0.0075	0.0222	0.1243	0.2251	0.3595	0.3847	0.2335	-0.1558	0.0155

					$3t_2$		$1t_1$			$3a_1$	$4t_2$			$2e$	
EIGENVALUES---					0.4305	0.4305	0.4305	0.4305	0.4305	1.0303	1.1402	1.1402	1.1402	1.2631	1.2631
					12	13	14	15	16	17	18	19	20	21	22
1	1	P	S		0.0000	-0.0000	0.0000	0.0000	0.0000	0.6868	-0.0000	0.0000	0.0000	0.0000	-0.0000
2	1	P	PX		-0.0001	-0.0641	-0.0000	0.0000	-0.0000	0.0000	0.0043	-0.7336	-0.0331	0.0000	0.0000
3	1	P	PY		-0.2196	-0.0012	-0.0000	0.0000	-0.0000	0.0000	0.7347	0.0042	0.0007	-0.0000	0.0000
4	1	P	PZ		0.0013	-0.2130	0.0000	-0.0000	0.0000	0.0000	0.0085	0.0391	-0.7337	-0.0000	-0.0000
5	1	P	DZ2		0.0020	-0.3160	-0.0000	0.0000	-0.0000	-0.0000	-0.0003	-0.0248	0.4559	-0.0000	0.0000
6	1	P	DXZ		0.0681	0.0597	-0.0000	0.0000	-0.0000	0.0000	0.0016	-0.2690	-0.0143	-0.0010	-0.7350
7	1	P	DYZ		0.1926	0.0011	-0.0000	0.0000	-0.0000	0.0000	0.2694	0.0016	0.0003	0.7350	-0.0010
8	1	P	DX-Y		-0.0002	-0.0747	0.0000	-0.0000	0.0000	-0.0000	-0.0022	0.3804	0.0203	-0.0147	-0.5197
9	1	P	DXY		0.2696	0.0015	-0.0000	-0.0000	-0.0000	0.0000	0.3809	0.0022	0.0004	-0.5197	0.0007
10	2	O	S		-0.0707	0.1144	0.0000	0.0000	-0.0000	-0.1551	-0.0001	-0.0050	0.0035	0.0000	0.0000
11	2	O	PX		-0.0002	0.3766	-0.0368	-0.0314	0.0114	-0.0000	-0.1115	0.2577	0.0137	0.0003	0.2176
12	2	O	PY		0.2426	0.0014	-0.0315	-0.3097	0.5258	-0.0000	-0.2560	-0.0015	-0.0002	-0.2178	0.0003
13	2	O	PZ		-0.0045	0.6767	0.0000	0.0000	0.0000	0.3287	0.0001	0.0106	-0.1997	-0.0000	-0.0000
14	3	O	S		0.0003	-0.0352	0.0100	-0.0000	0.0000	-0.1551	-0.0005	0.0098	-0.0265	-0.0000	-0.0000
15	3	O	PX		0.0013	0.0514	-0.2323	0.0271	-0.0038	0.3099	0.0008	-0.1566	0.1358	0.0001	0.0726
16	3	O	PY		0.2426	0.0014	0.3776	0.5954	0.1206	-0.0000	-0.2560	-0.0015	-0.0012	0.2178	-0.0003
17	3	O	PZ		-0.0019	0.2393	-0.5721	0.0768	-0.0138	-0.1096	-0.0010	0.1327	0.2145	0.0003	0.2053
18	4	O	S		-0.0674	-0.0551	-0.0000	0.0000	-0.0000	-0.1550	0.3767	-0.0420	-0.0335	-0.0000	-0.0000
19	4	O	PX		-0.1739	0.1718	-0.1499	0.4533	0.2524	-0.1550	0.1754	0.1609	-0.0634	0.1259	-0.1452
20	4	O	PY		0.5916	0.1765	-0.3131	-0.1428	-0.3232	-0.2684	0.0484	-0.1691	-0.1338	0.0002	0.1257
21	4	O	PZ		0.1249	0.3630	0.2440	-0.2913	0.4347	-0.1096	0.1249	-0.0822	0.2031	0.1777	-0.1029
22	5	O	S		0.0678	-0.0546	-0.0000	0.0000	0.0000	-0.1550	-0.0762	-0.0429	-0.0336	0.0000	0.0000
23	5	O	PX		-0.1794	0.1697	-0.2546	-0.3990	-0.2600	-0.1550	-0.1772	0.1588	-0.0637	0.1255	-0.1454
24	5	O	PY		0.5830	-0.1763	-0.3131	-0.1428	-0.3232	0.2684	0.0462	0.1697	0.1339	-0.0002	-0.1257
25	5	O	PZ		-0.1234	0.3614	0.4281	0.2145	-0.4239	-0.1096	-0.1244	-0.0836	0.2029	-0.1780	-0.1024

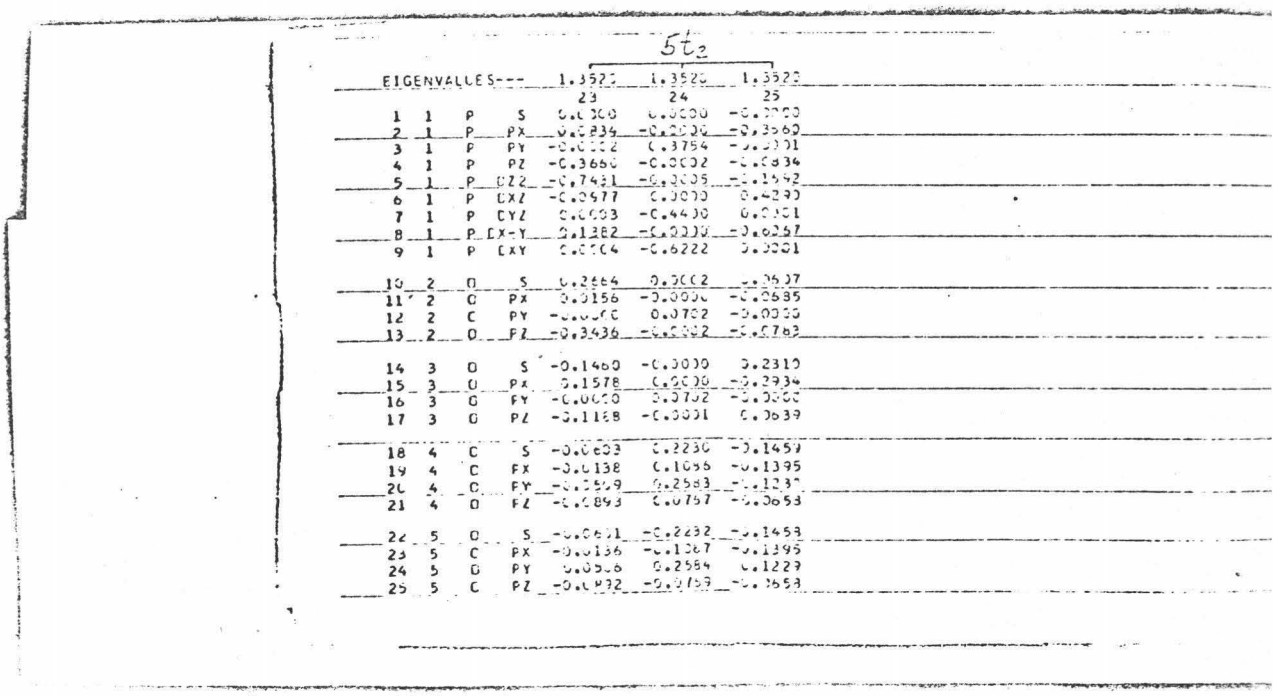

$5t_2$

EIGENVALUES---				1.3520	1.3520	1.3520
				23	24	25
1	1	P	S	0.0308	0.0000	-0.0000
2	1	P	PX	0.0834	-0.0000	-0.3660
3	1	P	PY	-0.0002	0.3754	-0.0001
4	1	P	PZ	-0.3660	-0.0002	-0.0834
5	1	P	DZ2	-0.7431	-0.0005	-0.1542
6	1	P	DXZ	-0.0977	0.0000	0.4290
7	1	P	DYZ	0.0003	-0.4400	0.0001
8	1	P	DX-Y	0.1382	-0.0000	-0.0257
9	1	P	DXY	0.0004	-0.6222	0.0001
10	2	D	S	0.2664	0.0002	-0.0607
11	2	D	PX	0.0156	-0.0000	-0.0685
12	2	D	PY	-0.0000	0.0702	-0.0000
13	2	D	PZ	-0.3436	-0.0002	-0.0783
14	3	D	S	-0.1460	-0.0000	0.2310
15	3	D	PX	0.1578	0.0000	-0.2934
16	3	D	PY	-0.0000	0.0702	-0.0000
17	3	D	PZ	-0.1188	-0.0001	0.0639
18	4	D	S	-0.0603	0.2230	-0.1459
19	4	D	PX	-0.0138	0.1096	-0.1395
20	4	D	PY	-0.2569	0.2583	-0.1237
21	4	D	PZ	-0.0893	0.0767	-0.0653
22	5	D	S	-0.0601	-0.2232	-0.1459
23	5	D	PX	-0.0136	-0.1087	-0.1395
24	5	D	PY	0.0506	0.2584	0.1229
25	5	D	PZ	-0.0892	-0.0769	-0.0653

EIGENVALUES AND EIGENVECTORS $H_2PO_2^-$

				1a₁	1b₂	2a₁	1b₁	2b₁	2b₂	3b₂	3a₁	4a₁	1a₂	5a₁
EIGENVALUES---				-1.0755	-1.0151	-0.5360	-0.3909	-0.3871	-0.2835	-0.2821	-0.2617	-0.2499	-0.2177	0.3450
				1	2	3	4	5	6	7	8	9	10	11
1	1	P	S	0.4131	0.0000	-0.6028	-0.0839	-0.0084	0.0000	-0.0000	0.0678	0.0016	0.0000	-0.6521
2	1	P	PX	-0.1583	-0.0000	-0.2023	0.3152	-0.3247	-0.0000	0.0000	-0.2424	0.0236	-0.0000	-0.1363
3	1	P	PY	0.0000	-0.3172	-0.0000	0.0000	0.0000	0.4132	-0.2485	-0.0000	-0.0000	0.0219	-0.0000
4	1	P	PZ	-0.1084	-0.0000	-0.1439	0.1883	0.4880	-0.0000	0.0000	-0.1650	-0.0751	-0.0000	-0.0901
5	1	P	DZ2	-0.0866	-0.0000	-0.0742	-0.0743	0.0134	-0.0000	-0.0000	-0.1443	-0.3914	0.0000	-0.0293
6	1	P	DXZ	0.0704	0.0000	0.0804	-0.1751	-0.0060	-0.0000	-0.0000	-0.0044	-0.1576	0.0000	-0.0093
7	1	P	DYZ	-0.0000	0.1356	0.0000	0.0000	0.0000	0.1636	0.3099	0.0000	-0.0000	0.1760	-0.0000
8	1	P	DX-Y	-0.0961	-0.0000	-0.0725	-0.2579	-0.0209	-0.0000	0.0000	-0.3391	0.1884	0.0000	-0.0510
9	1	P	DXY	-0.0000	0.1969	0.0000	0.0000	-0.0000	-0.1472	-0.1940	0.0000	0.0000	0.2528	-0.0000
10	2	H	S	0.0847	0.0000	-0.4046	0.0668	0.4107	-0.0000	-0.0000	-0.2575	-0.4286	-0.0000	0.4362
11	3	H	S	0.0832	0.0000	-0.4056	0.1034	-0.4050	-0.0000	0.0000	-0.3263	0.3762	-0.0000	0.4402
12	4	O	S	0.6126	0.6488	0.2244	0.0946	0.0040	0.1111	-0.0665	-0.0980	-0.0070	-0.0391	0.1064
13	4	O	PX	0.0145	0.0086	-0.1556	0.2597	-0.2165	-0.1969	0.5417	0.4302	-0.2351	-0.2487	0.1411
14	4	O	PY	0.0530	-0.0080	-0.1671	-0.5178	-0.0215	-0.2303	0.1355	0.2113	0.0230	0.5989	0.2017
15	4	O	PZ	0.0104	0.0062	-0.1110	0.1600	0.3379	-0.5350	-0.2934	0.2471	0.4145	-0.1738	0.0909
16	5	O	S	0.6126	-0.6488	0.2244	0.0946	0.0040	-0.1111	0.0665	-0.0980	-0.0070	0.0391	0.1064
17	5	O	PX	0.0145	-0.0086	-0.1556	0.2597	-0.2165	0.1969	-0.5417	0.4302	-0.2351	0.2487	0.1411
18	5	O	PY	-0.0530	-0.0080	0.1671	0.5178	0.0215	-0.2303	0.1355	-0.2113	-0.0230	0.5989	-0.2017
19	5	O	PZ	0.0104	-0.0062	-0.1110	0.1600	0.3379	0.5350	0.2934	0.2471	0.4145	0.1738	0.0909

				4b₁	4b₂	6a₁	2a₂	5b₁	7a₁	8a₁	5b₂
EIGENVALUES---				0.4380	0.4517	0.4752	0.5863	0.5953	0.6043	0.6749	0.7178
				12	13	14	15	16	17	18	19
1	1	P	S	0.1042	-0.0000	-0.0396	0.0000	0.0582	0.0066	0.1207	-0.0000
2	1	P	PX	-0.5190	0.0000	0.4785	-0.0000	-0.2992	0.0570	-0.2454	0.0000
3	1	P	PY	0.0000	0.6900	-0.0000	-0.0003	0.0000	0.0000	0.0000	0.4362
4	1	P	PZ	-0.4080	0.0000	-0.6329	0.0000	-0.1966	-0.1334	-0.1719	0.0000
5	1	P	DZ2	0.3148	-0.0000	0.1501	0.0000	0.0355	-0.7010	-0.4348	0.0000
6	1	P	DXZ	-0.5877	-0.0000	0.0938	0.0000	0.7021	-0.2295	0.1820	-0.0000
7	1	P	DYZ	-0.0000	0.3277	-0.0000	-0.7445	0.0000	-0.0000	-0.0000	-0.4075
8	1	P	DX-Y	0.1073	-0.0000	-0.1055	-0.0000	0.4023	0.4425	-0.5206	0.0000
9	1	P	DXY	-0.0000	0.4742	0.0000	0.5144	-0.0000	0.0000	-0.0000	-0.5904
10	2	H	S	0.0849	0.0000	0.2871	-0.0000	0.0504	0.3014	0.1807	-0.0000
11	3	H	S	0.0648	0.0000	-0.2861	0.0000	0.0998	-0.2898	0.1794	-0.0000
12	4	O	S	-0.0670	0.0575	0.0051	-0.0003	-0.0756	-0.0078	-0.1849	0.2397
13	4	O	PX	-0.0130	0.2506	-0.1611	0.1709	0.1334	0.1140	-0.2098	0.1176
14	4	O	PY	-0.1956	-0.0030	0.0122	-0.0000	-0.2507	-0.0242	-0.1144	0.2643
15	4	O	PZ	0.0056	0.1723	0.2327	-0.2477	0.1165	-0.1359	-0.1431	0.0801
16	5	O	S	-0.0670	-0.0575	0.0051	0.0003	-0.0756	-0.0078	-0.1849	-0.2397
17	5	O	PX	-0.0130	-0.2506	-0.1611	-0.1709	0.1334	0.1140	-0.2098	-0.1176
18	5	O	PY	0.1956	-0.0030	-0.0122	-0.0000	0.2507	0.0242	0.1144	0.2643
19	5	O	PZ	0.0056	-0.1723	0.2327	0.2477	0.1165	-0.1359	-0.1431	-0.0801

EIGENVALUES AND EIGENVECTORS $HPO_4^=$

				1a₁	2a₁	1e		3a₁	2e		4a₁	3e		5a₁
EIGENVALUES---				-0.9523	-0.7573	-0.6944	-0.6923	-0.3064	-0.1656	-0.1680	-0.0874	-0.0750	-0.0667	-0.0133
				1	2	3	4	5	6	7	8	9	10	11
1	1	P	S	-0.2480	0.4153	-0.0192	0.0221	-0.2527	0.0141	0.0019	0.3759	-0.0738	0.0294	0.2557
2	1	P	PX	0.0308	0.0166	0.3073	-0.0775	-0.0011	0.0566	0.1899	0.0252	0.0575	-0.2745	0.0186
3	1	P	PY	-0.0218	-0.3123	0.0762	0.3100	0.0014	-0.1754	0.1045	-0.0315	-0.2802	-0.0955	-0.0186
4	1	P	PZ	-0.1815	-0.1715	0.0216	0.0228	-0.2443	0.0300	0.0009	-0.3190	0.0467	-0.0167	0.1786
5	1	P	DZZ	-0.1414	-0.1381	0.0115	-0.0180	-0.1145	-0.0556	-0.3022	0.0865	0.0007	-0.0019	-0.3434
6	1	P	DXZ	0.0013	-0.0155	-0.1294	0.0247	0.0008	0.1413	0.2468	-0.0186	-0.0602	0.1732	-0.0056
7	1	P	DYZ	-0.1013	0.0140	-0.0364	-0.1152	-0.0017	-0.2550	0.1376	0.0229	0.1748	0.0606	0.0066
8	1	P	DX-Y	0.0026	0.0089	0.1844	-0.0480	-0.0014	0.0039	0.0028	-0.0347	-0.0998	0.3023	0.0013
9	1	P	DXY	0.0013	0.0096	-0.0452	-0.1875	-0.0017	0.0071	-0.0014	-0.0422	-0.2945	-0.1088	0.0010
10	2	O	S	-0.8450	-0.1437	0.0075	-0.0131	-0.1311	0.0013	-0.0002	-0.0692	0.0141	-0.0059	-0.1467
11	2	O	PX	0.0013	-0.0008	0.0315	-0.0112	0.0016	0.4286	0.7741	-0.0028	0.0109	0.0180	-0.0183
12	2	O	PY	-0.0018	0.0016	0.0066	0.0380	-0.0029	-0.7714	0.4304	0.0041	-0.0145	0.0118	0.0134
13	2	O	PZ	-0.0124	-0.0699	0.0054	-0.0065	0.6589	-0.0036	0.0002	0.1018	-0.0204	0.0083	0.1730
14	3	O	S	-0.0701	0.4556	-0.5457	-0.5103	0.0551	-0.0314	0.0466	-0.1806	-0.0189	-0.0634	-0.0865
15	3	O	PX	-0.0102	0.0295	0.0178	-0.0144	-0.0257	0.0223	0.0142	0.3073	0.4658	-0.2725	0.0555
16	3	O	PY	-0.0171	0.0423	-0.0091	0.0115	-0.0523	-0.0048	-0.0183	0.3350	-0.1673	0.3580	0.0469
17	3	O	PZ	-0.0204	0.0020	-0.0054	-0.0029	-0.8801	0.1235	-0.1974	-0.1441	-0.3791	-0.1080	0.4788
18	4	O	S	-0.0708	0.5350	0.7010	-0.1513	0.0543	-0.0293	-0.0487	-0.1860	0.0051	0.0548	-0.0915
19	4	O	PX	0.0200	-0.0526	0.0053	-0.0016	0.0594	-0.0057	-0.0066	-0.4717	-0.0089	0.2949	-0.0620
20	4	O	PY	0.0031	-0.0035	0.0076	0.0274	-0.0002	-0.0153	0.0183	-0.0809	-0.6158	-0.2266	-0.0185
21	4	O	PZ	-0.0220	0.0032	0.0056	0.0001	-0.0805	0.1166	0.2033	-0.1446	-0.0340	0.1257	0.4964
22	5	O	S	-0.0765	0.4411	-0.2297	0.7479	0.1028	0.0623	0.0007	-0.1583	0.0558	-0.0236	-0.0850
23	5	O	PX	-0.0107	0.0295	0.0156	0.0064	-0.0335	-0.0099	0.0453	0.1956	-0.2492	-0.5217	0.0527
24	5	O	PY	0.0183	-0.0415	0.0128	0.0323	0.0565	0.0178	0.0264	-0.3074	0.1903	-0.3775	-0.0791
25	5	O	PZ	-0.0241	-0.0009	-0.0022	0.0062	-0.0851	-0.2440	-0.0024	-0.1225	0.1641	-0.0329	0.4347
26	6	H	S	-0.3910	-0.1031	0.0067	-0.0110	0.5453	-0.0006	0.0005	0.0781	-0.0164	0.0066	0.1546

				4e		5e		1a₂	6a₁	7a₁	6e		8a₁	
EIGENVALUES---				0.0695	0.0712	0.0855	0.0907	0.1284	0.6732	0.7556	0.8248	0.8267	0.8611	0.9466
				12	13	14	15	16	17	18	19	20	21	22
1	1	P	S	0.0198	-0.0138	0.0037	0.0016	0.0001	0.6225	-0.2809	0.0014	-0.0034	0.1434	-0.0047
2	1	P	PX	-0.2547	0.1053	-0.0182	-0.0215	-0.0052	0.0299	0.0155	0.6810	-0.2183	-0.0123	-0.0600
3	1	P	PY	-0.1069	-0.2549	0.0308	-0.0161	-0.0043	-0.0123	-0.0200	0.2215	0.6760	0.0224	-0.0325
4	1	P	PZ	0.0015	-0.0087	-0.0029	-0.0010	0.0000	0.2676	0.6183	-0.0008	-0.0016	0.4054	0.0077
5	1	P	DZZ	-0.0058	0.0069	-0.0087	-0.0014	-0.0000	0.1398	-0.1637	-0.0069	0.0272	-0.4594	-0.0061
6	1	P	DXZ	0.0092	0.0037	0.1057	0.1883	-0.0014	0.0112	-0.0182	0.3306	-0.1007	-0.0267	0.6652
7	1	P	DYZ	0.0043	-0.0074	-0.1838	0.1076	-0.0015	-0.0147	0.0171	0.1109	0.3236	0.0298	0.3050
8	1	P	DX-Y	-0.2267	0.0784	-0.0776	-0.1151	-0.0009	0.0030	-0.0044	-0.3417	0.1212	0.0159	0.4654
9	1	P	DXY	0.0823	0.2182	-0.1425	0.0706	0.0016	0.0022	-0.0033	0.1067	0.3568	0.0257	-0.2156
10	2	O	S	-0.0057	0.0128	0.0083	0.0015	-0.0000	-0.3388	-0.2281	0.0053	-0.0184	0.1837	0.0003
11	2	O	PX	0.2140	-0.1069	-0.1247	-0.2253	0.0048	-0.0078	0.0022	-0.1838	0.0566	0.0085	-0.1378
12	2	O	PY	0.0973	0.2934	0.2119	-0.1261	0.0043	0.0101	-0.0013	-0.0669	-0.1795	-0.0105	-0.0629
13	2	O	PZ	0.0045	-0.0105	-0.0059	-0.0011	0.0000	-0.0278	-0.2716	0.0085	-0.0292	0.4758	0.0008
14	3	O	S	-0.0957	-0.0722	0.0282	-0.0417	0.0007	-0.1172	0.1020	0.0622	0.0561	-0.0266	-0.0130
15	3	O	PX	0.2249	0.0855	0.0957	0.3411	0.5109	-0.1267	0.1062	-0.1015	0.2168	0.0153	0.0826
16	3	O	PY	0.2774	0.2697	-0.3581	0.3219	-0.2717	-0.2235	0.2124	0.1763	-0.0234	0.0162	-0.1409
17	3	O	PZ	0.4675	0.3318	0.2007	-0.4143	-0.0109	-0.1644	-0.1151	0.1424	0.1333	-0.1833	0.1788
18	4	O	S	0.1113	-0.0356	0.0252	0.0393	-0.0006	-0.1181	0.1027	-0.0796	0.0258	-0.0283	0.0201
19	4	O	PX	0.4215	-0.1411	0.2569	0.4490	0.0157	0.2498	-0.2363	0.1246	-0.0381	-0.0285	-0.0995
20	4	O	PY	0.0286	0.0656	-0.2589	0.1333	0.5737	-0.0010	0.0109	-0.0785	-0.2541	-0.0096	0.1062
21	4	O	PZ	-0.4676	0.1677	0.2018	0.3494	0.0054	-0.1096	-0.1119	-0.1858	0.0634	-0.1846	-0.2008
22	5	O	S	-0.0240	0.1199	-0.0575	0.0010	-0.0002	-0.1157	0.1011	0.0173	-0.0819	-0.0361	0.0016
23	5	O	PX	0.1295	-0.2223	0.2468	0.2643	-0.5043	-0.1353	0.1140	-0.2118	-0.1212	-0.0024	0.1976
24	5	O	PY	-0.0312	0.4178	-0.4335	0.1532	-0.2850	0.2373	-0.2049	-0.1585	0.1003	0.0026	0.1179
25	5	O	PZ	0.5934	-0.5118	-0.5106	-0.0111	0.0015	-0.1348	-0.1324	0.0356	-0.1714	-0.1845	0.0208
26	6	H	S	0.0149	-0.0113	-0.0058	-0.0011	0.0000	0.2950	0.3782	-0.0100	0.0345	-0.4802	-0.0006

					9e	9a	10e	
C	EIGENVALUES---				0.9504	1.0246	1.0420	1.0443
					23	24	25	26
	1	1	P	S	-0.0160	0.0238	0.0005	-0.0013
C	2	1	P	PX	-0.0923	0.0206	0.1377	-0.3645
	3	1	P	PY	0.0761	-0.0261	-0.3664	-0.1357
	4	1	P	PZ	0.0152	-0.3507	0.0077	-0.0004
	5	1	P	DZZ	-0.0186	-0.7459	0.0785	-0.0247
	6	1	P	DXZ	0.3197	-0.0259	-0.1159	0.3760
	7	1	P	DYZ	-0.6944	0.0332	0.3241	0.1459
	8	1	P	DX-Y	0.1909	0.0353	0.2307	-0.5874
	9	1	P	DXY	0.4157	0.0470	0.6112	0.2197
	10	2	C	S	0.0011	0.1392	-0.0120	0.0036
	11	2	C	PX	-0.0651	0.0034	0.0111	-0.0416
	12	2	C	PY	0.1405	-0.0044	-0.0324	-0.0165
	13	2	C	PZ	-0.0026	-0.3983	0.0305	-0.0088
	14	3	C	S	0.0232	-0.1058	-0.1618	-0.2069
	15	3	C	PX	0.2002	-0.0440	-0.0371	-0.1691
	16	3	C	PY	-0.0285	-0.0903	-0.2070	-0.1929
	17	3	C	PZ	-0.1253	-0.1133	-0.0599	-0.0818
	18	4	C	S	0.0186	-0.1108	-0.0863	0.2503
	19	4	C	PX	-0.0579	0.1011	0.1045	-0.2966
	20	4	C	PY	-0.2153	-0.0062	-0.0845	-0.0265
	21	4	C	PZ	-0.0913	-0.1208	-0.0301	0.0978
	22	5	C	S	-0.0145	-0.0763	0.2681	-0.0456
	23	5	C	PX	-0.0630	-0.0368	0.1533	-0.1029
	24	5	C	PY	0.0632	0.0657	-0.2993	0.0063
	25	5	C	PZ	0.2261	-0.0220	0.0867	-0.0150
	26	6	H	S	0.0017	0.2150	-0.0158	0.0045

EIGENVALUES AND EIGENVECTORS $H_2PO_4^-$

				1a1	1b2	2a1	1b1	3a1	2b2	2b1	3b2	3b1	4a1	4b2
EIGENVALUES---				-1.2227	-1.1914	-1.0617	-1.0261	-0.5937	-0.5388	-0.4484	-0.4471	-0.4444	-0.3973	-0.3894
				1	2	3	4	5	6	7	8	9	10	11
1	1	P	S	0.3481	-0.0000	-0.3067	0.0011	-0.3798	0.0000	0.0504	0.0000	-0.0009	0.1820	-0.0000
2	1	P	PX	-0.0989	0.0000	-0.2323	-0.1773	0.1571	-0.0000	0.1879	-0.0000	-0.1647	0.2747	-0.0000
3	1	P	PY	0.0000	0.2447	-0.0000	-0.0000	-0.0000	-0.3613	0.0000	-0.0023	0.0000	-0.0000	0.1942
4	1	P	PZ	-0.0615	0.0000	-0.1283	0.2771	0.1301	0.0000	0.0992	0.0000	0.2737	0.1314	0.0000
5	1	P	DZ2	-0.0585	0.0000	-0.1212	0.1799	0.0892	-0.0000	-0.0644	-0.0000	-0.1801	-0.0961	0.0000
6	1	P	DXZ	0.0351	-0.0000	0.1024	0.3921	-0.0382	-0.0000	-0.1366	-0.0000	-0.1058	0.2934	-0.0000
7	1	P	DYZ	-0.0000	-0.0998	-0.0000	0.0000	-0.0000	0.3651	0.0000	0.3338	-0.0000	-0.0000	0.1765
8	1	P	DX-Y	-0.0679	0.0000	-0.1203	-0.1026	0.0655	0.0000	-0.2658	0.0000	0.0880	0.1036	-0.0000
9	1	P	DXY	-0.0000	-0.1576	0.0000	0.0000	0.0000	0.0937	-0.0000	-0.2104	0.0000	0.0000	0.2673
10	2	O	S	0.1367	-0.0000	-0.6028	0.6505	0.1367	-0.0000	-0.0523	-0.0000	-0.0772	-0.1105	-0.0000
11	2	O	PX	-0.0103	0.0000	-0.0148	-0.0100	0.0432	-0.0000	-0.0395	-0.0000	-0.2060	0.5384	-0.0000
12	2	O	PY	0.0000	0.0227	-0.0000	0.0000	-0.0000	-0.1376	0.0000	0.3760	-0.0000	-0.0000	0.3403
13	2	O	PZ	-0.0387	0.0000	0.0335	0.0037	0.1382	0.0000	-0.0873	-0.0000	-0.1374	-0.2542	-0.0000
14	3	O	S	0.1343	-0.0000	-0.6105	-0.6442	0.1354	0.0000	-0.0598	0.0000	0.0715	-0.1096	0.0000
15	3	O	PX	-0.0388	-0.0000	0.0246	0.0032	0.1422	-0.0000	-0.1061	0.0000	0.1965	-0.0083	0.0000
16	3	O	PY	0.0000	0.0218	-0.0000	-0.0000	0.0000	-0.1340	-0.0000	-0.3053	0.0000	0.0000	0.3442
17	3	O	PZ	0.0069	0.0000	-0.0272	0.0094	-0.0183	0.0000	0.0117	0.0000	0.1217	0.6012	-0.0000
18	4	O	S	0.5857	-0.6105	0.1538	-0.0020	-0.0335	0.0964	0.0020	0.0009	0.0001	-0.0253	0.0667
19	4	O	PX	0.0010	0.0066	-0.0357	-0.0167	-0.2083	0.3133	0.4664	0.3100	-0.2978	-0.0561	-0.2961
20	4	O	PY	0.0040	0.0314	-0.0332	0.0005	-0.4225	0.3611	-0.3628	0.0009	-0.0192	-0.0181	-0.4172
21	4	O	PZ	0.0010	0.0039	-0.0233	0.0275	-0.1325	0.2916	0.2598	-0.4834	0.5209	-0.0267	-0.1899
22	5	O	S	0.5857	0.6105	0.1538	-0.0020	-0.0335	-0.0964	0.0020	-0.0009	0.0001	-0.0253	-0.0667
23	5	O	PX	0.0010	-0.0066	-0.0357	-0.0167	-0.2083	-0.3133	0.4664	-0.3100	-0.2978	-0.0561	0.2961
24	5	O	PY	-0.0040	0.0314	0.0332	-0.0005	0.4225	0.3611	0.3628	0.0009	0.0192	0.0181	0.4172
25	5	O	PZ	0.0010	-0.0039	-0.0233	0.0275	-0.1325	-0.2916	0.2598	0.4834	0.5209	-0.0267	0.1899
26	6	H	S	0.2549	-0.2800	0.0920	-0.0013	0.3551	-0.3636	-0.0065	-0.0015	-0.0003	0.0336	-0.1061
27	7	H	S	0.2549	0.2800	0.0920	-0.0013	0.3551	0.3636	-0.0065	0.0015	-0.0003	0.0336	0.1061

				5a1	5b2	4b1	6b2	6a1	7a1	7b2	5b1	8a1	1a2	9a1
EIGENVALUES---				-0.3101	-0.2681	-0.2449	-0.2424	-0.2167	0.3268	0.4645	0.4839	0.4976	0.5663	0.5835
				12	13	14	15	16	17	18	19	20	21	22
1	1	P	S	-0.3256	-0.0000	0.0024	0.0000	0.0008	0.6555	-0.0000	-0.1602	0.0011	0.0000	0.1915
2	1	P	PX	-0.0731	-0.0000	-0.1929	-0.0000	0.0401	-0.2250	-0.0000	-0.6020	0.3847	0.0000	0.0234
3	1	P	PY	-0.0000	0.1735	-0.0000	-0.0023	-0.0000	0.0000	-0.7667	0.0000	-0.0000	0.1674	-0.0000
4	1	P	PZ	-0.0424	0.0000	0.3009	0.0000	-0.0619	-0.1479	-0.0000	-0.4016	-0.5742	-0.0000	0.0197
5	1	P	DZ2	-0.1824	0.0000	0.1648	0.0000	0.1381	-0.0715	-0.0000	0.2525	0.4264	0.0000	0.1972
6	1	P	DXZ	0.2295	0.0000	0.0953	0.0000	0.0728	0.0969	-0.0000	-0.0699	0.2241	0.0000	0.1062
7	1	P	DYZ	-0.0000	0.0929	0.0000	-0.1742	-0.0000	0.0000	-0.0659	-0.0000	-0.0000	0.3342	0.0000
8	1	P	DX-Y	-0.1088	-0.0000	-0.1050	-0.0000	-0.0796	-0.0415	0.0000	0.3535	-0.2550	0.0000	0.4415
9	1	P	DXY	-0.0000	0.1499	-0.0000	0.1092	-0.0000	-0.0000	-0.1059	0.0000	-0.0000	0.5284	-0.0000
10	2	O	S	0.1562	-0.0000	-0.1218	-0.0000	-0.0144	-0.1085	0.0000	0.0932	0.0668	-0.0000	-0.0938
11	2	O	PX	0.2940	0.0000	-0.0232	-0.0000	0.6450	0.0440	0.0000	0.1900	-0.2109	-0.0000	-0.2403
12	2	O	PY	-0.0000	0.5049	0.0000	-0.5872	-0.0000	0.0000	0.2554	-0.0000	0.0000	-0.1770	-0.0000
13	2	O	PZ	0.4488	-0.0000	-0.5959	-0.0000	-0.0922	0.3253	0.0000	-0.1940	-0.1700	-0.0000	0.1300
14	3	O	S	0.1564	0.0000	0.1200	0.0000	0.0137	-0.1088	-0.0000	0.0918	-0.0693	-0.0000	-0.0897
15	3	O	PX	0.5382	0.0000	0.5466	0.0000	-0.1769	0.0172	-0.0000	-0.0916	0.2442	0.0000	0.0998
16	3	O	PY	0.0000	0.5213	-0.0000	0.5713	-0.0000	-0.0000	0.2572	0.0000	0.0000	-0.1784	0.0000
17	3	O	PZ	0.0844	-0.0000	-0.2230	-0.0000	-0.6236	-0.0901	0.0000	0.2566	0.1159	0.0000	-0.0901
18	4	O	S	0.1219	0.0407	-0.0013	-0.0015	0.0035	-0.2674	-0.2390	-0.0534	0.0039	-0.2240	0.1910
19	4	O	PX	0.1613	0.3373	0.1094	0.1995	-0.1315	-0.0012	-0.0302	0.1441	-0.1047	0.1676	-0.0849
20	4	O	PY	0.0897	-0.2110	-0.0013	0.0007	0.0014	-0.1053	0.0904	-0.0841	0.0012	0.1625	-0.3341
21	4	O	PZ	0.1023	0.2102	-0.1741	-0.3217	0.2051	0.0020	-0.0185	0.0962	0.1558	0.1073	-0.0545
22	5	O	S	0.1219	-0.0407	-0.0013	0.0015	0.0035	-0.2674	0.2390	-0.0534	0.0039	0.2240	0.1910
23	5	O	PX	0.1613	-0.3373	0.1094	-0.1995	-0.1315	-0.0012	0.0302	0.1441	-0.1047	-0.1676	-0.0849
24	5	O	PY	-0.0897	-0.2110	0.0013	0.0007	-0.0014	0.1053	0.0904	0.0841	-0.0012	0.1625	0.3341
25	5	O	PZ	0.1023	-0.2102	-0.1741	0.3217	0.2051	0.0020	0.0185	0.0962	0.1558	-0.1073	-0.0545
26	6	H	S	-0.1346	-0.0435	0.0013	0.0013	-0.0004	0.1956	0.2571	0.0776	-0.0048	0.3709	-0.4171
27	7	H	S	-0.1346	0.0435	0.0013	-0.0013	-0.0004	0.1956	-0.2571	0.0776	-0.0048	-0.3709	-0.4171

				$6b_1$	$2a_2$	$8b_2$	$10a_1$	$11a_1$
EIGENVALUES---				0.6187	0.6219	0.7105	0.7216	0.7228
				23	24	25	26	27
1	1	P	S	-0.0812	0.0000	-0.0000	-0.0024	-0.0150
2	1	P	PX	0.1124	-0.0000	0.0000	-0.2657	-0.2577
3	1	P	PY	-0.0000	0.0009	0.3448	0.0000	-0.0000
4	1	P	PZ	0.0705	-0.0000	-0.0000	0.3271	-0.2320
5	1	P	DZ2	-0.1074	0.0000	-0.0000	0.5037	-0.5088
6	1	P	DXZ	0.6937	-0.0000	-0.0000	0.3443	0.3463
7	1	P	DYZ	-0.0000	-0.7570	-0.3421	-0.0000	0.0000
8	1	P	DX-Y	0.4366	-0.0000	0.0000	-0.3793	-0.3573
9	1	P	DXY	0.0000	0.4806	-0.5436	-0.0000	0.0000
10	2	O	S	0.0211	-0.0000	0.0000	-0.2128	0.1917
11	2	O	PX	-0.2634	0.0000	0.0000	-0.0619	-0.0699
12	2	O	PY	0.0000	0.2678	0.0556	0.0000	-0.0000
13	2	O	PZ	-0.0297	0.0000	-0.0000	0.2742	-0.2383
14	3	O	S	0.0206	-0.0000	-0.0000	0.2560	0.1287
15	3	O	PX	-0.1345	0.0000	0.0000	-0.2820	-0.1782
16	3	O	PY	-0.0000	-0.2651	0.0593	0.0000	0.0000
17	3	O	PZ	-0.2278	0.0000	-0.0000	0.1708	-0.0124
18	4	O	S	-0.0501	-0.0006	0.0657	-0.0073	-0.0564
19	4	O	PX	0.1679	0.0892	0.1655	-0.0439	-0.1463
20	4	O	PY	0.0622	0.0018	0.3398	-0.0277	-0.2136
21	4	O	PZ	0.1087	-0.1380	0.1054	0.0239	-0.0988
22	5	O	S	-0.0501	0.0006	-0.0657	-0.0073	-0.0564
23	5	O	PX	0.1679	-0.0892	-0.1655	-0.0439	-0.1463
24	5	O	PY	-0.0622	0.0018	0.3398	0.0277	0.2136
25	5	O	PZ	0.1087	0.1380	-0.1054	0.0239	-0.0988
26	6	H	S	0.1711	0.0022	0.2696	-0.0242	-0.1819
27	7	H	S	0.1711	-0.0022	-0.2696	-0.0242	-0.1819

EIGENVALUES AND EIGENVECTORS H_3PO_4

				1a₁	1e		2a₁	3a₁	2e		4a₁	3e		
EIGENVALUES---				-1.5314	-1.4712	-1.4668	-1.3522	-0.8988	-0.8081	-0.8068	-0.7518	-0.7445	-0.7407	-0.6824
				1	2	3	4	5	6	7	8	9	10	11
1	1	P	S	-0.3966	0.0213	0.0200	0.2026	-0.4235	-0.0136	-0.0092	0.1088	0.0277	-0.0188	0.0125
2	1	P	PX	-0.0169	-0.2539	-0.0456	0.0107	-0.0071	0.3843	-0.0478	0.0975	-0.0142	0.0155	-0.1299
3	1	P	PY	0.0681	-0.0442	0.2564	-0.0027	0.0038	-0.0493	-0.3864	-0.0184	0.0226	0.0154	-0.1119
4	1	P	PZ	0.1769	-0.0357	0.0336	0.2909	0.1464	0.0041	-0.0380	0.3187	0.3914	-0.0429	0.3044
5	1	P	DZ2	0.0482	-0.0014	-0.0150	0.2104	0.0376	0.0063	0.0078	-0.2465	-0.0568	0.0353	-0.1304
6	1	P	DXZ	0.0587	0.1303	0.0052	-0.0062	0.0021	-0.0769	0.0085	0.0799	-0.1479	0.2175	-0.2117
7	1	P	DYZ	-0.0068	0.0265	-0.1287	0.0009	-0.0033	0.0108	0.0845	-0.1344	0.2106	0.1469	-0.1328
8	1	P	DX-Y	-0.0121	-0.1534	-0.0286	0.0005	-0.0006	0.0336	-0.0276	0.0746	-0.1573	0.2335	-0.1612
9	1	P	DXY	-0.0037	0.0264	-0.1533	0.0018	0.0009	-0.0012	0.0205	0.0462	-0.2445	-0.1611	-0.1275
10	2	O	S	-0.1370	0.0348	0.0154	0.8898	0.1409	0.0034	0.0062	-0.1029	-0.0316	0.0133	0.0004
11	2	O	PX	-0.0011	-0.0154	-0.0038	0.0002	-0.0020	0.1453	-0.0186	0.0778	-0.1486	0.2163	-0.3580
12	2	O	PY	-0.0008	-0.0017	0.0158	0.0003	-0.0006	-0.0183	-0.1407	-0.0406	0.2132	0.1475	-0.3196
13	2	O	PZ	0.0399	-0.0020	-0.0028	-0.0153	0.1424	0.0047	0.0092	-0.1380	-0.0584	0.0256	0.0020
14	3	O	S	-0.4805	0.4817	-0.5174	-0.0885	0.0250	-0.0304	0.0683	0.0356	-0.0173	-0.0301	0.0442
15	3	O	PX	-0.0146	-0.0311	0.0028	0.0097	-0.2045	0.1167	-0.3298	-0.2146	0.3761	-0.1453	-0.3110
16	3	O	PY	-0.0200	-0.0119	0.0367	0.0166	-0.3426	-0.3026	0.3337	-0.1756	-0.2945	0.1917	-0.2132
17	3	O	PZ	0.0022	-0.0040	0.0354	0.0272	-0.1217	-0.1179	0.2459	0.4478	-0.0663	-0.4782	0.2403
18	4	O	S	-0.5247	-0.6684	-0.1017	-0.0913	0.0232	0.0749	-0.0109	0.0080	-0.0169	0.0229	0.0677
19	4	O	PX	0.0227	-0.0418	-0.0372	-0.0204	0.4137	-0.4878	0.0644	0.2178	0.0154	0.0424	-0.2761
20	4	O	PY	0.0626	-0.0052	0.0269	-0.0101	0.0043	-0.0411	-0.2924	0.0155	-0.4943	-0.3234	-0.2654
21	4	O	PZ	0.0021	0.0048	0.0019	0.0297	-0.1200	0.2740	-0.0505	0.5770	-0.1192	0.3075	-0.1527
22	5	O	S	-0.4360	0.2648	0.6844	-0.1096	0.0267	-0.0437	-0.0573	-0.0363	0.0347	0.0061	0.0168
23	5	O	PX	-0.0131	-0.0271	-0.0111	0.0106	-0.1935	0.0194	-0.3428	-0.1453	-0.0169	-0.4331	-0.3272
24	5	O	PY	0.0215	-0.0014	0.0370	-0.0184	0.3322	0.3766	0.2682	0.0914	0.3488	-0.2388	-0.2677
25	5	O	PZ	0.0016	-0.0020	-0.0040	0.0303	-0.1016	-0.1555	-0.2068	0.4126	0.5982	-0.0134	-0.0642
26	6	H	S	-0.1514	0.2099	-0.2272	-0.0489	0.2844	0.1545	-0.3396	-0.0156	0.0412	0.0698	0.1552
27	7	H	S	-0.2098	-0.2919	-0.0450	-0.0508	0.2931	-0.3667	0.0520	-0.0199	0.0395	-0.0519	-0.1233
28	8	H	S	-0.1727	0.1149	0.2988	-0.0550	0.2720	0.2326	0.2906	0.0153	-0.0365	-0.0154	-0.0314

				4e		1a₂	5a₁	5e		6a₁	6e		7a₁	6e		
EIGENVALUES---				-0.6819	-0.6810	-0.6810	-0.5721	-0.5477	-0.5467	0.0227	0.1764	0.1710	0.1738	0.2344	0.2353	
				12	13	14	15	16	17	18	19	20	21	22		
1	1	P	S	-0.0022	-0.0010	0.2850	0.0012	0.0048	0.6961	-0.0018	-0.0012	-0.0562	0.0028	0.0125		
2	1	P	PX	-0.1082	-0.0028	0.0014	-0.0875	-0.0420	-0.0028	-0.7234	-0.3203	-0.0336	-0.0132	-0.0303		
3	1	P	PY	0.1227	-0.0032	-0.0072	-0.0433	0.0865	0.0004	-0.3214	0.7245	-0.0218	0.0017	0.0103		
4	1	P	PZ	0.0072	-0.0001	0.2882	0.0001	0.0051	-0.1716	0.0111	-0.0193	-0.7113	-0.0023	-0.0025		
5	1	P	DZ2	0.0006	-0.0001	0.2473	0.0002	0.0060	-0.1110	-0.0103	0.0169	0.4932	0.0034	0.0021		
6	1	P	DXZ	-0.1807	-0.0020	0.0013	-0.1244	-0.0592	0.0011	-0.1258	-0.0521	0.0350	0.1789	0.0211		
7	1	P	DYZ	0.2193	-0.0019	-0.0099	-0.0615	0.1218	-0.0035	-0.0549	0.1214	-0.0151	0.0076	-0.1923		
8	1	P	DX-Y	0.1404	0.0029	0.0002	0.0200	0.0113	-0.0006	0.2286	0.1054	0.0034	-0.6314	-0.0466		
9	1	P	DXY	0.1514	-0.0046	0.0004	-0.0089	0.0713	0.0018	-0.0951	0.2235	-0.0133	0.0527	-0.4327		
10	2	O	S	-0.0032	0.0000	-0.2180	-0.0011	-0.0026	-0.1664	-0.0006	0.0323	0.1419	-0.0047	-0.0210		
11	2	O	PX	-0.3066	-0.0089	0.0095	-0.6420	-0.3151	0.0012	0.2644	0.1155	-0.0118	-0.0667	-0.0674		
12	2	O	PY	0.3641	-0.0092	-0.0210	-0.3123	0.6384	0.0072	0.1166	-0.2644	0.0178	-0.0023	0.0716		
13	2	O	PZ	-0.0079	0.0092	-0.7497	0.0023	-0.0202	0.3889	0.0034	-0.0383	-0.2534	0.0008	0.0018		
14	3	O	S	0.0288	0.0007	-0.0809	-0.0002	-0.0009	-0.2462	-0.1720	0.1255	-0.0677	-0.1715	0.2575		
15	3	O	PX	-0.2790	0.5069	-0.0315	0.1591	0.0621	-0.0597	0.1161	0.1462	-0.0412	-0.0407	-0.1556		
16	3	O	PY	0.3005	-0.2642	-0.0479	0.1074	-0.1673	-0.1076	-0.0556	-0.0953	-0.0773	0.1582	-0.1155		
17	3	O	PZ	-0.0786	-0.0114	-0.1380	-0.4029	0.2608	-0.0422	-0.0526	0.0427	0.2325	0.0316	-0.0513		
18	4	O	S	0.0588	-0.0020	-0.0812	0.0026	0.0008	-0.2445	0.1995	0.0352	-0.0566	0.3129	0.0275		
19	4	O	PX	-0.2349	0.0092	0.0608	0.1752	0.0823	0.1234	0.0075	0.0071	0.0782	0.2211	0.0194		
20	4	O	PY	0.3108	0.5649	0.0233	0.0643	-0.1513	-0.0025	0.0673	-0.1491	0.0057	-0.0130	0.1421		
21	4	O	PZ	-0.1492	0.0152	-0.1950	0.4372	0.2033	-0.0355	0.0497	0.0297	0.2946	-0.0616	-0.3072		
22	5	O	S	-0.0886	0.0015	-0.0821	-0.0011	-0.0085	-0.2455	-0.0202	-0.2164	-0.0475	-0.1326	-0.2809		
23	5	O	PX	-0.2738	-0.5040	-0.0375	0.1665	0.0838	-0.0645	0.1871	-0.0169	-0.0333	-0.0704	0.1458		
24	5	O	PY	0.2705	-0.2956	0.0540	0.0834	-0.1656	0.1110	0.1057	-0.0126	0.0676	-0.1335	-0.1274		
25	5	O	PZ	0.2706	-0.0039	-0.1797	-0.0327	-0.5089	-0.0309	-0.0690	-0.0518	0.2929	0.0252	0.0538		
26	6	H	S	-0.0530	-0.0003	0.0858	0.0057	-0.0027	0.1636	0.1652	-0.1203	0.0770	0.2491	-0.3778		
27	7	H	S	-0.1069	0.0017	0.0856	-0.0082	-0.0034	0.1616	-0.1924	-0.0822	0.0663	-0.4625	-0.0415		
28	8	H	S	0.1645	-0.0015	0.0179	0.0014	0.0137	0.1632	0.0195	0.2071	0.0558	0.1892	0.4029		

					1e		8a1	9a1	8e	
EIGENVALUES---					0.3175	0.3194	0.3405	0.4284	0.4351	0.4362
					23	24	25	26	27	28
1	1	P	S	-0.0003	-0.0080	-0.1975	-0.0139	-0.0016	-0.0016	
2	1	P	PX	0.0334	-0.0803	-0.0060	-0.0255	0.3414	0.0284	
3	1	P	PY	0.0277	0.0260	-0.0003	0.0459	0.0289	-0.3352	
4	1	P	PZ	0.0033	-0.0046	-0.0299	0.3963	0.0207	0.0472	
5	1	P	DZ2	-0.0010	-0.0104	-0.3349	0.6620	0.0328	0.1035	
6	1	P	DXZ	0.5482	-0.5373	0.0299	0.0266	-0.4042	-0.0228	
7	1	P	DYZ	0.5327	0.5515	-0.0417	-0.0036	-0.0458	0.3921	
8	1	P	DX-Y	0.3076	-0.2991	-0.0072	-0.0332	0.4373	0.0377	
9	1	P	DXY	-0.3029	-0.3096	0.0150	-0.0594	-0.0357	0.4313	
10	2	O	S	-0.0003	0.0055	0.1254	-0.2642	-0.0132	-0.0378	
11	2	O	PX	-0.1990	0.1931	-0.0092	-0.0041	0.0698	0.0029	
12	2	O	PY	-0.1928	-0.1976	0.0130	0.0133	0.0091	-0.0670	
13	2	O	PZ	-0.0006	-0.0093	-0.1809	0.3531	0.0174	0.0492	
14	3	O	S	-0.0840	-0.0301	-0.1423	0.0270	0.0405	-0.0524	
15	3	O	PX	0.0462	-0.1439	0.1515	0.0909	0.1442	-0.1523	
16	3	O	PY	-0.0135	0.0984	0.2515	0.1631	0.2142	-0.2901	
17	3	O	PZ	0.1931	0.0573	0.0674	0.1430	0.1068	-0.1219	
18	4	O	S	0.0551	-0.0614	-0.1357	0.0298	-0.0721	-0.0017	
19	4	O	PX	0.0039	-0.0171	-0.2982	-0.1809	0.4154	0.0124	
20	4	O	PY	0.1271	0.1300	-0.0075	0.0025	0.0007	-0.0234	
21	4	O	PZ	-0.1460	0.1454	0.0659	0.1353	-0.1534	0.0049	
22	5	O	S	0.0149	0.0583	-0.1582	0.0123	0.0268	0.0589	
23	5	O	PX	0.1481	-0.0303	0.1465	0.0450	0.1176	0.2001	
24	5	O	PY	0.0817	-0.0317	-0.2579	-0.0790	-0.1599	-0.3660	
25	5	O	PZ	-0.0480	-0.1887	0.0777	0.0949	0.0733	0.1574	
26	6	H	S	0.1477	0.0561	0.3828	0.1811	0.2173	-0.2709	
27	7	H	S	-0.0982	0.1141	0.3829	0.1716	-0.3412	-0.0076	
28	8	H	S	-0.0252	-0.0991	0.4026	0.0950	0.1650	0.3500	

EIGENVALUES AND EIGENVECTORS $Ni[S_2P(OCH_3)_2]_2$

					1a1	1b2	2a1	2b2	3a1	1b1	3b2	4a1	1a2	5a1	6a1
EIGENVALUES---					-1.3961	-1.3720	-0.9723	-0.9502	-0.8436	-0.7072	-0.6390	-0.6281	-0.6459	-0.6216	-0.5383
					1	2	3	4	5	6	7	8	9	10	11
1	1	P	S		-0.2790	-0.0000	0.2122	-0.0000	0.4631	-0.0177	0.0000	-0.0778	0.0000	0.0705	0.2019
2	1	P	PX		0.0862	0.0000	-0.0807	0.0000	0.1954	0.2917	-0.0000	0.0098	-0.0000	-0.0626	-0.3689
3	1	P	PY		-0.0000	-0.2349	-0.0000	-0.1074	0.0000	0.0000	0.2832	0.0000	-0.0406	0.0000	-0.0000
4	1	P	PZ		0.0572	0.0000	-0.1092	0.0000	0.1774	-0.2139	-0.0000	0.1117	0.0000	-0.1795	-0.1695
5	1	P	DZZ		0.0672	0.0000	-0.0042	-0.0000	0.0575	-0.0838	0.0000	-0.0033	0.0000	-0.1486	0.1200
6	1	P	DXZ		-0.0374	-0.0000	0.0666	-0.0000	-0.0386	-0.0472	-0.0000	-0.0566	-0.0000	-0.0342	0.0733
7	1	P	DYZ		0.0000	0.0778	0.0000	0.1218	0.0000	-0.0000	0.0870	0.0000	0.0419	0.0000	0.0000
8	1	P	DX-Y		0.1011	0.0000	0.0141	-0.0000	0.0785	0.0326	0.0000	-0.1916	0.0000	-0.1241	-0.0659
9	1	P	DXY		0.0000	0.1154	0.0000	0.0990	0.0000	-0.0000	-0.0393	-0.0000	-0.1731	-0.0000	0.0000
10	2	S	S		-0.0669	0.0000	0.0054	-0.0000	0.5192	-0.4332	-0.0000	0.1167	-0.0000	-0.5119	0.0271
11	2	S	PX		0.0093	-0.0000	0.0060	-0.0000	0.0469	0.0780	-0.0000	-0.0245	-0.0000	-0.1579	0.0050
12	2	S	PY		-0.0000	-0.0365	0.0000	0.0324	-0.0000	0.0000	0.1418	0.0000	0.0196	0.0000	0.0000
13	2	S	PZ		0.0478	-0.0000	-0.0252	0.0000	-0.1644	0.0420	-0.0000	-0.0318	-0.0000	-0.0095	-0.0032
14	2	S	DZZ		-0.0210	-0.0000	0.0236	-0.0000	0.0720	-0.0172	0.0000	0.0007	0.0000	-0.0174	0.0139
15	2	S	DXZ		-0.0088	-0.0000	0.0001	0.0000	-0.0336	-0.0565	0.0000	0.0162	0.0000	0.0239	-0.0001
16	2	S	DYZ		0.0000	0.0336	-0.0000	-0.0103	0.0000	-0.0000	-0.0741	-0.0000	-0.0034	-0.0000	-0.0000
17	2	S	DX-Y		0.0118	-0.0000	0.0127	-0.0000	0.0057	0.0137	0.0000	-0.0213	0.0000	-0.0203	-0.0061
18	2	S	DXY		0.0000	0.0097	0.0000	-0.0003	0.0000	-0.0000	-0.0133	-0.0000	-0.0238	-0.0000	0.0000
19	3	S	S		-0.0542	-0.0000	0.0592	-0.0000	0.4819	0.5593	0.0000	-0.3784	-0.0000	0.1266	-0.3114
20	3	S	PX		0.0429	-0.0000	-0.0379	0.0000	-0.1411	-0.0695	-0.0000	0.0118	-0.0000	-0.0143	-0.1191
21	3	S	PY		0.0000	-0.0262	0.0000	0.0015	-0.0000	-0.0000	0.0439	0.0000	-0.0311	-0.0000	0.0000
22	3	S	PZ		-0.0350	-0.0000	-0.0034	0.0000	0.0886	-0.0255	-0.0000	-0.0057	-0.0000	-0.0621	-0.0480
23	3	S	DZZ		0.0183	0.0000	-0.0094	0.0000	-0.0076	-0.0324	-0.0000	-0.0054	-0.0000	-0.0321	-0.0254
24	3	S	DXZ		0.0048	-0.0000	0.0011	-0.0000	-0.0597	0.0151	0.0000	0.0016	0.0000	0.0296	0.0265
25	3	S	DYZ		-0.0000	0.0000	0.0000	-0.0081	0.0000	-0.0000	0.0147	0.0000	-0.0085	0.0000	0.0000
26	3	S	DX-Y		-0.0151	-0.0000	0.0233	-0.0000	0.0556	0.0239	0.0000	-0.0239	0.0000	0.0082	0.0355
27	3	S	DXY		0.0000	0.0259	0.0000	0.0058	0.0000	0.0000	-0.0277	-0.0000	0.0547	0.0000	-0.0000
28	4	O	S		-0.5020	0.5031	0.3129	0.3483	-0.1578	-0.0308	0.0795	-0.0931	-0.1136	-0.0360	0.0006
29	4	O	PX		-0.0338	0.0293	-0.0117	-0.0034	0.0336	0.1638	-0.1254	0.2647	0.3173	0.0624	0.2799
30	4	O	PY		0.0430	-0.0677	0.1620	0.1020	0.0762	-0.1248	-0.1113	-0.1824	-0.1574	0.1992	0.3178
31	4	O	PZ		-0.0449	0.0420	-0.0569	-0.0587	0.0463	-0.1235	-0.2667	0.1228	-0.0717	0.1938	-0.2153
32	5	O	S		-0.5020	-0.5031	0.3129	-0.3483	-0.1578	-0.0308	-0.0795	-0.0931	0.1136	-0.0360	0.0006
33	5	O	PX		-0.0338	-0.0293	-0.0117	0.0034	0.0336	0.1638	0.1254	0.2647	-0.3173	0.0624	0.2799
34	5	O	PY		-0.0430	-0.0677	-0.1620	0.1020	-0.0762	0.1248	-0.1113	0.1824	-0.1574	-0.1992	-0.3178
35	5	O	PZ		-0.0449	-0.0420	-0.0569	0.0587	0.0463	-0.1235	0.2667	0.1228	0.0717	0.1938	-0.2153
36	6	C	S		-0.3226	0.3391	-0.3814	-0.3682	-0.0186	-0.0129	0.0192	-0.0427	-0.0352	0.0176	-0.0498
37	6	C	PX		-0.0410	0.0384	-0.0147	-0.0114	0.0530	0.1338	-0.1678	0.3227	0.3632	0.0516	0.1636
38	6	C	PY		-0.1214	0.1204	0.1675	0.1954	-0.0332	-0.0583	-0.2188	0.2151	0.0040	-0.0902	-0.3249
39	6	C	PZ		0.0620	-0.0577	-0.0718	-0.1037	0.1185	-0.1958	-0.3361	-0.0336	-0.2091	0.3459	0.0450
40	7	C	S		-0.3228	-0.3391	-0.3814	0.3682	-0.0186	-0.0129	-0.0192	-0.0427	0.0352	0.0176	-0.0498
41	7	C	PX		-0.0410	-0.0384	-0.0147	0.0114	0.0530	0.1338	0.1678	0.3227	-0.3632	0.0516	0.1636
42	7	C	PY		0.1214	0.1204	-0.1675	0.1954	0.0332	0.0583	-0.2188	-0.2151	0.0040	-0.0902	0.3249
43	7	C	PZ		0.0620	0.0577	-0.0718	0.1037	0.1185	-0.1958	0.3361	-0.0336	0.2091	0.3459	0.0450
44	8	H	S		-0.1204	0.1249	-0.2361	-0.2514	0.0772	-0.1652	-0.2572	-0.0475	-0.1917	0.2803	-0.0044
45	9	H	S		-0.1852	0.1912	-0.1764	-0.1639	0.0095	0.1546	-0.0291	0.2277	0.3263	-0.0408	0.1119
46	10	H	S		-0.1047	0.1144	-0.2630	-0.2672	-0.0527	0.0291	0.3140	-0.2844	-0.1121	-0.1733	0.1174
47	11	H	S		-0.1204	-0.1249	-0.2361	0.2514	0.0772	-0.1652	0.2572	-0.0475	0.1917	0.2803	-0.0044
48	12	H	S		-0.1852	-0.1912	-0.1764	0.1639	0.0095	0.1546	0.0291	0.2277	-0.3263	-0.0408	0.1119
49	13	H	S		-0.1047	-0.1144	-0.2630	0.2672	-0.0527	0.0291	-0.3140	-0.2844	0.1121	-0.1733	0.1174

					$4b_2$	$7a_1$	$5b_2$	$3b_1$	$4b_1$	$2a_2$	$8a_1$	$6b_2$	$9a_1$	$7b_2$	$10a_1$
	EIGENVALUES---				-0.4923	-0.4406	-0.3953	-0.3774	-0.3729	-0.3494	-0.2888	-0.2596	-0.2558	-0.1696	-0.1438
					12	13	14	15	16	17	18	19	20	21	22
1	1	P	S		-0.0000	-0.3223	0.0000	-0.0522	-0.1270	0.0000	0.2130	0.0000	0.0125	0.0000	-0.0081
2	1	P	PX		0.0000	0.0852	0.0000	-0.1255	-0.3182	0.0000	0.0000	0.0000	0.2527	-0.0000	0.0125
3	1	P	PY		-0.1563	-0.0000	-0.3141	0.0000	-0.0000	0.1325	-0.0000	0.2243	0.0000	0.0372	0.0000
4	1	P	PZ		-0.3070	-0.1683	-0.0000	0.1314	-0.1560	0.0000	0.0469	-0.0000	-0.3519	0.0000	0.0017
5	1	P	DZ2		-0.0000	0.1114	-0.0000	-0.0584	-0.0209	0.0000	0.1791	-0.0000	-0.1803	0.0000	-0.1648
6	1	P	DXZ		-0.0000	0.0622	-0.0000	0.1851	-0.2048	-0.0000	-0.3087	-0.0000	-0.0528	0.0000	-0.0495
7	1	P	DYZ		0.2460	-0.0000	-0.0404	-0.0000	-0.0000	-0.3247	-0.0000	0.2672	-0.0000	0.2089	0.0000
8	1	P	DX-Y		0.0000	0.0192	0.0000	0.1750	-0.0499	-0.0000	0.1481	0.0000	0.1352	-0.0000	0.0458
9	1	P	DXY		-0.0075	0.0000	0.0882	0.0000	0.0000	0.2437	0.0000	0.2141	-0.0000	-0.1508	-0.0000
10	2	S	S		0.0000	0.2658	-0.0000	-0.0585	0.2553	-0.0000	-0.1358	0.0000	0.1781	-0.0000	-0.0038
11	2	S	PX		0.0000	0.0638	0.0000	0.1157	-0.3843	0.0000	-0.4310	0.0000	0.1244	0.0000	-0.6618
12	2	S	PY		0.0640	0.0000	-0.1826	0.0000	-0.0000	0.0759	-0.0000	0.5503	-0.0000	0.6459	0.0000
13	2	S	PZ		0.0000	0.2449	0.0000	-0.0715	0.2911	-0.0000	-0.2820	0.0000	0.5071	-0.0000	0.1776
14	2	S	DZ2		-0.0000	-0.0835	-0.0000	0.0197	-0.0577	0.0000	0.0730	-0.0000	-0.0907	0.0000	-0.0239
15	2	S	DXZ		-0.0000	-0.0352	-0.0000	-0.0338	0.1417	0.0000	0.1141	0.0000	-0.0550	0.0000	0.0131
16	2	S	DYZ		-0.0299	0.0000	0.0754	-0.0000	0.0000	-0.0243	0.0000	-0.1484	0.0000	-0.1016	-0.0000
17	2	S	DX-Y		0.0000	-0.0115	0.0000	0.0207	-0.0031	-0.0000	0.0049	0.0000	0.0093	-0.0000	0.0461
18	2	S	DXY		-0.0049	0.0000	0.0004	0.0000	0.0000	0.0197	0.0000	0.0431	-0.0000	-0.0196	-0.0000
19	3	S	S		-0.0000	0.1907	-0.0000	0.0640	0.2902	-0.0000	-0.1049	-0.0000	-0.1824	0.0000	0.0158
20	3	S	PX		-0.0000	0.1441	-0.0000	0.1485	0.2730	0.0000	-0.3324	-0.0000	-0.5380	0.0000	-0.2325
21	3	S	PY		-0.0933	0.0000	-0.0935	0.0000	0.0000	0.2614	0.0000	0.5327	-0.0000	-0.6312	-0.0000
22	3	S	PZ		-0.0000	-0.0547	0.0000	0.2127	-0.4071	0.0000	-0.3461	-0.0000	-0.0439	-0.0000	0.6839
23	3	S	DZ2		-0.0000	0.0278	-0.0000	0.0512	-0.0237	-0.0000	-0.0595	-0.0000	-0.0698	0.0000	-0.0442
24	3	S	DXZ		0.0000	0.0307	-0.0000	-0.0704	0.1319	0.0000	0.0743	0.0000	0.0235	-0.0000	-0.0319
25	3	S	DYZ		0.0108	-0.0000	-0.0149	0.0000	-0.0000	0.0224	-0.0000	0.0703	-0.0000	0.0029	0.0000
26	3	S	DX-Y		0.0000	-0.0330	0.0000	-0.0468	-0.0463	0.0000	0.0748	0.0000	0.0866	-0.0000	-0.0764
27	3	S	DXY		0.0536	0.0000	0.0452	-0.0000	0.0000	-0.0949	-0.0000	-0.1252	0.0000	0.0993	0.0000
28	4	O	S		0.0954	0.1241	-0.0820	-0.0080	-0.0202	0.0160	-0.0378	-0.0149	-0.0310	-0.0226	0.0175
29	4	O	PX		0.2808	-0.0371	0.1798	-0.4062	0.0127	-0.3651	-0.2367	0.2727	-0.1673	-0.1541	0.0632
30	4	O	PY		0.3709	-0.0806	0.1877	0.1986	0.1322	0.3017	-0.1199	-0.0419	0.0316	0.0392	-0.0154
31	4	O	PZ		-0.2460	-0.4080	0.4502	0.0471	0.1756	0.1288	-0.2077	0.1410	0.1319	0.1333	-0.0598
32	5	O	S		-0.0954	0.1241	0.0820	-0.0080	-0.0202	-0.0160	-0.0378	0.0149	-0.0310	0.0226	0.0175
33	5	O	PX		-0.2808	-0.0371	-0.1798	-0.4062	0.0127	0.3651	-0.2367	-0.2727	-0.1673	0.1541	0.0632
34	5	O	PY		0.3709	0.0806	0.1877	-0.1986	-0.1322	0.3017	0.1199	-0.0419	-0.0316	0.0392	0.0154
35	5	O	PZ		0.2460	-0.4080	-0.4502	0.0471	0.1756	-0.1288	-0.2077	-0.1410	0.1319	-0.1333	-0.0598
36	6	C	S		-0.0683	-0.0123	-0.0101	-0.0061	-0.0083	-0.0204	0.0046	0.0492	0.0241	0.0342	-0.0166
37	6	C	PX		0.0582	0.0904	-0.1211	0.2923	0.0482	0.2767	0.0639	-0.0448	0.0147	-0.0094	0.0016
38	6	C	PY		-0.3161	0.0151	-0.0518	-0.1048	-0.3505	-0.1579	0.0112	0.0755	0.0357	0.0420	-0.0223
39	6	C	PZ		0.1774	0.2112	-0.1798	-0.0297	-0.0691	-0.0305	0.0069	0.0110	-0.0178	0.0153	0.0087
40	7	C	S		0.0683	-0.0123	0.0101	-0.0061	-0.0083	0.0204	0.0046	-0.0492	0.0241	-0.0342	-0.0166
41	7	C	PX		-0.0582	0.0904	0.1211	0.2923	0.0482	-0.2767	0.0639	0.0448	0.0147	0.0094	0.0016
42	7	C	PY		-0.3161	-0.0151	-0.0518	0.1048	0.3505	-0.1579	-0.0112	0.0755	-0.0357	0.0420	0.0223
43	7	C	PZ		-0.1774	0.2112	0.1798	-0.0297	-0.0691	0.0305	0.0069	-0.0110	-0.0178	-0.0153	0.0087
44	8	H	S		0.1076	0.2302	-0.2234	-0.0613	-0.0913	-0.0672	0.0341	0.0279	-0.0157	0.0088	0.0120
45	9	H	S		-0.0175	0.0111	-0.0578	0.2845	0.0935	0.2644	0.0697	-0.0474	0.0455	0.0285	-0.0118
46	10	H	S		0.1086	-0.1766	0.2210	-0.0834	0.0917	-0.0311	-0.0834	-0.0021	-0.0250	-0.0309	0.0054
47	11	H	S		-0.1076	0.2302	0.2234	-0.0613	-0.0913	0.0672	0.0341	-0.0279	-0.0157	-0.0088	0.0120
48	12	H	S		0.0175	0.0111	0.0578	0.2845	0.0935	-0.2644	0.0697	0.0474	0.0455	-0.0285	-0.0118
49	13	H	S		-0.1086	-0.1766	-0.2210	-0.0834	0.0917	0.0311	-0.0834	0.0021	-0.0250	0.0309	0.0054

				EIGENVALUES---	0.2588	0.2953	0.3060	0.3430	0.3689	0.3801	0.4213	0.4377	0.4478	0.4585	0.4646
					23	24	25	26	27	28	29	30	31	32	33
1	1	P	S		0.5041	0.0000	-0.3146	-0.1272	-0.0000	0.0414	-0.0000	0.0304	0.1457	-0.1474	-0.0000
2	1	P	PX		-0.2453	0.0000	-0.2303	0.1614	0.0000	0.4478	-0.0000	-0.0191	-0.0981	0.1627	-0.0000
3	1	P	PY		-0.0000	0.4986	0.0000	0.0000	0.0432	0.0000	-0.1325	0.0000	-0.0000	-0.0000	-0.1877
4	1	P	PZ		-0.2624	-0.0000	-0.1627	-0.4444	0.0000	-0.1048	0.0000	-0.1608	-0.0888	0.1185	-0.0000
5	1	P	DZ2		0.1361	-0.0000	0.1164	0.3451	-0.0000	0.0583	0.0000	-0.2827	-0.2778	-0.1562	0.0000
6	1	P	DXZ		-0.0943	0.0000	-0.3466	0.2736	-0.0000	-0.2153	-0.0000	-0.0607	0.0911	-0.1389	0.0000
7	1	P	DYZ		-0.0000	0.2267	0.0000	-0.0000	-0.4645	0.0000	-0.0392	-0.0000	0.0000	0.0000	0.0763
8	1	P	DX-Y		0.0658	-0.0000	0.0661	-0.0085	-0.0000	-0.3419	0.0000	0.3428	-0.2096	0.0281	0.0000
9	1	P	DXY		-0.0000	0.2795	0.0000	-0.0000	0.3078	-0.0000	0.2049	0.0000	-0.0000	-0.0000	0.1017
10	2	S	S		-0.0712	-0.0000	0.1031	0.0940	0.0000	0.0302	0.0000	0.0878	0.0584	0.0329	0.0000
11	2	S	PX		0.2214	-0.0000	0.2634	-0.2155	0.0000	-0.0111	0.0000	0.0269	-0.0136	0.0411	-0.0000
12	2	S	PY		-0.0000	-0.3775	-0.0000	0.0000	0.2365	0.0000	0.0555	0.0000	-0.0000	-0.0000	0.0990
13	2	S	PZ		0.2662	0.0000	-0.3208	-0.3252	-0.0000	-0.0833	0.0000	-0.2260	-0.1531	-0.0361	-0.0000
14	2	S	DZ2		0.0411	-0.0000	-0.1392	-0.1697	-0.0000	-0.0313	0.0000	-0.4798	-0.4764	0.1073	0.0000
15	2	S	DXZ		0.1706	-0.0000	0.3674	-0.3193	0.0000	-0.0192	0.0000	0.0964	0.0035	0.2259	-0.0000
16	2	S	DYZ		0.0000	-0.3768	-0.0000	-0.0000	0.4197	0.0000	0.2127	0.0000	-0.0000	-0.0000	0.0472
17	2	S	DX-Y		0.0042	-0.0000	0.0179	0.0073	-0.0000	-0.2415	-0.0000	0.3294	-0.3774	-0.0219	-0.0000
18	2	S	DXY		-0.0000	0.0913	0.0000	0.0000	0.1293	0.0000	0.1712	0.0000	-0.0000	-0.0000	0.6337
19	3	S	S		-0.0765	-0.0000	0.1033	-0.0161	-0.0000	-0.0952	0.0000	-0.0969	0.0175	-0.0331	0.0000
20	3	S	PX		0.3624	0.0000	-0.2671	0.0811	0.0000	0.3330	-0.0000	0.2368	-0.3692	0.0944	-0.0000
21	3	S	PY		-0.0000	-0.3744	-0.0000	0.0000	-0.2410	-0.0000	-0.0639	-0.0000	0.0000	0.0000	0.0761
22	3	S	PZ		0.2014	-0.0000	0.3196	0.0398	-0.0000	0.0876	0.0000	-0.0960	-0.0286	-0.0337	0.0000
23	3	S	DZ2		-0.0865	0.0000	-0.0627	0.0854	-0.0000	-0.3260	-0.0000	-0.0173	-0.2550	-0.4417	-0.0000
24	3	S	DXZ		0.1728	-0.0000	0.3797	0.1070	-0.0000	0.1775	-0.0000	-0.3134	-0.1283	-0.2641	-0.0000
25	3	S	DYZ		-0.0000	0.1755	0.0000	0.0000	-0.0719	0.0000	0.0763	-0.0000	0.0000	0.0000	0.5914
26	3	S	DX-Y		0.0952	-0.0000	-0.0350	0.1108	-0.0000	0.2337	0.0000	0.3523	-0.5211	0.1522	0.0000
27	3	S	DXY		0.0000	-0.3450	-0.0000	-0.0000	-0.4623	-0.0000	-0.1789	-0.0000	0.0000	0.0000	0.1885
28	4	O	S		-0.1947	0.0274	0.0463	-0.0568	0.0794	0.0973	-0.1570	0.0152	-0.0985	0.0165	-0.0702
29	4	O	PX		-0.0559	0.0988	0.0369	-0.0127	0.0858	-0.1528	0.0365	0.0562	-0.0551	0.0474	-0.0525
30	4	O	PY		-0.0971	0.0279	0.0321	0.1347	-0.1018	-0.0413	0.1655	-0.0865	-0.0165	0.1645	-0.0618
31	4	O	PZ		-0.1296	0.0787	0.0395	0.0432	-0.0246	0.1110	-0.2100	0.0166	-0.1076	-0.0785	0.0372
32	5	O	S		-0.1947	-0.0274	0.0463	-0.0568	-0.0794	0.0973	0.1570	0.0152	-0.0985	0.0165	0.0702
33	5	O	PX		-0.0559	-0.0988	0.0369	-0.0127	-0.0858	-0.1528	-0.0365	0.0562	-0.0551	0.0474	0.0525
34	5	O	PY		0.0971	0.0279	-0.0321	-0.1347	-0.1018	0.0413	0.1855	0.0865	0.0165	-0.1645	-0.0618
35	5	O	PZ		-0.1296	-0.0787	0.0395	0.0432	0.0246	0.1110	0.2100	0.0166	-0.1076	-0.0785	0.0372
36	6	C	S		0.0959	0.0251	-0.0076	0.1661	-0.1161	-0.1586	0.3127	-0.0745	-0.0449	0.2520	-0.1604
37	6	C	PX		-0.0705	-0.0015	0.0068	-0.1249	0.1318	0.1201	-0.2676	0.0773	-0.0727	-0.1959	0.0001
38	6	C	PY		0.0975	0.0156	-0.0036	0.1490	-0.0732	-0.0878	0.0730	-0.0276	0.0386	-0.0465	0.0511
39	6	C	PZ		-0.0631	-0.0224	0.0051	-0.0634	0.0378	0.0619	-0.0209	-0.0557	-0.0284	0.0963	-0.0763
40	7	C	S		0.0959	-0.0251	-0.0076	0.1661	0.1161	-0.1586	-0.3127	-0.0745	-0.0449	0.2520	0.1604
41	7	C	PX		-0.0705	0.0015	0.0068	-0.1249	-0.1318	0.1201	0.2676	0.0773	-0.0727	-0.1959	0.0001
42	7	C	PY		-0.0975	0.0156	0.0036	-0.1490	-0.0732	0.0878	0.0730	0.0276	-0.0386	0.0465	0.0511
43	7	C	PZ		-0.0631	0.0224	0.0051	-0.0634	-0.0378	0.0619	0.0209	-0.0557	-0.0284	0.0963	0.0763
44	8	H	S		-0.0030	0.0130	-0.0034	-0.0668	0.0327	0.0360	-0.2021	0.1050	0.0163	-0.2389	0.1402
45	9	H	S		0.0253	0.0111	0.0099	0.0667	-0.0728	-0.0388	0.1160	-0.0498	0.0610	0.0777	0.0634
46	10	H	S		-0.0836	-0.0202	0.0106	-0.0984	0.1108	0.1286	-0.2744	0.0413	0.0095	-0.2265	0.0953
47	11	H	S		-0.0030	-0.0130	-0.0034	-0.0668	-0.0327	0.0360	0.2021	0.1050	0.0163	-0.2389	-0.1402
48	12	H	S		0.0253	-0.0111	0.0099	0.0667	0.0728	-0.0388	-0.1180	-0.0498	0.0610	0.0776	-0.0634
49	13	H	S		-0.0836	0.0202	0.0106	-0.0984	-0.1108	0.1286	0.2744	0.0413	0.0095	-0.2265	-0.0953

				EIGENVALUES---	0.4824	0.4834	0.4932	0.4934	0.4995	0.5022	0.5091	0.5413	0.5508	0.5669	0.5815
					34	35	36	37	38	39	40	41	42	43	44
1	1	P	S		0.0821	0.0000	0.0000	-0.0904	0.0000	0.0768	0.1015	0.0000	-0.0005	0.0000	-0.0294
2	1	P	PX		-0.0110	-0.0000	0.0000	-0.0644	0.0000	0.1498	0.1398	0.0000	0.3047	-0.0000	0.1355
3	1	P	PY		-0.0600	0.0618	0.0841	0.0000	-0.0173	0.0000	0.0000	-0.3507	0.0000	0.5125	0.0000
4	1	P	PZ		-0.0079	-0.0636	0.0000	-0.0167	0.0000	-0.0353	0.1846	0.0000	-0.2029	-0.0000	0.3694
5	1	P	DZ2		-0.0645	-0.0000	-0.0000	0.0347	-0.0000	0.0435	-0.1559	-0.0000	0.1731	-0.0000	-0.1127
6	1	P	DXZ		-0.0030	-0.0330	-0.0000	0.0399	-0.0000	-0.0436	-0.1351	-0.0000	0.0259	-0.0000	0.0060
7	1	P	DYZ		-0.0000	-0.0091	-0.0196	-0.0000	-0.0269	0.0000	-0.0000	0.1698	-0.0000	0.0413	-0.0000
8	1	P	DX-Y		-0.1052	-0.0000	-0.0000	0.0882	-0.0000	-0.1797	-0.1852	-0.0000	-0.1917	-0.0000	0.1513
9	1	P	DXY		0.0000	-0.0349	-0.0463	-0.0000	0.0357	-0.0000	-0.0000	0.1411	0.0000	-0.0376	-0.0000
10	2	S	S		0.0080	0.0000	-0.0000	0.0126	-0.0000	-0.0003	-0.0333	-0.0000	-0.0005	0.0000	-0.0565
11	2	S	PX		-0.0111	-0.0000	0.0000	-0.0022	0.0000	0.0083	-0.0005	0.0000	-0.0438	-0.0000	-0.0211
12	2	S	PY		0.0000	0.0078	-0.0105	-0.0000	0.0225	-0.0000	-0.0000	0.0392	0.0000	-0.0383	0.0000
13	2	S	PZ		-0.0220	-0.0000	0.0000	-0.0174	0.0000	-0.0045	0.0512	0.0000	-0.0016	-0.0000	-0.2059
14	2	S	DZ2		-0.1691	-0.0000	-0.0000	0.1944	-0.0000	-0.0060	-0.3050	-0.0000	0.0974	-0.0000	0.2059
15	2	S	DXZ		-0.0483	-0.0000	0.0000	-0.0203	-0.0000	-0.0409	0.3088	0.0000	0.6291	-0.0000	0.0987
16	2	S	DYZ		-0.0000	0.0046	0.0360	0.0000	0.2363	-0.0000	-0.0000	-0.1840	0.0000	0.4878	-0.0000
17	2	S	DX-Y		-0.0554	-0.0000	0.0000	-0.2842	0.0000	0.7264	-0.0987	0.0000	0.0428	-0.0000	0.1493
18	2	S	DXY		-0.0000	-0.0584	-0.0913	-0.0000	-0.6813	0.0000	0.0000	-0.1646	0.0000	0.0313	0.0000
19	3	S	S		0.0081	0.0000	-0.0000	0.0234	-0.0000	-0.0357	-0.0250	-0.0000	-0.0183	0.0000	0.0111
20	3	S	PX		-0.0206	-0.0000	0.0000	-0.0323	0.0000	0.0544	0.0352	0.0000	0.0415	-0.0000	-0.0268
21	3	S	PY		0.0000	0.0023	-0.0032	0.0000	-0.0151	0.0000	-0.0000	0.0769	-0.0000	-0.0330	0.0000
22	3	S	PZ		0.0060	0.0000	-0.0000	0.0069	-0.0000	-0.0136	0.0024	-0.0000	0.0321	0.0000	-0.0391
23	3	S	DZ2		0.1419	0.0000	0.0000	-0.1791	0.0000	-0.2202	0.5523	0.0000	0.3345	0.0000	-0.0837
24	3	S	DXZ		0.1033	0.0000	0.0000	-0.0775	0.0000	0.1508	0.2129	0.0000	-0.3985	0.0000	0.2742
25	3	S	DYZ		0.0000	-0.2539	0.3102	0.0000	0.6236	-0.0000	-0.0000	-0.0855	-0.0000	-0.0638	0.0000
26	3	S	DX-Y		-0.0606	-0.0000	-0.0000	0.3919	-0.0000	-0.4228	0.1842	-0.0000	-0.2172	-0.0000	0.1529
27	3	S	DXY		-0.0000	-0.0931	0.0650	0.0000	-0.0806	0.0000	0.0000	-0.3019	-0.0000	0.3578	-0.0000
28	4	O	S		0.0159	-0.0249	0.0188	0.0061	-0.0042	0.0357	0.0439	-0.2036	-0.0225	-0.0095	-0.0954
29	4	O	PX		-0.0392	0.0286	-0.0071	0.0380	0.0086	-0.0363	-0.0068	-0.0807	-0.0564	0.0574	-0.0069
30	4	O	PY		-0.0606	0.0699	-0.0116	0.0286	0.0041	-0.0230	0.0161	0.1048	0.0855	0.2417	0.0072
31	4	O	PZ		0.0216	-0.0464	-0.0489	0.0740	0.0111	0.0622	0.0032	-0.1806	0.0142	-0.0312	-0.1684
32	5	O	S		0.0159	0.0249	-0.0188	0.0061	0.0042	0.0357	0.0439	0.2036	-0.0225	0.0095	-0.0954
33	5	O	PX		-0.0392	-0.0286	0.0071	-0.0380	-0.0086	-0.0363	-0.0068	0.0807	-0.0564	-0.0574	-0.0069
34	5	O	PY		0.0606	0.0699	-0.0116	-0.0286	0.0041	0.0230	-0.0161	0.1048	-0.0855	0.2417	-0.0072
35	5	O	PZ		0.0216	0.0464	0.0489	0.0740	-0.0111	0.0622	0.0032	0.1806	0.0142	0.0312	-0.1684
36	6	C	S		0.3141	-0.2919	0.0634	-0.0357	-0.0620	-0.0296	-0.0383	0.0340	0.0139	0.0674	0.0809
37	6	C	PX		0.2611	-0.2862	0.1096	-0.0663	-0.0821	-0.0932	-0.2573	0.2067	0.0524	0.0959	0.0934
38	6	C	PY		-0.2208	0.2212	0.2036	-0.1829	-0.0408	-0.1567	-0.1815	0.3168	0.0670	0.2212	0.2841
39	6	C	PZ		-0.0268	0.0644	0.4165	-0.4128	-0.1050	-0.0638	-0.0051	-0.1565	-0.0914	-0.1762	-0.2277
40	7	C	S		0.3141	0.2919	-0.0634	-0.0357	0.0620	-0.0296	-0.0383	-0.0340	0.0139	-0.0674	0.0809
41	7	C	PX		0.2611	0.2862	-0.1096	-0.0663	0.0821	-0.0932	-0.2573	-0.2067	0.0524	-0.0959	0.0934
42	7	C	PY		0.2208	0.2212	0.2036	0.1829	-0.0408	0.1567	0.1815	0.3168	-0.0670	0.2212	-0.2841
43	7	C	PZ		-0.0268	-0.0644	-0.4165	-0.4128	0.1050	-0.0638	-0.0051	0.1565	-0.0914	0.1762	-0.2277
44	8	H	S		-0.1402	0.0889	-0.3767	0.3603	0.1267	0.0080	0.0043	0.1013	0.0618	0.0945	0.1138
45	9	H	S		-0.4167	0.4346	0.0016	-0.0451	0.0658	0.0448	0.2053	-0.1639	-0.0541	-0.0939	-0.1006
46	10	H	S		-0.1964	0.1853	0.2534	-0.2356	-0.0561	-0.1330	-0.1892	0.1922	0.0262	0.0784	0.0885
47	11	H	S		-0.1402	-0.0889	0.3767	0.3603	-0.1267	0.0080	0.0043	-0.1013	0.0618	-0.0945	0.1138
48	12	H	S		-0.4167	-0.4346	-0.0016	-0.0451	-0.0658	0.0448	0.2053	0.1639	-0.0541	0.0938	-0.1006
49	13	H	S		-0.1964	-0.1853	-0.2534	-0.2356	0.0561	-0.1330	-0.1892	-0.1922	0.0262	-0.0784	0.0885

EIGENVALUES---				0.6153	0.6347	0.6350	0.6557	0.6604
				45	46	47	48	49
1	1	P	S	-0.0649	0.0000	0.0096	0.0000	0.0235
2	1	P	PX	-0.2976	-0.0000	-0.2087	-0.0000	0.0269
3	1	P	PY	-0.0000	-0.0021	0.0000	0.0821	-0.0000
4	1	P	PZ	-0.2161	0.0000	0.1937	-0.0000	0.0356
5	1	P	DZ2	-0.3316	0.0000	0.5598	0.0000	-0.0860
6	1	P	DXZ	0.0198	0.0000	0.0540	-0.0000	0.7034
7	1	P	DYZ	0.0000	-0.3979	0.0000	-0.5967	0.0000
8	1	P	DX-Y	-0.5967	-0.0000	-0.2655	0.0000	0.0057
9	1	P	DXY	-0.0000	0.5847	-0.0000	-0.4665	0.0000
10	2	S	S	0.0957	-0.0000	-0.1449	0.0000	0.0154
11	2	S	PX	0.0125	0.0000	0.0045	0.0000	-0.1188
12	2	S	PY	0.0000	0.0733	-0.0000	0.0971	-0.0000
13	2	S	PZ	-0.1479	0.0000	0.2299	-0.0000	-0.0190
14	2	S	DZ2	0.2671	-0.0000	-0.4082	0.0000	0.0070
15	2	S	DXZ	-0.0879	-0.0000	0.0127	-0.0000	0.4550
16	2	S	DYZ	0.0000	-0.3497	0.0000	-0.3855	0.0000
17	2	S	DX-Y	0.1879	0.0000	0.3670	-0.0000	0.0242
18	2	S	DXY	0.0000	-0.1620	0.0000	0.1033	-0.0000
19	3	S	S	0.1059	0.0000	0.1374	-0.0000	0.0429
20	3	S	PX	-0.1577	-0.0000	-0.2084	0.0000	-0.0847
21	3	S	PY	0.0000	-0.1158	0.0000	0.0451	-0.0000
22	3	S	PZ	0.0475	0.0000	0.0771	0.0000	-0.0936
23	3	S	DZ2	0.0544	-0.0000	-0.1892	0.0000	-0.1833
24	3	S	DXZ	-0.1502	-0.0000	-0.3171	-0.0000	0.3479
25	3	S	DYZ	0.0000	-0.0510	0.0000	0.1975	-0.0000
26	3	S	DX-Y	0.3224	0.0000	0.2320	-0.0000	0.1623
27	3	S	DXY	-0.0000	0.5460	-0.0000	-0.1391	0.0000
28	4	O	S	-0.1125	-0.0440	0.0261	0.0921	-0.0144
29	4	O	PX	-0.1146	0.0537	-0.0311	0.0729	0.0024
30	4	O	PY	-0.0428	-0.0164	-0.0431	0.2380	-0.1475
31	4	O	PZ	-0.1100	-0.1017	0.0755	-0.0179	0.0481
32	5	O	S	-0.1125	0.0440	0.0261	-0.0921	-0.0144
33	5	O	PX	-0.1146	-0.0537	-0.0311	-0.0729	0.0024
34	5	O	PY	0.0428	-0.0164	0.0431	0.2380	0.1475
35	5	O	PZ	-0.1100	0.1017	0.0755	0.0179	0.0481
36	6	C	S	-0.0197	-0.0020	-0.0183	0.0516	-0.0353
37	6	C	PX	-0.0091	-0.0041	-0.0108	-0.0074	-0.0167
38	6	C	PY	-0.0020	0.0148	-0.0568	0.0967	-0.0784
39	6	C	PZ	-0.0085	-0.0136	0.0241	-0.1017	0.0636
40	7	C	S	-0.0197	0.0020	-0.0183	-0.0516	-0.0353
41	7	C	PX	-0.0091	0.0041	-0.0108	0.0074	-0.0167
42	7	C	PY	0.0020	0.0148	0.0568	0.0967	0.0784
43	7	C	PZ	-0.0085	0.0136	0.0241	0.1017	0.0636
44	8	H	S	0.0138	0.0043	-0.0145	0.0383	-0.0224
45	9	H	S	-0.0010	0.0073	0.0160	-0.0170	0.0179
46	10	H	S	0.0009	0.0027	-0.0177	0.0038	-0.0150
47	11	H	S	0.0138	-0.0043	-0.0145	-0.0383	-0.0224
48	12	H	S	-0.0010	-0.0073	0.0160	0.0170	0.0179
49	13	H	S	0.0009	-0.0027	-0.0177	-0.0038	-0.0150

EIGENVALUES AND EIGENVECTORS $Ni[S_2P(C_2H_5)_2]_2$

					1a$_1$	1b$_2$	2a$_1$	1b$_1$	2b$_2$	3a$_1$	3b$_2$	2b$_1$	4a$_1$	4b$_2$	5a$_1$
EIGENVALUES---					-1.6350	-1.5854	-0.9755	-0.8792	-0.8697	-0.8090	-0.7853	-0.6829	-0.6105	-0.5576	-0.5295
					1	2	3	4	5	6	7	8	9	10	11
1	1	P	S		0.2270	0.0000	-0.4506	-0.1588	0.0000	-0.2706	0.0000	-0.0626	0.1789	0.0000	-0.1472
2	1	P	PX		-0.0691	0.0000	-0.1442	0.1155	-0.0000	-0.0325	-0.0000	0.3098	-0.1578	-0.0000	0.0501
3	1	P	PY		-0.0000	0.1789	0.0000	-0.0000	-0.1849	0.0000	-0.0966	-0.0000	0.0000	0.3479	-0.0000
4	1	P	PZ		-0.0426	-0.0000	0.0749	0.1036	-0.0000	-0.3297	-0.0000	-0.0710	-0.1790	-0.0000	-0.0718
5	1	P	DZ2		-0.0526	-0.0000	-0.0377	-0.0244	-0.0000	-0.0603	-0.0000	-0.1276	-0.1101	0.0000	0.1222
6	1	P	DXZ		0.0162	0.0000	0.0085	-0.0792	0.0000	-0.0014	-0.0000	-0.0370	-0.0050	0.0000	0.0779
7	1	P	DYZ		0.0000	-0.0444	-0.0000	0.0000	0.1056	0.0000	0.1771	0.0000	-0.0000	-0.0104	0.0000
8	1	P	DX-Y		-0.0658	-0.0000	0.0143	-0.0995	0.0000	-0.1009	0.0000	0.1612	0.0145	0.0000	0.0727
9	1	P	DXY		0.0000	-0.0810	-0.0000	-0.0000	-0.0968	0.0000	0.0201	-0.0000	0.0000	-0.1390	0.0000
10	2	S	S		0.0534	0.0000	-0.1937	0.0049	-0.0000	-0.6089	-0.0000	-0.3434	-0.4450	-0.0000	0.2127
11	2	S	PX		-0.0114	0.0000	-0.0379	0.0001	-0.0000	-0.0140	-0.0000	0.0889	-0.0735	-0.0000	0.0601
12	2	S	PY		-0.0000	0.0311	0.0000	-0.0000	-0.0185	0.0000	0.0058	0.0000	0.0000	0.1513	0.0000
13	2	S	PZ		-0.0400	-0.0000	0.0950	0.0125	-0.0000	0.1462	-0.0000	0.0171	-0.0452	-0.0000	0.1108
14	2	S	DZ2		0.0171	0.0000	-0.0511	-0.0163	0.0000	-0.0610	0.0000	-0.0180	0.0001	0.0000	-0.0381
15	2	S	DXZ		0.0103	-0.0000	0.0278	-0.0046	0.0000	0.0089	0.0000	-0.0603	0.0379	0.0000	-0.0322
16	2	S	DYZ		0.0000	-0.0268	-0.0000	0.0000	0.0155	-0.0000	-0.0274	-0.0000	-0.0000	-0.0798	-0.0000
17	2	S	DX-Y		-0.0080	-0.0000	-0.0231	-0.0177	-0.0000	-0.0058	-0.0000	0.0203	-0.0141	-0.0000	0.0092
18	2	S	DXY		0.0000	-0.0092	-0.0000	-0.0000	-0.0104	-0.0000	-0.0086	-0.0000	0.0000	-0.0203	0.0000
19	3	S	S		0.0493	0.0000	-0.3609	-0.0316	0.0000	-0.1873	0.0000	0.7685	0.0132	-0.0000	0.0486
20	3	S	PX		-0.0385	-0.0000	0.1581	0.0171	-0.0000	0.0369	-0.0000	-0.0210	-0.0236	-0.0000	0.0334
21	3	S	PY		-0.0000	0.0231	0.0000	-0.0000	-0.1058	0.0000	-0.0375	0.0000	0.0000	0.0603	-0.0000
22	3	S	PZ		-0.0016	0.0000	-0.0060	0.0012	-0.0000	-0.1151	-0.0000	0.0218	-0.0639	-0.0000	-0.0021
23	3	S	DZ2		-0.0158	-0.0000	0.0363	-0.0008	-0.0000	-0.0213	-0.0000	-0.0098	-0.0274	0.0000	0.0208
24	3	S	DXZ		0.0012	-0.0000	0.0049	-0.0031	0.0000	0.0757	0.0000	-0.0130	0.0295	-0.0000	0.0073
25	3	S	DYZ		0.0000	-0.0023	-0.0000	0.0000	0.0056	0.0000	0.0170	0.0000	-0.0000	0.0058	0.0000
26	3	S	DX-Y		0.0127	0.0000	-0.0592	-0.0181	0.0000	-0.0233	0.0000	0.0174	0.0156	0.0000	-0.0077
27	3	S	DXY		0.0000	-0.0229	-0.0000	0.0000	0.0727	-0.0000	0.0298	0.0000	-0.0000	-0.0412	0.0000
28	4	C	S		0.4020	-0.3853	-0.0602	-0.1919	0.0190	0.1243	0.2554	-0.0697	-0.0111	-0.0924	0.0203
29	4	C	PX		-0.0187	0.0250	-0.3044	0.2068	0.4113	0.1609	0.0247	-0.1195	-0.0031	-0.0756	-0.0979
30	4	C	PY		-0.0742	0.1242	-0.1520	-0.2491	0.0110	-0.0341	0.1112	-0.1425	0.3082	-0.3279	0.0760
31	4	C	PZ		0.0914	-0.0957	0.0723	0.1302	-0.0523	-0.1784	-0.2211	-0.0118	0.1672	-0.2301	-0.3663
32	5	C	S		0.4020	0.3853	-0.0602	-0.1919	-0.0190	0.1243	-0.2554	-0.0697	-0.0111	0.0924	0.0203
33	5	C	PX		-0.0187	-0.0250	-0.3044	0.2068	-0.4113	0.1609	-0.0247	-0.1195	-0.0031	0.0756	-0.0979
34	5	C	PY		0.0742	0.1242	0.1520	0.2491	0.0110	0.0341	0.1112	0.1425	-0.3082	-0.3279	-0.0760
35	5	C	PZ		0.0914	0.0957	0.0723	0.1302	0.0523	-0.1784	0.2211	-0.0118	0.1672	0.2301	-0.3663
36	6	C	S		0.2900	-0.3116	0.1142	0.3088	0.0530	-0.0458	-0.3336	0.0483	0.0768	0.1423	0.1932
37	6	C	PX		-0.0004	0.0021	-0.1431	0.1601	0.2512	0.0955	-0.0342	-0.0757	-0.0448	0.0719	0.0107
38	6	C	PY		0.1382	-0.1407	0.0247	-0.0476	-0.0518	-0.0305	0.0615	-0.0186	-0.0026	-0.1869	-0.2918
39	6	C	PZ		-0.0726	0.0788	-0.0138	0.0548	-0.0018	-0.1309	-0.1917	-0.0567	0.3349	-0.3031	0.1391
40	7	C	S		0.2900	0.3116	0.1142	0.3088	-0.0530	-0.0458	0.3336	0.0483	0.0768	-0.1423	0.1932
41	7	C	PX		-0.0004	-0.0021	-0.1431	0.1601	-0.2512	0.0955	0.0342	-0.0757	-0.0448	-0.0719	0.0107
42	7	C	PY		-0.1382	-0.1407	-0.0247	0.0476	-0.0518	0.0305	0.0615	0.0186	0.0026	-0.1869	0.2918
43	7	C	PZ		-0.0726	-0.0788	-0.0138	0.0548	0.0018	-0.1309	0.1917	-0.0567	0.3349	0.3031	0.1391
44	8	H	S		0.1651	-0.1512	-0.2526	-0.0037	0.2854	0.2116	0.2150	-0.0776	-0.0543	-0.0410	0.0510
45	9	H	S		0.1794	-0.1719	0.1281	-0.2768	-0.2320	0.0131	0.1941	0.0492	-0.0599	0.0804	0.2448
46	10	H	S		0.1651	0.1512	-0.2526	-0.0037	-0.2854	0.2116	-0.2150	-0.0776	-0.0543	0.0410	0.0510
47	11	H	S		0.1794	0.1719	0.1281	-0.2768	0.2320	0.0131	-0.1941	0.0492	-0.0599	-0.0804	0.2448
48	12	H	S		0.0947	-0.1015	0.0454	0.1930	0.0271	-0.1171	-0.3041	-0.0202	0.2923	-0.1662	0.2341
49	13	H	S		0.1496	-0.1589	-0.0569	0.2556	0.2242	0.0869	-0.1378	-0.0175	-0.0863	0.2198	0.0829
50	14	H	S		0.2558	-0.3059	0.1762	-0.0411	-0.1918	-0.0742	-0.0262	0.0636	-0.0115	-0.0352	-0.1539
51	15	H	S		0.0947	0.1015	0.0454	0.1930	-0.0271	-0.1171	0.3041	-0.0202	0.2923	0.1662	0.2341
52	16	H	S		0.1496	0.1589	-0.0569	0.2556	-0.2242	0.0869	0.1378	-0.0175	-0.0863	-0.2198	0.0829
53	17	H	S		0.2558	0.3059	0.1762	-0.0411	-0.1918	-0.0742	0.0262	0.0636	-0.0115	0.0352	-0.1539

					$5b_2$	$6a_1$	$3b_1$	$4b_1$	$6b_2$	$7b_2$	$7a_1$	$5b_1$	$8b_2$	$9a_1$	$8a_1$
EIGENVALUES---					-0.4967	-0.4102	-0.3529	-0.3203	-0.3153	-0.2893	-0.2715	-0.2253	-0.1991	-0.1999	-0.1616
					12	13	14	15	16	17	18	19	20	21	22
1	1	P	S		0.0000	0.2733	0.0005	0.2744	-0.0000	-0.0000	-0.0532	-0.0766	-0.0000	0.0000	0.0164
2	1	P	PX		-0.0000	0.1879	-0.3432	-0.0249	0.0000	0.0000	-0.1777	0.2040	0.0000	-0.0000	-0.0127
3	1	P	PY		0.0586	-0.0000	-0.0000	-0.0000	-0.1286	-0.2385	0.0000	0.0000	0.0110	0.2461	-0.0000
4	1	P	PZ		0.0000	0.2010	0.0942	0.0174	-0.0000	0.0000	0.3763	0.1123	0.0000	-0.0000	-0.0068
5	1	P	DZ2		-0.0000	-0.0111	-0.0345	0.1205	-0.0000	0.0000	0.2136	0.0207	-0.0000	0.0000	0.1652
6	1	P	DXZ		-0.0000	0.1985	0.0458	-0.3626	0.0000	0.0000	0.0084	-0.1578	0.0000	-0.0000	0.0563
7	1	P	DYZ		0.1214	-0.0000	-0.0000	-0.0000	-0.1526	-0.2200	0.0000	-0.0000	-0.2182	-0.0868	-0.0000
8	1	P	DX-Y		-0.0000	0.0830	0.0151	0.0912	-0.0000	0.0000	-0.1318	0.0006	0.0000	-0.0000	-0.0916
9	1	P	DXY		-0.0123	0.0000	0.0000	0.0000	0.1288	-0.3372	0.0000	-0.0000	0.1453	-0.1542	-0.0000
10	2	S	S		-0.0000	-0.3396	-0.0332	-0.0901	0.0000	0.0000	-0.1813	-0.0372	0.0000	-0.0000	0.0044
11	2	S	PX		-0.0000	0.2862	-0.1539	-0.4737	0.0000	-0.0000	-0.1010	-0.1304	-0.0000	0.0000	0.6579
12	2	S	PY		0.0647	-0.0000	-0.0000	-0.0000	-0.2627	-0.4953	0.0000	-0.0000	-0.6391	-0.0024	0.0000
13	2	S	PZ		-0.0000	-0.3669	-0.0634	-0.2051	0.0000	-0.0000	-0.5105	-0.0996	-0.0000	0.0000	-0.1687
14	2	S	DZ2		0.0000	0.0934	0.0151	0.0717	-0.0000	-0.0000	0.0933	0.0055	-0.0000	0.0000	0.0269
15	2	S	DXZ		0.0000	-0.1060	0.0648	0.1343	-0.0000	-0.0000	0.0452	0.0113	-0.0000	0.0000	-0.0139
16	2	S	DYZ		-0.0421	0.0000	0.0000	0.0000	0.0858	0.1454	-0.0000	-0.0000	0.0995	-0.0282	0.0000
17	2	S	DX-Y		0.0000	0.0134	0.0069	0.0072	-0.0000	0.0000	-0.0122	-0.0229	0.0000	-0.0000	-0.0474
18	2	S	DXY		0.0022	0.0000	0.0000	0.0000	0.0068	-0.0501	0.0000	-0.0000	0.0199	-0.0057	-0.0000
19	3	S	S		-0.0000	-0.3014	0.2278	-0.0803	-0.0000	0.0000	0.1346	-0.0395	0.0000	-0.0000	-0.0022
20	3	S	PX		-0.0000	-0.2678	0.3571	-0.2537	-0.0000	-0.0000	0.4312	-0.1958	-0.0000	0.0000	0.0649
21	3	S	PY		-0.0003	0.0000	-0.0000	0.0000	0.0900	-0.6166	0.0000	-0.0000	0.5990	0.0362	-0.0000
22	3	S	PZ		-0.0000	0.3730	0.0247	-0.4330	0.0000	-0.0000	0.0607	-0.1323	-0.0000	0.0000	-0.6877
23	3	S	DZ2		-0.0000	0.0038	0.0347	-0.0643	0.0000	0.0000	0.3624	-0.0261	0.0000	-0.0000	0.0551
24	3	S	DXZ		0.0000	-0.1326	-0.0060	0.0950	-0.0000	-0.0000	-0.0254	0.0102	-0.0000	0.0000	0.0110
25	3	S	DYZ		0.0154	-0.0000	-0.0000	-0.0000	-0.0256	-0.0724	0.0000	-0.0000	-0.0715	-0.0223	-0.0000
26	3	S	DX-Y		0.0000	0.0538	-0.0716	0.0726	-0.0000	-0.0000	-0.0762	0.0264	-0.0000	0.0000	0.0950
27	3	S	DXY		0.0015	-0.0000	0.0000	-0.0000	-0.0292	0.1628	-0.0000	0.0000	-0.0882	-0.0140	0.0000
28	4	C	S		0.0704	-0.0337	0.0110	-0.0919	0.0285	-0.0719	0.0378	-0.0043	0.0256	-0.0208	-0.0137
29	4	C	PX		-0.0793	-0.0743	-0.1325	-0.0715	-0.1599	-0.0615	0.0965	-0.0711	0.0886	0.0284	-0.0287
30	4	C	PY		0.1757	0.0057	0.1757	-0.0625	0.1908	-0.1104	-0.1136	-0.1553	-0.0822	-0.3066	0.0256
31	4	C	PZ		-0.3392	-0.0409	0.0916	-0.0552	0.0517	-0.0912	-0.1480	-0.0931	-0.1185	-0.1514	0.0428
32	5	C	S		-0.0704	-0.0337	0.0110	-0.0919	-0.0285	0.0720	0.0378	-0.0043	-0.0256	0.0208	-0.0137
33	5	C	PX		0.0793	-0.0743	-0.1325	-0.0715	0.1599	0.0615	0.0965	-0.0711	-0.0886	-0.0284	-0.0287
34	5	C	PY		0.1757	-0.0057	-0.1757	0.0625	0.1908	-0.1104	0.1136	0.1553	-0.0822	-0.3066	-0.0256
35	5	C	PZ		0.3392	-0.0409	0.0916	-0.0552	-0.0517	0.0912	-0.1480	-0.0931	0.1185	0.1514	0.0428
36	6	C	S		0.1432	0.0475	-0.0324	0.1008	-0.1053	0.0102	-0.0062	-0.2293	0.0300	-0.2071	0.0036
37	6	C	PX		-0.0390	0.0747	0.3264	-0.0739	0.3897	-0.0874	-0.1216	0.2808	-0.1107	0.1835	0.0218
38	6	C	PY		-0.2551	-0.1039	-0.0398	-0.1830	0.0291	-0.0530	0.0156	0.3457	-0.0623	0.3978	0.0105
39	6	C	PZ		0.2402	-0.0716	-0.0818	-0.1305	0.0041	-0.0372	0.0500	0.2327	-0.0462	0.2239	-0.0051
40	7	C	S		-0.1432	0.0475	-0.0324	0.1008	0.1053	-0.0102	-0.0062	-0.2293	-0.0300	0.2071	0.0036
41	7	C	PX		0.0390	0.0747	0.3264	-0.0739	-0.3897	0.0874	-0.1216	0.2808	0.1107	-0.1835	0.0218
42	7	C	PY		-0.2551	0.1039	0.0398	0.1830	0.0291	-0.0530	-0.0156	-0.3457	-0.0623	0.3978	-0.0105
43	7	C	PZ		-0.2402	-0.0716	-0.0818	-0.1305	-0.0041	0.0372	0.0500	0.2327	0.0462	-0.2239	-0.0051
44	8	H	S		0.0926	-0.0911	-0.1785	-0.0527	-0.1976	-0.0028	0.1553	-0.0003	0.1137	0.0824	-0.0503
45	9	H	S		0.2598	0.0769	0.0970	0.0333	0.2208	0.0751	-0.0191	0.2051	-0.0489	0.0893	0.0006
46	10	H	S		-0.0926	-0.0911	-0.1785	-0.0527	0.1976	0.0028	0.1553	-0.0003	-0.1137	-0.0824	-0.0503
47	11	H	S		-0.2598	0.0769	0.0970	0.0333	-0.2208	-0.0751	-0.0191	0.2051	0.0489	-0.0893	0.0006
48	12	H	S		0.2938	-0.0494	-0.1208	-0.0735	-0.0718	-0.0130	0.0740	0.1527	-0.0017	0.1870	-0.0154
49	13	H	S		-0.0133	0.1174	0.3100	0.0344	0.3078	-0.0524	-0.1446	0.0581	-0.0915	-0.0311	0.0264
50	14	H	S		-0.1520	-0.0470	-0.0873	-0.0181	-0.1087	-0.0052	-0.0153	-0.0406	-0.0279	0.0012	0.0179
51	15	H	S		-0.2938	-0.0494	-0.1208	-0.0735	0.0718	0.0130	0.0740	0.1527	0.0017	-0.1870	-0.0154
52	16	H	S		0.0133	0.1174	0.3100	0.0344	-0.3078	0.0524	-0.1446	0.0581	0.0915	0.0311	0.0264
53	17	H	S		0.1520	-0.0470	-0.0873	-0.0181	0.1087	0.0052	-0.0153	-0.0406	0.0279	-0.0012	0.0179

				EIGENVALUES---	0.2388	0.2539	0.2707	0.3013	0.3278	0.3405	0.3997	0.4005	0.4105	0.4240	0.4259
					23	24	25	26	27	28	29	30	31	32	33
1	1	P	S		-0.5789	0.0000	-0.1759	0.0590	-0.0947	0.0000	0.1053	0.0000	0.0194	-0.0609	-0.0000
2	1	P	PX		0.1136	0.0000	-0.2757	0.1994	0.4005	-0.0000	-0.2543	-0.0000	0.0209	0.1431	-0.0000
3	1	P	PY		0.0000	0.5068	-0.0000	-0.0000	0.0000	0.0207	-0.0000	0.0779	-0.0000	-0.0000	-0.3627
4	1	P	PZ		0.1254	-0.0000	-0.2087	-0.4978	-0.1037	-0.0000	-0.2133	-0.0000	-0.1386	0.1038	-0.0000
5	1	P	DZ2		0.0018	0.0000	0.1760	0.4633	0.0036	0.0000	-0.1556	-0.0000	-0.3983	-0.1461	-0.0000
6	1	P	DXZ		0.1472	-0.0000	-0.3874	0.2161	-0.1908	0.0000	0.1802	0.0000	-0.0401	-0.1294	-0.0000
7	1	P	DYZ		0.0000	0.2359	-0.0000	-0.0000	0.0000	0.4590	0.0000	-0.0271	-0.0000	0.0000	0.2756
8	1	P	DX-Y		0.0972	0.0000	0.1877	0.0465	-0.4895	0.0000	-0.2795	-0.0000	0.2904	-0.1236	0.0000
9	1	P	DXY		0.0000	0.2746	-0.0000	-0.0000	0.0000	-0.4196	-0.0000	0.1021	-0.0000	0.0000	0.1854
10	2	S	S		0.0880	0.0000	0.0574	0.0495	0.0621	0.0000	0.0708	0.0000	0.1137	0.0205	0.0000
11	2	S	PX		-0.1876	0.0000	0.3172	-0.1914	-0.0173	0.0000	-0.0466	-0.0000	0.0242	0.0424	0.0000
12	2	S	PY		0.0000	-0.4027	0.0000	0.0000	-0.0000	-0.2540	0.0000	-0.0195	0.0000	-0.0000	-0.0557
13	2	S	PZ		-0.3491	-0.0000	-0.2424	-0.2243	-0.1725	0.0000	-0.2262	-0.0000	-0.2929	-0.0228	-0.0000
14	2	S	DZ2		-0.0621	-0.0000	-0.0957	-0.0900	-0.0720	-0.0000	-0.3979	-0.0000	-0.5190	0.0247	0.0000
15	2	S	DXZ		-0.1355	0.0000	0.3735	-0.2427	-0.0069	-0.0000	-0.0385	0.0000	0.0827	0.2107	-0.0000
16	2	S	DYZ		-0.0000	-0.3249	0.0000	0.0000	-0.0000	-0.4131	0.0000	-0.0402	0.0000	-0.0000	-0.2191
17	2	S	DX-Y		0.0386	0.0000	0.0444	0.0091	-0.2017	0.0000	-0.1622	0.0000	0.1843	-0.3092	0.0000
18	2	S	DXY		0.0000	0.0732	-0.0000	-0.0000	0.0000	-0.1580	-0.0000	0.1384	-0.0000	0.0000	0.3192
19	3	S	S		0.0843	-0.0000	0.0680	-0.0489	-0.0377	0.0000	0.0969	0.0000	-0.1120	0.0079	-0.0000
20	3	S	PX		-0.3825	0.0000	-0.1927	0.2103	0.1849	0.0000	-0.2641	-0.0000	0.2549	0.0252	0.0000
21	3	S	PY		0.0000	-0.3880	0.0000	0.0000	0.0000	0.2600	0.0000	-0.0462	0.0000	-0.0000	-0.0240
22	3	S	PZ		-0.1240	0.0000	0.3272	0.0580	0.1106	0.0000	-0.0011	-0.0000	-0.0857	0.0040	-0.0000
23	3	S	DZ2		0.0997	-0.0000	-0.0330	0.0636	-0.2172	0.0000	0.1234	0.0000	-0.1823	-0.4079	0.0000
24	3	S	DXZ		-0.1119	0.0000	0.3888	0.1131	0.1943	-0.0000	0.0215	0.0000	-0.2978	-0.0554	0.0000
25	3	S	DYZ		0.0000	0.1303	-0.0000	-0.0000	0.0000	0.0627	-0.0000	0.2078	-0.0000	0.0000	0.2836
26	3	S	DX-Y		-0.0724	0.0000	-0.0309	0.1773	0.0560	-0.0000	-0.4435	-0.0000	0.3007	0.0427	0.0000
27	3	S	DXY		-0.0000	-0.3059	0.0000	0.0000	-0.0000	0.4531	0.0000	-0.1919	0.0000	-0.0000	-0.0143
28	4	C	S		0.1311	0.0930	-0.0221	0.0071	-0.0836	-0.0854	-0.0040	-0.3099	-0.0265	0.3231	0.0228
29	4	C	PX		0.0066	-0.0066	-0.0357	-0.0548	0.0469	-0.0510	0.0937	0.0716	0.0029	-0.0120	0.1646
30	4	C	PY		0.2404	0.0904	0.0353	-0.0009	-0.1208	0.0701	-0.1469	-0.0215	-0.0531	0.0367	-0.2113
31	4	C	PZ		0.1060	0.0006	-0.0301	-0.0897	0.2213	0.0889	-0.0491	0.2985	0.0158	-0.1926	-0.0480
32	5	C	S		0.1311	-0.0930	-0.0221	0.0071	-0.0836	0.0854	-0.0040	0.3099	-0.0265	0.3231	-0.0228
33	5	C	PX		0.0066	0.0066	-0.0357	-0.0548	0.0469	0.0510	0.0937	-0.0716	0.0029	-0.0120	-0.1646
34	5	C	PY		-0.2404	0.0904	-0.0353	0.0009	-0.1208	0.0701	0.1469	-0.0215	0.0531	-0.0367	-0.2113
35	5	C	PZ		0.1060	-0.0006	-0.0301	-0.0897	0.2213	-0.0889	-0.0491	-0.2985	0.0158	-0.1926	0.0480
36	6	C	S		0.0166	-0.0074	-0.0074	-0.0042	0.0338	-0.0063	0.0191	0.0602	-0.0079	-0.0479	0.0361
37	6	C	PX		-0.0001	0.0285	0.0222	0.0298	-0.0357	0.0025	-0.0280	-0.0323	0.0033	0.0219	-0.0173
38	6	C	PY		-0.0590	0.0112	0.0211	0.1022	-0.0820	0.0195	0.0344	-0.0010	-0.0085	-0.0521	0.0663
39	6	C	PZ		0.0014	0.0023	0.0056	-0.0030	0.0027	0.0230	-0.0587	0.0029	-0.0144	-0.0173	-0.0917
40	7	C	S		0.0166	0.0074	-0.0074	-0.0042	0.0338	0.0063	0.0191	-0.0602	-0.0079	-0.0479	-0.0361
41	7	C	PX		-0.0001	-0.0285	0.0222	0.0298	-0.0357	-0.0025	-0.0280	0.0323	0.0033	0.0219	0.0173
42	7	C	PY		0.0590	0.0112	-0.0211	-0.1022	0.0820	0.0195	-0.0344	-0.0010	0.0085	0.0521	0.0663
43	7	C	PZ		0.0014	-0.0023	0.0056	-0.0030	0.0027	-0.0230	-0.0587	-0.0029	-0.0144	-0.0173	0.0917
44	8	H	S		0.0782	0.0091	0.0436	-0.1560	0.0273	-0.0102	-0.1922	0.3195	0.0820	-0.2913	-0.3192
45	9	H	S		-0.0811	-0.1295	-0.0381	-0.1681	0.2698	0.0373	0.0723	0.3768	0.0231	-0.2475	0.1085
46	10	H	S		0.0782	-0.0091	0.0436	-0.1560	0.0273	0.0102	-0.1922	-0.3195	0.0820	-0.2913	0.3192
47	11	H	S		-0.0811	0.1295	-0.0381	-0.1681	0.2698	-0.0373	0.0723	-0.3768	0.0231	-0.2475	-0.1085
48	12	H	S		-0.0514	0.0030	-0.0010	0.0143	-0.0801	-0.0175	0.0429	-0.0722	0.0206	0.0540	0.0834
49	13	H	S		0.0356	0.0375	0.0357	0.0621	-0.0190	0.0554	-0.0769	-0.0274	-0.0193	-0.0189	-0.1108
50	14	H	S		0.0588	0.0533	0.0379	0.1277	-0.0426	0.0970	-0.1292	-0.0866	-0.0461	0.0036	-0.2003
51	15	H	S		-0.0514	-0.0030	-0.0010	0.0143	-0.0801	0.0175	0.0429	0.0722	0.0206	0.0540	-0.0834
52	16	H	S		0.0356	-0.0375	0.0357	0.0621	-0.0190	-0.0554	-0.0769	0.0274	-0.0193	-0.0189	0.1108
53	17	H	S		0.0588	-0.0533	0.0379	0.1277	-0.0426	-0.0970	-0.1292	0.0866	-0.0461	0.0036	0.2003

				EIGENVALUES---	0.4535	0.4568	0.4794	0.4809	0.4879	0.5169	0.5179	0.5478	0.5531	0.5681	0.5704
					34	35	36	37	38	39	40	41	42	43	44
1	1	P	S		0.0000	-0.0797	0.0000	0.0145	-0.1652	-0.0000	-0.0033	-0.0000	-0.0206	0.0561	0.0000
2	1	P	PX		-0.0000	0.0459	0.0000	0.1297	-0.2422	-0.0000	0.1590	-0.0000	-0.1124	0.1526	0.0000
3	1	P	PY		-0.0430	0.0000	-0.0393	-0.0000	0.0000	-0.4840	0.0000	0.1281	0.0000	0.0000	0.0947
4	1	P	PZ		-0.0000	0.0340	-0.0000	-0.0666	-0.2312	-0.0000	-0.1724	0.0000	0.1671	0.1480	0.0000
5	1	P	DZ2		-0.0000	-0.0058	0.0000	0.0785	0.1341	-0.0000	0.1423	-0.0000	-0.0762	0.1909	0.0000
6	1	P	DXZ		0.0000	-0.0943	-0.0000	-0.0153	0.1535	0.0000	0.0278	-0.0000	0.0086	0.0001	-0.0000
7	1	P	DYZ		-0.0427	-0.0000	-0.0093	0.0000	-0.0000	0.1565	-0.0000	0.1396	-0.0000	-0.0000	0.0614
8	1	P	DX-Y		-0.0000	-0.0732	-0.0000	-0.1280	0.2209	-0.0000	-0.1051	-0.0000	-0.0717	0.2925	0.0000
9	1	P	DXY		-0.0051	-0.0000	0.0371	0.0000	-0.0000	0.1655	-0.0000	-0.0847	-0.0000	0.0000	0.1341
10	2	S	S		0.0000	-0.0072	-0.0000	0.0103	0.0509	0.0000	-0.0086	-0.0000	-0.0175	-0.0620	-0.0000
11	2	S	PX		-0.0000	0.0103	-0.0000	0.0160	-0.0047	-0.0000	-0.0313	0.0000	0.0134	-0.0066	-0.0000
12	2	S	PY		0.0270	0.0000	0.0133	-0.0000	0.0000	0.0071	-0.0000	-0.0327	0.0000	0.0000	-0.0096
13	2	S	PZ		-0.0000	0.0178	-0.0000	-0.0212	-0.0773	-0.0000	0.0171	0.0000	0.0363	0.1032	0.0000
14	2	S	DZ2		0.0000	0.0686	0.0000	0.0883	0.4198	0.0000	0.0361	-0.0000	-0.1212	-0.2396	-0.0000
15	2	S	DXZ		-0.0000	0.0558	-0.0000	0.0763	-0.0452	0.0000	0.6366	-0.0000	-0.1020	0.0478	0.0000
16	2	S	DYZ		0.1972	0.0000	0.1612	-0.0000	0.0000	-0.2519	0.0000	0.2838	0.0000	-0.0000	0.1372
17	2	S	DX-Y		-0.0000	0.3581	0.0000	0.7687	-0.1570	0.0000	-0.1687	0.0000	0.0485	-0.1031	-0.0000
18	2	S	DXY		0.5295	0.0000	-0.7104	0.0000	0.0000	-0.1423	0.0000	0.0441	-0.0000	0.0000	-0.0601
19	3	S	S		0.0000	0.0182	-0.0000	-0.0189	0.0541	0.0000	0.0093	0.0000	0.0370	-0.0493	-0.0000
20	3	S	PX		-0.0000	-0.0192	0.0000	0.0306	-0.0812	-0.0000	-0.0164	-0.0000	-0.0655	0.0765	0.0000
21	3	S	PY		0.0154	0.0000	-0.0170	-0.0000	-0.0000	0.0126	-0.0000	0.0049	0.0000	-0.0000	-0.0213
22	3	S	PZ		-0.0000	0.0149	-0.0000	-0.0185	0.0065	0.0000	0.0379	-0.0000	-0.0132	-0.0220	-0.0000
23	3	S	DZ2		-0.0000	0.4231	-0.0000	-0.3621	-0.4514	0.0000	0.3132	-0.0000	-0.1005	-0.0478	-0.0000
24	3	S	DXZ		-0.0000	0.1005	-0.0000	-0.0700	-0.2484	-0.0000	-0.5459	0.0000	0.1180	0.0869	0.0000
25	3	S	DYZ		0.5788	0.0000	0.6598	-0.0000	0.0000	-0.1362	0.0000	-0.0043	-0.0000	0.0000	-0.0544
26	3	S	DX-Y		-0.0000	0.4123	-0.0000	-0.4380	0.1207	0.0000	-0.0747	0.0000	0.2014	-0.2677	-0.0000
27	3	S	DXY		0.2286	0.0000	-0.0970	0.0000	0.0000	-0.4105	0.0000	-0.0561	0.0000	0.0000	0.1562
28	4	C	S		-0.0645	0.2173	0.0210	0.0282	-0.0488	-0.2683	-0.0777	-0.0721	-0.0802	0.0648	-0.0006
29	4	C	PX		-0.1898	0.2023	0.0040	0.0261	0.1665	-0.1369	0.0570	0.1991	0.1232	0.0206	0.0082
30	4	C	PY		0.0390	-0.0355	-0.0217	0.0202	-0.0737	-0.0513	0.0593	0.1381	-0.1080	-0.0429	-0.0093
31	4	C	PZ		-0.1205	0.0634	-0.0100	-0.0177	0.0944	-0.1764	-0.0420	-0.1482	-0.1910	0.0035	0.0910
32	5	C	S		0.0645	0.2173	-0.0210	0.0282	-0.0488	0.2683	-0.0777	0.0721	-0.0802	0.0648	0.0006
33	5	C	PX		0.1898	0.2023	-0.0040	0.0261	0.1665	0.1369	0.0570	-0.1991	0.1232	0.0206	-0.0082
34	5	C	PY		0.0390	0.0355	-0.0217	-0.0202	0.0737	-0.0513	-0.0593	0.1381	-0.1080	-0.0429	-0.0093
35	5	C	PZ		0.1205	0.0634	0.0100	-0.0177	0.0944	0.1764	-0.0420	0.1482	-0.1910	0.0035	-0.0910
36	6	C	S		-0.0696	0.0598	0.0082	0.0022	0.0966	-0.0793	0.0374	0.1531	0.1117	0.3271	-0.2904
37	6	C	PX		0.0081	0.0181	0.0091	-0.0165	-0.0227	-0.0735	-0.0623	-0.2835	-0.3184	0.1967	-0.2981
38	6	C	PY		-0.0285	-0.0001	0.0045	0.0084	0.1131	0.0327	0.0642	0.2678	0.2514	0.1094	0.0112
39	6	C	PZ		0.0433	-0.0580	-0.0014	0.0304	-0.0682	0.0544	0.0514	0.1689	0.1804	0.1334	-0.2373
40	7	C	S		0.0696	0.0598	-0.0082	0.0022	0.0966	0.0793	0.0374	-0.1531	0.1117	0.3271	0.2904
41	7	C	PX		-0.0081	0.0181	-0.0091	-0.0165	-0.0227	0.0735	-0.0623	0.2835	-0.3184	0.1967	0.2981
42	7	C	PY		-0.0285	0.0001	0.0045	-0.0084	-0.1131	0.0327	-0.0642	0.2678	-0.2514	-0.1094	0.0112
43	7	C	PZ		-0.0433	-0.0580	0.0014	0.0304	-0.0682	-0.0544	0.0514	-0.1689	0.1804	0.1334	0.2373
44	8	H	S		0.1106	-0.2644	-0.0409	-0.0790	-0.0620	0.1112	-0.0302	-0.1524	-0.0973	-0.0130	0.0164
45	9	H	S		-0.1679	0.0937	-0.0079	-0.0000	0.1630	-0.0623	0.0422	0.0795	0.0278	-0.0005	0.0254
46	10	H	S		-0.1106	-0.2644	0.0409	-0.0790	-0.0620	-0.1112	-0.0302	0.1524	-0.0973	-0.0130	-0.0164
47	11	H	S		0.1679	0.0937	0.0079	-0.0000	0.1630	0.0623	0.0422	-0.0795	0.0278	-0.0005	-0.0254
48	12	H	S		-0.0122	0.0374	0.0098	-0.0090	0.0154	-0.0030	-0.0773	-0.2392	-0.2262	-0.2834	0.3436
49	13	H	S		0.1111	-0.1400	-0.0210	0.0172	-0.0794	0.1741	0.0710	0.2375	0.2874	-0.2633	0.3030
50	14	H	S		0.1663	-0.1985	-0.0211	0.0193	-0.1608	0.1861	0.0681	-0.0157	-0.0284	-0.0988	-0.1032
51	15	H	S		0.0122	0.0374	-0.0098	-0.0090	0.0154	0.0030	-0.0773	0.2392	-0.2262	-0.2834	-0.3436
52	16	H	S		-0.1111	-0.1400	0.0210	0.0172	-0.0794	-0.1741	0.0710	-0.2375	0.2874	-0.2633	-0.3030
53	17	H	S		-0.1663	-0.1985	0.0211	0.0193	-0.1608	-0.1861	0.0681	0.0157	-0.0284	-0.0988	0.1032

				EIGENVALUES---	0.5742	0.5787	0.5892	0.5933	0.6095	0.6142	0.6168	0.6547	0.6566
					45	46	47	48	49	50	51	52	53
1	1	P	S		-0.0347	0.0000	-0.0000	-0.0065	-0.0010	0.0000	0.0025	0.0000	0.0293
2	1	P	PX		-0.2451	0.0000	0.0000	0.1347	-0.0484	0.0000	0.1189	-0.0000	-0.0353
3	1	P	PY		0.0000	0.0428	0.0568	0.0000	0.0000	0.0548	-0.0000	-0.0333	0.0000
4	1	P	PZ		-0.1026	0.0000	0.0000	-0.2711	-0.0894	0.0000	0.0391	-0.0000	-0.0409
5	1	P	DZ2		-0.1671	0.0000	0.0000	-0.4703	0.0607	0.0000	-0.2238	0.0000	0.1406
6	1	P	DXZ		0.0212	-0.0000	0.0000	-0.0492	-0.5745	0.0000	0.2441	0.0000	0.2306
7	1	P	DYZ		-0.0000	0.3732	0.3852	-0.0000	-0.0000	-0.2888	0.0000	0.2238	-0.0000
8	1	P	DX-Y		-0.3653	0.0000	0.0000	0.0812	0.1695	0.0000	0.3100	0.0000	0.0468
9	1	P	DXY		0.0000	-0.3144	0.5238	-0.0000	0.0000	0.2503	-0.0000	0.0537	-0.0000
10	2	S	S		0.0489	-0.0000	-0.0000	0.1437	-0.0011	-0.0000	0.0414	-0.0000	-0.0136
11	2	S	PX		0.0084	0.0000	-0.0000	-0.0066	0.0963	-0.0000	-0.0413	-0.0000	-0.0365
12	2	S	PY		0.0000	-0.0644	-0.0572	0.0000	0.0000	0.0435	-0.0000	-0.0406	0.0000
13	2	S	PZ		-0.0738	0.0000	0.0000	-0.2340	-0.0024	0.0000	-0.0662	0.0000	0.0221
14	2	S	DZ2		0.1312	-0.0000	-0.0000	0.4683	0.0218	-0.0000	0.1070	-0.0000	-0.0506
15	2	S	DXZ		-0.0746	-0.0000	0.0000	-0.0128	-0.4493	0.0000	0.1733	0.0000	0.1215
16	2	S	DYZ		-0.0000	0.4417	0.3745	0.0000	0.0000	-0.2075	0.0000	0.1264	-0.0000
17	2	S	DX-Y		0.1155	-0.0000	-0.0000	-0.0358	-0.0918	-0.0000	-0.0617	-0.0000	-0.0166
18	2	S	DXY		-0.0000	0.1059	-0.1394	-0.0000	-0.0000	-0.0593	0.0000	-0.0023	0.0000
19	3	S	S		0.0871	-0.0000	-0.0000	-0.0959	-0.0528	-0.0000	-0.0638	0.0000	0.0213
20	3	S	PX		-0.1377	0.0000	-0.0000	0.1571	0.0952	0.0000	0.0910	-0.0000	-0.0372
21	3	S	PY		-0.0000	0.0559	-0.0788	0.0000	-0.0000	-0.0590	0.0000	0.0023	-0.0000
22	3	S	PZ		0.0263	-0.0000	-0.0000	-0.0275	0.0729	-0.0000	-0.0812	-0.0000	-0.0146
23	3	S	DZ2		-0.0442	-0.0000	-0.0000	0.2364	0.1420	0.0000	0.0210	-0.0000	-0.0636
24	3	S	DXZ		-0.1090	0.0000	0.0000	0.1479	-0.3394	0.0000	0.3338	0.0000	0.0511
25	3	S	DYZ		0.0000	-0.0192	-0.2023	-0.0000	-0.0000	0.0245	-0.0000	-0.0428	0.0000
26	3	S	DX-Y		0.2847	-0.0000	-0.0000	-0.2013	-0.2081	-0.0000	-0.1161	0.0000	0.0452
27	3	S	DXY		0.0000	-0.3845	0.4097	-0.0000	0.0000	0.2703	-0.0000	-0.0145	0.0000
28	4	C	S		-0.1098	-0.0452	-0.1754	0.0466	0.0793	-0.0421	-0.0881	0.1910	0.2015
29	4	C	PX		-0.0407	0.1496	-0.0561	-0.1554	0.1710	0.3390	0.3439	-0.0964	-0.0340
30	4	C	PY		-0.0532	0.0084	-0.0701	-0.0412	-0.0088	-0.0294	0.0087	-0.3107	-0.2908
31	4	C	PZ		-0.1464	0.0498	-0.0864	-0.0426	0.0028	-0.0685	-0.0654	0.1824	0.2070
32	5	C	S		-0.1098	0.0452	0.1754	0.0466	0.0793	0.0421	-0.0881	-0.1910	0.2015
33	5	C	PX		-0.0407	-0.1496	0.0561	-0.1554	0.1710	-0.3390	0.3439	0.0964	-0.0340
34	5	C	PY		0.0532	0.0084	-0.0701	0.0412	0.0088	-0.0294	-0.0087	-0.3107	0.2908
35	5	C	PZ		-0.1464	-0.0498	0.0864	-0.0426	0.0028	0.0685	-0.0654	-0.1824	0.2070
36	6	C	S		0.0992	-0.1250	0.0902	0.0952	-0.0684	-0.1561	-0.0874	-0.1447	-0.1567
37	6	C	PX		0.2481	0.1350	0.1407	-0.0551	-0.0245	0.0028	0.0427	-0.0929	-0.0957
38	6	C	PY		-0.1166	-0.1657	0.0410	0.0847	-0.1082	-0.2000	-0.1112	-0.2452	-0.2525
39	6	C	PZ		0.1939	-0.0739	-0.0258	0.0999	0.1287	0.1316	0.0363	0.3629	0.3504
40	7	C	S		0.0992	0.1250	-0.0902	0.0952	-0.0684	0.1561	-0.0874	0.1447	-0.1567
41	7	C	PX		0.2481	-0.1350	-0.1407	-0.0551	-0.0245	-0.0028	0.0427	0.0929	-0.0957
42	7	C	PY		0.1166	-0.1657	0.0410	-0.0847	0.1082	-0.2000	0.1112	-0.2452	0.2526
43	7	C	PZ		0.1939	0.0739	0.0258	0.0999	0.1287	-0.1316	0.0363	-0.3629	0.3504
44	8	H	S		0.0057	-0.0908	0.0351	0.0502	-0.1048	-0.1293	-0.1301	0.0177	0.0196
45	9	H	S		-0.0317	0.0920	-0.0145	-0.0936	0.0637	0.1412	0.1480	-0.0239	0.0063
46	10	H	S		0.0057	0.0908	-0.0351	0.0502	-0.1048	0.1293	-0.1301	-0.0177	0.0195
47	11	H	S		-0.0317	-0.0920	0.0145	-0.0936	0.0637	-0.1412	0.1480	0.0239	0.0063
48	12	H	S		-0.2045	0.1270	-0.0188	-0.1174	-0.0675	-0.0300	0.0161	-0.1919	-0.1787
49	13	H	S		-0.1876	-0.0831	-0.1258	0.0257	0.0522	0.0580	-0.0071	0.1236	0.1248
50	14	H	S		0.2480	0.2561	0.0440	-0.1723	0.1198	0.3432	0.3129	-0.1145	-0.0888
51	15	H	S		-0.2045	-0.1270	0.0188	-0.1174	-0.0675	0.0300	0.0161	0.1919	-0.1787
52	16	H	S		-0.1876	0.0831	0.1258	0.0257	0.0522	-0.0580	-0.0071	-0.1236	0.1248
53	17	H	S		0.2480	-0.2561	-0.0440	-0.1723	0.1198	-0.3432	0.3129	0.1145	-0.0888

EIGENVALUES AND EIGENVECTORS $Ni[S_2P(OC_2H_5)_2]_2$

					1a₁	1b₂	2a₁	2b₂	3a₁	3b₂	4a₁	4b₂	5a₁	1b₁	6a₁
EIGENVALUES---					-1.4351	-1.4221	-1.0370	-1.1871	-0.8851	-0.8733	-0.8445	-0.7395	-0.7795	-0.6861	-0.6642
					1	2	3	4	5	6	7	8	9	10	11
1	1	P	S		0.2131	0.0000	0.2424	0.0000	0.0171	0.0005	-0.4470	0.0001	-0.1756	-0.0380	-0.0620
2	1	P	PX		-0.0099	-0.0000	-0.0832	-0.0000	0.0766	0.0002	-0.1789	-0.0008	-0.0185	0.2934	0.0139
3	1	P	PY		-0.0000	0.1743	0.0000	-0.1840	0.0001	-0.0215	0.0002	-0.0847	-0.0009	-0.0001	-0.0010
4	1	P	PZ		-0.0389	-0.0000	-0.0501	-0.0000	0.1726	-0.0000	-0.0887	0.0003	-0.0834	-0.1479	0.2622
5	1	P	DZ2		-0.0557	-0.0000	-0.0394	-0.0000	0.0019	0.0000	-0.0523	0.0000	-0.0389	-0.0876	0.1046
6	1	P	DXZ		0.0282	0.0000	0.0424	0.0000	-0.0644	0.0000	0.0119	0.0001	-0.0052	-0.0611	-0.0166
7	1	P	DYZ		0.0000	-0.0511	-0.0000	0.0795	0.0001	0.1302	0.0002	0.0149	0.0000	0.0000	0.0002
8	1	P	DX-Y		-0.0812	-0.0000	-0.0496	0.0000	-0.0123	0.0000	-0.0628	0.0003	-0.1058	0.0722	-0.0364
9	1	P	DXY		0.0000	-0.0887	-0.0000	0.1124	0.0001	0.0425	0.0001	-0.0473	-0.0000	-0.0004	0.0000
10	2	S	S		0.0534	0.0000	0.0552	0.0000	0.1962	0.0003	-0.4083	0.0005	-0.2489	-0.3741	0.5156
11	2	S	PX		-0.0080	-0.0000	-0.0060	-0.0000	-0.0034	0.0001	-0.0550	-0.0002	-0.0082	0.0712	0.0033
12	2	S	PY		-0.0000	0.0393	0.0000	-0.0193	0.0001	0.0660	0.0002	-0.0274	-0.0004	-0.0000	-0.0003
13	2	S	PZ		-0.0375	-0.0000	-0.0408	-0.0000	-0.0524	-0.0001	0.1400	-0.0001	0.0646	0.0310	-0.0252
14	2	S	DZ2		0.0150	0.0000	0.0224	0.0000	0.0088	0.0001	-0.0665	0.0000	-0.0320	-0.0181	0.0202
15	2	S	DXZ		0.0075	0.0000	0.0069	0.0000	-0.0004	-0.0000	0.0373	0.0001	0.0062	-0.0537	0.0012
16	2	S	DYZ		0.0000	-0.0247	-0.0000	0.0193	-0.0000	-0.0333	-0.0001	0.0173	0.0002	0.0000	0.0002
17	2	S	DX-Y		-0.0105	-0.0000	-0.0029	0.0000	-0.0152	0.0000	-0.0085	0.0000	-0.0154	0.0133	0.0027
18	2	S	DXY		0.0000	-0.0076	0.0000	0.0076	0.0000	-0.0049	0.0000	-0.0086	-0.0000	-0.0001	-0.0000
19	3	S	S		0.0377	0.0000	0.0496	-0.0000	0.0569	0.0005	-0.4628	-0.0007	-0.1810	0.6115	-0.2232
20	3	S	PX		-0.0089	-0.0000	-0.0078	-0.0000	-0.0094	-0.0002	0.1430	0.0002	0.0391	-0.0517	0.0281
21	3	S	PY		-0.0000	0.0178	0.0000	-0.0137	0.0000	0.0036	0.0001	-0.0453	-0.0003	-0.0002	-0.0003
22	3	S	PZ		0.0044	0.0000	0.0045	-0.0000	0.0328	0.0001	-0.0719	0.0000	-0.0410	-0.0126	0.0563
23	3	S	DZ2		-0.0133	-0.0000	-0.0131	0.0000	0.0056	-0.0000	0.0141	0.0001	-0.0079	-0.0226	0.0293
24	3	S	DXZ		-0.0041	-0.0000	-0.0039	0.0000	-0.0237	-0.0000	0.0480	-0.0000	0.0263	0.0065	-0.0314
25	3	S	DYZ		-0.0000	0.0105	0.0000	0.0021	0.0000	0.0113	0.0000	-0.0063	-0.0001	-0.0000	-0.0000
26	3	S	DX-Y		0.0109	0.0000	0.0180	0.0000	-0.0025	0.0001	-0.0566	-0.0000	-0.0226	0.0215	-0.0162
27	3	S	DXY		0.0000	-0.0180	-0.0000	0.0164	-0.0000	0.0020	-0.0001	0.0288	0.0002	0.0001	0.0002
28	4	O	S		0.3599	-0.3809	0.3842	0.4172	-0.2497	0.2412	0.0684	-0.0195	0.0112	-0.0454	-0.0512
29	4	O	PX		0.0115	-0.0066	0.0124	0.0092	0.0220	0.0087	-0.1267	0.1605	0.1290	0.0555	-0.0239
30	4	O	PY		-0.0521	0.0689	0.0529	0.0157	-0.0870	0.0591	-0.1152	0.0110	-0.0731	-0.1747	-0.2333
31	4	O	PZ		0.0392	-0.0353	0.0272	0.0293	0.1489	-0.1382	-0.0163	0.0034	-0.0229	-0.0845	0.0008
32	5	O	S		0.3598	0.3809	0.3844	-0.4170	-0.2500	-0.2411	0.0678	0.0198	0.0111	-0.0449	-0.0515
33	5	O	PX		0.0115	0.0066	0.0125	-0.0093	0.0223	-0.0081	-0.1262	-0.1625	0.1271	0.0540	-0.0260
34	5	O	PY		0.0521	0.0689	-0.0529	0.0157	0.0871	0.0588	0.1151	0.0098	0.0742	0.1740	0.2350
35	5	O	PZ		0.0392	0.0353	0.0272	-0.0293	0.1491	0.1380	-0.0157	-0.0024	-0.0238	-0.0842	0.0009
36	6	C	S		0.3684	-0.3776	-0.0834	-0.0458	0.2889	-0.3046	0.1203	-0.0072	0.0391	0.0775	0.0176
37	6	C	PX		0.0077	-0.0037	0.0106	0.0059	0.0222	0.0011	-0.1598	0.3427	0.3042	-0.0158	0.0029
38	6	C	PY		0.0404	-0.0286	0.2396	0.2522	0.0059	0.0111	0.0358	-0.0058	0.0092	-0.0223	0.0792
39	6	C	PZ		-0.0658	0.0700	0.0106	-0.0014	0.2277	-0.2455	-0.0297	0.0113	-0.0429	-0.1649	-0.2366
40	7	C	S		0.3684	0.3776	-0.0835	0.0458	0.2893	0.3039	0.1211	0.0074	0.0392	0.0772	0.0184
41	7	C	PX		0.0076	0.0036	0.0109	-0.0062	0.0230	0.0001	-0.1584	-0.3465	0.3005	-0.0181	0.0002
42	7	C	PY		-0.0404	-0.0286	-0.2397	0.2521	-0.0058	0.0112	-0.0360	-0.0064	-0.0086	0.0221	-0.0789
43	7	C	PZ		-0.0658	-0.0700	0.0106	0.0014	0.2280	0.2453	-0.0285	-0.0088	-0.0452	-0.1639	-0.2385
44	8	H	S		0.1554	-0.1556	-0.0309	-0.0211	0.2503	-0.2525	-0.0493	0.1586	0.1732	-0.0365	-0.0814
45	9	H	S		0.1488	-0.1536	-0.0430	-0.0271	0.2270	-0.2557	0.1410	-0.1993	-0.1758	-0.0168	-0.0941
46	10	H	S		0.1554	0.1556	-0.0307	0.0209	0.2510	0.2527	-0.0477	-0.1997	0.1701	-0.0377	-0.0836
47	11	H	S		0.1488	0.1536	-0.0432	0.0272	0.2269	0.2546	0.1411	0.2027	-0.1744	-0.0150	-0.0927
48	12	C	S		0.2598	-0.2804	-0.3697	-0.3604	-0.1949	0.2003	-0.0753	0.0043	-0.0184	-0.0202	0.0363
49	12	C	PX		0.0019	-0.0009	0.0039	0.0025	0.0151	0.0007	-0.1277	0.3734	0.3555	-0.0588	0.0026
50	12	C	PY		0.0774	-0.0795	0.0168	0.0334	0.0958	-0.1009	0.1018	-0.0115	0.0578	0.2302	0.2283
51	12	C	PZ		0.0497	-0.0530	-0.0580	-0.0550	0.1343	-0.1513	0.0221	0.0026	-0.0019	-0.0464	-0.1952
52	13	C	S		0.2597	0.2805	-0.3698	0.3603	-0.1951	-0.1999	-0.0763	-0.0062	-0.0169	-0.0205	0.0363
53	13	C	PX		0.0017	0.0006	0.0047	-0.0033	0.0164	0.0009	-0.1258	-0.3775	0.3517	-0.0598	0.0023
54	13	C	PY		-0.0774	-0.0795	-0.0188	0.0334	-0.0960	-0.1006	-0.1015	-0.0093	-0.0602	-0.2287	-0.2310
55	13	C	PZ		0.0497	0.0530	-0.0580	0.0550	0.1344	0.1511	0.0228	-0.0038	-0.0035	-0.0457	-0.1960
56	14	H	S		0.1625	-0.1123	-0.2043	-0.2065	-0.1006	0.0998	-0.0380	0.0102	-0.0451	-0.1830	-0.2267
57	15	H	S		0.1157	-0.1244	-0.1655	-0.1628	-0.1270	0.1449	-0.1279	0.2503	0.2292	-0.0348	0.0877
58	16	H	S		0.1141	-0.1239	-0.1709	-0.1666	-0.1472	0.1451	0.0376	-0.2496	-0.2496	0.0491	0.0855
59	17	H	S		0.1625	0.1123	-0.2044	0.2064	-0.1008	-0.0995	-0.0873	-0.0069	-0.0485	-0.1814	-0.2290
60	18	H	S		0.1156	0.1243	-0.1651	0.1623	-0.1263	-0.1436	-0.1275	-0.2547	0.2280	-0.0360	0.0876
61	19	H	S		0.1142	0.1241	-0.1713	0.1669	-0.1482	-0.1458	0.0356	0.2507	-0.2456	0.0425	0.0862

					$5b_2$	$7a_1$	$6b_2$	$8a_1$	$7b_2$	$9a_1$	$8b_2$	$2b_1$	$10a_1$	$9b_2$	$3b_1$
C	EIGENVALUES---				-0.6580	-0.5594	-0.5567	-0.5501	-0.5498	-0.4923	-0.4299	-0.4134	-0.4018	-0.3855	-0.3710
					12	13	14	15	16	17	18	19	20	21	22
	1	1	P	S	0.0003	0.0536	0.0303	0.0422	0.0080	0.2600	-0.0005	-0.2764	0.0987	-0.0002	0.0968
	2	1	P	PX	0.0003	0.0171	-0.0010	0.0267	0.0042	-0.1540	-0.0005	-0.0788	-0.1059	-0.0001	0.2967
	3	1	P	PY	-0.1547	-0.0044	-0.1798	-0.0024	0.0206	0.0008	-0.1534	0.0007	0.0002	-0.1821	-0.0004
	4	1	P	PZ	-0.0009	-0.0057	-0.0012	-0.1002	-0.0171	-0.1021	0.0003	-0.0138	0.2155	-0.0001	0.1492
	5	1	P	DZZ	-0.0004	-0.0791	0.0023	0.1364	0.0222	-0.0063	-0.0002	0.0067	-0.1215	0.0000	0.0228
	6	1	P	DXZ	0.0000	-0.0752	0.0021	0.0698	0.0112	0.0262	0.0004	0.1394	0.0655	0.0001	0.2377
	7	1	P	DYZ	0.0232	-0.0013	-0.0194	-0.0288	0.1749	-0.0004	0.1663	-0.0005	-0.0002	0.0804	-0.0001
	8	1	P	DX-Y	0.0011	-0.1802	0.0032	-0.0487	-0.0092	0.0401	0.0006	0.1039	0.1117	0.0001	0.0738
	9	1	P	DXY	0.0562	-0.0006	-0.0789	0.0138	-0.0784	0.0004	0.0828	0.0000	-0.0002	-0.1842	0.0003
	10	2	S	S	-0.0018	-0.1714	0.0034	0.1606	0.0252	-0.1770	0.0001	0.1476	-0.1882	0.0001	-0.2361
	11	2	S	PX	0.0001	-0.0321	0.0007	0.0464	0.0074	-0.0561	0.0001	0.0461	0.0323	-0.0000	0.4048
	12	2	S	PY	-0.0542	-0.0027	-0.1306	-0.0166	0.1033	0.0002	0.0325	-0.0000	-0.0000	-0.0176	-0.0002
	13	2	S	PZ	0.0000	-0.0369	0.0007	0.0371	0.0058	-0.0930	0.0001	0.1705	-0.2062	0.0002	-0.2676
	14	2	S	DZZ	-0.0000	0.0064	-0.0001	-0.0022	-0.0003	0.0322	-0.0001	-0.0638	0.0543	-0.0001	0.0509
	15	2	S	DXZ	-0.0001	0.0175	-0.0003	-0.0223	-0.0035	0.0296	-0.0000	-0.0169	-0.0024	0.0000	-0.1475
	16	2	S	DYZ	0.0309	0.0014	0.0541	0.0083	-0.0518	-0.0001	-0.0113	-0.0000	0.0000	0.0162	0.0001
	17	2	S	DX-Y	0.0001	-0.0258	0.0004	-0.0031	-0.0007	0.0010	0.0000	-0.0040	0.0173	-0.0000	0.0059
	18	2	S	DXY	0.0102	-0.0001	-0.0105	0.0027	-0.0154	0.0001	0.0077	0.0000	-0.0000	-0.0136	0.0000
	19	3	S	S	0.0027	-0.1303	0.0004	-0.1906	-0.0329	-0.1543	0.0007	0.2375	-0.0020	0.0002	-0.2707
	20	3	S	PX	-0.0001	-0.0427	0.0002	-0.0582	-0.0102	-0.0928	0.0007	0.2393	0.0443	0.0002	-0.2383
	21	3	S	PY	-0.0116	-0.0018	-0.1138	0.0083	-0.0454	0.0006	-0.0397	0.0004	-0.0000	-0.2368	0.0000
	22	3	S	PZ	-0.0001	-0.0309	0.0003	-0.0138	-0.0026	-0.0266	0.0003	0.0158	0.1863	-0.0001	0.4207
	23	3	S	DZZ	-0.0000	-0.0238	0.0004	-0.0038	-0.0009	-0.0225	0.0002	0.0455	0.0266	0.0000	0.0314
	24	3	S	DXZ	0.0000	0.0116	-0.0001	0.0122	0.0021	0.0098	-0.0001	0.0006	-0.0729	0.0000	-0.1352
	25	3	S	DYZ	-0.0015	-0.0004	-0.0180	-0.0014	0.0094	0.0000	0.0113	-0.0000	-0.0000	-0.0134	-0.0000
	26	3	S	DX-Y	0.0001	0.0031	0.0002	0.0174	0.0030	0.0311	-0.0002	-0.0592	-0.0183	-0.0000	0.0365
	27	3	S	DXY	0.0112	0.0010	0.0513	-0.0048	0.0264	-0.0003	0.0254	-0.0002	-0.0000	0.0994	-0.0000
	28	4	O	S	0.0654	-0.0819	-0.0980	0.0401	0.1030	-0.0828	0.0301	0.0808	-0.0241	-0.0718	0.0186
	29	4	O	PX	0.0224	0.3119	0.2990	0.1635	0.1986	0.0118	0.1260	-0.2943	-0.3137	0.4608	-0.0639
	30	4	O	PY	0.2381	-0.0710	-0.0095	0.0775	0.0708	0.3630	0.4286	0.0846	0.0559	-0.1568	-0.0840
	31	4	O	PZ	0.1035	0.2137	0.1278	-0.2505	-0.3701	0.0948	-0.0604	-0.1560	0.2942	0.0102	-0.1994
	32	5	O	S	-0.0850	-0.0778	0.0915	0.0700	-0.0859	-0.0830	-0.0298	0.0806	-0.0241	0.0719	0.0188
	33	5	O	PX	-0.0250	0.3027	-0.3079	0.2222	-0.1302	0.0148	-0.1292	-0.2923	-0.3136	-0.4612	-0.0639
	34	5	O	PY	0.2366	0.0721	-0.0173	-0.0944	0.0412	-0.3637	0.4276	-0.0862	-0.0570	-0.1573	0.0848
	35	5	O	PZ	-0.1038	0.2041	-0.1392	-0.3558	0.2722	0.0945	0.0606	-0.1561	0.2942	-0.0105	-0.2012
	36	6	C	S	-0.1084	-0.0185	-0.0108	0.0155	0.0238	-0.0065	-0.0522	-0.0146	0.0187	0.0151	-0.0053
	37	6	C	PX	-0.0006	0.2009	0.2271	0.1224	0.1275	-0.0336	-0.0898	0.1961	0.1389	-0.2189	-0.0085
	38	6	C	PY	0.0416	0.1876	0.0910	-0.2301	-0.3200	-0.1762	-0.2307	-0.0003	-0.0527	0.0854	0.0400
	39	6	C	PZ	0.2827	0.0469	0.0202	-0.0608	-0.0857	0.0989	0.1981	0.1867	-0.1951	-0.0720	0.0945
	40	7	C	S	0.1084	-0.0170	0.0113	0.0227	-0.0178	-0.0066	0.0522	-0.0148	0.0185	-0.0151	-0.0053
	41	7	C	PX	-0.0035	0.1938	-0.2323	0.1598	-0.0782	-0.0328	0.0909	0.1952	0.1387	0.2193	-0.0084
	42	7	C	PY	0.0424	-0.1808	0.1032	0.3201	-0.2300	0.1768	-0.2304	0.0012	0.0533	0.0855	-0.0404
	43	7	C	PZ	-0.2814	0.0432	-0.0206	-0.0865	0.0628	0.0991	-0.1976	0.1873	-0.1947	0.0724	0.0954
	44	8	H	S	0.0596	0.1525	0.1762	0.0745	0.0639	0.0205	-0.0031	0.2841	0.0288	-0.2435	0.0628
	45	9	H	S	0.0599	-0.1397	-0.1655	-0.1099	-0.1216	0.0810	0.1688	-0.0854	-0.2557	0.1949	0.0616
	46	10	H	S	-0.0616	0.1462	-0.1797	0.0929	-0.0339	0.0212	0.0044	0.2836	0.0288	0.2442	0.0635
	47	11	H	S	-0.0566	-0.1353	0.1696	-0.1457	0.0778	0.0804	-0.1696	-0.0843	-0.2553	-0.1950	0.0621
	48	12	C	S	0.0024	0.0248	0.0273	-0.0255	-0.0586	0.0488	0.0357	-0.0023	0.0171	-0.0113	-0.0165
	49	12	C	PX	-0.0306	-0.2442	-0.2585	-0.1355	-0.1452	0.0244	0.0411	-0.0789	-0.0534	0.0749	0.0044
	50	12	C	PY	-0.4105	-0.1142	0.0344	0.1504	0.1294	0.2448	0.1631	-0.0423	0.1379	-0.0497	-0.0744
	51	12	C	PZ	0.1292	-0.1669	-0.1638	0.1884	0.3772	-0.1896	-0.1571	-0.1769	0.1956	0.0340	-0.0951
	52	13	C	S	-0.0026	0.0224	-0.0277	-0.0433	0.0479	0.0488	-0.0356	-0.0023	0.0171	0.0112	-0.0166
	53	13	C	PX	0.0297	-0.2356	0.2758	-0.1783	0.0895	0.0214	-0.0402	-0.0791	-0.0531	-0.0754	0.0043
	54	13	C	PY	-0.4096	0.1108	-0.0118	-0.1656	0.0748	-0.2452	0.1625	0.0412	-0.1086	-0.0501	0.0751
	55	13	C	PZ	-0.1286	-0.1554	0.1726	0.2985	-0.2987	-0.1896	0.1564	-0.1778	0.1959	-0.0348	-0.0960
	56	14	H	S	0.3396	0.0057	-0.0805	-0.0213	0.0833	-0.2910	-0.2365	-0.0921	0.0552	0.0681	-0.0125
	57	15	H	S	-0.0693	-0.1253	-0.1413	-0.1902	-0.2869	0.1360	0.1408	-0.0031	-0.1282	0.0539	0.0341
	58	16	H	S	-0.0248	0.2723	0.2972	0.0314	-0.0512	0.0945	0.0615	0.1586	-0.0179	-0.1092	0.0267
	59	17	H	S	-0.3387	0.0094	0.0784	0.0058	-0.0867	-0.2914	0.2358	-0.0931	0.0546	-0.0685	-0.0126
	60	18	H	S	0.0679	-0.1236	0.1442	-0.2748	0.2079	0.1331	-0.1395	-0.0029	-0.1276	-0.0542	0.0342
	61	19	H	S	0.0252	0.2599	-0.3063	0.0162	0.0635	0.0975	-0.0622	0.1592	-0.0190	0.1100	0.0271

					$10b_2$	$4b_1$	$11b_2$	$11a_1$	$12b_2$	$12a_1$					
EIGENVALUES---					-0.3766	-0.2848	-0.2590	-0.2531	-0.1870	-0.1421	0.2623	0.2975	0.3078	0.3473	0.3722
					23	24	25	26	27	28	29	30	31	32	33
1	1	P	S		0.0002	0.2061	-0.0000	0.0155	0.0000	0.0066	0.5095	-0.0000	0.3081	0.1194	-0.0004
2	1	P	PX		0.0006	0.3189	0.0000	0.2569	-0.0000	-0.0127	-0.2500	0.0000	0.2274	-0.1256	-0.0034
3	1	P	PY		0.2065	-0.0000	-0.2491	0.0000	-0.0055	-0.0000	0.0000	0.5012	-0.0000	0.0000	0.0395
4	1	P	PZ		0.0003	0.0607	-0.0000	-0.3425	-0.0000	0.0008	-0.2496	0.0000	0.1623	0.4371	0.0017
5	1	P	DZ2		0.0001	0.1799	-0.0000	-0.1817	0.0000	0.1627	0.1228	-0.0000	-0.1145	-0.3263	-0.0012
6	1	P	DXZ		0.0004	-0.3135	0.0000	-0.0655	0.0000	0.0475	-0.0996	0.0000	0.3529	-0.2682	0.0010
7	1	P	DYZ		0.0734	-0.0000	-0.2063	0.0000	-0.1983	0.0000	0.0000	0.2260	0.0000	0.0000	-0.3928
8	1	P	DX-Y		0.0001	0.1323	0.0000	0.1339	-0.0000	-0.0872	0.0733	0.0000	-0.0617	-0.0208	0.0024
9	1	P	DXY		-0.1665	-0.0000	-0.2296	0.0000	0.1505	0.0000	0.0000	0.2783	0.0000	-0.0000	0.2568
10	2	S	S		-0.0005	-0.1391	0.0000	0.1725	-0.0000	0.0040	-0.0740	0.0000	-0.0986	-0.0914	-0.0003
11	2	S	PX		0.0008	-0.4306	0.0000	0.1113	0.0000	0.6611	0.2249	-0.0000	-0.2665	0.2002	0.0004
12	2	S	PY		0.1685	-0.0000	-0.5765	0.0000	-0.6402	0.0000	-0.0000	-0.3731	0.0000	-0.0000	0.1935
13	2	S	PZ		-0.0005	-0.2914	0.0000	0.4974	-0.0000	-0.1783	0.2768	-0.0000	0.3156	0.3176	0.0010
14	2	S	DZ2		0.0001	0.0699	-0.0000	-0.0886	0.0000	0.0242	0.0643	-0.0000	0.1385	0.1778	0.0005
15	2	S	DXZ		-0.0003	0.1137	-0.0000	-0.0520	-0.0000	-0.0124	0.1766	-0.0000	-0.3723	0.3031	0.0008
16	2	S	DYZ		-0.0576	0.0000	0.1518	-0.0000	0.0971	-0.0000	-0.0000	-0.3783	0.0000	-0.0000	0.3571
17	2	S	DX-Y		0.0000	0.0008	0.0000	0.0076	-0.0000	-0.0459	0.0028	0.0000	-0.0158	-0.0087	0.0014
18	2	S	DXY		-0.0122	-0.0000	-0.0396	0.0000	0.0229	-0.0000	0.0000	0.0920	-0.0000	-0.0000	0.1169
19	3	S	S		-0.0006	-0.0974	-0.0000	-0.1824	0.0000	-0.0047	-0.0772	0.0000	-0.1018	0.0120	0.0008
20	3	S	PX		-0.0005	-0.2934	-0.0000	-0.5470	0.0000	0.0313	0.3572	-0.0000	0.2615	-0.0652	-0.0027
21	3	S	PY		-0.0301	-0.0000	-0.5523	0.0000	0.6326	-0.0000	-0.0000	-0.3751	0.0000	0.0000	-0.2014
22	3	S	PZ		0.0008	-0.3503	0.0000	-0.0550	-0.0000	-0.6848	0.1913	-0.0000	-0.3226	-0.0371	-0.0007
23	3	S	DZ2		0.0001	-0.0540	-0.0000	-0.0712	0.0000	0.0444	-0.0676	0.0000	0.0666	-0.0940	0.0019
24	3	S	DXZ		-0.0003	0.0731	0.0000	0.0241	0.0000	0.0315	0.1687	-0.0000	-0.3816	-0.1058	-0.0015
25	3	S	DYZ		0.0046	-0.0000	-0.0721	0.0000	-0.0008	-0.0000	0.0000	0.1750	-0.0000	0.0000	-0.0568
26	3	S	DX-Y		0.0001	0.0727	0.0000	0.0886	-0.0000	0.0082	0.0946	-0.0000	0.0323	-0.1081	-0.0019
27	3	S	DXY		0.0056	0.0000	0.1328	-0.0000	-0.0984	0.0000	-0.0000	-0.3461	0.0000	0.0000	-0.3916
28	4	O	S		0.0510	-0.0247	0.0163	-0.0224	0.0171	-0.0141	-0.1924	0.0273	-0.0478	0.0993	0.0727
29	4	O	PX		0.0107	-0.2212	-0.2290	-0.1715	0.1659	-0.0612	-0.0739	0.0967	-0.0365	0.0276	0.0916
30	4	O	PY		-0.1970	-0.1459	0.0140	0.0140	-0.0331	0.0117	-0.1024	0.0282	-0.0267	-0.1283	-0.1040
31	4	O	PZ		-0.4557	-0.2102	-0.1398	0.1400	-0.1448	0.0654	-0.1254	0.0738	-0.0385	-0.0485	-0.0259
32	5	O	S		-0.0509	-0.0247	-0.0163	-0.0224	-0.0171	-0.0141	-0.1924	-0.0273	-0.0478	0.0993	-0.0738
33	5	O	PX		-0.0109	-0.2212	0.2289	-0.1716	-0.1659	-0.0612	-0.0739	-0.0967	-0.0365	0.0276	-0.0896
34	5	O	PY		-0.1967	0.1459	0.0140	-0.0140	-0.0331	-0.0117	0.1024	0.0282	0.0267	0.1283	-0.1048
35	5	O	PZ		0.4549	-0.2102	0.1398	0.1399	0.1448	0.0654	-0.1254	-0.0738	-0.0385	-0.0499	0.0241
36	6	C	S		-0.0036	0.0023	-0.0496	0.0196	-0.0267	0.0116	0.0872	0.0368	0.0051	-0.1498	-0.0795
37	6	C	PX		0.0180	0.0544	-0.0252	0.0249	-0.0197	-0.0031	-0.0027	0.0207	-0.0062	0.0135	0.0200
38	6	C	PY		0.1040	0.0285	-0.0646	0.0323	-0.0312	0.0190	0.0950	0.0222	0.0036	-0.1418	-0.0537
39	6	C	PZ		0.2299	0.0276	-0.0032	-0.0263	0.0034	-0.0149	-0.0821	-0.0094	-0.0139	0.1231	0.1009
40	7	C	S		0.0036	0.0023	0.0496	0.0196	0.0267	0.0116	0.0872	-0.0368	0.0051	-0.1499	0.0807
41	7	C	PX		-0.0181	0.0544	0.0252	0.0248	0.0197	-0.0031	-0.0027	-0.0207	-0.0062	0.0135	-0.0196
42	7	C	PY		0.1038	-0.0285	-0.0646	-0.0323	-0.0312	-0.0190	-0.0950	0.0222	-0.0036	0.1418	-0.0544
43	7	C	PZ		-0.2295	0.0276	0.0032	-0.0263	-0.0034	-0.0149	-0.0821	0.0094	-0.0139	0.1231	-0.1027
44	8	H	S		0.1601	0.0914	-0.0044	0.0289	-0.0360	0.0009	0.0211	0.0035	0.0021	-0.0108	-0.0546
45	9	H	S		0.1375	-0.0395	-0.0195	-0.0484	0.0276	-0.0149	-0.0163	-0.0014	0.0069	0.0277	-0.0112
46	10	H	S		-0.1599	0.0914	0.0044	0.0289	0.0360	0.0008	0.0211	-0.0035	0.0021	-0.0109	0.0551
47	11	H	S		-0.1372	-0.0395	0.0195	-0.0484	-0.0276	-0.0149	-0.0163	0.0014	0.0069	0.0277	0.0121
48	12	C	S		-0.0405	-0.0161	0.0062	0.0011	0.0033	0.0017	-0.0219	-0.0054	-0.0045	-0.0270	-0.1026
49	12	C	PX		-0.0054	-0.0116	0.0045	-0.0048	0.0038	0.0004	0.0005	0.0021	-0.0007	0.0026	0.0063
50	12	C	PY		-0.1602	-0.0471	0.0249	0.0004	0.0081	0.0028	-0.0263	-0.0088	-0.0068	-0.0143	-0.0234
51	12	C	PZ		-0.2265	-0.0347	0.0160	0.0094	0.0036	0.0051	-0.0600	-0.0136	-0.0150	0.1476	0.2331
52	13	C	S		0.0405	-0.0162	-0.0062	0.0011	-0.0033	0.0017	-0.0218	0.0054	-0.0045	-0.0271	0.1046
53	13	C	PX		0.0056	-0.0116	-0.0045	-0.0048	-0.0038	0.0004	0.0004	-0.0021	-0.0008	0.0030	-0.0068
54	13	C	PY		-0.1799	0.0471	0.0249	-0.0004	0.0081	-0.0028	0.0263	-0.0088	0.0068	0.0144	-0.0240
55	13	C	PZ		0.2262	-0.0347	-0.0160	0.0094	-0.0036	0.0051	-0.0600	0.0136	-0.0150	0.1477	-0.2375
56	14	H	S		-0.0277	0.0111	-0.0105	0.0105	-0.0039	0.0052	0.0532	0.0064	0.0087	-0.1083	-0.1129
57	15	H	S		0.0657	-0.0121	0.0054	-0.0126	0.0061	-0.0022	-0.0301	-0.0087	-0.0050	0.1022	0.1845
58	16	H	S		0.0786	0.0204	-0.0065	0.0025	-0.0061	-0.0031	-0.0292	0.0007	-0.0082	0.1079	0.1943
59	17	H	S		0.0277	0.0111	0.0105	0.0105	0.0039	0.0052	0.0532	-0.0064	0.0087	-0.1084	0.1150
60	18	H	S		-0.0654	-0.0121	-0.0053	-0.0126	-0.0061	-0.0022	-0.0298	0.0087	-0.0049	0.1015	-0.1874
61	19	H	S		-0.0787	0.0203	0.0064	0.0024	0.0061	-0.0031	-0.0294	-0.0007	-0.0082	0.1086	-0.1986

EIGENVALUES---				0.3724	0.3820	0.3936	0.4336	0.4406	0.4454	0.4502	0.4532	0.4568	0.4621	0.4639
				34	35	36	37	38	39	40	41	42	43	44
1	1	P	S	0.0445	-0.0000	0.0060	0.0001	-0.0102	-0.0758	0.0026	-0.1464	0.1139	0.0024	0.0384
2	1	P	PX	0.3795	-0.0001	0.2503	-0.0002	-0.0241	0.0382	-0.0025	0.1234	-0.1223	-0.0028	-0.0025
3	1	P	PY	0.0004	-0.0223	0.0000	0.1280	-0.0005	0.0004	-0.0441	-0.0008	0.0004	-0.0220	0.0009
4	1	P	PZ	-0.1841	-0.0000	0.0549	0.0003	0.1267	0.0354	-0.0021	0.1017	-0.0361	-0.0017	-0.0245
5	1	P	DZZ	0.1336	0.0000	-0.0531	0.0002	0.3153	0.2014	-0.0047	0.1768	0.1167	0.0011	-0.0295
6	1	P	DXZ	-0.1170	0.0001	-0.1862	0.0002	0.0757	-0.0377	0.0015	-0.0990	0.0965	0.0010	0.0346
7	1	P	DYZ	-0.0035	-0.2478	-0.0000	-0.0237	0.0001	-0.0001	0.0147	0.0002	-0.0001	0.0040	-0.0006
8	1	P	DX-Y	-0.2734	0.0001	-0.2340	-0.0010	-0.3182	0.1611	-0.0010	0.1218	0.0055	0.0024	-0.0998
9	1	P	DXY	0.0023	0.2228	0.0000	-0.1355	0.0005	-0.0002	0.0206	-0.0001	-0.0001	-0.0065	-0.0015
10	2	S	S	0.0348	0.0000	0.0018	-0.0002	-0.0912	-0.0388	0.0010	-0.0387	-0.0244	-0.0005	0.0141
11	2	S	PX	-0.0452	-0.0000	0.0263	-0.0001	-0.0378	0.0054	-0.0002	0.0179	-0.0290	-0.0003	-0.0077
12	2	S	PY	0.0017	0.1419	0.0000	-0.0266	0.0001	0.0000	-0.0021	-0.0002	0.0001	-0.0068	-0.0004
13	2	S	PZ	-0.1062	-0.0000	0.0050	0.0004	0.2245	0.1015	-0.0027	0.1088	0.0259	0.0004	-0.0291
14	2	S	DZZ	-0.0488	-0.0000	0.0303	0.0005	0.4608	0.2933	-0.0091	0.4011	-0.0950	-0.0041	-0.0629
15	2	S	DXZ	-0.0862	-0.0000	0.0661	-0.0001	-0.1404	-0.0227	0.0002	0.0383	-0.1637	-0.0021	-0.0320
16	2	S	DYZ	0.0032	0.2839	-0.0000	-0.1142	0.0004	-0.0001	0.0238	0.0002	-0.0000	-0.0052	-0.0007
17	2	S	DX-Y	-0.1659	0.0001	-0.1356	-0.0012	-0.3164	0.3018	-0.0025	0.1957	0.1145	0.0069	-0.1633
18	2	S	DXY	0.0011	0.1059	-0.0000	-0.1566	0.0007	-0.0008	0.0729	0.0020	-0.0013	0.1196	0.0001
19	3	S	S	-0.0647	0.0000	-0.0446	0.0003	0.1031	-0.0105	0.0000	-0.0164	0.0152	-0.0002	0.0116
20	3	S	PX	0.2992	-0.0001	0.1537	-0.0007	-0.2253	0.0395	-0.0006	0.0653	-0.0541	-0.0002	-0.0259
21	3	S	PY	-0.0018	-0.1397	-0.0000	0.0270	-0.0001	-0.0000	-0.0019	0.0001	-0.0001	0.0078	0.0003
22	3	S	PZ	0.0832	-0.0000	0.0367	0.0001	0.0941	0.0177	-0.0008	0.0202	0.0193	-0.0001	0.0058
23	3	S	DZZ	-0.2179	0.0001	-0.2506	-0.0001	0.1078	0.2228	-0.0013	0.0478	0.3585	0.0107	-0.1221
24	3	S	DXZ	0.1704	-0.0000	0.0623	0.0005	0.3476	0.0875	-0.0030	0.0656	0.1876	0.0019	0.0234
25	3	S	DYZ	-0.0005	-0.0311	-0.0000	-0.1043	0.0005	-0.0005	0.0626	0.0014	-0.0008	0.0804	-0.0009
26	3	S	DX-Y	0.2124	-0.0000	0.0915	-0.0014	-0.3547	0.3275	-0.0059	0.3861	-0.0964	0.0017	-0.1910
27	3	S	DXY	-0.0035	-0.2913	-0.0000	0.0646	-0.0001	-0.0003	0.0176	0.0012	-0.0007	0.0682	0.0017
28	4	O	S	0.0636	-0.0225	0.0783	0.1412	-0.0182	0.0626	-0.0275	0.0689	-0.0088	-0.0125	-0.0317
29	4	O	PX	-0.1083	0.0480	-0.0560	0.0221	-0.0538	0.0427	-0.0003	0.0220	-0.0140	-0.0571	-0.0782
30	4	O	PY	-0.0468	0.0415	-0.0023	-0.1620	0.0542	-0.0164	0.0128	0.0701	-0.1363	0.0060	0.0122
31	4	O	PZ	0.0988	-0.0862	0.0433	0.1519	0.0069	0.0643	-0.0483	0.0682	0.0566	-0.0124	-0.0310
32	5	O	S	0.0623	0.0224	0.0782	-0.1415	-0.0171	0.0618	0.0250	0.0696	-0.0095	0.0137	-0.0333
33	5	O	PX	-0.1099	-0.0480	-0.0560	-0.0221	-0.0535	0.0417	0.0010	0.0234	-0.0156	0.0611	-0.0755
34	5	O	PY	0.0449	0.0415	0.0023	-0.1623	-0.0531	0.0154	0.0155	-0.0698	0.1355	0.0139	-0.0129
35	5	O	PZ	0.0993	0.0861	0.0433	-0.1522	0.0081	0.0635	0.0454	0.0699	0.0560	0.0150	-0.0317
36	6	C	S	-0.0721	-0.0155	-0.1555	-0.3086	0.0642	0.1523	0.3408	-0.0893	-0.3629	0.0572	0.0933
37	6	C	PX	-0.0318	0.0130	-0.0162	0.0221	-0.0679	0.0291	-0.0760	0.1358	0.0538	0.3479	0.3392
38	6	C	PY	-0.0439	0.0019	-0.0811	-0.0481	0.0170	-0.0367	-0.0509	0.0005	0.0981	-0.0063	-0.0103
39	6	C	PZ	0.1001	-0.0471	0.0415	0.0956	0.0125	0.1092	0.1276	-0.0572	-0.0667	0.0058	0.0106
40	7	C	S	-0.0707	0.0156	-0.1655	0.3088	0.0609	0.1540	-0.3371	-0.1055	-0.3621	-0.0662	0.0836
41	7	C	PX	-0.0320	-0.0129	-0.0152	-0.0251	-0.0679	0.0346	0.0645	0.1290	0.0629	-0.3690	0.3184
42	7	C	PY	0.0430	0.0019	0.0811	-0.0481	-0.0169	0.0366	-0.0506	-0.0035	-0.0984	-0.0081	0.0070
43	7	C	PZ	0.0983	0.0470	0.0415	-0.0956	0.0128	0.1085	-0.1254	-0.0638	-0.0678	-0.0019	0.0043
44	8	H	S	-0.0187	0.0341	0.0789	0.0935	-0.0005	-0.1394	-0.1976	0.0054	0.1843	-0.2963	-0.3240
45	9	H	S	-0.0559	0.0552	0.0685	0.1294	-0.0882	-0.1151	-0.3043	0.1870	0.2501	0.2214	0.1948
46	10	H	S	-0.0179	-0.0342	0.0789	-0.0912	0.0012	-0.1444	0.2025	0.0233	0.1775	0.3153	-0.2997
47	11	H	S	-0.0556	-0.0551	0.0685	-0.1320	-0.0866	-0.1113	0.2920	0.1936	0.2571	-0.2349	0.1877
48	12	C	S	-0.1131	0.2370	0.3090	0.3348	-0.0242	0.2025	0.1561	-0.1660	0.1607	0.0193	0.0214
49	12	C	PX	-0.0020	-0.0031	-0.0102	0.0053	-0.0352	0.0162	-0.0492	0.0940	0.0397	0.2860	0.2914
50	12	C	PY	-0.0260	0.0714	0.0734	-0.0587	0.0119	-0.2323	-0.3058	0.1976	0.0472	-0.0529	-0.0768
51	12	C	PZ	0.2486	-0.2814	-0.1893	0.1649	-0.0210	0.0644	0.0178	-0.0953	0.1993	0.0005	-0.0029
52	13	C	S	-0.1114	-0.2370	0.3088	-0.3357	-0.0229	0.2011	-0.1502	-0.1744	0.1594	-0.0064	0.0146
53	13	C	PX	-0.0015	0.0035	-0.0100	-0.0105	-0.0356	0.0241	0.0367	0.0843	0.0488	-0.3042	0.2748
54	13	C	PY	0.0256	0.0715	-0.0734	-0.0594	-0.0129	0.2325	-0.2983	-0.2126	-0.0474	-0.0483	0.0672
55	13	C	PZ	0.2445	0.2814	-0.1892	-0.1653	-0.0200	0.0635	-0.0145	-0.0963	0.1986	0.0094	-0.0037
56	14	H	S	-0.1178	0.1003	-0.0003	-0.2934	0.0308	-0.3001	-0.3066	0.2642	-0.1274	-0.0459	-0.0620
57	15	H	S	0.2097	-0.2888	-0.2572	-0.1130	0.0353	-0.0965	-0.0388	-0.0267	-0.0321	-0.2432	-0.2494
58	16	H	S	0.1971	-0.2877	-0.2818	-0.1000	-0.0269	-0.0680	-0.1212	0.1286	0.0333	0.2171	0.2164
59	17	H	S	-0.1159	-0.1003	-0.0002	0.2944	0.0303	-0.2990	0.2970	0.2799	-0.1260	0.0308	-0.0503
60	18	H	S	0.2057	0.2881	-0.2671	0.1183	0.0355	-0.1032	0.0477	-0.0143	-0.0394	0.2556	-0.2329
61	19	H	S	0.1946	0.2884	-0.2815	0.0955	-0.0276	-0.0609	0.1087	0.1346	0.0412	[illegible]	[illegible]

				EIGENVALUES---	0.4678	0.4970	0.5002	0.5033	0.5038	0.5139	0.5240	0.5261	0.5288	0.5512	0.5541
					45	46	47	48	49	50	51	52	53	54	55
1	1	P	S		-0.0001	0.1750	-0.0301	0.0492	0.0001	0.0272	-0.0001	-0.0054	0.0000	0.0035	0.0000
2	1	P	PX		0.0002	0.1060	-0.0301	0.1218	-0.0001	0.0100	-0.0009	0.0056	-0.0007	0.3465	-0.0000
3	1	P	PY		-0.1796	-0.0002	-0.0130	-0.0002	-0.1759	0.0003	-0.1136	-0.0011	0.1004	0.0000	0.5079
4	1	P	PZ		-0.0000	0.1017	-0.0301	-0.0405	0.0001	0.0669	-0.0004	-0.0028	-0.0003	-0.1304	-0.0001
5	1	P	DZ2		-0.0000	-0.1071	0.0301	0.0642	-0.0002	-0.0657	0.0000	0.0058	-0.0000	0.1319	0.0000
6	1	P	DXZ		0.0001	-0.1019	0.0301	-0.0174	0.0000	-0.0454	0.0004	-0.0052	0.0003	0.0028	0.0000
7	1	P	DYZ		0.0818	0.0001	-0.0294	0.0001	0.0562	-0.0002	0.0989	0.0002	-0.0947	-0.0000	-0.0230
8	1	P	DX-Y		-0.0004	-0.2025	0.0002	-0.1427	0.0001	-0.0488	0.0009	-0.0117	0.0008	-0.2297	0.0000
9	1	P	DXY		0.0962	0.0002	0.0320	0.0001	0.0911	-0.0002	0.0756	0.0005	-0.0690	-0.0000	-0.0835
10	2	S	S		0.0001	-0.0315	0.0300	0.0092	0.0000	0.0006	0.0002	-0.0021	0.0001	-0.0088	0.0000
11	2	S	PX		-0.0000	-0.0004	0.0100	0.0067	-0.0000	-0.0063	-0.0000	-0.0016	0.0000	-0.0430	-0.0000
12	2	S	PY		0.0048	0.0000	0.0167	-0.0000	0.0011	-0.0000	0.0026	0.0001	0.0010	0.0000	-0.0388
13	2	S	PZ		-0.0001	0.0390	-0.0301	-0.0217	-0.0000	-0.0030	-0.0003	0.0029	-0.0002	0.0141	-0.0000
14	2	S	DZ2		0.0003	-0.3653	0.0303	0.0589	-0.0003	-0.0865	0.0004	0.0090	0.0002	0.0445	0.0001
15	2	S	DXZ		-0.0000	-0.0358	-0.0000	-0.0901	-0.0002	-0.0219	-0.0012	0.0342	-0.0012	0.6371	0.0000
16	2	S	DYZ		0.0410	0.0002	0.2101	-0.0001	-0.0102	0.0000	-0.0209	-0.0001	0.0295	0.0000	0.5116
17	2	S	DX-Y		-0.0009	0.1910	-0.0300	0.7225	-0.0014	-0.2023	-0.0018	0.0294	-0.0012	0.0581	-0.0000
18	2	S	DXY		0.6290	-0.0007	-0.6620	0.0002	0.0681	-0.0000	-0.1172	0.0015	0.1550	0.0000	0.0773
19	3	S	S		0.0000	-0.0286	0.0300	-0.0300	0.0000	-0.0025	0.0001	0.0017	0.0000	-0.0234	0.0000
20	3	S	PX		-0.0001	0.0356	-0.0300	0.0469	-0.0000	0.0029	-0.0001	-0.0038	-0.0000	0.0487	-0.0000
21	3	S	PY		0.0048	-0.0000	-0.0165	-0.0000	-0.0035	0.0000	-0.0024	-0.0000	0.0000	-0.0000	-0.0328
22	3	S	PZ		0.0000	0.0022	-0.0000	-0.0140	0.0000	0.0052	0.0000	-0.0000	0.0000	0.0254	0.0000
23	3	S	DZ2		-0.0011	0.5203	-0.0306	-0.3362	0.0007	0.2132	-0.0007	0.0089	-0.0007	0.3657	0.0000
24	3	S	DXZ		0.0000	0.2695	-0.0302	0.1017	0.0004	0.1259	0.0005	-0.0446	0.0008	-0.3331	-0.0001
25	3	S	DYZ		0.6128	0.0007	0.6975	-0.0004	-0.1449	0.0003	-0.0751	-0.0001	0.0708	0.0000	-0.0366
26	3	S	DX-Y		-0.0007	-0.0027	-0.0002	-0.4469	0.0007	0.1395	0.0005	-0.0109	0.0004	-0.1881	-0.0000
27	3	S	DXY		0.1915	-0.0003	-0.0594	-0.0002	-0.1131	0.0003	-0.1368	-0.0005	0.1330	0.0000	0.4247
28	4	O	S		-0.0664	0.0513	-0.0315	0.0214	-0.0847	0.0336	-0.1176	0.0080	0.1486	-0.0312	0.0497
29	4	O	PX		-0.0428	-0.0443	0.0304	-0.0399	-0.0226	-0.0063	0.0061	0.0471	0.0583	-0.0617	0.0815
30	4	O	PY		-0.0694	-0.0856	-0.0313	-0.0140	0.0769	-0.0111	0.0967	-0.0051	-0.1626	0.1359	0.2106
31	4	O	PZ		-0.0448	0.0132	0.0348	0.0521	-0.0318	0.0629	-0.1220	0.0117	0.1613	-0.0152	0.0160
32	5	O	S		0.0661	0.0514	0.0314	0.0217	0.0846	0.0332	0.1175	0.0069	-0.1488	-0.0312	-0.0497
33	5	O	PX		0.0419	-0.0449	-0.0304	-0.0398	0.0217	-0.0060	-0.0074	0.0450	-0.0598	-0.0618	-0.0814
34	5	O	PY		-0.0700	0.0854	-0.0314	0.0144	0.0769	0.0110	0.0975	0.0020	-0.1620	-0.1360	0.2107
35	5	O	PZ		0.0445	0.0133	-0.0348	0.0523	0.0317	0.0627	0.1223	0.0096	-0.1612	-0.0152	-0.0159
36	6	C	S		-0.1324	0.0520	0.0049	0.0057	0.0052	0.0404	-0.0172	-0.0070	-0.0039	0.0202	0.0435
37	6	C	PX		-0.0388	0.0009	0.0329	0.0041	-0.0036	0.0121	-0.2608	-0.3594	-0.2188	0.0198	-0.0197
38	6	C	PY		0.0738	-0.1317	-0.0444	-0.1296	-0.1037	-0.3362	0.2793	-0.0313	-0.3721	0.0914	0.1381
39	6	C	PZ		-0.0094	0.2233	-0.0597	-0.0754	-0.4393	-0.3264	-0.0039	-0.0231	0.0286	-0.0946	-0.1010
40	7	C	S		0.1331	0.0523	-0.0350	0.0057	-0.0049	0.0403	0.0174	-0.0066	0.0041	0.0202	-0.0435
41	7	C	PX		0.0435	0.0054	-0.0323	0.0041	0.0102	0.0087	0.2727	-0.3419	0.2320	0.0203	0.0195
42	7	C	PY		0.0739	0.1320	-0.0447	0.1295	-0.1036	0.3360	0.2805	0.0239	-0.3718	-0.0916	0.1382
43	7	C	PZ		0.0088	0.2230	0.0593	-0.0742	0.4392	-0.3272	0.0019	-0.0193	-0.0292	-0.0947	0.1011
44	8	H	S		0.1021	-0.1419	0.0228	0.0466	0.2121	0.1275	0.1586	0.2262	0.1322	0.0172	0.0396
45	9	H	S		0.0270	-0.1265	0.0357	0.0419	0.1979	0.1446	-0.1463	-0.1913	-0.1284	0.0422	0.0144
46	10	H	S		-0.1057	-0.1449	-0.0230	0.0460	-0.2164	0.1300	-0.1649	0.2139	-0.1297	0.0170	-0.0394
47	11	H	S		-0.0236	-0.1236	-0.0351	0.0413	-0.1940	0.1430	0.1539	-0.1832	0.1360	0.0425	-0.0146
48	12	C	S		0.0759	-0.0515	-0.0234	-0.0620	-0.0901	-0.1767	0.1054	-0.0116	-0.1255	0.0093	0.0171
49	12	C	PX		-0.0362	0.0197	0.0132	-0.0240	0.0004	-0.0253	0.3268	0.4207	0.2379	-0.0133	0.0114
50	12	C	PY		0.0323	0.1431	-0.0593	-0.0848	-0.3532	-0.3180	0.0632	-0.0198	-0.0642	-0.0340	-0.0233
51	12	C	PZ		0.0951	-0.1263	-0.0176	-0.0677	-0.0045	-0.1555	0.1472	-0.0146	-0.1893	0.0385	0.0492
52	13	C	S		-0.0768	-0.0518	0.0236	-0.0616	0.0901	-0.1765	-0.1040	-0.0111	0.1268	0.0094	-0.0171
53	13	C	PX		0.0394	0.0181	-0.0135	-0.0240	-0.0049	-0.0225	-0.3401	0.4003	-0.2534	-0.0142	-0.0108
54	13	C	PY		0.0323	-0.1429	-0.0589	0.0841	-0.3529	0.3186	0.0677	0.0125	-0.0618	0.0341	-0.0232
55	13	C	PZ		-0.0957	-0.1265	0.0180	-0.0676	0.0046	-0.1552	-0.1458	-0.0132	0.1904	0.0386	-0.0492
56	14	H	S		-0.0514	0.1565	-0.0211	-0.0033	-0.1768	-0.0689	-0.0500	-0.0021	0.0693	-0.0320	-0.0302
57	15	H	S		0.0290	-0.0262	-0.0093	0.0126	0.0138	0.0177	-0.1878	-0.2522	-0.1539	0.0123	0.0007
58	16	H	S		-0.0270	0.0005	0.0093	-0.0177	0.0140	-0.0144	0.2028	0.2462	0.1238	-0.0016	0.0123
59	17	H	S		0.0523	0.1566	0.0205	-0.0032	0.1765	-0.0696	0.0448	0.0033	-0.0727	-0.0321	0.0302
60	18	H	S		-0.0313	-0.0251	0.0095	0.0125	-0.0109	0.0159	0.1956	-0.2395	0.1634	0.0128	-0.0010
61	19	H	S		0.0296	-0.0006	-0.0095	-0.0178	-0.0168	-0.0126	-0.2110	0.2347	-0.1335	-0.0021	-0.0120

EIGENVALUES---				0.5740	0.6175	0.6364	0.6365	0.6563	0.6619
				56	57	58	59	60	61
1	1	P	S	-0.0212	-0.0644	-0.0000	-0.0076	0.0000	0.0219
2	1	P	PX	0.1324	-0.2924	0.0001	0.2060	0.0000	0.0339
3	1	P	PY	0.0001	-0.0000	0.0012	-0.0000	0.0779	-0.0000
4	1	P	PZ	0.4132	-0.2164	-0.0001	-0.2028	0.0000	0.0377
5	1	P	DZ2	-0.1701	-0.3393	-0.0003	-0.5514	-0.0000	-0.1016
6	1	P	DXZ	-0.0445	0.0207	-0.0000	-0.0764	0.0000	0.7049
7	1	P	DYZ	0.0000	0.0000	0.4154	-0.0002	-0.5917	0.0000
8	1	P	DX-Y	-0.1427	-0.5966	0.0002	0.2765	0.0000	0.0143
9	1	P	DXY	0.0000	-0.0000	-0.5710	0.0004	-0.4849	0.0000
10	2	S	S	-0.0544	0.0973	0.0001	0.1451	0.0000	0.0178
11	2	S	PX	0.0085	0.0116	-0.0000	-0.0008	-0.0000	-0.1191
12	2	S	PY	-0.0000	-0.0000	-0.0760	0.0000	0.0954	-0.0000
13	2	S	PZ	0.0962	-0.1501	-0.0001	-0.2305	-0.0000	-0.0228
14	2	S	DZ2	-0.2333	0.2688	0.0002	0.4086	0.0000	0.0149
15	2	S	DXZ	-0.0283	-0.0839	-0.0000	-0.0307	0.0000	0.4558
16	2	S	DYZ	0.0001	0.0000	0.3626	-0.0002	-0.3866	0.0000
17	2	S	DX-Y	0.1431	0.1851	-0.0000	-0.0732	0.0000	0.0255
18	2	S	DXY	0.0000	0.0000	0.1565	-0.0001	0.1116	-0.0000
19	3	S	S	0.0004	0.1044	-0.0001	-0.1406	-0.0000	0.0398
20	3	S	PX	-0.0113	-0.1552	0.0001	0.2140	-0.0000	-0.0803
21	3	S	PY	-0.0000	0.0000	0.1145	-0.0001	0.0492	-0.0000
22	3	S	PZ	-0.0440	0.0465	-0.0000	-0.0741	-0.0000	-0.0969
23	3	S	DZ2	-0.0735	0.0573	0.0001	0.1975	-0.0000	-0.1828
24	3	S	DXZ	0.3512	-0.1439	0.0002	0.3028	0.0000	0.3609
25	3	S	DYZ	-0.0000	0.0000	0.0443	-0.0000	0.2021	-0.0000
26	3	S	DX-Y	0.1747	0.3205	-0.0002	-0.2436	0.0000	0.1579
27	3	S	DXY	0.0001	-0.0000	-0.5431	0.0003	-0.1557	0.0000
28	4	O	S	-0.0844	-0.1142	0.0382	-0.0196	0.0991	-0.0182
29	4	O	PX	-0.0042	-0.1176	-0.0550	0.0327	0.0700	0.0060
30	4	O	PY	0.3072	-0.0393	0.0156	0.0347	0.2292	-0.1392
31	4	O	PZ	-0.1760	-0.1123	0.0974	-0.0690	-0.0104	0.0414
32	5	O	S	-0.0844	-0.1142	-0.0382	-0.0195	-0.0991	-0.0182
33	5	O	PX	-0.0042	-0.1176	0.0550	0.0326	-0.0700	0.0060
34	5	O	PY	-0.3071	0.0393	0.0156	-0.0347	0.2292	0.1392
35	5	O	PZ	-0.1760	-0.1123	-0.0975	-0.0689	0.0104	0.0414
36	6	C	S	0.0687	-0.0120	0.0001	0.0129	0.0478	-0.0306
37	6	C	PX	-0.0200	-0.0043	0.0048	-0.0115	-0.0256	-0.0032
38	6	C	PY	0.2670	0.0009	-0.0086	0.0500	0.0880	-0.0657
39	6	C	PZ	-0.1673	-0.0035	0.0185	-0.0055	-0.0783	0.0526
40	7	C	S	0.0687	-0.0120	-0.0000	0.0129	-0.0478	-0.0306
41	7	C	PX	-0.0196	-0.0043	-0.0048	-0.0115	0.0256	-0.0032
42	7	C	PY	-0.2670	-0.0009	-0.0086	-0.0500	0.0880	0.0657
43	7	C	PZ	-0.1673	-0.0035	-0.0185	-0.0055	0.0783	0.0526
44	8	H	S	0.0427	-0.0029	-0.0088	0.0063	0.0161	-0.0084
45	9	H	S	0.0264	0.0028	-0.0004	-0.0063	0.0031	-0.0084
46	10	H	S	0.0425	-0.0029	0.0089	0.0063	-0.0161	-0.0084
47	11	H	S	0.0265	0.0028	0.0004	-0.0063	-0.0031	-0.0084
48	12	C	S	0.0385	0.0007	0.0013	0.0101	0.0022	-0.0029
49	12	C	PX	0.0099	0.0009	-0.0017	0.0034	0.0077	0.0010
50	12	C	PY	-0.0345	-0.0040	0.0070	0.0058	-0.0133	0.0091
51	12	C	PZ	0.0994	0.0045	-0.0036	0.0156	0.0172	-0.0146
52	13	C	S	0.0385	0.0007	-0.0013	0.0101	-0.0022	-0.0029
53	13	C	PX	0.0090	0.0009	0.0017	0.0033	-0.0077	0.0011
54	13	C	PY	0.0345	0.0040	0.0069	-0.0058	-0.0133	-0.0091
55	13	C	PZ	0.0994	0.0045	0.0036	0.0156	-0.0172	-0.0146
56	14	H	S	-0.0548	-0.0031	0.0035	-0.0033	-0.0082	0.0065
57	15	H	S	0.0066	-0.0001	-0.0004	-0.0006	-0.0006	-0.0018
58	16	H	S	0.0162	0.0004	-0.0012	0.0024	0.0052	-0.0013
59	17	H	S	-0.0547	-0.0031	-0.0035	-0.0033	0.0082	0.0065
60	18	H	S	0.0071	-0.0001	0.0005	-0.0006	0.0006	-0.0018
61	19	H	S	0.0158	0.0004	0.0012	0.0024	-0.0052	-0.0013

REFERENCES

[1]D. S. Urch, Jour. Phy-C-Solid State, 3, No. 6, 1275 (1970).

[2]G. Andermann, private communication.

[3]K. Siegbahn, et al, "Electron Spectroscopy for Chemical Analysis," Air Force Materials Lab. Technical Report A.F.M.L. TR-68-189 (1968).

[4]A. Compton and S. Allison, "Xrays in Theory and Experiment," 2nd Edition, Van Nostrand Company, Inc., N.Y. (1935).

[5]P. E. Best, Jour. Chem. Phys. 44, No. 9, 3248 (1966).

[6]W. Seka and H. Hanson, Jour. Chem. Phys. 50, 344 (1969).

[7]D. W. Fischer, Reprint, Air Force Material Lab. Publication (1970).

[8]D. W. Fischer, Reprint, Air Force Materials Lab. Publication (1969).

[9]G. Andermann, N.S.F. Research Proposal 1967.

[10]C. Dodd and G. Glenn, Jour. Appl. Phys. 39, No. 12, 5377 (1968).

[11]P. E. Best, Jour. Chem. Phys. 49, No. 6, 2797 (1968).

[12]G. Andermann and H. C. Whitehead, Adv. Xray Analysis 14, 453, Plenum Press, New York (1969).

[13]V. I. Nefedov, Zh. Strukt. Khim. 8, No. 6, 1037 (1967).

[14]V. I. Nefedov, Zh. Strukt. Khim. 9, No. 1, 126 (1968); No. 2, 279 (1968).

[15]V. I. Nefedov, Zh. Strukt. Khim. 8, No. 4 686 (1967).

[16]R. Manne, Reprint, Preliminary Research Report No. 257, Quantum Chemistry Group, Uppsala, Sweden.

[17]J. Connor, I. Hillier and V. Saunders, Preprint.

[18]D. Bishop, M. Randic and J. Morton, Jour. Chem. Phys. 45, 1880 (1966).

[19]D. Bishop, Theor. Chim. Acta. 8, 285 (1967).

[20]D. S. Urch, Jour. Chem. Soc. A1969, 3026 (1969).

[21]D. Boyd and W. Lipscomb, Jour. Chem. Phys. 48, No. 11, 498 (1968).

[22]M. Fichter, Ph.D. Dissertation, Univ. Munchen (1966).

[23]B. L. Henke and E. N. Smith, Jour. Appl. Phys. 37, 922 (1966).

[24]Liebhafsky, et al., "Xray Absorption and Emission in Analytical Chemistry," John Wiley and Sons Inc., New York (1960).

[25]W. Hume-Rothery, "Electrons, Atoms, Metals and Alloys," 3rd Revised Edition, Dover Publications, Inc., New York, N.Y. (1963).

[26]Ballhausen and Gray, "Molecular Orbital Theory," W. A. Benjamin, Inc., New York (1965).

[27]R. S. Drago, "Physical Methods in Inorganic Chemistry," Reinhold Pub. Corp., New York, N.Y. (1965).

[28]Lowdin, "Molecular Orbitals in Chemistry, Physics and Biology," Academic Press, Inc., New York, N.Y. (1964).

[29]G. King, "Spectroscopy and Molecular Structure," Holt, Reinhart and Winston, Inc., New York (1964).

[30]R. Manne, Jour. Chem. Phys. 52, No. 11, 5733 (1970).

[31]K. A. R. Mitchell, Chem. Revs. 69, No. 2, 157 (1969).

[32]D. P. Craig, et al., Jour. Chem. Soc., 332 (1954).

[33]L. S. Bartel, et al., Inorg. Chem. 9, 1903 (1970).

[34]G. S. Chandler and T. Thirunamachandran, Jour. Chem. Phys. 47, 1192 (1967).

[35]C. A. Coulson, Nature 221, 1106 (1969).

[36]G. S. Chandler and T. Thirunamachandran, Jour. Chem. Phys. 49, 3640 (1968).

[37]D. W. J. Cruickshank, et al., Jour. Chem. Phys. 40, 3733 (1964).

[38]I. H. Hillier and V. R. Saunders, Chem. Comm. 1970, 1183.

[39]D. W. Jones and D. W. J. Cruickshank, Z. Krist. 116, 101 (1961).

[40]H. C. Whitehead, J. Layfield and G. Andermann, Revs. Sci. Instr. in press.

[41]G. Wiech, Z. für Phys. 216, 472 (1968).

[42]R. W. Mooney and M. A. Aia, Chem. Revs. 61, 433 (1961).

[43]A. D. Mighell, et al., Acta. Cryst. (1969) B25, 776.

[44]D. E. C. Corbridge, Acta Cryst. 1956 9, 991.

[45]M. Ebert and J. Sedivy, Czech. J. Phys. 13 (10), 765 (1963).

[46]Chem. Abstr. 53:6725d.

[47]M. Pelavin, W. L. Jolly, et al., Jour. Phys. Chem. 74, No. 5, 1164 (1970).

[48]Q. Fernando and C. D. Green, J. Inorg. Nucl. Chem., 1967, 29, 647.

[49]Q. Fernando, Inorg. Chem. 6, 1558 (1967).

[50]P. S. Shetty and Q. Fernando, Acta. Cryst. (1969), B25, 1294.

[51]F. A. Cotton, "Chemical Applications of Group Theory," Interscience Publishers, New York, N.Y. (1963).

[52]D. S. Urch, "Orbitals and Symmetry," Penguin Education Ltd., London U.K. (1970).

[52]D. S. Urch, Adv. Xray Analysis 14, 250, Plenum Press, New York (1971).

[53]J. A. Pople, et al., Jour. Chem. Phys. 43, No. 10, s129 (1965).

[54]J. A. Pople and G. A. Segal, Jour. Chem. Phys. 43, No. 10, s136 (1965).

[55]J. A. Pople and G. A. Segal, Jour. Chem. Phys. 44, No. 9, 3289 (1965).

[56]J. A. Pople and G. A. Segal, Jour. Chem. Phys. 47, No. 1, 158 (1967).

[57]J. A. Pople and D. L. Beveridge, "Approximate Molecular Orbital Theory," McGraw-Hill Inc., New York, N.Y. (1970).